nagra
National Cooperative for
the Disposal of Radioactive Waste

TECHNICAL REPORT 91-04

GRIMSEL TEST SITE

THE RADIONUCLIDE MIGRATION EXPERIMENT – OVERVIEW OF INVESTIGATIONS 1985 – 1990

MARCH 1992

U. Frick [1], W.R. Alexander [2], B. Baeyens [3]
P. Bossart [4][5], M.H. Bradbury [3], Ch. Bühler [6]
J. Eikenberg [3], Th. Fierz [6], W. Heer [3]
E. Hoehn [3], I.G. McKinley [1] and P.A. Smith [3]

[1] Nagra, Hardstrasse 73, CH-5430 Wettingen, Switzerland
[2] Rock-Water Interaction Group, Institute for Mineralogy and Petrography, University of Bern, Baltzerstrasse 1, CH-3012 Bern, Switzerland
[3] Paul Scherrer Institute, CH-5232 Villigen PSI, Switzerland
[4] Kellerhals & Haefeli AG, Geological Contractors, Kapellenstrasse 22, CH-3011 Bern, Switzerland
[5] Geotechnical Institute AG, Gartenstrasse 13, CH-3007 Bern, Switzerland
[6] SOLEXPERTS AG, Research and Consulting Office for Applied Rock & Soil Mechanics and Hydraulics, Ifangstrasse 12, CH-8603 Schwerzenbach, Switzerland

Hardstrasse 73, CH-5430 Wettingen/Switzerland, Telephone + 41-56-37 11 11

nagra National Cooperative for the Disposal of Radioactive Waste

TECHNICAL REPORT 91-04

GRIMSEL TEST SITE

THE RADIONUCLIDE MIGRATION EXPERIMENT – OVERVIEW OF INVESTIGATIONS 1985 – 1990

MARCH 1992

U. Frick [1], W.R. Alexander [2], B. Baeyens [3]
P. Bossart [4][5], M.H. Bradbury [3], Ch. Bühler [6]
J. Eikenberg [3], Th. Fierz [6], W. Heer [3]
E. Hoehn [3], I.G. McKinley [1] and P.A. Smith [3]

[1] Nagra, Hardstrasse 73, CH-5430 Wettingen, Switzerland
[2] Rock-Water Interaction Group, Institute for Mineralogy and Petrography, University of Bern, Baltzerstrasse 1, CH-3012 Bern, Switzerland
[3] Paul Scherrer Institute, CH-5232 Villigen PSI, Switzerland
[4] Kellerhals & Haefeli AG, Geological Contractors, Kapellenstrasse 22, CH-3011 Bern, Switzerland
[5] Geotechnical Institute AG, Gartenstrasse 13, CH-3007 Bern, Switzerland
[6] SOLEXPERTS AG, Research and Consulting Office for Applied Rock & Soil Mechanics and Hydraulics, Ifangstrasse 12, CH-8603 Schwerzenbach, Switzerland

Hardstrasse 73, CH-5430 Wettingen/Switzerland, Telephone + 41-56-37 11 11

FOREWORD

Concepts for the disposal of radioactive waste in geological formations place a significant emphasis on acquiring extensive knowledge of the proposed host rock and the surrounding strata. For this reason, Nagra has, since May 1984, been operating the **Grimsel Test Site (GTS)** which is located at a depth of 450 m in the crystalline rock of the Aare Massif of the Central Swiss Alps. The general objectives of the research being carried out in this underground laboratory include

- the build-up of know-how in planning, performing and interpreting field experiments in various scientific and technical disciplines and

- the acquisition of practical experience in the development of investigation methodologies, measuring techniques and test equipment which will be of use during actual repository site explorations.

The GTS is operated by Nagra and, on the basis of a German-Swiss co-operative agreement, various experiments are carried out by Nagra, the "Bundesanstalt für Geowissenschaften und Rohstoffe, Hannover" (BGR) and the "Forschungszentrum für Umwelt und Gesundheit, München" (GSF). The Grimsel projects of both GSF and BGR are supported by the German Federal Ministry for Research and Technology (BMFT). NTB 85-46 (German version NTB 85-47) provide an overview of the German-Swiss investigation programme. In a special issue of the Nagra Bulletin 1988 (German version "Nagra Informiert 1+2/1988") the status of the programme up to 1988 is described.

The **Radionuclide Migration Experiment (MI)** is the most significant contribution from Nagra to the Grimsel programme. MI is a multidisciplinary study aimed at investigating solute transport in fractured media. Extensive field work is complemented by a substantial programme of hydrodynamic, chemical and transport modeling, along with supporting laboratory studies. This project, initiated in 1985 and currently planned to be terminated in 1994, was initially conceived as a collaborative project between Nagra and the Paul Scherrer Institute (PSI). Since 1987, radiotracer field tests have also been carried out with the Institute of Hydrology of GSF Munich-Neuherberg. In 1989 a bilateral collaboration agreement was signed with the Japanese Power Reactor and Nuclear Fuel Development Corporation (PNC) and the support under this cooperation resulted in a substantial extension of the project.

This report, issued simultaneously as Nagra NTB and PSI Report #120, was produced in accordance with the cooperation agreements mentioned above. The authors have presented their own opinions and conclusions which do not necessarily coincide with those of Nagra or its participating partners.

VORWORT

Bei Konzepten, welche die Endlagerung radioaktiver Abfälle in geologischen Formationen vorsehen, ist die Kenntnis des Wirtgesteins und der angrenzenden Gesteinsschichten von grundlegender Bedeutung. Die Nagra betreibt deshalb seit Mai 1984 das **Felslabor Grimsel (FLG)** in 450 m Tiefe im Kristallin des Aarmassivs. Die generelle Zielsetzung für die Arbeiten in diesem System von Versuchsstollen umfasst

- den Aufbau von Know-how in der Planung, Ausführung und Interpretation von Untergrundversuchen in verschiedenen wissenschaftlichen und technischen Fachgebieten, und

- den Erwerb praktischer Erfahrung in der Entwicklung und der Anwendung von Untersuchungsmethoden, Messverfahren und Messgeräten, die für die Erkundung von potentiellen Endlagerstandorten in Frage kommen.

Im Felslabor der Nagra werden, auf der Basis eines deutsch-schweizerischen Zusammenarbeitsvertrages, verschiedene Versuche von den beiden deutschen Partnern Bundesanstalt für Geowissenschaften und Rohstoffe, Hannover (BGR) und Forschungszentrum für Umwelt und Gesundheit GmbH, München (GSF) durchgeführt. Das Deutsche Bundesministerium für Forschung und Technologie (BMFT) fördert die Arbeiten der BGR und der GSF im FLG. Der NTB 85-47 (englische Version NTB 85-46) enhält eine Uebersicht des FLG und die Zusammenfassung der Untersuchungsprogramme mit Status August 1985. In der Ausgabe 1+2/1988 des Heftes "Nagra informiert" bzw. der englischen Spezialausgabe "Nagra Bulletin 1988" ist der Stand der Arbeiten anfangs 1988 beschrieben.

Der **Migrationsversuch (MI)** ist ein sehr wesentlicher Beitrag zum Grimsel Programm. MI ist ein multidisziplinäres Experiment zur Untersuchung des Transportverhaltens von Radionukliden im Grundwasser eines geklüftetem Gesteins. Die ausgedehnten Feldversuche werden unterstützt durch ein umfangreiches Programm zur hydrodynamischen und chemischen Charakterisierung des MI-Bereichs und zur Modellierung der Transportprozesse sowie durch ergänzende Laboruntersuchungen. Das 1985 begonnene und, gemäss jetziger Planung, bis 1994 dauernde Projekt MI war ursprünglich als gemeinsames Vorhaben der Nagra und des Paul Scherrer Instituts (PSI) konzipiert worden. Seit 1987 führt das Institut für Hydrologie der GSF, München-Neuherberg die Radiotracer-Analysen bei den Feldversuchen durch. Im Jahre 1989 unterzeichnete dann Nagra mit der japanischen Power Reactor and Nuclear Fuel Corporation (PNC) einen Vertrag zur Beteiligung der PNC am Migrationsversuch, wodurch eine wesentliche Erweiterung des Untersuchungsprogrammes ermöglicht wurde.

Der vorliegende Bericht erscheint gleichzeitig als Nagra NTB und als PSI Bericht Nr. 120 und wurde im Rahmen der erwähnten Zusammenarbeitsverträge erstellt. Die Autoren haben ihre eigenen Ansichten und Schlussfolgerungen dargelegt. Diese müssen nicht unbedingt mit denjenigen der Nagra oder der beteiligten Partner übereinstimmen.

AVANT - PROPOS

Lors d'études de concepts de stockage de déchets radioactifs dans des formations géologiques, on attache une grande importance à l'acquisition d'informations étendues sur la roche d'accueil et les formations rocheuses environnantes. C'est pour cette raison que la Cédra exploite depuis mai 1984 son **laboratoire souterrain du Grimsel (LSG)** situé à 450 m de profondeur dans le cristallin du massif de l'Aar, situé au milieu des Alpes centrales. Les principaux objectifs des recherches effectuées dans ce réseau de galeries comprennent:

- l'acquisition de savoir-faire dans diverses disciplines techniques et scientifiques en ce qui concerne la conception, la réalisation et l'interprétation d'expériences in situ, ainsi que

- l'accumulation d'expériences pratiques dans la mise au point et l'application de méthodes d'investigation, de techniques et d'appareillages de mesure, qui pourraient être utilisés lors de l'exploration de sites potentiels de dépôts finals.

Le LSG est exploité par la Cédra et diverses expériences y sont réalisées par celle-ci et deux institutions allemandes: la "Bundesanstalt für Geowissenschaften und Rohstoffe, Hannover" (BGR) et le "Forschungszentrum für Umwelt und Gesundheit GmbH, München" (GSF) dans le cadre d'un traité de collaboration germano-suisse. Les projets poursuivis au Grimsel par la BGR et le GSF sont financés par le Ministère fédéral allemand de la recherche et de la technologie (BMFT). Les rapports NTB 85-46 (version anglaise) et NTB 85-47 (version allemande) présentent un aperçu du laboratoire souterrain et un résumé des programmes de recherches avec état au mois d'août 1985. L'état d'avancement de ce programme en 1988 est présenté dans la publication "Cédra informe 1+2/1988" (version française) et "Nagra informiert 1+2/1988" (version allemande), ainsi que dans une édition spéciale en anglais (Nagra Bulletin 1988).

L'expérience de migration de radionucléides (MI) représente la contribution essentielle de la Cédra au programme du Grimsel. MI est une étude multidisciplinaire ayant pour objectif l'étude du transport en solution en milieu fissuré. Les travaux de terrain intensifs sont complétés par un programme de modélisation hydrodynamique, chimique et de transport, ainsi que par des essais en laboratoire. Ce projet, qui a débuté en 1985 et devrait se terminer en 1994, fut initialement conçu comme une collaboration entre la Cédra et l'Institut Paul Scherrer (IPS). Depuis 1987 des essais de terrain avec des traceurs radioactifs ont été réalisés par l'institut d'hydrologie de la GSF de Munich-Neuherberg. En 1989 un accord bilatéral de collaboration a été signé avec la "Power Reactor and Nuclear Fuel Development Corporation" (PNC) du Japon qui a conduit à une extension substantielle du programme d'investigation.

Le présent rapport, publié simultanément en tant que rapport technique Cédra (NTB) et rapport IPS N° 120, a été élaboré dans le cadre des accords de collaboration mentionnés. Les auteurs ont présenté leurs vues et conclusions personnelles. Celles-ci ne doivent pas forcément correspondre à celles de la Cédra ou à celles de ses partenaires participants.

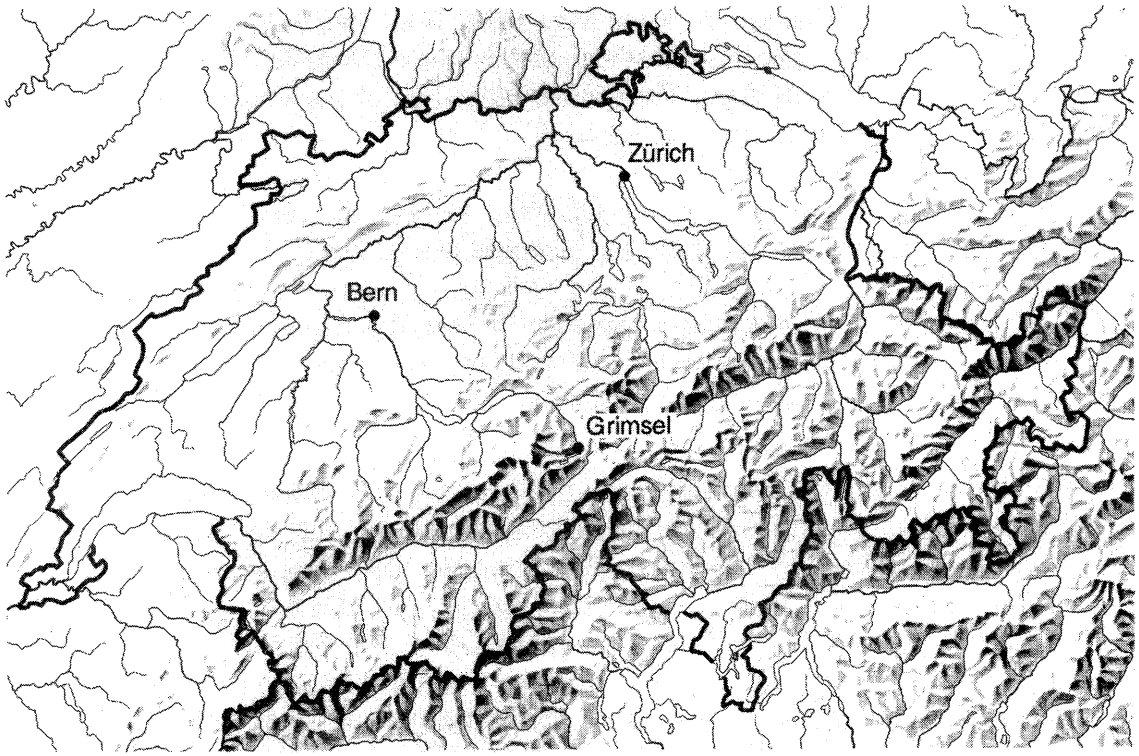

Location of Nagra's underground test facility at the Grimsel Pass in the Central Alps (Bernese Alps) of Switzerland (approximate scale 1 cm = 25 km).

Geographische Lage des Nagra Felslabors am Grimselpass (Berner Oberland) in den schweizerischen Zentralalpen (Massstab: 1 cm = ca. 25 km)

GRIMSEL-GEBIET

Blick nach Westen

1 Felslabor
2 Juchlistock
3 Räterichsbodensee
4 Grimselsee
5 Rhonetal

GRIMSEL AREA

View looking West

1 Test Site
2 Juchlistock
3 Lake Raeterichsboden
4 Lake Grimsel
5 Rhone Valley

FLG FELSLABOR GRIMSEL
GTS *GRIMSEL TEST SITE*

Situation

0 100 m

- Zugangsstollen/*Access tunnel*
- Fräsvortrieb/*by tunnel boring machine*
- Sprengvortrieb/*excavated by blasting*
- Zentraler Aaregranit ZAGR / *Central Aaregranite CAGR*
- Biotitreicher ZAGR / *CAGR with high content of biotite*
- Grimsel-Granodiorit / *Grimsel-Granodiorite*
- Scherzone/*Shear zone*
- Lamprophyr/*Lamprophyre*
- Wasserzutritt/*Water inflow*
- SB Sondierbohrung/*Exploratory borehole*
- US US Bohrung/*US borehole*
- ZB Zentraler Bereich/*Central facilities*
- AU Auflockerung/*Excavation effects*
- BK Bohrlochkranz/*Fracture system flow*
- EM El.magn. HF-Messungen/*-measurements*
- FRI Kluftzone/*Fracture zone investigation*
- GS Gebirgsspannungen/*Rock stresses*
- HPA Hydr. Parameter/*Hydr. parameters*
- MI Migration/*Migration*
- MOD Hydrodyn. Modellierung/*H. modeling*
- NM Neigungsmesser/*Tiltmeters*
- UR Untertageradar/*Underground radar*
- US Seismik/*Underground seismic testing*
- VE Ventilationstest/*Ventilation test*
- WT Wärmeversuch/*Heat test*

A — A Schnitt/*Section*

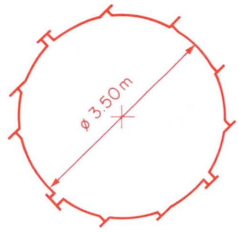

6/88

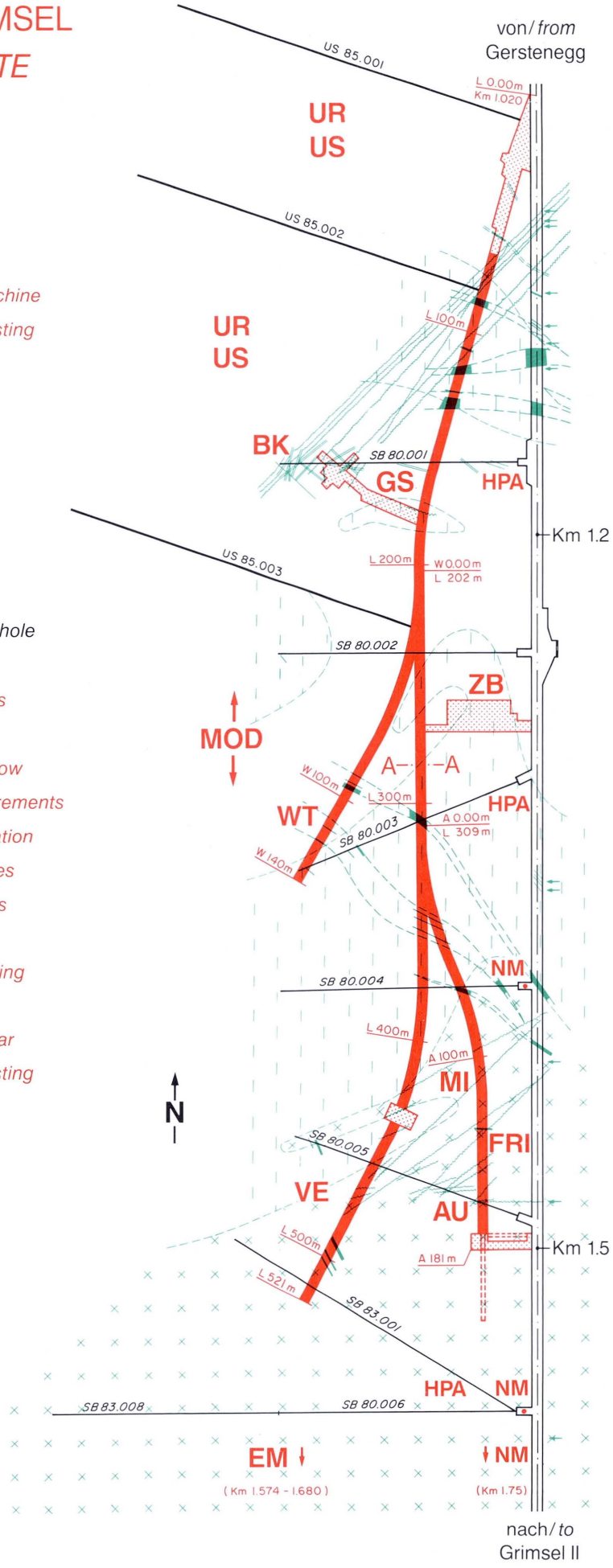

TABLE OF CONTENTS

ABSTRACT

This paper provides an overview of the investigations conducted from 1985 to 1990 as a part of the radionuclide migration experiment which is currently in progress in the Nagra underground research laboratory at the Grimsel pass in the Central Swiss Alps. The major aims of the project are (1) to test the extrapolation of laboratory sorption data to field conditions, (2) to analyse retardation processes in a fractured rock, (3) to improve and develop the necessary methodologies for site characterization and (4) to test existing geochemical, hydrodynamic, and solute transport models or their associated data bases. Field and modeling work are complemented by an extensive laboratory support programme.

The field experiments are carried out in a water conducting fracture within a tectonically active, granitic rock mass. On the scale of several meters this fracture can be described as a two-dimensional feature. The major water flow paths are the product of relatively recent tectonic deformation (alpine uplift). Brittle processes reactivated older, ductile shear zones and led to the formation of a few centimeter wide, asymmetrical array of conductive fractures in an otherwise relatively impermeable mylonitic fabric. These fractures are partially filled with highly porous, unconsolidated micaceous fault gouge. The migration fracture and the surrounding environs were extensively characterized in terms of mineralogy, hydrochemistry and hydrology prior to performing the migration test.

The water in the migration fracture is anoxic, has a high pH (~ 9.6) and a low ionic strength (0.0012 M) with the cation content dominated by Na^+ and Ca^{2+} while F^-, HCO_3^-, Cl^-, SO_4^{2-} and $SiO(OH)_3^-$ are the major anions. Further studies included the definition of ambient microbiological and colloidal populations as well as alteration and natural trace element transport processes in the fracture vicinity.

Hydrogeological exploration involved the drilling of 8 boreholes (6 to 24 m long). Subsequent hydraulic testing revealed local heterogeneities of the transmissivity from $5 \cdot 10^{-6}$ to about 10^{-8} m^2s^{-1} (single hole tests). On a scale of several meters, however, the fracture appears rather homogeneous with an average transmissivity of about $2 \cdot 10^{-6}$ m^2s^{-1} based on the results of cross-hole tests. Various hydrodynamic models satisfactorily predict stationary conditions (pressure distribution, flow) but have some difficulty in reproducing the observed transient response from long-term pumping tests.

At distances between 6 and 12 m from the tunnel wall, hydraulic pressures average around 1.5 bar. This hydraulic setting is well suited to maintain artificially stressed, closed flow fields (unequal strength dipoles with input/output flow ratios always less than 1/2) for tracer experiments. A series of pilot experiments utilizing conservative tracers (uranine, ^4He and $^{82}Br^-$ was performed in order to test the equipment and to identify appropriate borehole constellations and flow conditions (travel times) for the planned migration experiments. A variety of novel techniques, including quartz fiber fluorometry (optrodes) and the He tracer method were developed and successfully tested.

For the first series of reactive tracer migration experiments, isotopes of Na^+ and Sr^{2+} were chosen on the basis of laboratory studies, consisting of rock-water interaction, batch radionuclide sorption and dynamic sorption experiments. These studies indicated that at low concentrations the sorption of the Na^+ and Sr^{2+} tracersat low concentrations is dominated by reversible cation (isotope) exchange under equilibrium conditions and is proportional to the available cation exchange capacity CEC. Sorption coefficients (K_d) for Na and Sr under the chemical conditions prevailing in the migration fracture were expected to range from 0.3 - 0.4 ml g^{-1} and from 16 - 25 ml g^{-1}, respectively.

The first field tests performed, using a pulse injection of short-lived $^{24}Na^+$, showed a small retardation of the breakthrough peak. To prolong the interaction time of the tracer with fracture materials, a complex setup for continuous injection was constructed with tracer dosage and input/output flow being provided by highly precise (modified) HPLC pumps. In an attempt to minimize uncertainties from instrumental dispersion, equipment volumes were reduced as much as possible and down-hole tracer analyses implemented. A 7-day continuous injection of $^{22}Na^+$, together with uranine (and pulses of $^{82}Br^-$ and ^4He) was monitored over 2 months. Utilizing the same equipment, several pulse injection runs with $^{24}Na^+$, uranine, $^{82}Br^-$ and $^{123}I^-$, and input/output ratios of 1/3 and 1/15, were carried out. Pulse tests with moderately sorbing $^{85}Sr^{2+}$ were still underway at the end of the period considered in this report.

Laboratory rock-water interaction studies, a field-scale equilibration experiment and a preliminary interpretation of Na tracer breakthrough experiments by a dual-porosity modeling approach yield roughly consistent sorption values. With the transport model calibrated by the Na experiments, detailed predictions for the breakthrough of Sr are available. Ongoing field experiments with $^{85}Sr^{2+}$ will provide a critical test for the applicability of the radionuclide retardation model. After the tests with chemically simple and weakly sorbing tracers, it is planned to use chemically more complex nuclides of relevance to repository safety assessment studies (including isotopes of Cs, Se, Ni, Tc, and potentially Pd, Sn and Np). The final stage of the migration experiment is intended to be an excavation of part or all of the tracer flow path.

The Grimsel migration experiment demonstrates conclusively how the combined efforts of modeling, laboratory and field investigations can substantially widen the understanding of radionuclide transport in a geological environment.

ZUSAMMENFASSUNG

Im Felslabor der Nagra am Grimselpass in den Schweizer Zentralalpen findet gegenwärtig ein Radionuklid-Migrationsexperiment statt. Dieses Dokument soll einen Überblick geben über die Arbeiten, die im Rahmen dieses Projektes von 1985-1990 durchgeführt wurden. Die wichtigsten Ziele sind (1) die Übertragbarkeit von Laborsorptionsdaten auf Feldbedingungen zu prüfen, (2) realistische Hinweise auf die Retardierung beim Wassertransport in einem geklüfteten Gestein zu erhalten, (3) wichtige Methoden zur Standortcharakterisierung zu entwickeln oder zu verbessern, und (4) dabei bereits vorhandene geochemische, hydrodynamische und Transport-Modelle, sowie die dazu verwendeten Datenbasen zu testen. Feld- und Modellierungsarbeiten werden dabei durch ein umfassendes Laborprogramm ergänzt.

Die Feldexperimente werden in einer wasserführenden Kluft in einem tektonisch aktiven, granitischen Gestein durchgeführt. Auf einer Skala von mehreren Metern erscheint diese Kluft als 2-dimensionale, planare Struktur. Die typischen Fliesspfade sind das Resultat jüngster tektonischer Verformung im Zusammenhang mit der alpinen Hebung; spröde Prozesse reaktivierten dabei ältere, duktile Scherzonen, was zu einem wenigen cm breiten Netz von feinen, wasserführenden Öffnungen in den schmalen, relativ undurchlässigen Myloniten führte. Diese Öffnungen sind mindestens teilweise mit einer sehr porösen, feinkörnigen, praktisch unzementierten und glimmerreichen Kluftbreccie ("Kluftletten") gefüllt. Bevor die eigentlichen Markierversuche begannen, wurde die Migrationskluft, wie auch deren unmittelbare Umgebung, mineralogisch, hydrochemisch und hydraulisch gründlich charakterisiert.

Das Wasser in der Migrationskluft zeichnet sich durch eine geringe Ionenstärke (0.0012 M) aus, ist sehr sauerstoffarm (<0.1 ppb; anoxisch) und hat einen hohen pH von etwa 9.6. Gelöste Kationen werden durch Na^+ und Ca^{2+} dominiert, während F^-, HCO_3^-, Cl^-, SO_4^{2-} und $SiO(OH)_3^-$ die wichtigsten Anionen darstellen. Die mikrobiologische Populationen und der Kolloidgehalt dieses Wassers wurden beschrieben. Zusätzlich wurde die Mineralumwandlung, sowie auch der natürliche Transport verschiedener Spurenelemente in der unmittelbaren Nähe des Wasserfliesspfades untersucht.

Die hydrogeologische Erkundung der Migrationskluft erforderte das Abteufen von 8 gekernten Bohrungen von 6 bis 24 m Länge. Die unmittelbar darauf durchgeführten hydraulischen Einbohrlochtests ergaben lokal verschiedene Transmissivitäten im Bereich von $5 \cdot 10^{-6}$ bis weniger als 10^{-9} $m^2 s^{-1}$. Interferenzversuche ("cross hole tests") zeigten hingegen auf der Skala von wenigen Metern (2 - 15 m) eine homogene, repräsentative Durchlässigkeit von $2 \cdot 10^{-6}$ $m^2 s^{-1}$. Verschiedene hydrodynamische Modelle wurden angewendet; die beobachtete Verteilung der Drücke und Flüsse bei stationären Bedingungen konnte dabei durchwegs befriedigend nachvollzogen werden. Hingegen hatten sämtliche Modelle Schwierigkeiten, die transienten Reaktionen des Systems während langdauernder Pumpversuche zu reproduzieren.

Auf einer Distanz von 6 bis 12 m von der Stollenwand verlief der Druckanstieg im konvergenten Fliessfeld zum Laborstollen sehr flach. Hydraulische Drücke lagen um 1.5 bar und eröffneten günstige Bedingungen für künstlich gespannte, geschlossene Fliessfelder für Tracerversuche. Dipolfelder mit ungleichen Injektions- und Extraktionsfliessraten, mit Verhältnissen stets kleiner als 1:2, wurden eingerichtet. Eine erste Serie von Versuchen mit Pulsinjektion von nicht-sorbierenden Markierstoffen (Uranin, $^{82}Br^-$, und ^4He) wurde durchgeführt, um die Ausrüstung zu prüfen, geeignete Bohrlochkonstellationen oder Fliessbedingungen zu finden und den experimentell möglichen Bereich von Durchbruchszeiten abzutasten. Verschiedene neuartige Techniken wurde entwickelt und erfolgreich eingesetzt, unter anderem die Quarzfaser-Fluorometrie (Optroden) und die Helium-Tracermethode.

Für erste Versuche mit sorbierenden Stoffen wurden bei Laborarbeiten (Fels/Wasser Interaktion ohne Tracer, Batchversuche mit Radionukliden und dynamische Infiltrationstests) Isotopen von Na^+ und Sr^{2+} ausgewählt. Bei niedrigen Konzentrationen stehen diese Kationen mit dem Kluftmaterial unter reversiblem Kationenaustausch, wobei die sorbierte Menge jeweils proportional zur verfügbaren Kationen-Austauschkapazität (CEC) ist. Für die chemischen Bedingungen im Grimselwasser wurden die Verteilungskoeffizienten (K_d) bestimmt; der erwartete Bereich war etwa 0.3 - 0.4 ml g^{-1} für Na und 16 - 25 ml g^{-1} für Sr.

Die ersten Pulsversuche im Felde mit kurzlebigem $^{24}Na^+$ zeigten lediglich eine relativ geringe Verzögerung des Na-Durchbruchpeaks gegenüber dem konservative Tracer. Um die Kontaktzeit mit dem Kluftmaterial wesentlich verlängern zu können, wurde eine komplexe Einrichtung aufgebaut, die eine langfristig stabile, kontinuierliche Dosierung erlaubt. Die hohen Anforderungen an eine solche Tracerdosierung, wie auch an die Kontrolle des Injektions- und des Extraktionsstroms, wurden durch den Einsatz hochpräziser, modifizierter HPLC-Pumpen erfüllt. Um Unsicherheiten durch gerätebedingte Dispersion eliminieren zu können, wurde das Volumen der Ausrüstung soweit als möglich reduziert und die in-situ Traceranalyse in den Kluftintervallen verschiedener Bohrungen implementiert. Eine Experiment, das mit einer 7 Tage dauernden, kontinuierlichen Dosierung von Uranin und $^{22}Na^+$ begann und mit sporadischen Pulsen von $^{82}Br^-$ und ^4He begleitet wurde, erforderte Messungen über 2 Monate. Mit ähnlicher Ausrüstung wurden weitere Pulsversuche mit $^{24}Na^+$, $^{82}Br^-$ und $^{123}I^-$ über dieselbe Distanz von etwa 5 m durchgeführt, wobei jeweils die Verhältnisse der Injektions-/Extraktionsraten 1 : 3 und 1 : 15 waren. Ein Pulsversuch mit schwach bis mässig sorbierendem $^{85}Sr^{2+}$ zeigte eine grosse Retardierung und war bei Redaktionschluss dieses Berichtes noch nicht abgeschlossen.

Die verschiedenen Laborexperimente (Gestein/Wasser Wechselwirkung, Druckinfiltration) und die Resultate verschiedener Feldversuche (Equilibriertest, Modellierung der Durchbruchskurven mit doppelt-porösem Konzept) ergaben erstaunlich kohärente Sorptionswerte. Das Transportmodell konnte mit den Durchbruchskurven konservativer Tracer und Na geeicht werden und ermöglicht detaillierte Voraussagen über den Durchbruch von Sr. Die Resultate der noch andauernden Versuche mit $^{85}Sr^{2+}$ sind ein kritischer Test für die Verwendbarkeit des gewählten Konzepts und die Gültigkeit gewisser Parameter. Nach Abschluss der Experimente mit den chemisch einfachen, schwach sorbierenden Kationen, sind weitere Versuche mit chemisch komplexeren und für Endlager sicherheitsrelevanten Nukliden (Cs, Se, Ni, Tc; eventuell auch Pd, Sn and Np) geplant. Als letzte Phase des Migrationsexperimentes besteht die Absicht, den Fliesspfad, oder mindestens einen Teil desselben, auszugraben und zu untersuchen.

Das Migrationsexperiment zeigt deutlich, wie das koordinierte Zusammenwirken von Modellierung, Laborprogramm und Feldversuchen eindrückliche Resultate zum Verständnis des Radionuklidtransports in einem geologischen Umfeld erbringen kann.

RÉSUMÉ

Cet article présente un survol des recherches effectuées par la Cédra de 1985 à 1990 dans le cadre du programme d'étude de la migration des radionucléides au laboratoire souterrain du Grimsel, dans les Alpes suisses. Ce projet vise principalement (1) à tester l'extrapolation de données de laboratoire aux conditions de terrain, (2) à prouver par les faits les processus de retardation en milieu fissuré, (3) à améliorer ou développer les méthodologies nécessaires à la caractérisation d'un site, (4) ainsi qu' à tester les modèles géochimiques, hydrodynamiques et de transport existants, ou les bases de données qui y sont liées. Les travaux de terrain et de modélisation sont complétés par un programme de laboratoire étendu.

Les investigations de terrain sont effectuées sur une faille aquifère dans un massif de granite tectoniquement actif. A l'échelle de quelques mètres, cette faille peut être considérée comme un élément bidimensionnel. Les conduits d'écoulement principaux résultent d'une déformation tectonique assez récente (soulèvement alpin). Une déformation cassante a réactivé d'anciens cisaillements ductiles et formé un réseau asymétrique de fractures perméables dans une matrice mylonitique por le reste relativement imperméable. Ces fractures sont partiellement colmatées par une fine brèche de faille micacée, non consolidée et très poreuse. Avant les essais de migration, la faille sélectionnée et son voisinage ont été caractérisés de manière détaillée sur les plans minéralogique, hydrochimique et hydrologique.

L'eau contenue dans la faille est pauvre en oxygène ("anoxic"), de pH élevé (~9.6) et de faible force ionique (0.0012 M); les cations principaux sont Na^+ et Ca^{2+}, et les anions dominants F^-, HCO_3^-, Cl^-, SO_4^{2-} et $SiO(OH)_3^-$. On a également étudié les populations microbiologique et colloïdale ambiantes, ainsi que l'altération et le transport d'éléments trace naturels au voisinage de la faille.

Huit forages, de 6 à 24 m de long, ont été effectués pour les investigations hydrogéologiques. Les tests hydrauliques (en puits simple) ultérieurs ont révélé une transmissivité hétérogène à l'échelle locale, entre $5 \cdot 10^{-6}$ et 10^{-8} m^2s^{-1}. Toutefois, à l'échelle de quelques mètres (essais entre puits), la faille peut se caractériser par une transmissivité assez homogène d'environ $2 \cdot 10^{-6}$ m^2s^{-1}. Les divers modèles hydrodynamiques utilisés ont reproduit de manière satisfaisante le régime d'écoulement stationnaire (champ des pressions, flux), mais beaucoup moins bien les valeurs transitoires observées lors d'essais de pompage de longue durée.

A des distances de 6 à 12 m de la paroi du tunnel, les pressions hydrauliques sont d'environ 1.5 bar en moyenne. Cette situation permet de garantir lors des essais de traçage un circuit d'écoulement fermé sur lui-même, stimulé artificiellement (dipôle à débit d'injection toujours inférieur à la moitié du débit de soutirage). A fin de tester l'équipement et d'identifier la constellation de forages appropriée et les durées d'écoulement pour les essais de migration envisagés, on a effectué une série d'essais pilote avec des traceurs conservatifs (uranine, ^4He et $^{82}Br^-$).

Un certain nombre de techniques nouvelles ont été développées et testées avec succès, parmi lesquelles la fluorométrie à fibre de quartz (optrodes) et le traçage à l'hélium.Pour les premiers essais de migration d'un traceur réactif, on a utilisé des isotopes du sodium et du strontium, à la suite d'essais en laboratoire sur l'interaction eau-roche, l'adsorption en chaîne de radionucléides et l'adsorption dynamique. Ces essais ont montré qu'en situation d'équilibre l'adsorption des traceurs Na^+ et Sr^{2+} est dominée par un échange réversible des cations (isotopes), et qu'elle est proportionnelle à la capacité d'échanche cationique CEC disponible. Aux conditions chimiques régnant dans la faille étudiée, on s'attendait à des valeurs du coefficient d'adsorption (K_d) de 0.3 - 0.4 $ml \cdot g^{-1}$ pour Na et 16 - 25 $ml \cdot g^{-1}$ pour Sr.

Les premiers essais in situ, mettant en oeuvre une injection instantanée de $^{24}Na^+$ à courte demi-vie , ont montré que la retardation du pic d'apparition de Na était faible. Afin de prolonger le temps d'interaction entre le traceur et les matériaux de la faille, on a mis au point un dispositif complexe d'injection en continu, avec dosage du traceur et contrôle très précis des débits d'injection et de soutirage par des pompes HPLC modifiées. A fin de réduire les incertitudes liées à la dispersion instrumentale, les volume des équipements furent réduits le plus possible et des analyses de traceurs effectuées en forage même. On a réalisé un essai comprenant 7 jours d'injection continue de $^{22}Na^+$ et d'uranine (avec des injections instantannées de $^{82}Br^-$ et He^4) et une période d'observation de deux mois. Avec le même équipement, on a effectué plusieurs essais d'injection instantanée de $^{24}Na^+$, d'uranine, de $^{82}Br^-$ et de $^{123}I^-$, avec un rapport des débits d'injection et de soutirage de 1/3 et 1/15. Des essais d'injection instantanée de $^{85}Sr^{2+}$ modérément adsorbant étaient toujours en cours pour ce qui concerne la période considérée dans le présent rapport.

Des études d'interaction eau-roche en laboratoire, une expérience de mise à l'équilibre à l'échelle du terrain, ainsi que l'interprétation préliminaire du temps de parcours du traceur Na à l'aide d'un modèle à double porosité ont fourni des valeurs d'adsorption grossièrement compatibles entre elles. Le modèle de transport étant calibré grâce au traceur Na, on dispose maintenant de prédictions détaillées concernant le parcours du Sr. Les essais de terrain en cours utilisant le $^{85}Sr^{2+}$ permettront de tester de manière critique l'applicabilité du modèle de retardation des radionucléides. Après avoir utilisé des traceurs chimiquement simples et faiblement adsorbants, on prévoit maintenant d'utiliser des nucléides au comportement chimique plus complexe, représentatifs pour les analyses de sûreté de dépôts radioactifs (notamment des isotopes de Cs, Se, Ni, Tc, et éventuellement de Pd, Sn et Np). Le stade final de l'expérience de migration consistera à excaver une partie ou l'ensemble des chenaux d'écoulement empruntés par les divers traceurs.

L'expérience de migration montre de manière concluante comment les efforts combinés d'essais en laboratoire, d'essais sur le terrain et de modélisation permettent d'élargir considérablement la compréhension du transport des radionucléides en milieu rocheux.

1 INTRODUCTION

1.1 Background

It is widely recognized that field studies are an essential component of a waste management programme, not only for the characterization of potential sites but also to study processes which are inaccessible in a normal laboratory. The Grimsel Test Site (GTS) was constructed with the latter thought in mind. Even in the early planning stages, a comprehensive radionuclide migration study was foreseen.

The basic aim of the migration experiment, as defined in the initial planning proposals in 1981, was to test the conceptual and calculational models of radionuclide transport used in performance assessment. The basic aim was considerably expanded upon in a detailed project proposal prepared by McKINLEY & GROGAN (1984). The latter proposed an **integrated** migration project with much wider aims, including:

1. Study of the hydrology and geochemistry of a fractured rock
2. Testing models of radionuclide transport
3. Development of the methodology for site characterization
4. Focussing laboratory, field and modeling studies to the detailed characterization of a single site

Aim (1) is fundamentally, a characterization of what, in the Nagra performance assessment jargon, is called a "flow-system". The flow-system description is used for solute transport modeling and thus must, on a microscopic scale, consider the environment a migrating nuclide "sees" during its travels. This characterization requires a very detailed analysis of flow hydrology, water chemistry, mineralogy and structural geology. The pore space available to solute in flowing water is identified, for example, by injection of fluorescent resins or natural analogue studies. Potentially perturbing factors like colloids, natural organics and microbes, also need to be considered.

Aim (2) involves the comparison of predicted radionuclide transport with field observations. The predictive model has three potential weaknesses - the conceptual model of transport, the algorithm for evaluating this transport and the database used. The algorithm may be tested as part of conventional verification studies. The database is composed, among other things, of descriptions of radionuclide sorption/retardation which must be measured under appropriate conditions in laboratory batch and column studies as well as in-situ. The conceptual model is based on interpretation of hydrologic and geochemical information and is, in principle, directly testable only by post-mortem analysis of a tracer test (identifying exactly where nuclides have moved and where they have been immobilized). The field observations require tracer tests with a range of sorbing and non-sorbing solutes in a well characterized hydraulic system.

Aim (3) involves the establishment of the technical capacity to carry out the field work required for (1) and (2) above. The work involved in combining the hydrological and geochemical aspects mentioned above in a single study was unique and required the design, construction and testing of a range of new equipment. This investment is justified by the requirement to carry out similar work during characterization of a candidate repository site.

Aim (4) involved overcoming the general problems of communciation between specialists and integration of the effort in a complete hydrogeochemical characterization. The cross-fertilization of ideas resulting from such communication is a valuable output but, more fundamentally, such multi-disciplinary teams are a key component of the final assessment of a repository site. This has also involved including a suite of safety relevant radionuclides in the planned final tracer test, to develop the ability to characterize the behaviour of these key elements in a real rock/water system.

The project thus envisaged was much more extensive (and expensive!) than the simpler tracer tests which had been carried out elsewhere previously (e.g., Studsvik: LANDSTRÖM et al., 1982; Finnsjön: MORENO et al., 1983; Stripa 1: ABELIN 1986; ABELIN et al., 1985; Stripa 2: ABELIN et al., 1987; Chalk River: NOVAKOWSKI et al., 1985; Béthune, France: GARNIER et al., 1985; Fannay-Augère, France: CACAS et al. 1990a,b). The technical components for the Grimsel radionuclide migration experiment included:

1. Geology, geochemistry, hydrogeology
2. Trace element chemistry, radiochemistry, sorption
3. Modelling - hydraulic, transport, geochemical
4. Colloids, microbiology, natural analogues
5. Engineering, equipment design
6. Performance assessment (integration of sub-projects)

These disciplines represent a significant cross-section of any waste management programme.

Finally, it should be noted that such an extensive study was only justified by some of the particular advantages of the Grimsel Test Site as a location for this project:

- Well characterized, relevant geology
- Very good technical infrastructure
- Clearance for work with radionuclides
- High public relations profile

1.2 Historical development

From the earliest stages of planning, it was recognized that there was no precedent for such an integrated study and hence a considerable degree of flexibility was built into the programme. In principle the project developed in a series of phases, the exact composition of each being dependant on the results of that preceding. The field programme consists of the following sequence:

i site selection; geological and hydrochemical characterization

ii drilling the first boreholes; passive hydraulic tests (minimizing geochemical perturbations)

iii completion of the borehole array, performing extended hydrotesting

iv non-sorbing tracer tests

v simple, weakly sorbing tracer tests

vi simple, medium sorbing tracer tests (in progress)

vii complex, strongly sorbing, tracer tests (safety relevant, non-linearly sorbing, or redox-sensitive species; in planning)

viii "post mortem" analysis (in planning)

Figure 1-1 summarizes the significant field activities conducted since 1986 related to the hydrogeologic characterization of the groundwater flow and radionuclide transport properties of the MI fracture. The principal activities are devided into (1) borehole drilling and instrumentation, (2) hydrogeologic characterization using single- and cross-borehole hydraulic tests, (3) hydrogeologic characterization using conservative (i.e. non-sorbing) tracers, and (4) hydrogeologic characterization using non-conservative reactive tracers.

This fieldwork is supported by an extensive programme of laboratory studies and modeling. It has been a principle in this project to precede all field tests by a prediction of the expected behaviour and to follow each test by a comparison of the observations with the predictions. This post-test analysis may lead to alteration of the laboratory programme, alteration of the model or changing the field test methodology, as required.

Because of the lack of precedent, and the inherently flexible planning, the development of the project has taken considerable time and manpower. Since the initiation of field work in 1985, the effort expended has been about the equivalent of 35 man-years. This corresponds to about 60 % of the total expenditure expected by completion of the project in 1994.

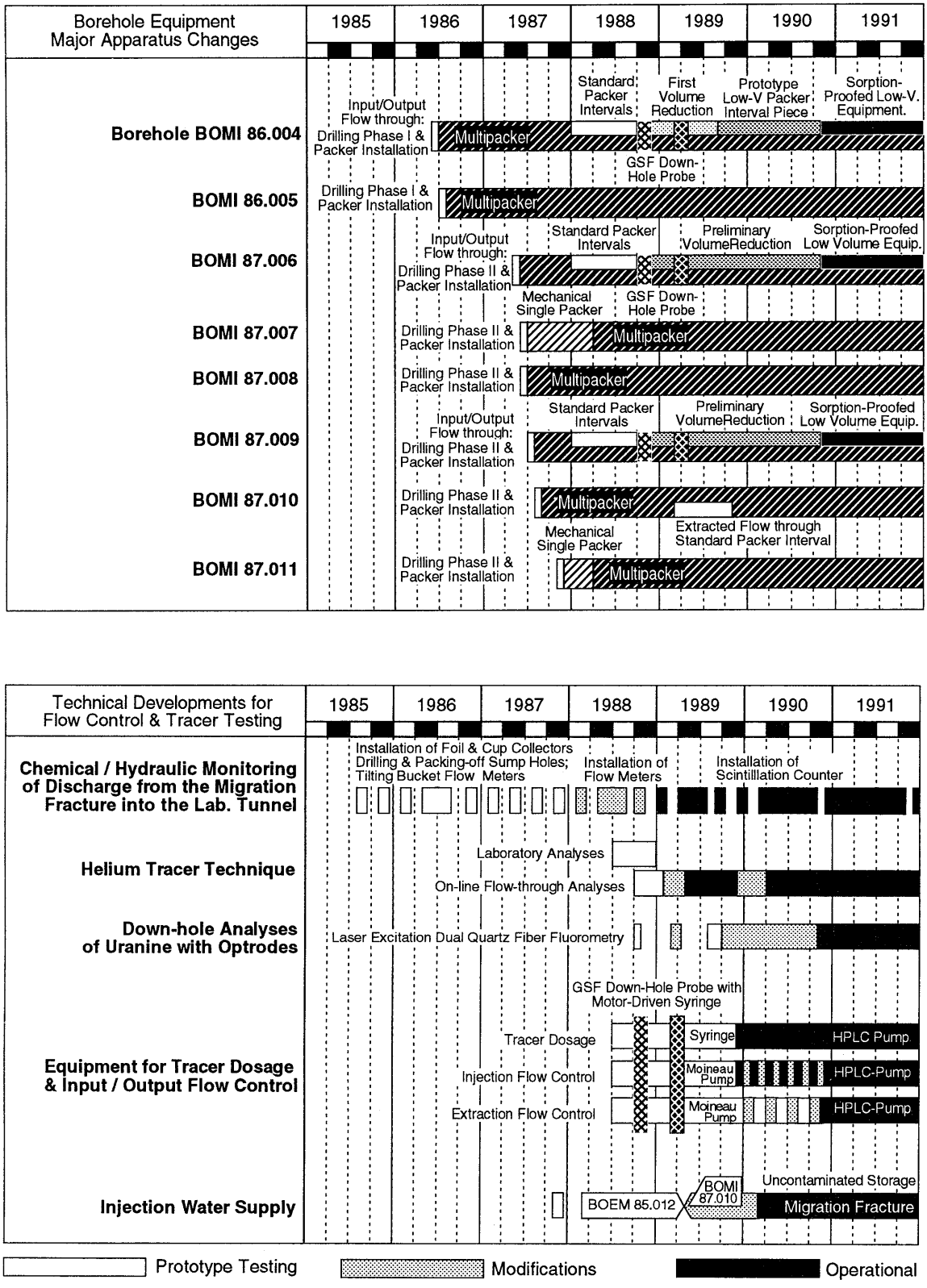

Fig. 1-1: Time sequence of major field activities 1985-1991

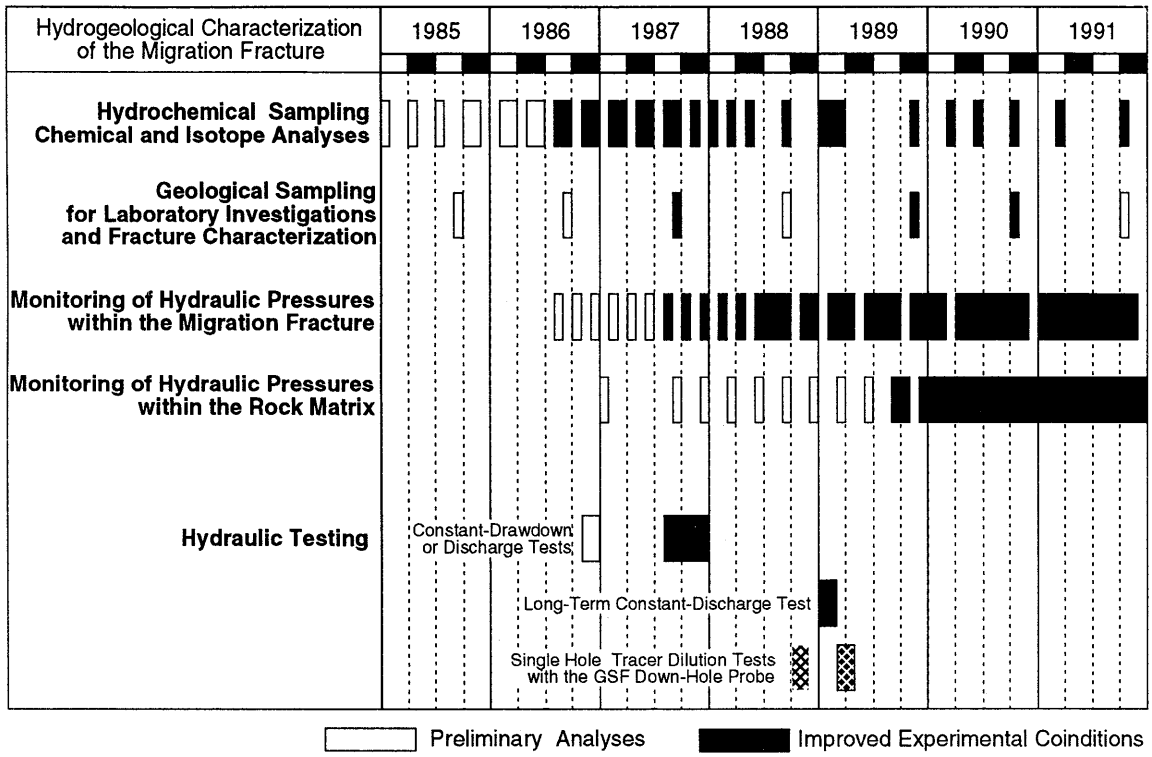

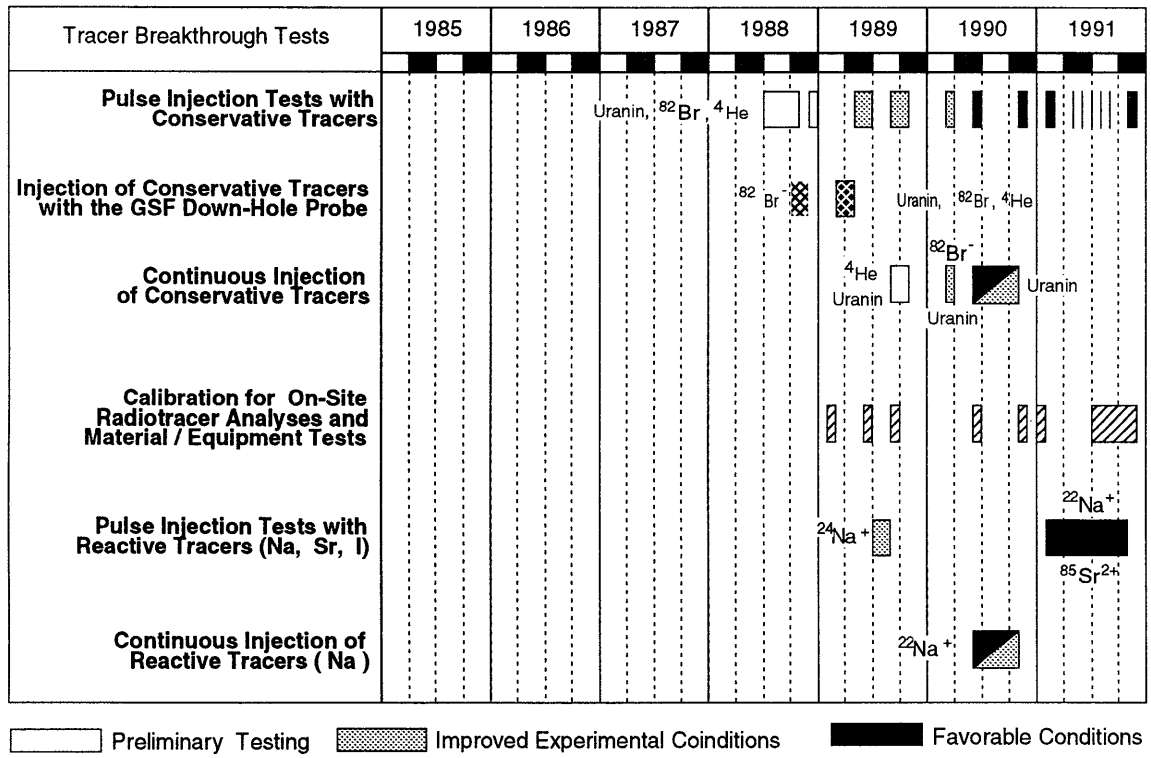

Fig. 1-1: (continued) Time sequence of major field activities 1985-1991

1.3 Layout of the report

To date this project has produced about a dozen papers or openly distributed reports which are referenced in appropriate sections of this document, a large number of internal documents and megabytes of data from field, laboratory and modeling programmes. This report can only provide an overview of the Migration Project. For more detail the interested reader is referred to supporting technical reports referenced throughout.

As emphasized in the previous sections, the project has very specific aims but developed in a rather organic manner. For ease of presentation, therefore, this report describes the project in terms of work areas rather than the specific aims listed previously or chronological order of development. An initial description of the overall setting of the Grimsel underground research facility GTS is given in Chapter 2. This is followed by a discussion of the field characterization of the geology, geochemistry, and hydrogeology of the migration test zone in Chapter 3, a description of the hydrogeologic test programme and major findings in Chapter 4, and the laboratory support programme in Chapter 5. Chapter 6 describes the non-reactive tracer testing while Chapter 7 lists the reactive tracer tests and gives a couple of examples of how the processes of pre-test prediction, testing and post-test analysis are carried out.

Progress so far to achieve the aims specified is summarized in Chapter 8, which is followed by an outline of the future programme.

2 OVERVIEW OF THE GRIMSEL TEST SITE (GTS)

The migration experiment is carried out at the Grimsel Test Site (GTS), Nagra's underground research facility situated at 1'730 m above sea level in the Central Aare Massif of the Swiss Alps (see Preface Section). The GTS is located in a region which is not under consideration for nuclear waste disposal. The test site was selected due to the general relevance of the geology as well as the excellent logistical support (including ready access and the infrastructure provided by a nearby underground hydroelectric power station).

The GTS lies at 8°19'E / 46°35'N under about 450 m of crystalline rock overburden. The site was selected after a series of 100 m long, subhorizontal exploration boreholes had been drilled from various adits to the access tunnel for an underground power station. The access to the power station was excavated 1974 and the initial exploratory borings were drilled in 1980. The Grimsel Test Site facility was built in 1983 by full-face drilling of a tunnel system of about 800 m long with a diameter of 3.5 m (Fig. 2-1).

An overview on the initial investigations performed by NAGRA and its German partners is summarized in NTB 85-46. A more recent summary of activities is documented in a special issue of NAGRA BULLETIN (1+2/1988). The environs of the facility have been well characterized by a variety of geological, geophysical, rock mechanical, hydrological and hydrogeochemical techniques. A list of the major references detailing the relevant characterisation efforts is presented in Table 2-1.

2.1 Regional Geological Setting

The rocks in the center of the Aare Crystalline basement (frequently termed the Aare Massif) consist mainly of pre-Hercynian gneisses and Hercynian granites. Aplitic and more mafic (lamprophyric) dykes intersect the rock mass as early stage, magmatic differentiation products. During alpine orogenesis, the rocks were buried to depths of at least 8 km and then subsequently uplifted, a process which is still continuing in the region. While the rocks were at these depths, they underwent the peak of greenschist facies metamorphism. At this stage, tectonic deformation resulted in ductile structures such as shearzones and mylonites. During uplift and after subsequent cooling, the deformation characteristics of the metamorphic event were further complicated by brittle re-activation of these structures. A schematic relationship of these geological processes and their related structures is provided in Fig. 2-2.

The Grimsel area is subject to various largescale tectonic movements. This is indicated by recent earthquakes, analyses of high-precision levelling by the Federal Office of Topography, and rock stress measurements (e.g., PAHL et al., NTB 88-39). It appears that brittle deformation occurs continually within the rocks adjacent to old ductile shear-zones and lamprophyre dykes, as well as in the shear zones oriented along the direction of regional alpine foliation. The regional orientation of the major shear zones at GTS has a dip of 70-90° and a principal strike from NE-SW (see Fig. 2-3).

Table 2-1: Major references for the various investigations at the Grimsel Test Site

Geology:	NTB 81-07; STALDER (1981); NTB 85-46 GEOTEST (1988); NTB 87-14; MÜLLER (1988) MAJER et al.(1990c); MARTEL & PETERSON (1990)
Structural Geology and Tectonics:	LABHART (1966); STECK (1968) CHOUKRONE & GAPAIS (1983); MARQUER et al. (1985) BOSSART & MARTEL (1990); BOSSART & MAZUREK (1990) MAJER et al.(1990c); MARTEL & PETERSON (1990) NTB 91-12; MARTEL & PETERSON (1991)
Geophysics:	NTB 87-13; NTB 88-06; BLüMLING & SATTEL (1988) NTB 88-31; NTB 89-37; NTB 89-11; NOELL & ZÜRN (1991) MAJER et al. (1990a,b); MARTEL & PETERSON (1990)
Rock Mechanics, Neotectonics:	EGGER (1986); PAHL et al.(1986) NTB 88-37; NTB 88-39; NTB 88-40; NTB 89-11 MAJER et al.(1990c); NOELL & ZÜRN (1991)
Hydrology:	NTB 81-07; NTB 87-13; GEOTEST (1988) NTB 88-31; BREWITZ et al.(1988); FRICK et al.(1988) LIEDKE & ZUIDEMA (1988); NTB 89-01; NTB 89-15 NTB 89-16; MAJER et al.(1990c); KELLEY & FRIEG (1990) NTB 91-01; WATANABE (1991); NTB 91-02; NTB 91-12
Hydrodynamic Modeling:	HUFSCHMIED & ADANK (1988); KUHLMANN (1989) NTB 89-16; WYSS (1990); FINSTERLE et al. (1990) STIESS (1990); LONG et al., (1990); DAVEY et al., (1990); NTB 91-03; NTB 91-31
Hydrochemistry:	OHSE (1983); FRICK et al. (1988); GEOTEST (1988) DEGUELDRE et al.(1989); NTB 88-23; NTB 89-15; NTB 90-01 EIKENBERG (1989); NTB 90-15; NTB 90-39; NTB 91-06
Isotope and Analogue Studies:	NTB 84-46; NTB 87-08; NTB 90-15; ALEXANDER et al. (1990)
Migration Experiment:	HOEHN et al. (1988); FRICK et al.(1988); McKINLEY et al. (1988) NTB 88-23; NTB 89-15; NTB 89-16; NTB 90-39; NAGRA (1990) FRICK et al. (1991); NTB 91-06; NTB 91-12; NTB 91-31, EIKENBERG et al. (1992)

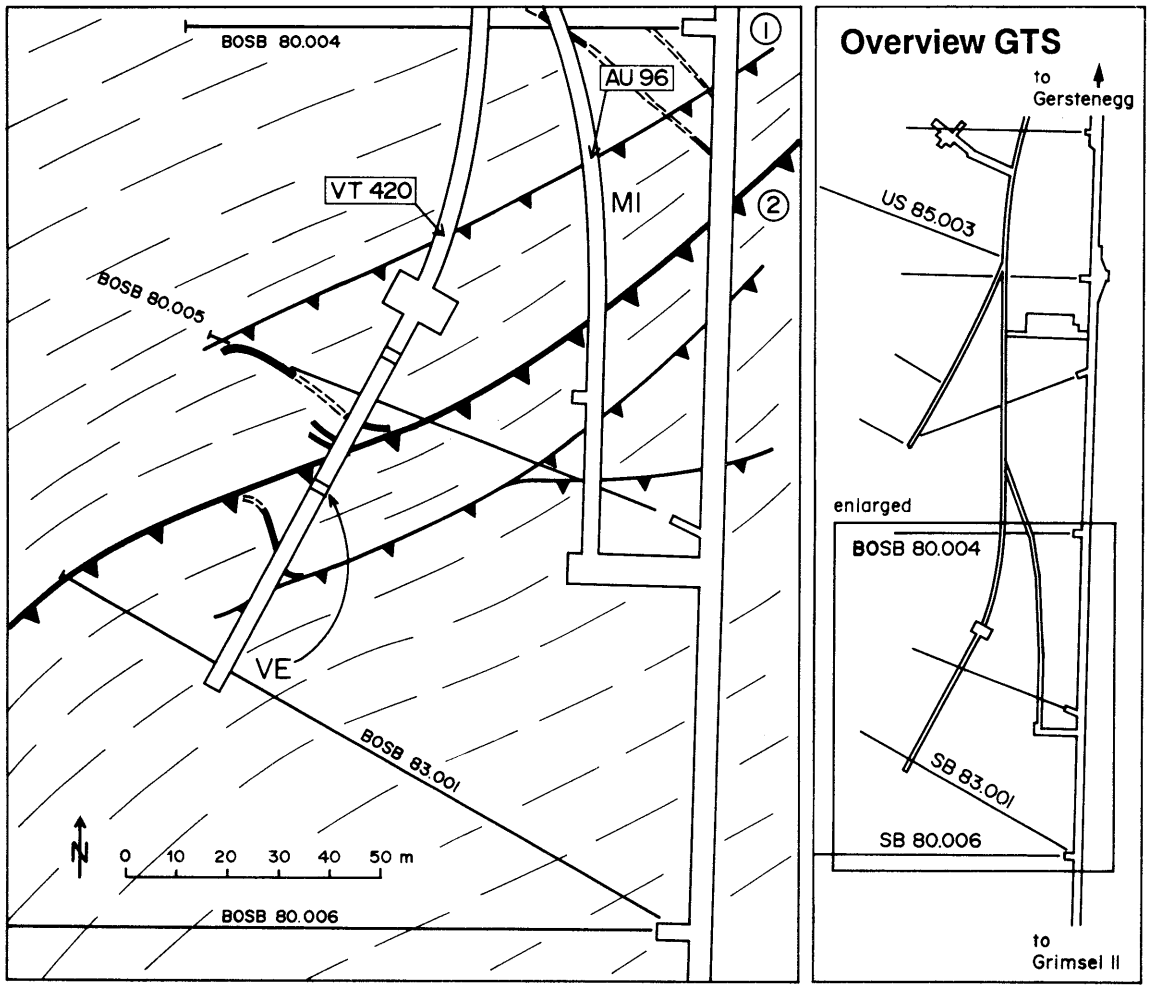

Shear-Zone (Thrust)

Lamprophyre Dyke

Trace of Cleavage

① "Migration" Shear-Zone (MI)

② "Ventilation" Shear-Zone (VE)

VE Site of the Ventilation Experiment

MI Site of the Migration Experiment

BO Projection of Borehole

Fig. 2-1: Situation of the Grimsel Test Site (GTS) and location of the migration experiment (MI)

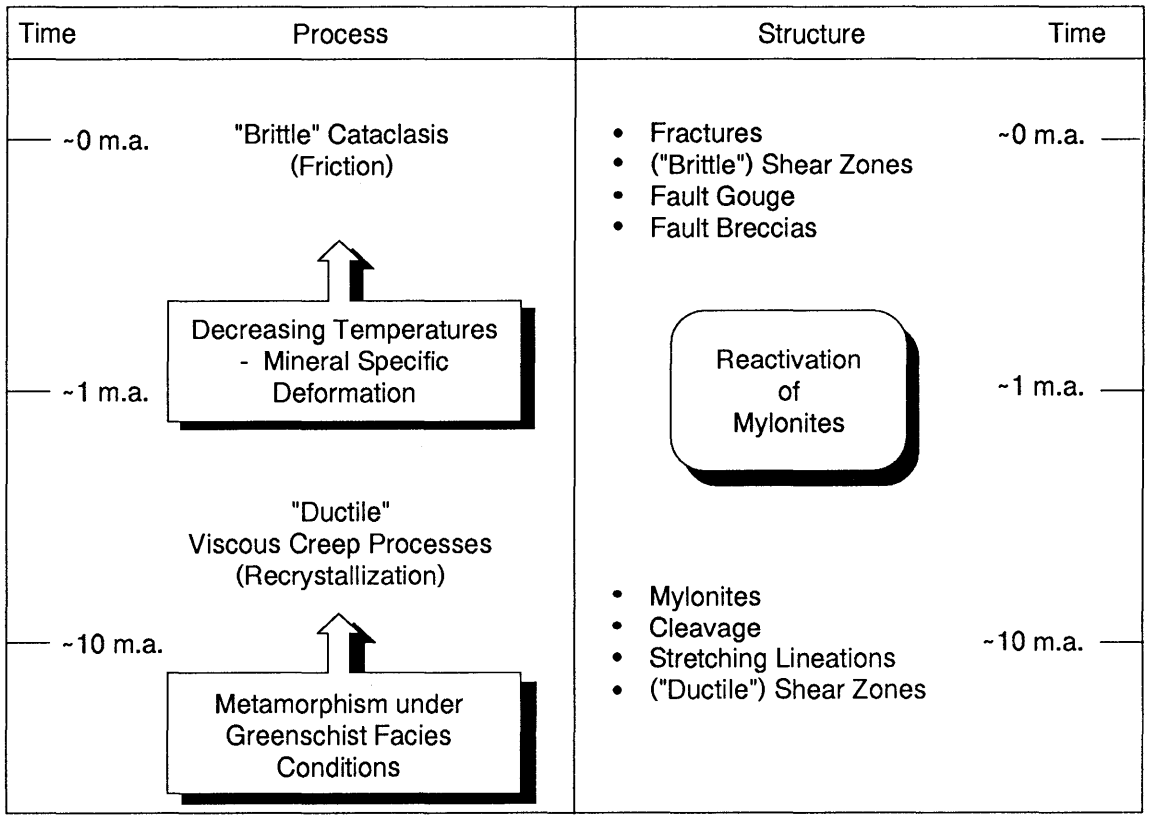

Fig. 2-2: Schematic relationship of alpine history, geological processes and their associated structures during ductile and brittle shear displacement within the Grimsel crystalline rock mass

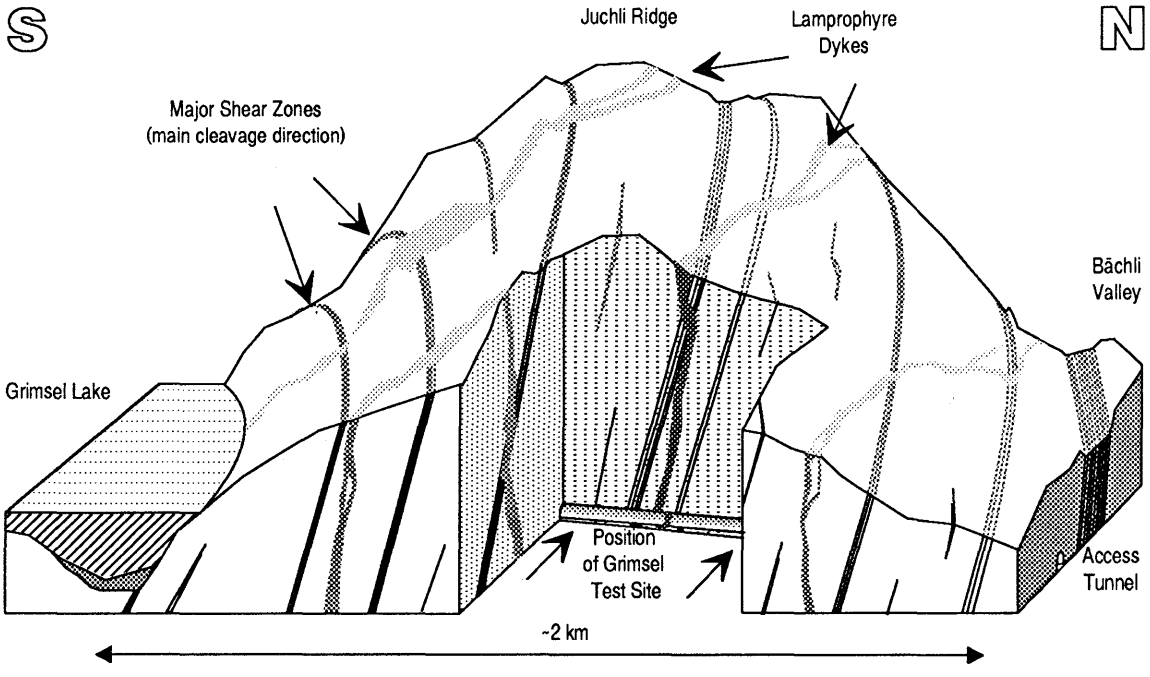

Fig. 2-3: Schematic of major pathways for groundwater flow around the Grimsel underground facility

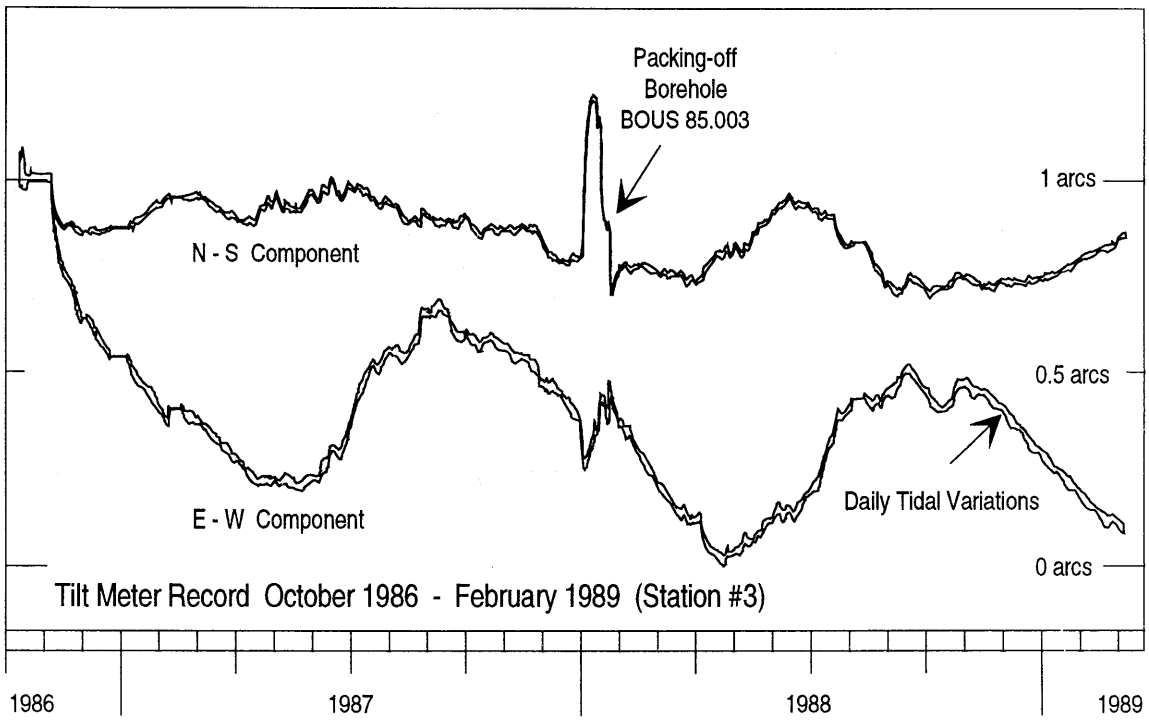

Fig. 2 - 4a: Typical long-term tilt meter record (October 1986 to February 1988)

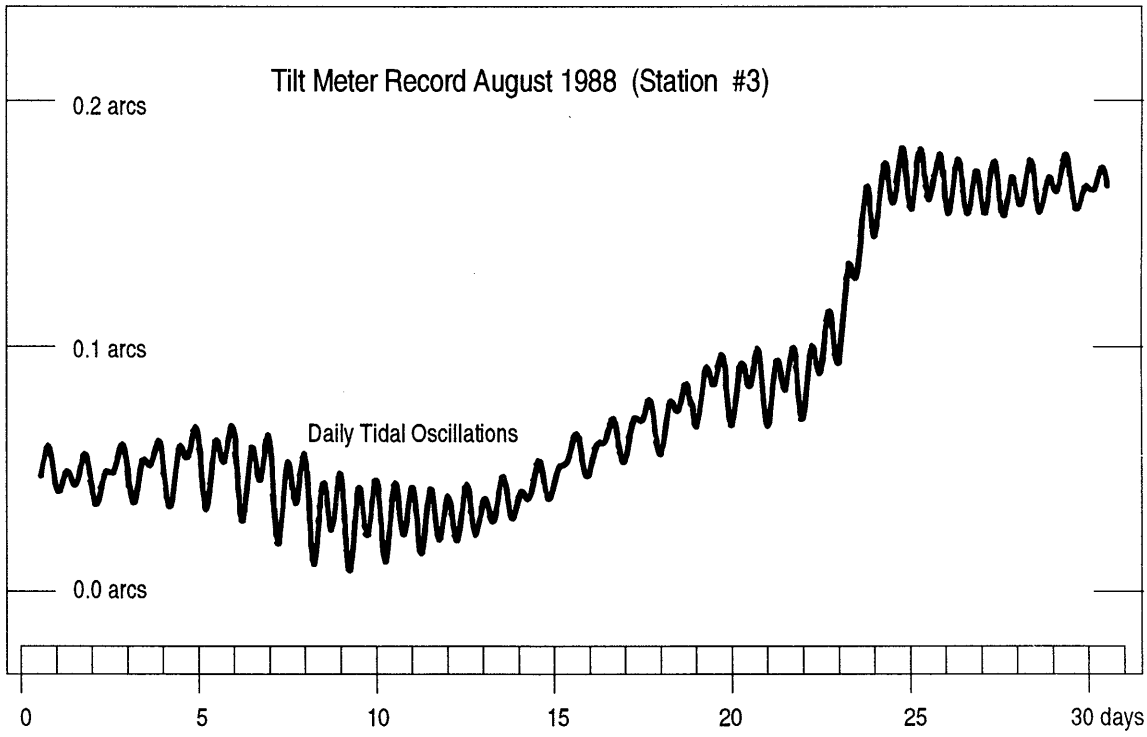

Fig. 2 - 4b: Typical monthly tilt meter record showing earth tidal oscillations

Recent displacement measurements were observed by a series of tilt meters installed in the GTS (FLACH & NOELL, NTB 89-11). They primarily reveal oriented, reversible, annual cycles of local dislocations (with a magnitude of roughly 1 arcs; NOELL & ZÜRN, 1991). These annual cycles (Fig. 2-4a) are caused by elastic deformation of the rock mass due to the seasonally varying level of the nearby reservoir on the eastern slope of the overlying mountain ridge. Non-periodic signals, such as those sporadically caused by the large-scale uplift of the Alps (at a rate of roughly 1 mm y^{-1}), are more difficult to identify. Tilt meter records also reveal (with a magnitude of roughly 0.05 arcs) the daily oscillations due to earth tides (Fig. 2-4b).

2.2 Regional Hydrogeologic Setting of the Grimsel Test Site

First clues on the general hydrology were obtained from the exploratory boreholes drilled prior to the construction of the GTS (NTB 81-07). Hydraulic pressures indicated that the overlying rock was fully water saturated almost to the top of the Juchli ridge.

Table 2-2: Range in groundwater composition from all known analyses of samples taken within or near the Grimsel underground facility.

Cations:		Anions:	
Na^+	6 - 16	SO_4^{2-}	4 - 11
K^+	0.1 - 3	Cl^-	0.2 - 6.1
Li^+	~0.1	F^-	0.9 - 9.6
Ca^{2+}	2.9 - 11	Br^-	0.03 - 0.05
Sr^{2+}	0.08 - 0.34	I^-	0.001 - 0.002
Mg^{2+}	0.01 - 0.5	NO_3^-	<0.3
Mn^{2+}	0.002 - 0.015	S^{2-}	<0.3
Fe^{2+}	<0.02	CO_3^{2-}	2 - 12
Fe_{tot}	0.006 - 0.04	HCO_3^-	4 - 16
Other Species:		Gases:	
Al	0.01 - 0.07	N_2	20 - 23
SiO_2	2.6 - 18.0	O_2	<0.1[f]
B	~0.1	Ar	0.7 - 1.1
DOC*	<0.9		

[f] detection limit for usual on-site electrode measurements

* dissolved organic carbon

all concentrations in mg l^{-1}; based on BAERTSCHI et al.(1982); OHSE (1983); FRESENIUS (1986, 1987); BALDERER (1987); GEOTEST (1988); HOEHN et al. (NTB 89-15); and unpublished Nagra data.

Within the 800 m of GTS laboratory tunnels, some 500 fracture planes have been observed with approximately 25 % of them (about 0.01 fractures per m^2 of tunnel surface), conducting water visibly. The total discharge into the tunnel systems of the GTS was initially around 2 l min^{-1}. All of the water bearing features seem associated with the ductile/brittle deformation pattern of the Grimsel rocks (details in NTB 85-46; NTB 87-14; GEOTEST 1988, MARTEL & PETERSON 1990, 1991). The observed geological structures provided the basis to define the water-conducting network in a recent attempt to model groundwater flow in the rock body surrounding the underground laboratory (NTB 91-03).

2.3 Regional Geochemical Setting of the Grimsel Test Site

2.3.1 Hydrochemistry

A large number of regional hydrochemical data have been gathered since the initiation of the test activities at Grimsel. These data are contained in unpublished Nagra internal files; OHSE, 1983; FRESENIUS, 1986; FRESENIUS, 1987 and GEOTEST, 1988. The observed variation in the major element chemistry between different discharge locations within the GTS or in the immediately adjacent area is rather small. Generally the groundwater is relatively poorly mineralized with an ionic strength of about 1 mM or less, electric conductivities from 60 to 120 µS cm^{-1} and, typically, a rather high pH ranging from 8.5 to 10.3. The range in groundwater composition observed in the GTS region is indicated in Table 2-2.

Table 2-3: Dissolved gases in Grimsel groundwater from early sampling campaigns in the exploration boreholes

	N_2	He	Ne	Ar	Kr	Xe
measured [f]		$9.3 \cdot 10^{-7}$	$8.6 \cdot 10^{-7}$	$6.3 \cdot 10^{-4}$	$1.2 \cdot 10^{-7}$	$1.4 \cdot 10^{-8}$
measured [*]	$1.6\text{-}1.8 \cdot 10^{-2}$			$3.9\text{-}4.1 \cdot 10^{-4}$		
saturation (calculated for 12°C, 830mbar)	$1.5 \cdot 10^{-2}$	$0.4 \cdot 10^{-7}$	$1.8 \cdot 10^{-7}$	$3.5 \cdot 10^{-4}$	$0.8 \cdot 10^{-7}$	$1.1 \cdot 10^{-8}$

concentrations are given in ccSTP ml^{-1}

[f] BALDERER 1987 (BOSB 80.001; sampled October 10, 1982)

[*] BAERTSCHI et al., 1982 (BOSB 80.001/002/003, sampled June 26, 1981)

Observed dissolved gases contained in the Grimsel groundwaters are comprised of mainly N_2 and Ar which amounted to about 97 % and 3 % of the total, respectively (Table 2-3). The dissolved Argon exists in apparent equilibrium with the atmospheric isotopic composition ($^{40}Ar/^{36}Ar \sim 300$; BALDERER 1987; EIKENBERG 1990). Methane and H_2S are below the detection limit (BAERTSCHI et al., 1982), although there is a perceptible smell of the latter. Small amounts of H_2 (0.1-20 $\mu g\ l^{-1}$) have been detected occasionally (BAERTSCHI et al., 1982).

2.3.2 Stable Isotope Data

It is outside the scope of this report to discuss the results of a large number of various isotope analyses contained in mostly unpublished GSF Munich data. Available δ^2H and $\delta^{18}O$ data reveal some interesting clues about the ambient hydrogeological regime.

There exist a total of 31 analyses of δ^2H and $\delta^{18}O$ available from various groundwater discharges into the GTS tunnel system. The mean and standard deviation of these samples are calculated to be

$$\delta^2H = -93.7\ (\pm 4.7)\ ‰ \qquad \delta^{18}O = -13.29\ (\pm 0.61)\ ‰$$

In spite of the relatively small spread of data, they correlate very close to the regression line for modern infiltration waters in Switzerland (Fig. 2-5). Based on the $\delta^{18}O$ versus altitude diagrams of modern recharge waters from the Bernese Alps climatic region, a plausible average infiltration altitude of about 2'000 m could be inferred for GTS groundwater. However, this might be a fortuitous result, since the local recharge compositions are not adequately known for the upper Hasli Valley (cf. KULLIN & SCHMASSMANN, in NTB 88-01).

Large-scale hydrologic interconnections within the Grimsel rock are indicated by the isotopic compositions from various sampling locations within the GTS access tunnel and the surrounding area (see Fig. 2-6). Systematic trends would have been expected if the pronounced fault zones which run from the Juchli Ridge, down to the main access tunnel, acted as preferential groundwater pathways. The neccessary (mixing) interconnections are probably provided by additional water-bearing fracture systems (e.g., associated with lamprophyre dyke zones) which transsect the main fault zones.

2.3.3 Groundwater Dating

Several attempts have been made to isotopically date the GTS groundwaters. Observed tritium (^3H, $t_{1/2}$=12.3 y) contents are 20-40 tritium units (TU) outside the actual GTS. However, there is little or no observed tritium in any groundwater discharge from within the GTS area (see Fig 2-6). The lack of tritium would indicate an age of this water of at least 35 years, i.e. older than the period of atmospheric nuclear bomb tests. This age limit is confirmed by very low concentrations of anthropogenic ^{85}Kr (BALDERER 1987; LOOSLI et al. in NTB 88-01).

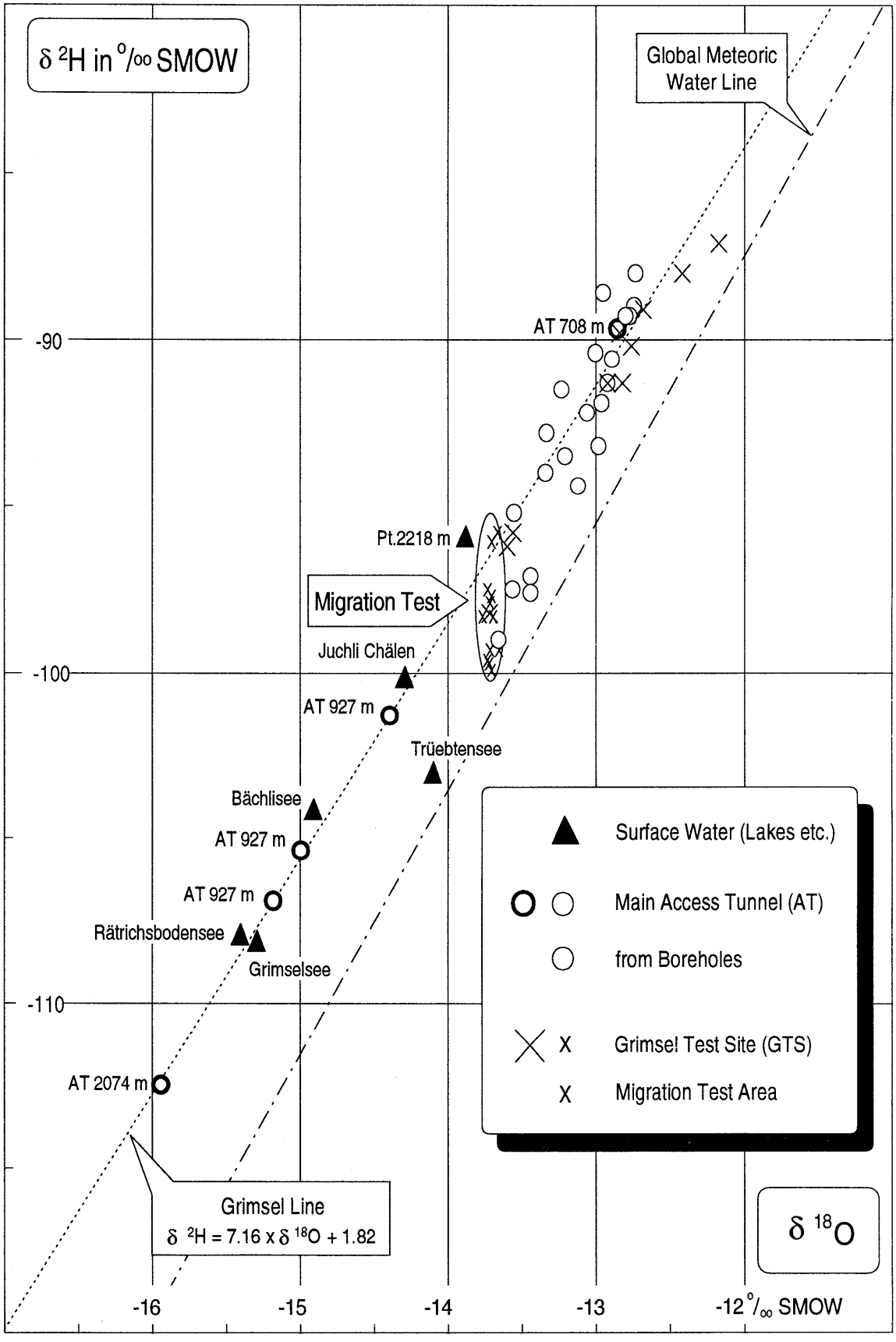

Fig. 2-5: Stable isotope data from various groundwaters at the Grimsel area

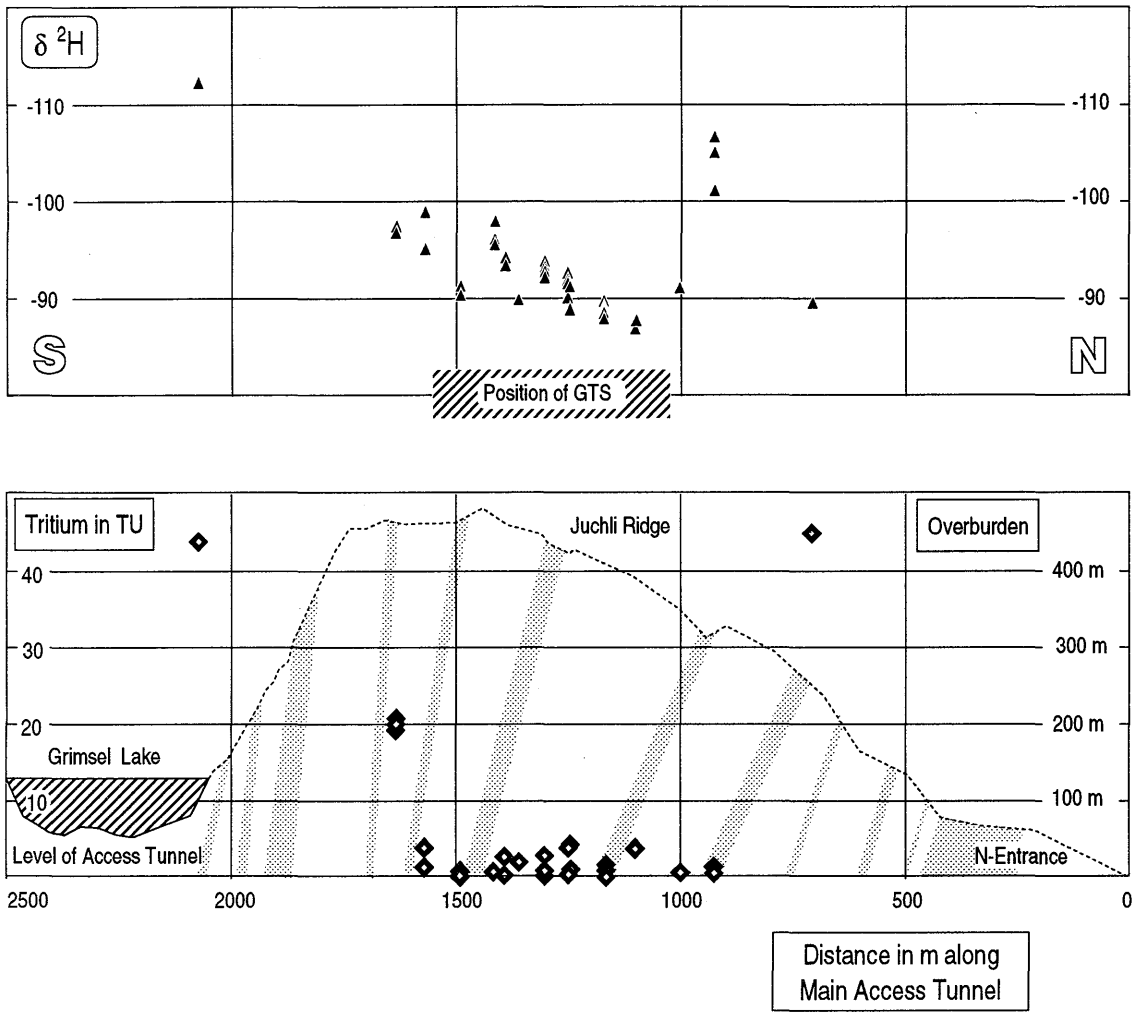

Fig. 2-6: Isotopic composition of groundwater at various locations within the Grimsel Test Site and the surrounding area.

Radiocarbon dating proved to be unsuccessful and was discontinued after one analysis of ^{14}C ($t_{1/2}$=5'730 y) contained about 50 % of the modern atmospheric concentration (BALDERER 1987). This anomaly is likely due to contamination from "fossil" carbonates and the very low CO_2 and carbonate content of the Grimsel water. Other methods of groundwater dating do not appear promising, either because of overly long half-lives of dateable isotopes or by excessive nucleogenic production in the granite, as exemplified by a value of 140 % of modern atmospheric composition for ^{39}Ar ($t_{1/2}$=269 y) (BALDERER 1987).

Additional isotope data reveal low ^{222}Rn ($t_{1/2}$=3.8d) concentrations in Grimsel groundwater with typical values from 10 - 30 Bq l^{-1} (FRESENIUS 1986; FRESENIUS 1987; HOEHN et al., NTB 89-15). One analysis of the U/Th series has been reported by IVANOVICH et al. (1986) which indicates a uranium content of 1.38 μg l^{-1} and the following activity ratios:

$^{234}U / ^{238}U$	2.12 ± 0.04
$^{230}Th / ^{234}U$	0.003 ± 0.001
$^{230}Th / ^{232}Th$	1.8 ± 0.5
$^{228}Ra / ^{226}Ra$	3.86 ± 0.28

These data should only be regarded as qualitative because of probable sampling perturbations. Realistic U contents in constantly discharging Grimsel groundwater are usually in the order of 0.2 $\mu g\ l^{-1}$ or less (BAERTSCHI et al., 1982; BAERTSCHI et al., NTB 90-15).

In summary, all geochemical observations to date are consistent with the GTS water being a relatively young meteoric water which infiltrated some 30 or more years ago and has undergone as slight increase in mineralization and accumulation of nucleogenic gases (^{4}He and ^{40}Ar). The infiltrating water generally follows 2 major steeply dipping pathways; the most prominent along almost vertical shear zones following the alpine strike (ENE-WSW) and the other representing shear zones along steeply dipping lamprophyre dykes striking NW-SE. The different orientations of the principal pathways leads to a mixing of the infiltrating water within a scale of approximately 100 m.

2.4 Selection of the Migration Experimental Site

To accomodate the major aims of the migration project, the following site selection criteria were defined:

- steady state hydrochemistry (i.e., constant chemical composition of major and trace elements in the groundwater),
- steady state hydrology (i.e., constant discharge rates and stable hydraulic pressures over the time scale of typical experiments),
- practicable experimental timescales, i.e. breakthrough of moderately retarded nuclides over distances of a few meters should occur within a few weeks or less,
- minimal disturbance, i.e. uncontaminated setting and no interference with other activities at the underground facility,
- saturated flow conditions.

This led to selection of the present site (laboratory designation AU 96 m) which was particularly notable for its relatively large water discharge (on the order of 10 ml s^{-1}) into the laboratory tunnel from an isolated fault of geometrically simple structure (HOEHN et al., NTB 89-15). This fault can be followed over a distance of almost 70 m as it intersects the principal access tunnel, the AU drift, the VT drift and borehole SB 80.005 (see Fig. 2-1). The fault is hereafter termed the migration (or MI) fracture. Further studies at the location, described in the next Chapter, confirmed that the selection criteria were all met at this site. A photograph of the experimental site, taken in summer 1989, is shown in Figure 2-7.

Fig. 2-7: Partial view of the test area with the migration fracture being covered by plastic sheets (photograph taken in spring 1990).

3 HYDROGEOLOGICAL CHARACTERIZATION OF THE MIGRATION SITE

The migration experiments were designed to be carried out under well defined and stable hydrological and hydrogeochemical conditions. Therefore, a comprehensive characterization of the migration fracture as well as the immediately surrounding environs was an important first step prior initiating the tracer tests. In this section the main geological features, the site exploration, and the principal hydrogeological and hydrochemistry observations are summarized. The hydraulic characterization based on hydrotesting is thoroughly discussed in HOEHN et al. (NTB 89-15) and briefly summarized in Section 4.

3.1 Geological Characterization of the Migration Fracture AU 96 m

3.1.1 Geology of the Migration Site

The rock mass at the migration site, a gneissose granodiorite, appears rather sparsely fractured on a macroscopic scale, while on a microscopic scale, the fabric of the country rock near shear zones or fractures is often heavily micro-fractured. The main mineralogical constituents of this rock are quartz, plagioclase (albite), K-feldspar, and biotite while minor constituents are muscovite, chlorite, epidote, allanite, zircon, and apatite (e.g., NTB 81-07, ALEXANDER et al., NTB 87-08; NTB 87-14; MÜLLER 1988; MEYER et al. in NTB 88-23 and references cited therein). Details on the mineralogy and petrography of the fracture are documented in MEYER et al.(NTB 88-23), ALEXANDER et al. (NTB 87-08), BOSSART & MAZUREK (1990) and BOSSART & MAZUREK (NTB 91-12).

3.1.2 Structural Features

Thorough investigations of the Grimsel fracture systems have recently been carried out by MARTEL & PETERSON (1990, 1991) and BOSSART & MARTEL (1990). The structural features of the migration fracture run parallel to the mean regional cleavage trends (BOSSART & MARTEL, 1990). The fault zone at AU 96m, usually referred to as the "migration fracture", is not a single fracture but rather represents a narrow, few cm wide, asymmetrical array of (small) shear zones and/or fractures. On the scale of several meters, however, this network can be described as a two-dimensional feature.

In a recent attempt to structurally characterize the MI fracture BOSSART & MAZUREK (1990, NTB 91-12) used oriented samples drilled at the tunnel face (Fig. 3-1). The application of particularly careful techniques provided samples while preserving their infilling fault gouge. Detailed structural and mineralogical investigations of the fracture zone indicate a complex anastomosing distribution of mineral assemblages and open pore space (Fig. 3-2 and 3-3).

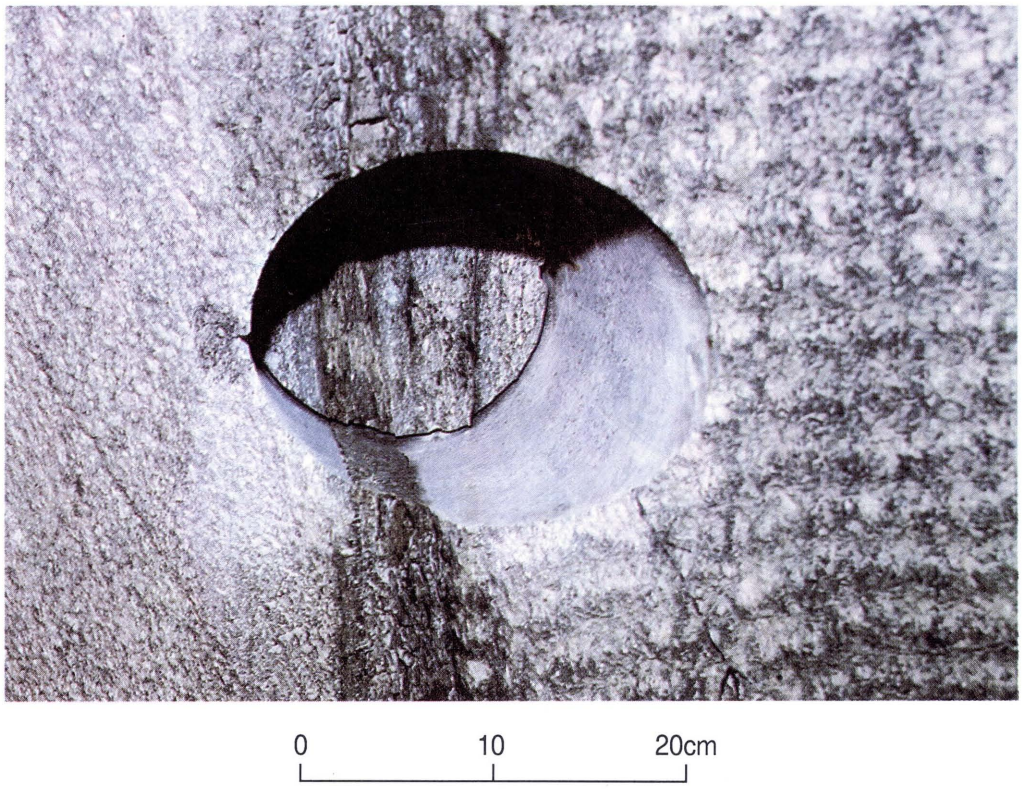

Fig. 3-1: Photographic view of the migration fracture (Eastern side of tunnel wall of the Ventilation Drift at VT 420 m, see Fig.2-1)

A simplified schematic presentation of the migration fracture is depicted in Fig. 3-3. Generally, the fracture consists of a re-crystallized portion (deformation under elevated temperatures) and a microbrecciated portion due to the recent brittle deformations (see Table 2-2 for a schematic representation of the local geological processes and their associated structural features. Recent shear movements and dilatation changes re-activate by brittle process (e.g., cataclasis) features of initially ductile deformation (e.g., mylonite bands) and cause frictional sliding and rotation of clasts. The net result is an unconsolidated breccia with coarse, internally unaltered rock components and fine grained gouge (see Fig. 3-3).

The asymmetric array of shear zones forms an abrupt interface with the country rock to the north. This interface is often referred to as "the migration fracture". Occasional branching of this main feature is observed. Subsequent, smaller shear zones run parallel to the main feature with their highest density within the first 3 cm. There is clear evidence of microfractures extending some 6-10 cm from the main zone into the nearby gneiss or granodiorite. The apparent fracture width (ranging from about 0.1 to 10 mm) could be determined from core investigations (ALEXANDER et al., NTB 87-08; BOSSART & MAZUREK, 1990; and BOSSART & MAZUREK, NTB 91-12) as well as from the apparent openings along the intersection of the tunnel with the fracture (HOEHN, 1987).

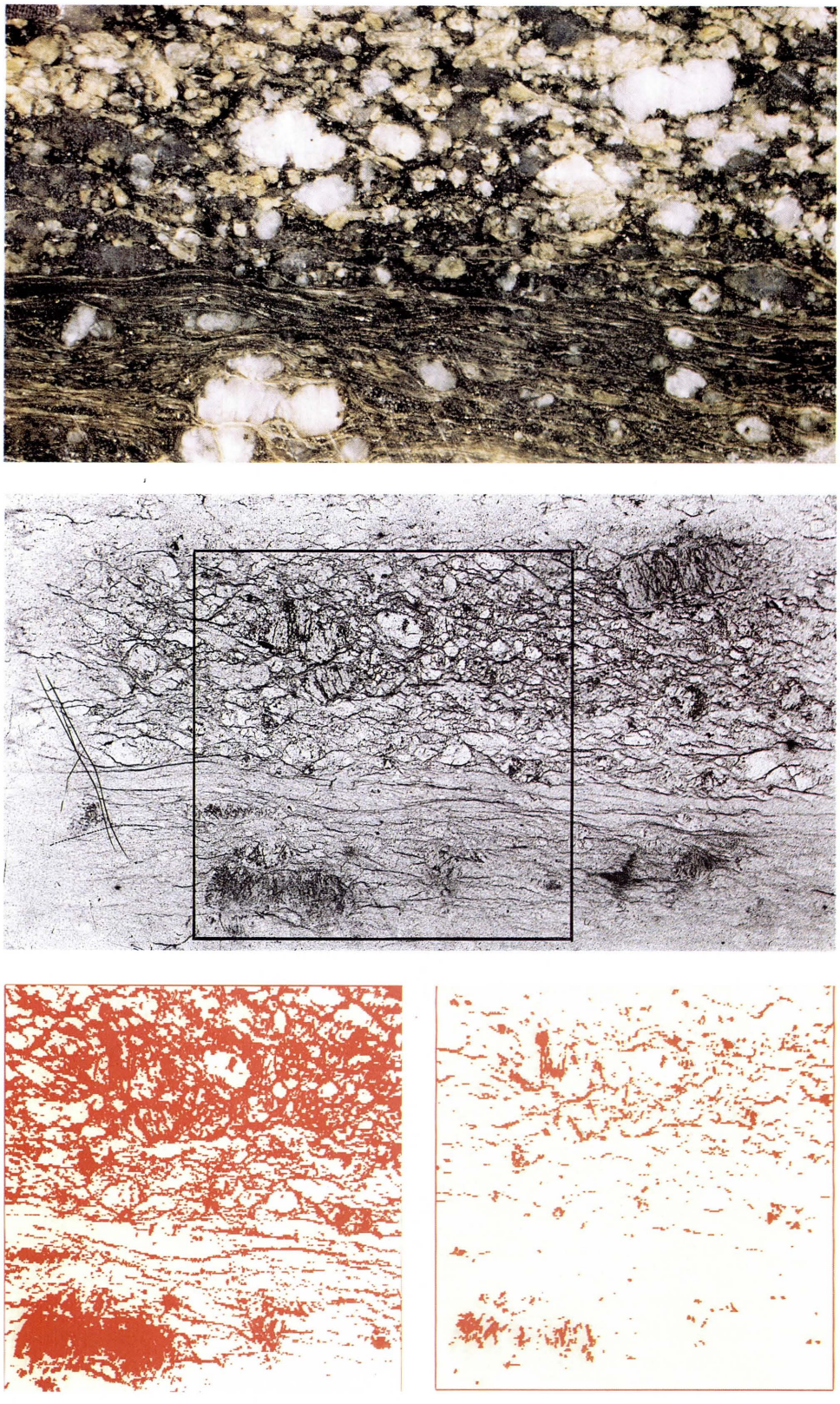

Fig. 3-2: Shear zone sample (width 6 cm; weakly deformed granodiorite and mica-rich mylonite) *top:* rock photograph; *center:* β-autoradiograph of the same sample, impregnated with a ^{14}C doped resin; *bottom:* processed images showing porosities of 0.6 % *(left)* and 0.2% *(right)* (taken from NTB 91-12)

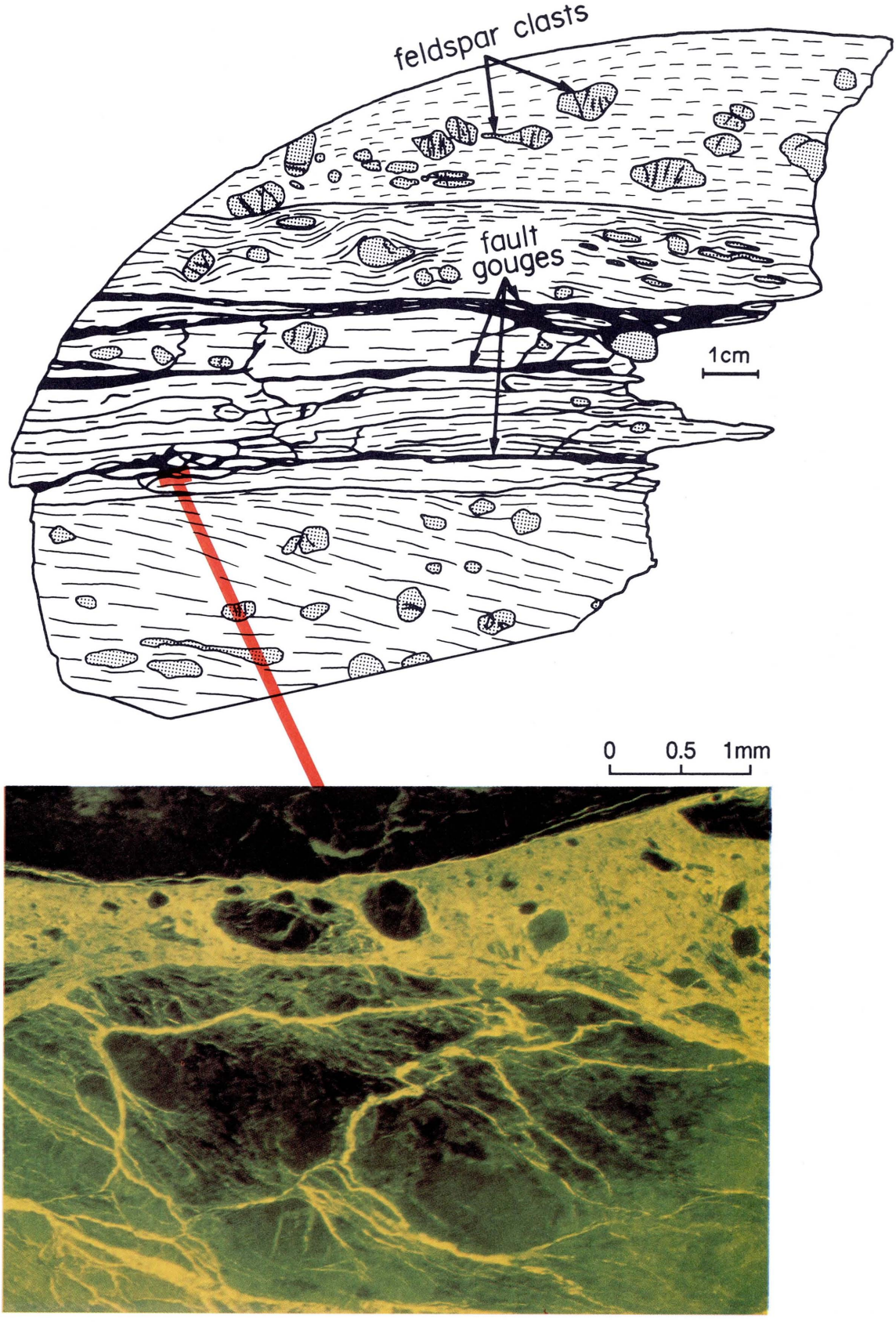

Fig. 3-3: Simplified presentation *(top)* of the migration shear zone; (*black:* open pore space caused by brittle deformation of mica-rich mylonite); and micrograph of fault gouge *(bottom)* impregnated with a fluorescent resin.

At the intersection of the fracture with the tunnel, small amounts of fault-gouge material have accumulated. The degree of filling in the MI fracture cannot be estimated because the drilling operations have washed away much of this infill material from the core samples. However, at least some of this infill did survive the careful drilling, cutting, and polishing procedures followed by BOSSART and MAZUREK (1990, and NTB 91-12), indicating an occasionally more coherent (or even slightly cemented) fabric.

3.1.3 Laboratory Sample Characterization of the Migration Zone

Laboratory samples of the MI fracture were required to determine the mineralogical and sorption characteristics relevant to tracer testing. Since the required amounts of material for the laboratory studies (~ 60 kg) could not be obtained from the narrow migration fracture at the MI site without potentially disturbing the local hydrology, samples were taken at a nearby fault (AU 126 m) located 30 m from the MI site. This fault zone is similar in several observable respects to the fracture zone at the MI site (AU 96 m). The fault at AU 126 m is also characterized by a substantially wider zone of intense deformation of a few decimetres width. This fault zone is highly cleaved, more or less incoherent, and rich of argillaceous material with white segregations of coarse grained quartz. It bears noting that during early investigations of the MI zone (MEYER et al. in NTB 88-23; AKSOYOGLU et al., NTB 91-06), material from the sampled fault and from the MI fracture was provisionally termed *"mylonite"* and *"protomylonite"*, respectively, regardless of the additional features of brittle deformation in both and the well developed characteristics of ductile deformation in the MI fracture.

Sampling of Laboratory Material: The first collection of laboratory samples for rock-water interaction experiments was achieved by breaking off chips and chunks from the mylonite and is documented in (BAJO et al. in NTB 88-23). A subsequent drillcore sampling with a portable (HILTI) drillcorer mounted on the wall, provided short (20-40 cm) borecores of 5-7 cm diameter across the fracture into the mylonite. Although the first 10-20 cm of damp, near-tunnel fault material were discarded, it cannot be ruled out that the sampled material had been at least partially in contact with air since the time the tunnel was constructed. The samples were placed in a nitrogen-flushed container and immediately transferred into a glove box at the Paul Scherrer Institute. All further handling of the samples for radiotracer batch experiments was carried out in a controlled atmosphere (AKSOYOGLU et al., NTB 91-06). The results of these laboratory analyses are presented in Section 5.

The Mineralogical Composition of Laboratory Samples was investigated by MEYER et al. (NTB 88-23) and is summarized in Table 3-1. The mylonite and the surrounding granodiorite have a similar mineralogy, except that the mylonite is more mica-rich with 21 % muscovite/sericite and 13 % biotite. A feature of possible importance with respect to sorption is the presence of plagioclase (originally magmatic) and albite (grown during alpine metamorphism). These grains appear sometimes to be intensely altered, as they are transformed into an irregular assemblage of very fine-grained, syn- and postmetamorphic minerals such as sericite, epidote and chlorite. It is possible that the altered plagioclases could substantially enhance the sorption capacity with respect to unaltered rock (ALEXANDER et al., NTB 87-08; MEYER et al. in NTB 88-23; BOSSART & MAZUREK, 1990; BOSSART & MAZUREK, NTB 91-12).

Table 3-1: Petrography of various typical rock samples from the migration site (modal composition in volume - %).

Sample[1]	Protocataclasite	Protomylonite	Mylonite	Fault Gouge	Granodiorite
	>2 cm away from Migration fracture	0.5-2 cm away from Migration fracture	from nearby fault	from nearby fault	from adjacent country rock
location	AU 96m	AU 96m	AU 126m	AU 126m	AU 96m
number of samples analyzed	6	1[2]	13	2[3]	8
method[4]	PCA	XRD+ETS	XRD+PCA	XRD	MCA+PCA
quartz	32	27	30	23	28.3
albite	32.4	25	20	15	29.1
K-feldspar	19.1	15	13	10	24.4
chlorite	1.0		0	10	
biotite	9.1		13		11.4
muscovite+sericite	2.3		21		3.4
16 / 33 / 37 / 52 / 18					
epidote	1.3		2.2		2.0
carbonate	<0.2		<0.1		<0.2
accessories[5]	2.3		0.8		1.5

1 for sampling location see Fig.1 in MEYER et al. in (NTB 88-23)

2 limited data due to insufficiently available sample material

3 uncertain data due to limited amounts of highly heterogeneous sample material

4 MCA: macroscopic counter analysis
PCA: point counter analysis
XRD: X-ray diffractometer analysis of bulk powder
ETS: estimates from thin section survey

5 includes minerals such as sphene, zircon, allanite, apatite, and opaques

The overall oxidation state of mylonite, characterized by the ratio Fe_{II}/Fe_{tot} is comparable with values from their parent granodiorite. This implies that there was no major oxidation of the fracture material by atmospheric contamination.

Comparison of Laboratory Samples and Material from the MI Fracture: A careful comparison of material from both the MI fracture and the fault zone sampled for laboratory analyses was carried out by MEYER et al. (NTB 88-23). As both faults underwent the same metamorphic processes and exhibit the same features of ductile and brittle deformation, they have a similar bulk geochemistry and mineralogy (see Table 3-1). The differences of the two faults (width of shear zones, cleavage intensity, etc.) are mainly of a structural nature and related to the different degree of shear deformation.

As fault gouge predominantly consists of finely ground minerals due to friction in phyllosilicate-rich mylonite bands, it is expected to be more phyllosilicate-rich than the parent mylonite. Its mineralogical composition (see Table 3-1 for fault gouge from AU 126 m) can therefore be expected to be the same in the migration fracture. With fault gouge partially filling the predominant water bearing features (see below), this material might be most relevant for water-rock interactions.

Of special interest for sorption studies is the presence of minerals with high surface areas. X-ray diffractograms of the clay size fraction from the mylonite show scant evidence of chlorite-smectite mixed layer structures. The maximum mixed-layer contents are approximately 1 volume % for AU 126 m mylonite and 0.2 volume % for the AU 96 m (c.f. MEYER et al. in NTB 88-23). There was not enough material available to determine the abundance of these minerals in the fault gouge.

3.1.4 Geologic Characterization of the Water-Filled Pore Space in the Migration Shear Zone

The characteristics of the water-filled pore space greatly influences flow and solute transport in a fractured rock. Thin sections of samples impregnated with a β-emitting resin (Fig. 3-2) or an UV fluorescent resin (see Fig. 3-3) show evidence of a major network of channels, transgranular microcracks and grain boundary porosity (MEYER et al. in NTB 88-23; BOSSART & MAZUREK, 1990; BOSSART & MAZUREK, NTB 91-12). Although it is not clear how much water flow might occur through these open voids these fluorescence microscopic examinations reveal important features of the network of open and closed pores on the order of 1 μm width.

Brittle deformation of the mylonitic structure has apparently opened dominant features for water flow. The resulting channels have apertures in the order of 0.01 to some cm (BOSSART & MAZUREK, 1990, NTB 91-12) which are filled with fault gouge (i.e., coarse rock components and unconsolidated, finely ground rock material; see also Fig. 3-3). This infill has a porosity of about 10-30 %. The additional pore space (typically 0.001-0.05 mm wide) is found within the parallel channels of the mica-rich mylonite bands and the deformed portion of the country rock. Mercury injection microporosimetry measurements on various samples (from the AU 96 m, VT 420 m, and AU 126 m fault zones) yielded porosity values of about 1-2 volume % (MEYER et al. in NTB 88-23; BOSSART & MAZUREK, NTB 91-12). These values seem

representative for the mica-rich matrix adjacent to the major, gouge-filled channels. Current investigations are underway to measure some typical hydraulic parameters (permeability and flow porosity) of selected samples from the migration fracture.

The main features of water filled pore space of the migration shear zone are depicted in a simplified manner in Fig. 3-4:

a) the usually deformed country rock is characterized by an average porosity of about 1%

b) the mylonite fabric is virtually impermeable perpendicular to the shear zone (except for a few parallel fractures)

c) the dominant openings are filled with fault gouge and have show a porosity around 10 - 30 %

For solute transport modeling (see Sections 6.4, 7.3.4 and 7.4.3) this setting is conceptualized as a dual-porosity medium of limited width, i.e., the pore space of the country rock is not accessed by the tracer.

3.1.5 Natural Decay Series Disequilibrium in the Migration Fracture

Natural decay series disequilibria have been measured in a profile across the MI shear zone and provide unambiguous evidence of solute mobility at distances of several centimetres into the rock matrix surrounding the main water conducting fracture (ALEXANDER et al., NTB 87-08). Although the $^{234}U/^{238}U$ and $^{230}Th/^{234}U$ daughter/parent pairs are in isotopic equilibrium, the $^{226}Ra/^{230}Th$ activity ratios display significant disequilibria indicating relatively recent ($< 8x10^3$ y) rock-water interaction.

Comparison of pore diffusion coefficients derived from the above data with those from laboratory studies have also been carried out (ALEXANDER et al., 1990). Simple model calculations indicate that the ^{226}Ra migration in and around the main water conducting fracture can be ascribed to matrix diffusion, even though the rock matrix is characterized by numerous, potentially water bearing microfractures. This provided the first clear evidence that matrix diffusion occurred in the mylonite and granodiorite of the migration shear zone. In addition, because Ra is a chemical analogue of Sr in this system, detailed mapping of the distribution of the excess ^{226}Ra could provide useful information on the potential sites of Sr (and Na) exchange in the water conducting fractures. Just such a study is currently underway (MAZUREK et al., 1991) and the preliminary results emphasize the importance of the role of minor amounts of critical secondary minerals such as smectite on the uptake of radiotracers in the migration shear zone.

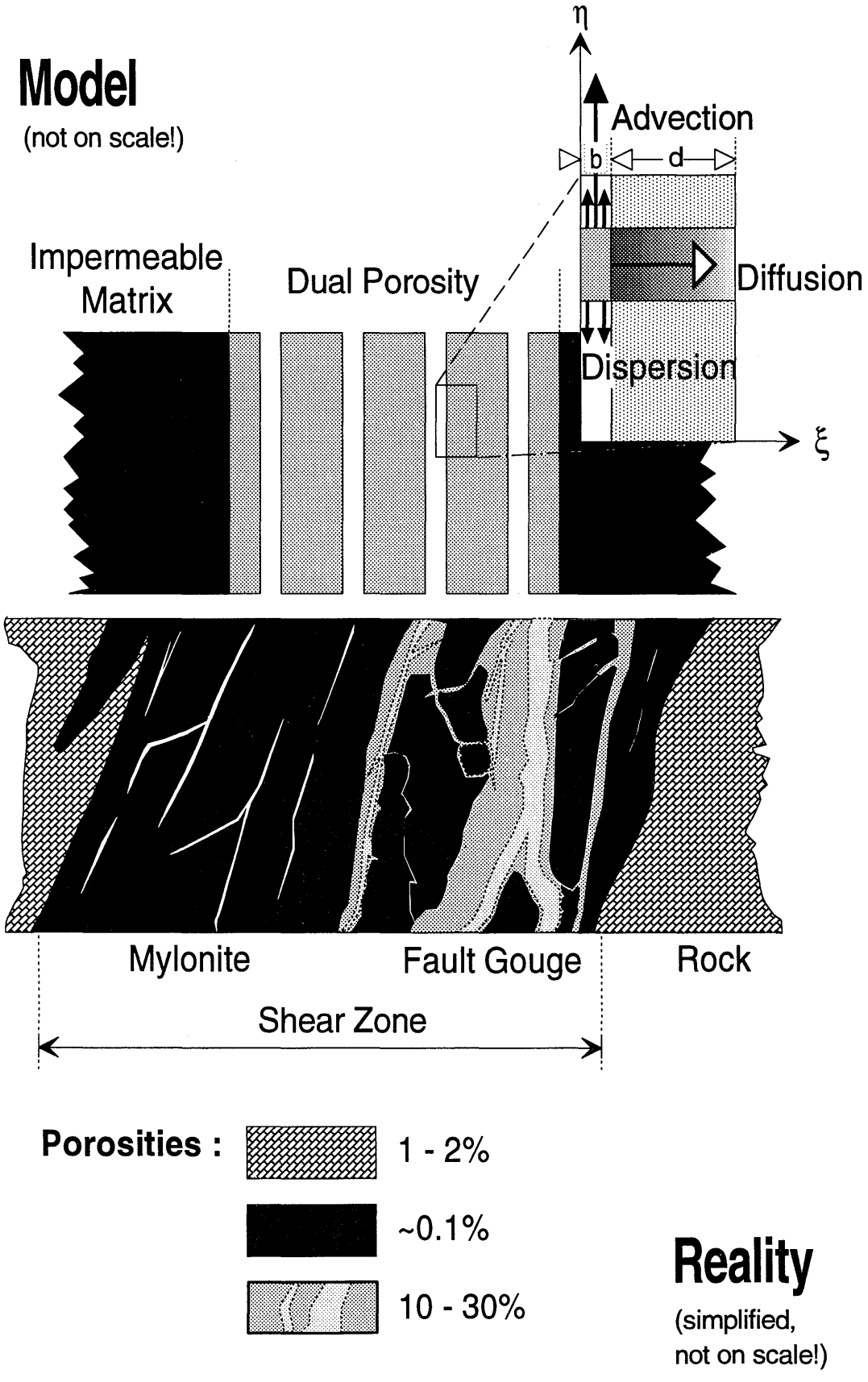

Fig. 3-4: Simplified presentation of the water filled pore space in the migration fracture and the dual-porosity concept for transport modeling.

3.2 Site Exploration

After the shear zone at tunnel meter AU 96 had been selected for the migration experiments, it was necessary to further explore its location and hydrology by drilling into the fracture on both sides of the laboratory tunnel. Figure 2-7 depicts the MI fracture (covered by plastic sheets for water collection and part of the apparatus used during tracer tests in the MI fracture.

3.2.1 Preliminary Instrumentation and Monitoring

The purpose of the hydrogeological monitoring before, during, and after the drilling campaign was to (a) obtain information on the hydrologic stability, (b) determine the spatial and temporal variability of the water chemistry in the MI fracture among the several discharging channels, and (c) identify hydraulic connections. Further details on the rationale and results of these efforts are given in (HOEHN et al., NTB 89-15).

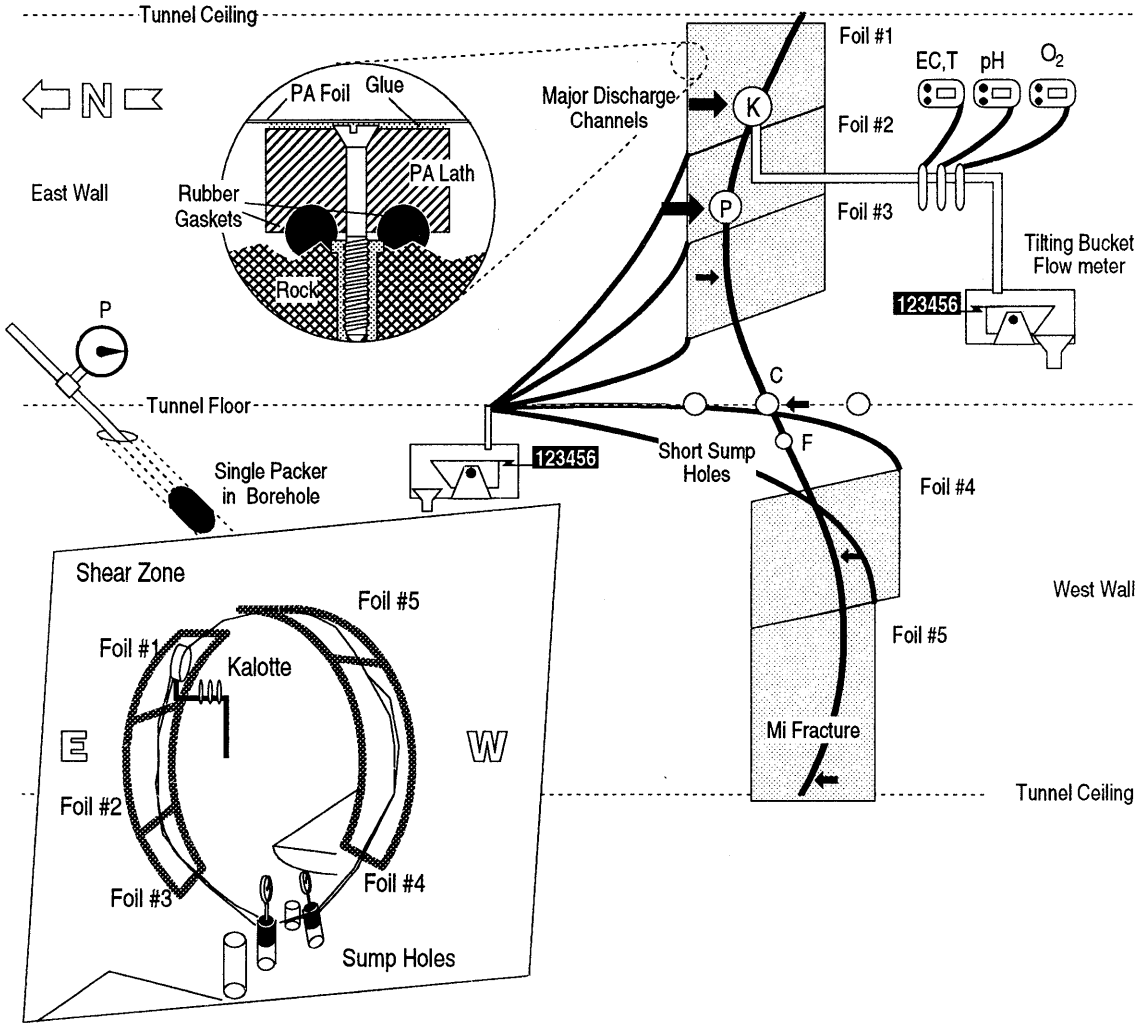

Fig. 3-5: Preliminary equipment setup for hydrogeological monitoring.

The first stage of site exploration involved collecting and analyzing water from the 5 main discharge points (channels) where the tunnel wall intersects the fracture (see Fig. 3-5). These five zones represent about 90 % of the local inflow. A major channel, located at point K on Figure 3-5, contributed more than 70 % of the local inflow into the drift from the MI fracture. This zone was equipped with a steel cup collector, which was later replaced by a teflon manifold with flow-through electrodes to measure electrical conductivity, pH, temperature, and dissolved oxygen. The flow from this channel was initially about 600 ml min^{-1}. The remaining flow was collected in 5 segments by polyethylene sheets glued to a frame of sealed plastic laths mounted on the relatively smooth rock surface. One or two collectors were temporarily connected to simple flow meters (tilting buckets) to monitor discharge rates.

The next stage involved monthly water sampling from the fracture (tunnel discharge, borehole intervals) and adjacent areas for hydrochemical and isotopic analyses. The sampling frequency was increased during drilling activities.

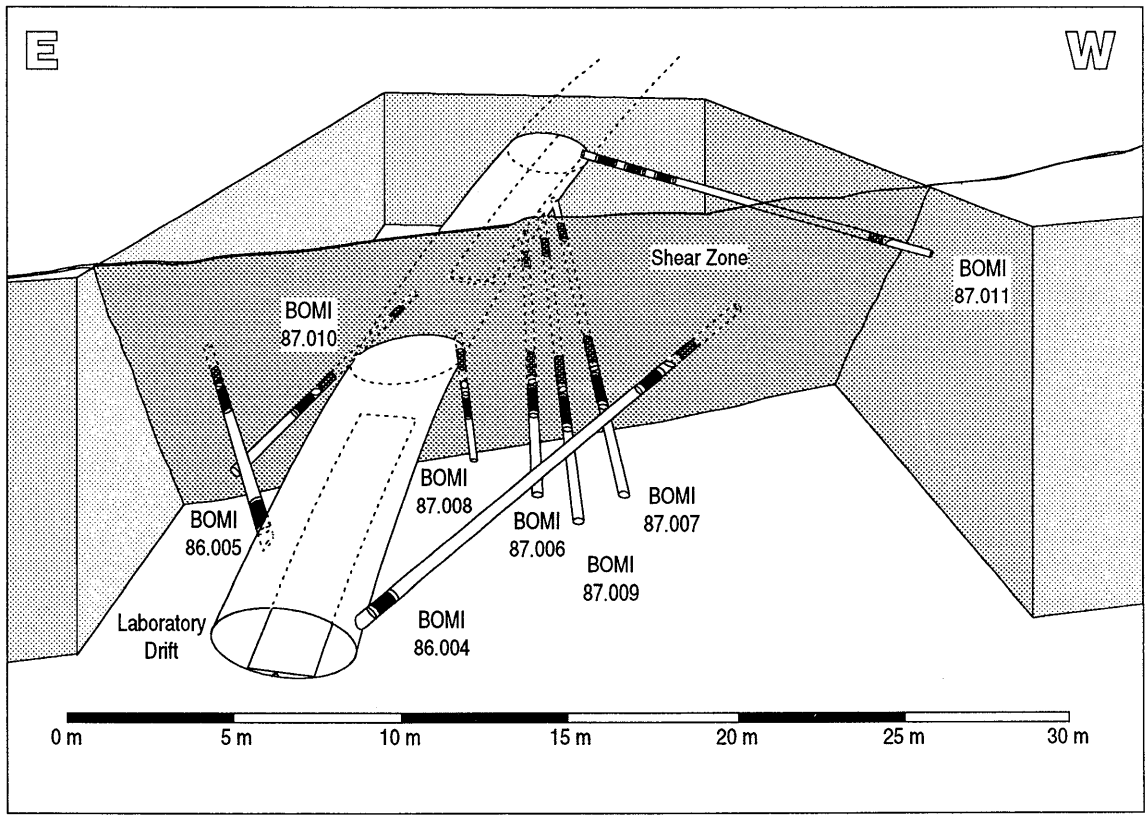

Fig. 3-6: 3-D perspective of the migration fracture indicating the location of the explorating boreholes.

A series of short (~ 0.3 m) sump holes of between 80 and 170 mm diameter were drilled into the tunnel floor with a portable powerdrill. Two of these sump holes labelled C and F on Figure 3-5 were drilled in the migration fracture at locations, where no significant water discharge had been observed. Surprizingly, when drilling C, the total water inflow to the tunnel from the previously flowing zones ceased and all the discharge began to occur through this sump hole. This hole was immediately packed-off. The same occurred when drilling sump hole F, which was intended to collect the small discharge (in the order of a few ml min^{-1}) seeping along the fracture at its intersection with the tunnel floor. Packing-off these two sump holes was successful and no measurable discharge could be detected in the lower portion of the fracture, where it intersected the tunnel. Both packers were equipped with manometers and one pressure transducer. Initially, pressures in C and F were nearly identical at about 0.8 bar (note this anomalously high pressure near the tunnel is described in Section 3.3.1). The pressure in C was continuously monitored by a data logger to obtain indications of the hydrologic stability of the fracture and to delineate possible pressure interferences resulting from subsequent drilling activities.

3.2.2 Drilling Campaigns

As design calculations indicated that distances of a few meters appeared adequate for the migration experiments with moderately sorbing tracers, it was planned to intersect the migration fracture some 3 to 12 m away from the tunnel by drilling a number of boreholes into the rock on both sides of the laboratory tunnel. The boreholes were drilled downwards to preclude any air reaching the fracture and to avoid creation of any unsaturated zones such as those which form along the upper half of the tunnel wall. Preliminary hydrodynamic modeling was utilized to optimize the position of the intersection of the boreholes with the presumably planar, water conducting shear zone.

In two campaigns during Summer 1986 and Summer 1987 a total of 8 boreholes of 86 mm diameter, 6 to 25 m long, were drilled to intersect the fracture plane at distances of 3 to 16 m from the tunnel wall (Table 3-2). The location of the boreholes is schematically represented in Figure 3-6. The boreholes were designated BOMI YY.XXX, with YY coresponding the year of drilling, and XXX the consecutive number of the hole. Partially aerated water of low mineralization (about 20 µS cm^{-1}) from a small lake (Trüebtensee) at 2365 m altitude, of known tritium content and stable isotope composition was used as the drilling fluid. In an attempt to minimize possible contamination, the pressure on the drill bit, as well as in the drilling fluid, was kept as low as manageable immediately before and after intersecting the fracture.

Usually, subcores of 3 m length were taken and broken into 1 m long pieces. They were immediately rinsed with water from the migration fracture. Subsequently, the petrographic features and structural information were mapped (GEOTEST 1986, 1987). They were then photographed (PHOTODOCUMENTATION, 1987) while still wet and heat-sealed, into one or two layers of transparent polyethylene foil (for unfractured cores and fracture samples, respectively). This process was usually completed within one hour of sampling. The wet wrapping was intended to provide short-term protection from contamination or drying-out prior to laboratory investigations. The suitability of this procedure has not been investigated for storage over extended periods.

Table 3-2: Dates of Drilling and Instrumentation

Borehole	Dates of Drilling	Multi Packer System Instrumentation Date
BOMI 86.004	15.7.–21.7.1986	21./22. 7. 1986
BOMI 86.005	22.7.–24.7.1986	29./30. 7. 1986
BOMI 87.006	11.6.–16.6.1987	2. 7. 1987
BOMI 87.007	17.6.–22.6.1987	21./22. 3. 1988
BOMI 87.008	14.7.–15.7.1987	12. 8. 1987
BOMI 87.009	16.7.–20.7.1987	12. 8. 1987
BOMI 87.010	21.6.–22.7.1987	12. 8. 1987
BOMI 87.011	26.8.–9.9.1987	21./22. 3. 1988

Instrumentation with improved,
(low volume, teflon coated and optical fiber) test interval tool

Borehole	Instrumentation Date	
BOMI 86.004	12. Sept. 1989	no teflon coating
BOMI 87.006	29./31. Jan. 1991	
BOMI 87.009	29./31. Jan. 1991	
BOMI 86.004	29./31. Jan. 1991	

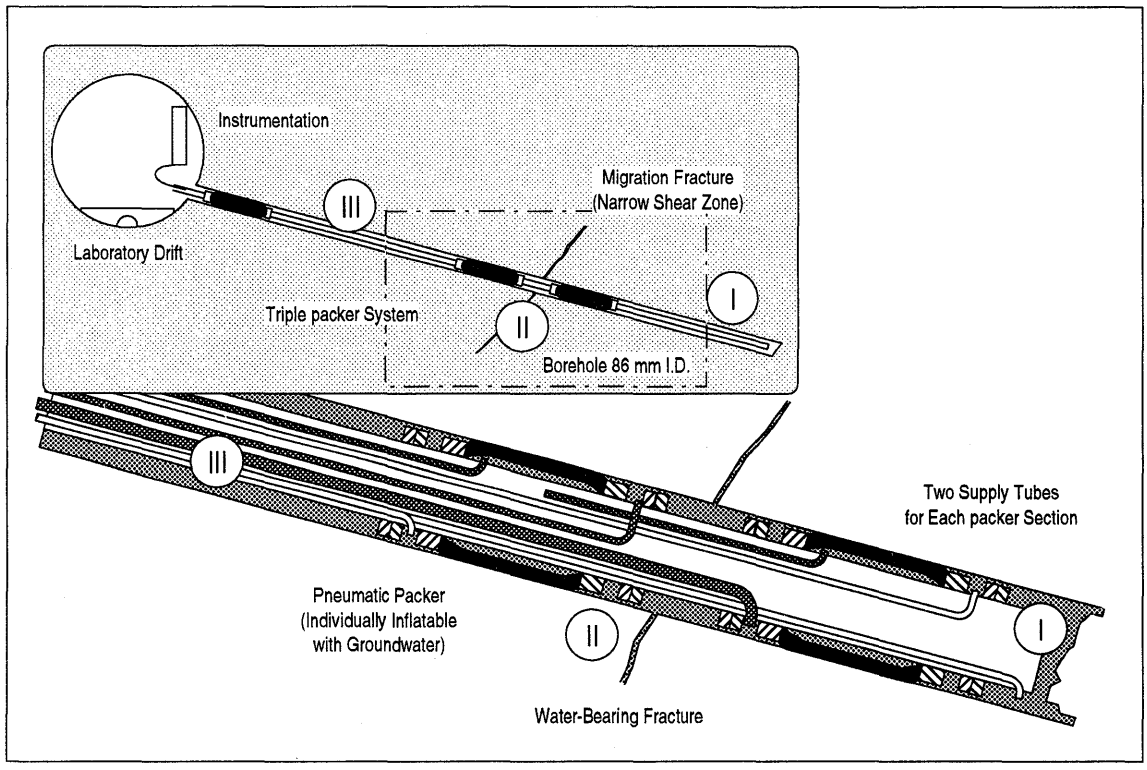

Fig. 3-7 Schematic representation of the packer arrangement in the boreholes which penetrate the migration fracture. Packer interval pieces were modified later during tracer migration tests (see Fig. 6-8).

During the drilling of all boreholes (except for BOMI 87.007/87.011) noticeable pressure drops were observed at all monitoring stations in the fracture whenever the drill passed through the migration fracture. Drilling was then briefly interrupted and the discharge (i.e., non-steady state flow) from the borehole was measured. Subsequently the boreholes were extended another 2-3 m and, immediately thereafter, closed with a single packer (equipped with a pressure transducer) near the tunnel wall. Triple-packer systems, schematically depicted in Figure 3-7, were installed (see also Table 3-2) (FRICK et al., 1988; HOEHN et al., NTB 89-15; THORNE, 1990a).

An obvious breakthrough of drilling fluid to the tunnel was seen only when drilling BOMI 87.008, intersecting the fracture 3.5 m from the tunnel wall (HOEHN et al., NTB 89-15). Some noticeably turbid water discharged into the drift for a few hours, with an oxygen content measurably increased from below detection limit (i.e. 0.05 %) to about 0.4 % saturation, undoubtedly caused by mixed-in, fully aerated drilling fluid.

3.3 Hydrogeological Monitoring

3.3.1 General Hydrologic Observations

The most relevant observations of fluid pressure and water flow out of the 8 boreholes intersecting the migration fracture produced short-time flow rates ranging from about 0.02 to 2 l min^{-1}. The flow rates correspond to transmissivities on the order of 10^{-5} to 10^{-7} m^2s^{-1} (see Section 4). Of the boreholes drilled only BOMI 87.007 and BOMI 87.011 showed no measurable flow. The static pressures are a uniform 1.5 bar at distances of 6 to 11 m from the drift (see Fig. 3-8). This constant value may represent the draw down caused by neighboring drifts which also intersect the MI fracture (see Fig. 2-1). The pressures in packed-off intervals appeared relatively stable over periods of a few months.

Over the years following the multipacker installation, a pressure decline of a few % per year was observed. This decline paralleled a small decrease of the discharge into the drift (from about 700 ml min^{-1} to about 500 ml min^{-1} during the period of 1984 to 1990). Although reasonably steady-state conditions can be assumed over the time of typical experiments, it is apparent that the hydraulic system has not yet reached complete equilibrium over the time since tunnel construction in 1983. Further details on the local hydrology are discussed in HOEHN et al. (NTB 89-15).

Many hydraulic observations were made at the early stages of site exploration. The following illustrate the anomalous features of water flow near the tunnel. The distribution of volumetric fluxes has occasionally changed. Once a new discharge started for unknown reasons with a net flow of about 150 ml min^{-1}. There is an uneven, but locally sharp, pressure increase within a few dm from the drift (see Fig. 3-8). The discharge channels supply partially degassed water to the tunnel as observed by slightly lower N_2 contents and substantially reduced levels of ^4He (degassing nitrogen bubbles would effectively strip noble gases from the groundwater; EIKENBERG & KIPFER, 1989) when compared with groundwater in the borehole fracture intervals.

These indicate the existence of unsaturated, but not aerated (no ingress of O_2 measured) zones. Since the water is only slightly oversaturated with nitrogen (the measured N_2 contents of about 22 mg l^{-1} or about 1.7 ccSTP ml^{-1} correspond to 110-120 % saturation at 830 mbar ambient pressure and a temperature of 12°C; cf. also Table 2-3), the degassing most probably occurred very close to the tunnel wall where the pressures are the lowest. Such nitrogen bubbles may be unstable and potentially might cause some channeling near the drift and slowly grow or bleed out into drift. In addition, it cannot be excluded that portions of eroded fracture infill are plugging the fracture at its intersection with the tunnel. Also the near-tunnel hydrologic effects might be related to stress relief after excavation of the laboratory tunnel. From the above it can be concluded that the channeled discharge pattern observed in the drift may not be representative of the actual channeling or transmissivity distribution within the fracture.

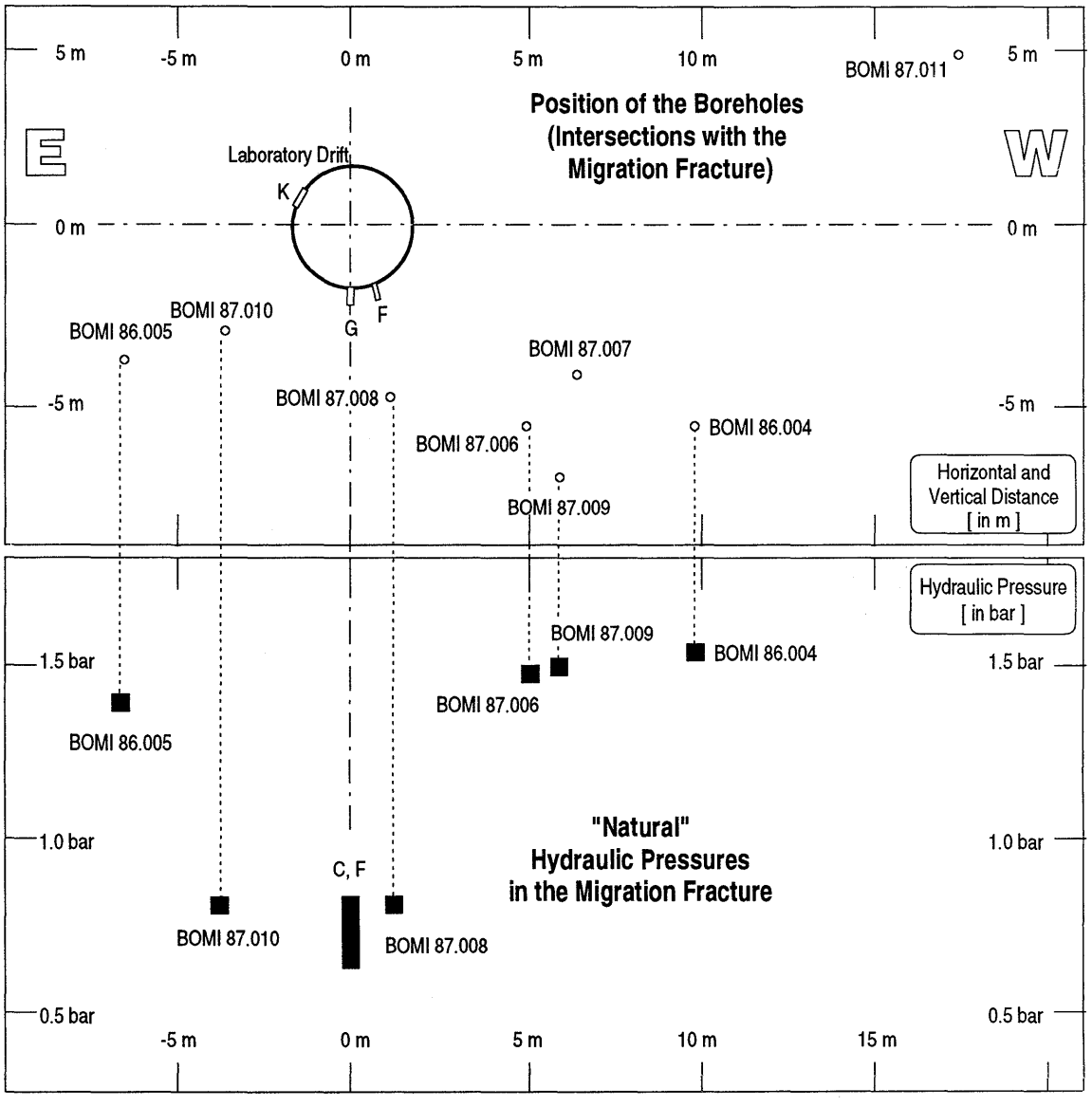

Fig. 3-8: Hydraulic pressure distribution within the MI fracture.

3.3.2 Effects from Unsaturated Rock at the Tunnel Wall

At the migration experiment site, the drift is drilled through almost unfractured rock. The walls appear completely dry for at least 30 m on either side of the intersection with the migration fracture. This dryness is believed to be a result of the lower humidity ventilation air being in the drift. Values of water evaporation rates on the order of 0.1 - 0.5 mg $m^{-2}s^{-1}$ were measured at 90-98 % relative humidity in this section (WATANABE, 1991). This rate of evaporation indicates substantial transport through the partially saturated, unfractured rock mass with hydraulic conductivities of about 10^{-10} to 10^{-11} m s^{-1} (estimates by BAERTSCHI et al., NTB 90-15).

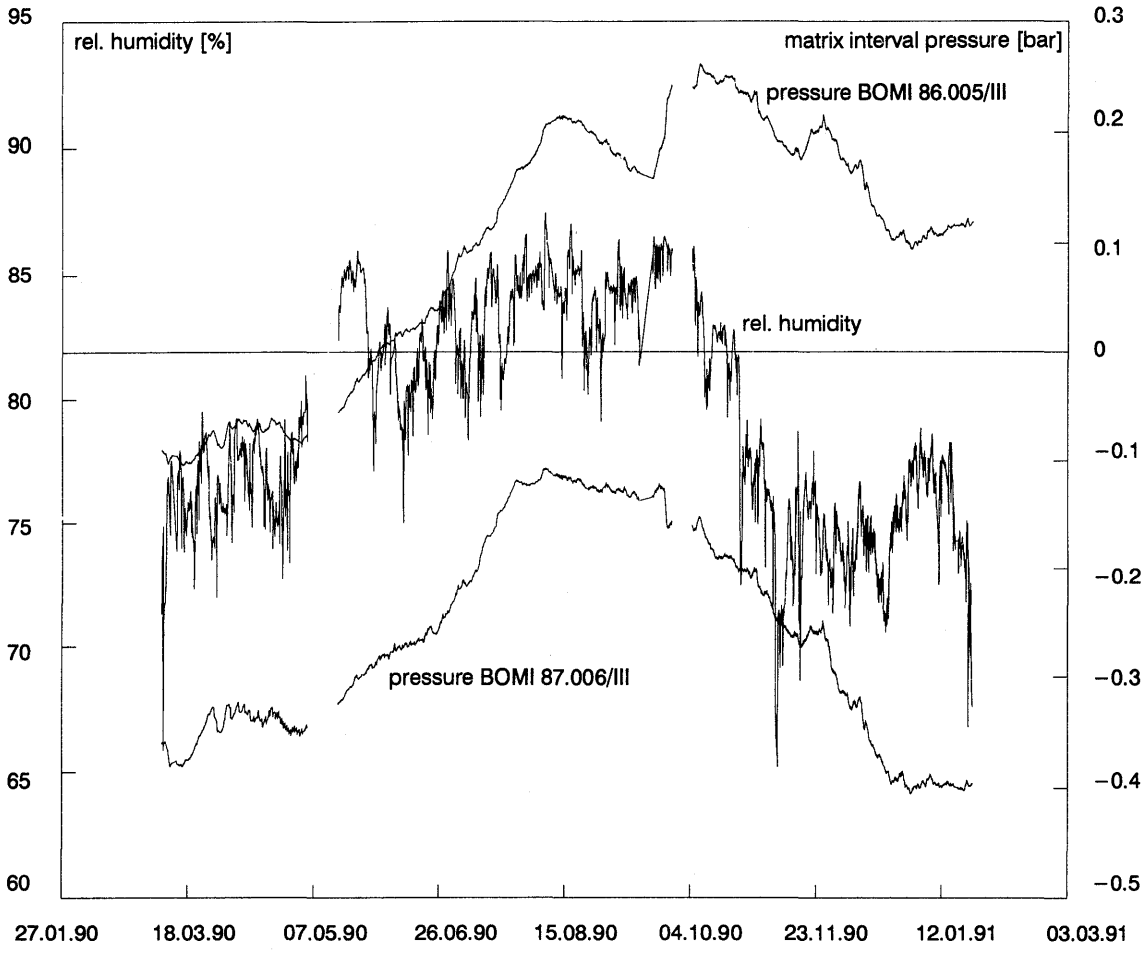

Fig. 3-9: Seasonal variations of the relative humidity int the laboratory tunnel and fluctuations of hydraulic pressure in rock matrix borehole intervals.

Unsaturated zones around the tunnel and the associated capillary suction cause significantly decreased pressures in packed-off borehole sections within the adjacent rock when compared with the pressures in the fracture intervals (see also Section 4.1.5). In borehole intervals which extend up to several meters from the tunnel wall, negative pressures (relative to the tunnel axis) were frequently measured (see Fig. 3-9). The stability of hydraulic pressures within the unfractured rock mass has been monitored over extended periods. Altough the pressure responses are complex, there are some indications of pressure increases near the drift face and pressure decrease in sections a few m away from the tunnel wall. These indicate a possibly growing unsaturated zone. In addition, the pressure changes appear also correlated with the seasonal changes of humidity in the tunnel (see Fig. 3-9). Such effects are now under systematic study (e.g. SCHNEEBELI et al., 1990) within another Nagra project at the Ventilation Test Site (see map in Preface section of this report), because they may significantly hamper conventional interpretation of a variety of experiments which are usually carried out near tunnel walls.

Although the anomalously low pressure regime within the unfractured rock mass does not appear to affect pressures in the more transmissive sections of the migration fracture, it is possible that the low observed pressures in less transmissive areas of the fracture (e.g. in the vicinity of boreholes BOMI 87.007 and BOMI 87.011) could be caused by capillary suction from unsaturated rock near the tunnel. It is not clear, however, to what extent these pressure anomalies might affect water transport in the fracture. Perpendicular to the plane of the shear zone, induced pressure gradients could reach in the order of 1 bar m^{-1}. The maximum estimates for related mass flow (i.e. at hydraulic conductivities of less than 10^{-10} m s^{-1} in the rock matrix) would then be less than 0.1 ml min^{-1} per m^2 of fracture area. This appears to be a negligible quantity in view of the extraction rates used during migration experiments (typically from 150 to 250 ml min^{-1}).

3.3.3 Earth Tide Effects

Earth tides cause pressure oscillations of 5-15 mbar amplitude with about a 12.5 h periode in the packed-off borehole intervals (Fig. 3-10; see also HUFSCHMIED & FRIEG, 1989 and NTB 91-12). As such pressure signals are related with relative movement of the rock mass on both sides of shear zones, it was suspected that the pattern measured by the tilt meters (FLACH & NOELL, NTB 89-11) might be similar. This is indeed the case (see Fig. 2-4b) and, moreover, tilt meter data reveal a pronounced phase-shift (18.25 min for the 12.5 h/M2 wave) between different tilt meter stations within the GTS and the access tunnel (NOELL & ZÜRN, 1991). These effects were explained by the existence of active fracture zones between the different tilt meter stations. It has therefore been postulated that earth tidal data could potentially be utilized as a diagnostic tool for locating major water conducting fault zones in a fractured rock. To check the suitability of precise pressure measurements in boreholes, as a relatively inexpensive and standard technique, the relationship of tilt meter and hydraulic pressure data is currently being investigated.

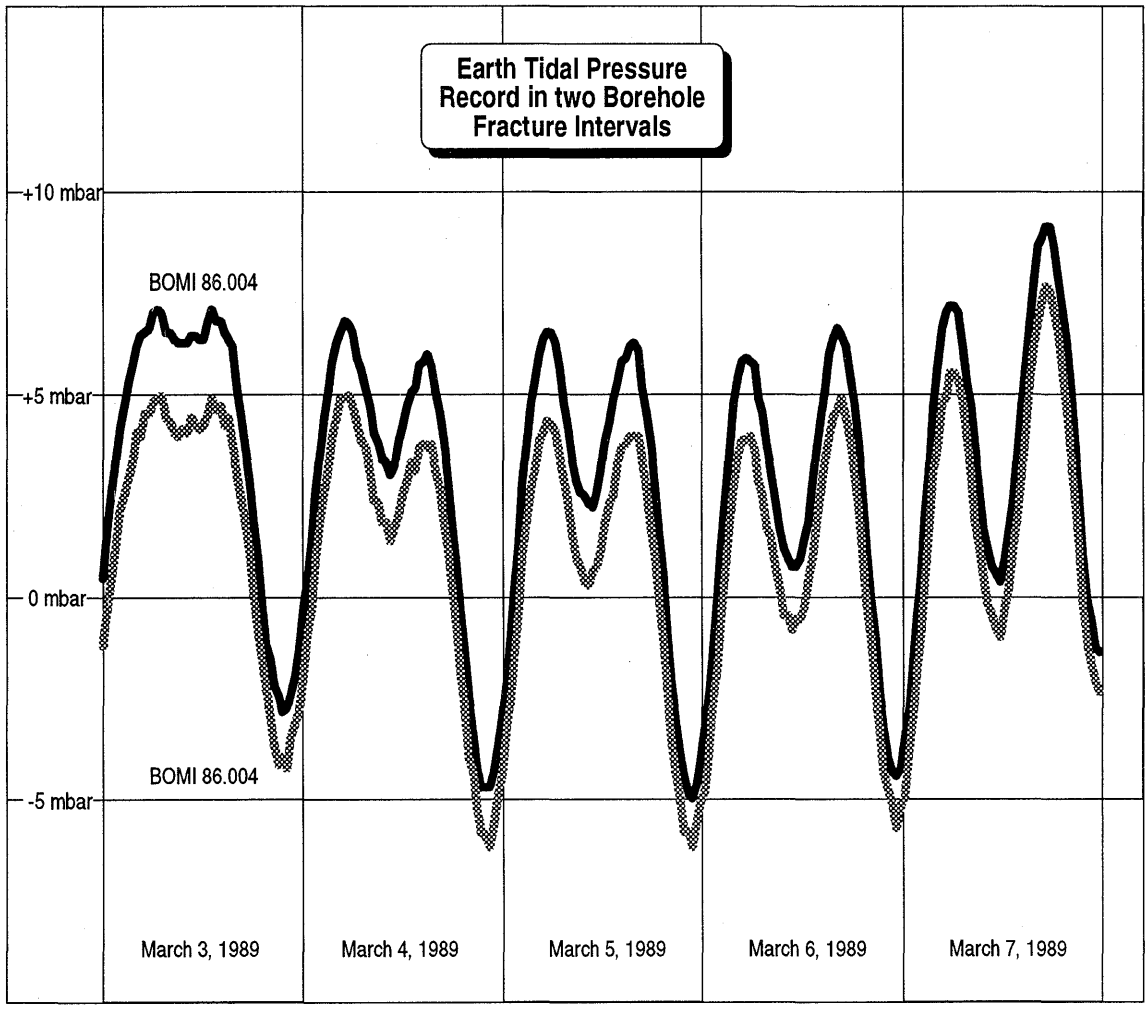

Fig. 3-10: Pressure oscillations due to earth tides.

Earth tide induced pressure waves are attenuated within the rock matrix with a penetration depth depending upon the hydraulic properties of the rock. Indeed, packed-off borehole sections, approximately 1 m away from the fracture, reveal much smaller pressure oscillations. It has been speculated (KUHLMANN et al., 1989) that earth tides might thereby enhance storage of solute in the rock matrix. So far, however, it was not possible to realistically estimate the magnitude of this effect, due to the unknown details of the pore space and effective pathways.

3.4 Characterization of Migration Site Groundwater

The chemical composition of the aqueous phase is of importance for the solubility, speciation and rock-solute interaction properties of dissolved radionuclides. Aside from the material properties (mineralogy, etc.) of the solid phase, detailed knowledge of the hydrochemical conditions in the natural groundwater is required to allow extrapolation of laboratory results to field conditions.

Water was sampled over several years under two main programmes:

- comprehensive analyses, including a large range of major and trace constituents, in order to understand the origin of the water (inlcluding mineral-groundwater interactions etc.), the capacity for pH and Eh buffering and to define a reference water for laboratory experiments.

- special analyses for specific questions, including dissolved gases to determine gas saturation and origin of the water, members of the U decay series for dating studies, colloid concentrations, microbes, and organics (as a basis for potential perturbations to the system).

3.4.1 Longtime Hydrochemical Monitoring

Hydrochemical Data: Extensive sampling at the migration site started in Summer 1986 and continued until spring 1988. The results available up to the Summer of 1987 are compiled by BAJO et al. in (NTB 88-23), and additional data are given in the Appendix of HOEHN et al. (NTB 89-15). The following conclusions can be drawn:

1. The chemical composition of the groundwater at the migration site does not show any significant spatial variability, i.e., within analytical errors, water sampled from all the boreholes as well as from the various discharge channels in the drift is of identical composition.

2. There are no significant temporal variations in chemical composition, i.e., neither long-term trends nor seasonal fluctuations can be detected.

Stable Isotope Data: A suite of water samples from the migration fracture was also analyzed for stable isotopes and tritium (i.e. δD, $\delta^{18}O$, and ^{3}H) in an attempt to obtain indications of hydraulic connections during the drilling of the first borehole (BOMI 86.004, from July 15-21, 1986). The major results can be summarized as follows:

1. No significant variation of δD, $\delta^{18}O$, and ^{3}H was detected during drilling (see also 3. below); average isotope composition was $\delta D = -98.2 \pm 1.4‰$ [SMOW], $\delta^{18}O = -13.72 \pm 0.03‰$ [SMOW] and 2.2 ± 0.6 TU)

2. The stable isotope composition (δD, $\delta^{18}O$) of the July 1986 samples is identical to that measured during the Winter of 1983/84 and plots exactly on a trend line defined by all available groundwater samples from the Grimsel rock mass (see Fig. 2-5).

3. The tritium content of samples taken during the winter of 1983/84 and summer 1991 (KRALIK, 1991) was between 0.6 to 0.9 ($\pm$ 0.6) TU. Samples from July 1986 and April 1988 (KRALIK, 1991) yielded consistently enhanced values of 2 to 4 TU. Obviously, the groundwater in the migration fracture was temporarily contaminated either by tritium containing drilling fluid or tritium containing injection water, respectively (see Section 7.1).

It may be concluded that, over a few years, there is most probably no significant variation of the isotopic abundances at the migration site and that, at least for this site, the excavation of the laboratory drift in the summer of 1983 did not noticeably lead to a major change in the local flow system. It bears noting that other groundwaters discharging to the tunnel are characterized by detectably different stable isotope contents.

3.4.2 Chemical Composition of Water in the Migration Fracture

A thorough characterization of the water in the migration fracture is given in BAJO et al. (NTB 88-23), EIKENBERG et al. (NTB 90-39) and AKSOYOGLU et al. (NTB 91-06). The range of the major constituents of the groundwater in the migration fracture (= MI water) are set out in Table 3-3. The water is poorly mineralized with an ionic strength of roughly 10^{-3} M. The pH is relatively high with a value of 9.6 and the CO_2-concentration is below the detection limit of 7×10^{-7} M.

Saturation indices, SI, were calculated for SiO_2, calcite and fluorite. For in-situ conditions (pH ~ 9.6, 12°C) the groundwater is saturated with respect to calcite (SI = -0.01) and slightly undersaturated with respect to fluorite (SI = -0.32). The small oversaturation of silicic acid calculated with respect to crystalline quartz (SI = +0.41) is probably due to the presence of amorphous silica which is metastable in this system. Detailed results from these applications are documented in BAJO et al. in (NTB 88-23) and EIKENBERG et al. (NTB 90-39).

Additional water speciation calculations using the geochemical code MINEQL/PSI are aimed at understanding the potential response of the Grimsel groundwater system to sometimes unavoidable changes of the water chemistry during certain experiments (see e.g. Section 7.2).

Table 3-3: Range of measured chemical composition of discharging groundwater from the migration fracture (MI water).

	pH		9.6 ± 0.2
	ionic strength [M]		0.0012
	Temperature [°C]		12 ± 1
	electrical conductivity [$\mu S\ cm^{-1}$]		103 ± 5
Cations :	Na^+	[M]	6.9×10^{-4}
	K^+	[M]	$3.8 - 5.0 \times 10^{-6}$
	Mg^{2+}	[M]	$5.4 - 6.2 \times 10^{-7}$
	Ca^{2+}	[M]	$1.3 - 1.4 \times 10^{-4}$
	Sr^{2+}	[M]	$1.8 - 2.0 \times 10^{-6}$
	Rb^+	[M]	2.5×10^{-8}
	Cs^+	[M]	5×10^{-9}
Anions :	SO_4^{2-}	[M]	$5.7 - 6.1 \times 10^{-5}$
	F^-	[M]	$3.3 - 3.6 \times 10^{-4}$
	Cl^-	[M]	$1.5 - 1.6 \times 10^{-4}$
	Br^-	[M]	3.8×10^{-7}
	I^-	[M]	1.0×10^{-9}
	alk [1]	[eq l^{-1}]	$4.2 - 4.5 \times 10^{-4}$
Other Species:	Si	[M]	2.5×10^{-4}
	CO_2	[M]	$< 7 \times 10^{-7}$
	O_2 [2]	[M]	$< 3 \times 10^{-8}$
	N_2	[M]	$7. - 8 \times 10^{-4}$
calculated[3]	HCO_3^- [4]	[M]	$2.7 - 2.9 \times 10^{-4}$
	CO_3^{--} [4]	[M]	$4.2 - 3.5 \times 10^{-5}$
	OH^- [4]	[M]	$1.2 - 1.3 \times 10^{-5}$
	$H_3SiO_4^-$ [4]	[M]	$4.2 - 4.1 \times 10^{-5}$
	H_4SiO_4	[M]	2.1×10^{-4}
total cations [5]		[eq l^{-1}]	$9.5 - 9.9 \times 10^{-4}$
total anions [5]		[eq l^{-1}]	$10.2 - 10.4 \times 10^{-4}$

1 alk = alkalinity

2 on site measurements at the Grimsel facility

3 calculated for relevant pH and temperatures (PHREEQE and MINEQL codes)

4 major species contributing to alkalinity

5 total anion concentrations are slightly smaller than the cation content; this might be caused by small systematic errors of the alkalinity which is particularly sensitive to precise pH determination in MI water.

Data are compiled from BAJO et al. in (NTB 88-23); EIKENBERG et al. (1990); AKSOYOGLU et al. (NTB 91-06), and KRALIK (1991).

3.4.3 pH and Redox Buffer Capacity of the Migration Fracture

It is intended that a variety of pH and Eh sensitive tracers (e.g. Se, Tc, Np) will be utilized in future field experiments. It is thus of paramount importance to identify the major components which exert control over these parameters in the migration site groundwater system. Not only will this enable a better understanding of the mechanisms involved in radionuclide retention within the fracture but, from a purely experimental point of view, it is necessary to have an idea of the pH and Eh buffer capacity of the rock-water system so that it can be ensured that the introduction of tracers does not change the existing (equilibrium) conditions.

The application of geochemical codes suggest that the pH of the rock-water system is well buffered by amorphous SiO_2 and calcite (EIKENBERG 1989, 1990). EIKENBERG (1989) also proposed field experiments to determine the pH buffering capacity of the mineral-MI water system in order to check the assumed equilibria conditions and the availability of sufficient $CaCO_3$ and SiO_2 for maintaining saturation.

Table 3-4: Concentrations of elements and species of interest to the definition of Eh in the migration site rock-water system (from ALEXANDER, 1991)

Species	Concentration [M]
Fe (total)	3×10^{-9}
Mn (total)	5×10^{-9}
Cu (total)	6×10^{-10}
U (total)	6×10^{-10}
SO_4^{-2}	6×10^{-5}
SO_3^{-2}	5×10^{-7}
HS^-	1×10^{-6}
$H_2S_{(g)}$	1×10^{-6}
NH_4^+	5×10^{-10}
NO_2^-	not detected
NO_3^-	1×10^{-6}
$O_{2(g)}$	$<3 \times 10^{-8}$

The Eh state of the system is much less clear, however, due to marked disequilibrium between various redox couples (ALEXANDER, 1991), a not unusual situation in natural waters (c.f. LINDBERG & RUNNELLS, 1984). In addition, all Eh electrode values have been discarded as meaningless due to the low concentration of electrode relevant species (see Table 3-3). Further, it is not yet clear if the relatively high O_2 concentrations in the groundwater are real or merely an artifact. Trace levels of O_2 of less than 0.1 ppb, measured by highly sensitive (ORBISPHERE) flow-through electrodes, should not be strictly taken as an indication of positive Eh in the groundwater because it cannot be excluded that these low O_2 levels may represent equipment contamination or leakage.

Unfortunately, an inability to rigorously define the Eh state of the groundwater also effectively precludes meaningful calculation of the Eh buffer capacity of the rock-water system. This in turn effectively restricts tracer migration experiments to the use of non-redox sensitive elements such as Na and Sr which are under investigation at present. ALEXANDER (1991) indicated that the appropriate solution to this problem is to define the Eh buffer capacity experimentally, using MI fracture material and groundwater and conducting the experiments under in situ conditions.

3.4.4 Investigations of Colloids, Organics and Microbes

The role of colloids, organics and microbes during radionuclide transport is, to date, only poorly understood. It was stated in Projekt-Gewähr (NAGRA NGB 85-09E) that *"....organic material can be produced as a by-product of microbial activity in the near-field but this could not be taken into account quantitatively in the base case as no data are available for calculations. For similar reasons, the effect of colloids on nuclide transport in the far-field and on uptake in the biosphere is not modelled in the base case".*

Certainly, since 1985, much work has been carried out on colloids, organics and microbes (see for example, the reviews of McCARTHY & ZACHARA, 1989) but many gaps remain. It is still uncertain to which degree radionuclide solubility, speciation and migration will be influenced by the combined (and single) effects of colloids, microbes and organics. To this end it became clear that these three groups should be studied in the MI experiment simply to ascertain whether they would significantly alter the results of particular tracer experiments. Further, because the MI system is so well characterized, it could prove possible to disentangle any effects of colloids, microbes and organics from other processes and thus provide generic information on the impact of these three groups on radionuclide migration and retardation.

The colloid concentration in the migration water was determined by various groups (see DEGUELDRE et al., 1987a,b; DEGUELDRE et al., 1989 and DEGUELDRE et al., NTB 90-01). There are approximately 10^{14} colloids l^{-1} of greater than 10 nm diameter, 10^{12} colloids l^{-1} of greater than 50 nm diameter and 10^{7} colloids l^{-1} of greater than 450 nm diameter. The mass of material involved is estimated to be around 50-100 ppb for the size range 10-450 nm or about 100-200 ppb if colloids greater than 450 nm are included. In general, the colloids consist of amorphous silica with smaller amounts of mica and calcium silicates although, in the larger colloid size range (100-1'000 nm), composite or aggregrate colloids, which include a significant organic component, have been identified (DEGUELDRE et al., 1987b). Although the significance of the colloidal population to radionuclide migration is still being debated for the MI water (see, for example VILKS & DEGUELDRE, 1991), it is clear that the large expenditure of effort on analytical methodology and technique development has been fruitful. Many of the lessons learned have already been employed in other areas of Nagra's colloid programme and have led to a greater degree of standardization of techniques internationally following a PSI/NAGRA/CEC intercomparison exercise on colloid sampling and characterization (DEGUELDRE et al., NTB 90-01). This effort will allow a more realistic intercomparison of colloid data.

To date, only two small scale studies have been carried out on the microbiology of the migration site (MILNER & CHRISTOFI, 1985; CHRISTOFI & MILNER, 1990). These report a maximum microbial population of $5x10^{6}$ bacteria l^{-1} consisting of aerobic and anaerobic heterotrophic spore-forming bacteria, heterotrophic iron precipitating bacteria, fungi, sulphate reducing bacteria, denitrifying bacteria and nitrifying bacteria. Although there are some inconsistencies between the above reports, it appears likely that the bacterial population is, at least in part, native and not wholly introduced by transport from soil horizons above or drilling operations. It is of note that the total organic carbon (TOC) levels of 0.5-0.9 mg l^{-1} (DEGUELDRE et al., NTB 90-01) which are present in the groundwater would, theoretically, support some two orders of magnitude more bacteria l^{-1} than are observed. This suggests that either part of the TOC is unavailable for microbial growth or that other factors are responsible for limiting the bacterial population. While the microbial populations are not high in the MI water, there is evidence to suggest that they might play an important (perhaps dominant) role in defining the redox state of the MI waters (ALEXANDER, 1991).

However, as an assessment of the microbial populations and activities on the solid phase (surface of fracture material, down-hole field equipment) remains to be done, the full significance of the microbiological impact on the migration experiment in particular (and radionuclide transport in general) remains speculative.

4 HYDRAULIC CHARACTERIZATION OF THE MIGRATION FRACTURE

In this section various hydrologic investigations performed at the migration site are reported. It was paramount to keep hydraulic and hydrochemical conditions at steady-state at all stages of the experiment. Therefore, severe experimental restrictions for exploration, testing and tracer analysis had to be maintained, occasionally demanding novel techniques. Additional experiments at nearby locations within the GTS, which are of interest in the context of solute migration in fractured Grimsel rock, are reported in FRICK et al. (1988) and ALEXANDER et al. (NTB 87-08).

4.1 Hydraulic Testing

The objective of the hydraulic testing programme carried out in the migration fracture was to determine the transmissivity and storage coefficient values of the migration fracture. These values and the porosity are necessary to predict the groundwater residence times for the planned tracer experiments. To maintain the hydrogeochemical condition within the fracture, no foreign water was injected (i.e. only discharge tests were performed). Drawdown and recovery of hydraulic potential (or pressure) were analyzed in the packed-off borehole intervals. The flow rates from the extraction borehole as well as the intersection of the migration fracture with the tunnel were carefully monitored. The hydraulic characterization of the site is documented in detail by HOEHN et al. (NTB 89-15).

It was intended to evaluate the results of relatively short (1 - 75 hours) hydraulic tests using standard hydrogeologic analysis. Such methods assume a homogeneous 2-dimensional aquifer of infinite extent. The drawdown effects from the nearby laboratory tunnel were not taken into account. To check the validity of these first analyses, more sophisticated analytical procedures were applied and an additional hydraulic test of a duration of 35 days was performed. The tests conducted solely for hydraulic characterization are tabulated in Table 4-1.

Initially, hydraulic pulse tests were performed in 1986, in the boreholes available at that time (BOMI 86.004 and 86.005; see also Table 3-2). The transmissivity values from these preliminary pulse tests revealed favorable conditions for the planned migration experiment. Therefore, six additional boreholes were drilled during 1987 to explore the fracture in more detail and to provide the facilities for injection, withdrawal, and monitoring of tracers.

Table 4-1: Hydraulic testing of the migration fracture

Preliminary Pulse Tests	
Borehole	Date
BOMI 86.004	25./26. Sept. 1986
BOMI 86.005	25./26. Sept. 1986

Constant–Drawdown Tests	
Borehole	Date
BOMI 86.004	6. Nov. 1986; 8. Dec. 1987
BOMI 86.005	16. Dec. 1986; 10. Dec. 1987
BOMI 87.006	9. Jul. 1987; 26. Aug. 1987
BOMI 87.008	28. Aug. 1987
BOMI 87.009	27. Aug. 1987
BOMI 87.010	31. Aug. 1987

Constant–Discharge Tests	
Borehole	Date
BOMI 86.004	9. Dec. 1987; 10. Dec. 1987
BOMI 87.009	1. Sept. 1987, Jan./Feb. 1989

Single Hole Dilution Tests	
Borehole	Date
BOMI 86.004	27. Oct. 1988
BOMI 87.006	25. Oct. 1988
BOMI 87.009	26. Oct. 1988; 21. April 1989

4.1.1 Equipment used for Hydraulic Testing

Systems of two (BOMI 87.008) and three (BOMI 86.004, 86.005, 87.006, 87.009, 87.010) inflatable packers were installed in six boreholes to isolate the fracture interval and an adjacent interval on each side of the fracture (see Fig. 3-6). Two boreholes (BOMI 87.007, 87.011) were isolated with mechanical packers during the hydraulic testing phase and later equipped with a 3- and 4-packer systems. Each of the isolated intervals in the borehole was equipped with two lines, one for measuring pressure and one as a flow line for injecting or withdrawing water (Fig. 3-7). During the hydraulic tests, piezoresistive pressure transducers were used to measure the pressures in the packed-off fracture intervals.

Three different devices were used at different times to measure withdrawal rates from the tested boreholes during the hydraulic testing phase. During the early tests, a balance measured the weight change versus time as water flowed from the flow line into a vessel. This system was used to measure discharge rates during the constant-pressure withdrawal tests performed in boreholes BOMI 86.004 and BOMI 86.005. An electromagnetic flow meter (FISCHER & PORTER) was installed to determine the flow rate during the constant-rate withdrawal tests in boreholes BOMI 86.004 and BOMI 87.009. A MICROMOTION (Model D12) flow meter was used to measure the flow rate during all other hydraulic tests.

The constant-pressure withdrawal tests were performed by fully opening a ball valve on the flow line from the fracture interval of the test borehole. Water was allowed to flow out under atmospheric pressure conditions and the changing flow rate was monitored. For the constant-rate tests performed in boreholes BOMI 86.004 and BOMI 87.009, a needle valve was manipulated to keep the flow rate constant as the pressure in the test interval dropped. For the long-term constant-discharge test in borehole BOMI 87.009 a Moineau pump (manufactured by WANGEN Pumps GmbH; Wangen, Bavaria) was used. Data collected during the hydraulic tests included pressure measurements in the fracture intervals of the tested borehole and of the observation boreholes, the flow rate from the tested borehole and, during later tests, the flow rate from the fracture into the drift. These data were collected and stored on site using a PC controlled data acquisition system.

Borehole instrumentation, measurement equipment and data acquisition for the hydraulic testing is described in detail by THORNE (1990a).

Examples of typical pressure interferences are illustrated elsewhere (e.g. FRICK et al., 1988; HOEHN et al., NTB 89-15; DAVEY et al., 1989). Short-term cross-hole testing of any borehole revealed no pressure response in BOMI 87.007 and BOMI 87.011. Testing BOMI 86.005 did not produce discernible pressure signals in any of the other boreholes due to the low transmissivity of its fracture interval (c.f. Table 4-2 and 4-3).

4.1.2 Methods Used for Hydraulic Test Interpretation

Two types of analyses for hydraulic tests were applied: a) single-borehole test analysis to obtain transmissivity values around the tested well, and b) cross-hole interference test analysis to obtain average transmissivities between various boreholes. For both types of tests several standard methods were used to calculate transmissivity (T) and the storage coefficient (S) from flow and pressure data. For the analysis, the following methods were utilized:

Flow-period, constant-drawdown (T):	JACOB & LOHMAN (1952)
Flow-period, constant-discharge (T, S):	COOPER & JACOB (1946)
Steady state (T):	e.g., LOHMAN (1972)
Recovery (T):	HORNER (1951)

Table 4-2: Calculated transmissivity values determined from single-hole tests

Tested Borehole	Test Date	Transmissivity (x 10^{-6} m^2 s^{-1}) Flow Period	Steady State	Recovery	Type of Test
BOMI 86.004	06/11/86	1.3	0.37	1.9	CDRT
	08/12/87	1.6	0.43	0.3 - 1.5	CDRT
	09/12/87	1.4	0.56	0.9 - 1.6	CDIT
	10/12/87	1.4	0.44	1.7	CDIT
BOMI 86.005	16/12/86	0.042	0.010	0.082	CDRT
	10/12/87	0.041	0.021	0.003 - 0.067	CDRT
BOMI 87.006	26/08/87	1.1	0.20	2.0	CDRT
BOMI 87.008	28/08/87	0.7 - 2.4	0.50	0.4 - 0.9	CDRT
BOMI 87.009	27/08/87	4.4	0.93	0.4 - 2.2	CDRT
	01/09/87	1.9	1.1	n.a.	CDIT
	12/01-09/03/89	1.5-1.7	n.a.	1.6-3.2	LT-CDIT [f]
BOMI 87.010	27/08/87	n.a.	0.54	0.3 - 4.9	CDRT

[f] for comparison, calculated transmissivities from the long-term (35 days), constant-drawdown test (LTCDIT), analysis by different methods (GEMPERLE, 1989)

n.a. not analyzed due to insufficient data quality

(based on flow-period data, steady-state assumption and recovery data of constant-drawdown (CDRT) and constant-discharge tests (CDIT) (compiled from Appendix B of HOEHN et al., NTB 89-15).)

The equations for the calculations and descriptions of the methods are compiled by HOEHN et al. (NTB 89-15). All these methods represent various solutions to the flow equation, assuming 2-dimensional flow in a homogeneous porous aquifer of infinite extent. Pressure data from observation boreholes as well as from the tested boreholes, allowed an additional determination of transmissivities by assuming steady-state flow conditions at the end of the flow-period. The method of HORNER (1951) was used for analysis of the pressure recovery data from both the tested and observation boreholes following the constant-drawdown tests. This method, like the one of (COOPER & JACOB, 1946) ideally assumes a period of constant-discharge. This introduces an error in the analysis, if steady-state conditions are not precisely met.

4.1.3 Results of Short-Duration Hydraulic Tests

Preliminary Pulse Tests were performed in the fracture interval at the two available boreholes, BOMI 86.004 and BOMI 86.005 during September 25 - 26, 1986. The tests were conducted by opening the flow line of the packed-off fracture interval for about 30 seconds to depressurize it and monitoring the pressure recovery after closing the flow line. The transmissivity values obtained from the pulse test were about $3 \times 10^{-6} m^2 s^{-1}$ for borehole BOMI 86.004 and $5 \times 10^{-8} m^2 s^{-1}$ for BOMI 86.005, well within the required range for the planned migration experiments.

Constant-Drawdown Tests (CDRT) were conducted in boreholes BOMI 86.004 and BOMI 86.005 during November/December 1986. After drilling the additional exploration boreholes more tests were performed in boreholes BOMI 86.004, 86.005, 87.006, 87.008, 87.009 and 87.010 during August 1987. Each borehole was tested by opening the flow line from the packed-off fracture interval and allowing the groundwater to flow out under atmospheric pressure. The flow rates were measured continuously by a balance. Pressures in the fracture intervals of the tested borehole as well as of all other boreholes were monitored by piezoresistive pressure transducers connected to a data logger. The discharge from the fracture into the plastic sheets along the drift wall (Fig. 3-5) was also monitored. The results of the CDRT are tabulated in Table 4-2 for the single-hole test and Table 4-3 for cross-hole tests.

Constant-Discharge Tests (CDIT): Because of the uncertainties in the use of the (COOPER & JACOB, 1946) and (HORNER, 1951) methods of analysis for constant-drawdown tests, constant-discharge tests were conducted in the two boreholes BOMI 86.004 and BOMI 87.009. These tests are more difficult to perform as the flow rate must be controlled during the entire test and kept constant under changing interval pressure conditions. However, they have an advantage over constant-drawdown tests in that they yield a more reliable analysis of observation borehole data. Constant-flow from the tested borehole was maintained by manually regulating a control valve, while continuously monitoring the flow rates measured by MICRO MOTION flowmeters. The results of the CDIT are also tabulated in Table 4-2 for the single-hole tests and Table 4-3 for the cross-hole tests.

The results presented in Table 4-2 reveal no significant discrepancy between constant-drawdown and constant-discharge tests. Results obtained from the steady-state data are listed merely for completeness. While they can be used for a rough estimation of the transmissivity, the flow-period and recovery data are more reliable.

The variation of the calculated transmissivities for the same hydraulic connection in the cross-hole tests can be taken as a measure of either the spatial heterogeneity of the fracture or the experimental error of the applied method. It is interesting to observe no significant difference of transmissivity among all the various boreholes.

In view of a potential influence from the laboratory tunnel the small variability of transmissivity is surprizing. On the basis of these data, the apparent homogeneity of the cross-hole transmissivities indicates that the tested section of the migration fracture, on a scale of 2 - 17 m, can be characterized by a rather homogeneous average transmissivity. By taking flow-period data only (the scatter for steady-state and recovery data is substantially larger), calculated transmissivities are all within a factor of 2 of the average value from 35 cross-hole tests (mean $\pm 1\sigma$ of transmissivity is $2.2 \pm 0.7 \times 10^{-6} m^2 s^{-1}$; see also Section 4.1.6).

Table 4-3: Calculated transmissivity values from cross-hole interference tests

Stimulus Borehole	Observation Borehole	Transmissivity (x 10^{-6} m^2 s^{-1}) Flow Period	Steady State	Recovery	Type of Test
BOMI 87.009	BOMI 87.009	3.2[a]	1.0[a]	0.4-2.2	SIH-CDRT+CDIT
BOMI 87.009	BOMI 87.009	1.5-1.7[b]	n.a.	1.6-3.2[b]	LT-CDIT
BOMI 86.004	BOMI 87.009	2.2	2.2	n.a.	CRH-CDRT
BOMI 86.004	BOMI 87.009	1.2	1.7	1.6	CRH-CDIT
BOMI 86.004	BOMI 87.009	1.8	2.4	1.0-2.0	CRH-CDIT
BOMI 87.009	BOMI 86.004	2.4	2.0	9.0-20.0	CRH-CDRT
BOMI 87.009	BOMI 86.004	1.9	2.2	n.a.	CRH-CDRT
BOMI 87.009	BOMI 86.004	1.4-2.0[b]	n.a.	3.0[b]	CRH-LT-CDIT
BOMI 86.004	BOMI 86.004	1.4[a]	0.37[a]	1.9[a]	SIH-CDRT+CDIT
BOMI 86.004	BOMI 87.006	2.2	2.3	n.a.	CRH-CDRT
BOMI 86.004	BOMI 87.006	1.2	1.8	1.8	CRH-CDIT
BOMI 86.004	BOMI 87.006	1.8	2.5	1.2	CRH-CDIT
BOMI 87.006	BOMI 86.004	2.1	2.7	1.7	CRH-CDRT
BOMI 87.006	BOMI 87.006	1.1	0.20	2.0	SIH-CDRT
BOMI 87.006	BOMI 87.009	2.1	1.8	1.6	CRH-CDRT
BOMI 87.009	BOMI 87.006	4.2	1.1	0.7-2.0	CRH-CDRT
BOMI 87.009	BOMI 87.006	1.9	1.3	n.a.	CRH-CDIT
BOMI 87.009	BOMI 87.006	1.4-2.0[b]	n.a.	1.4[b]	CRH-LT-CDIT
BOMI 87.009	BOMI 87.009	3.2[a]	1.0[a]	0.4-2.2	SIH-CDRT+CDIT
BOMI 87.009	BOMI 87.009	1.5-1.7[b]	n.a.	1.6-3.2[b]	LT-CDIT
BOMI 87.009	BOMI 87.008	2.3	5.8	2.0-3.0	CRH-CDRT
BOMI 87.009	BOMI 87.008	3.0	9.6	n.a.	CRH-CDIT
BOMI 87.009	BOMI 87.008	1.6-1.9[b]	n.a.	2.6[b]	CRH-LT-CDIT
BOMI 87.008	BOMI 87.009	3.9	8.2	1.7	CRH-CDRT
BOMI 87.008	BOMI 87.008	0.7-2.4	0.50	4.0-9.0	SIH-CDRT

[a] average of all available single-hole transmissivities from Table 4-2

[b] results from various analyses of the long-term, constant discharge test (GEMPERLE, 1989)

n.a. not analyzed due to insufficient data quality

Data are based on flow-period data, steady-state assumption and recovery data of constant-drawdown (CDRT) and constant-discharge tests (CDIT) (compiled from Appendix B of HOEHN et al., NTB 89-15). Single hole data (SIH) and data from the long-term constant-discharge test (LTCDIT) in BOMI 87.009 are given for comparison.

Table 4-3: Calculated transmissivity values from cross-hole interference tests

Stimulus Borehole	Observation Borehole	Transmissivity (x 10^{-6} m^2 s^{-1}) Flow Period	Steady State	Recovery	Type of Test
BOMI 86.004	BOMI 86.005	2.0	n.a.	n.a.	CRH-CDRT
BOMI 86.004	BOMI 86.005	1.7	3.3	2.0	CRH-CDRT
BOMI 86.004	BOMI 86.005	1.2	2.5	1.0-2.0	CRH-CDIT
BOMI 86.004	BOMI 86.005	1.8	3.4	1.0-3.0	CRH-CDIT
BOMI 86.005	BOMI 86.004		no response		CRH-CDRT
BOMI 86.004	BOMI 87.010	2.7	9.6	1.8	CRH-CDRT
BOMI 86.004	BOMI 87.010	2.3	7.4	2.0	CRH-CDIT
BOMI 86.004	BOMI 87.010	2.3	10.0	2.0	CRH-CDIT
BOMI 87.010	BOMI 86.004	3.0	11.0	3.2	CRH-CDRT
BOMI 87.009	BOMI 87.010	2.1	6.2	1.0-9.0	CRH-CDRT
BOMI 87.009	BOMI 87.010	2.7	8.3	n.a.	CRH-CDIT
BOMI 87.009	BOMI 87.010	1.9-2.0[b]	n.a.	1.6[b]	CRH-LT-CDIT
BOMI 87.010	BOMI 87.009	3.0	9.6	3.0	CRH-CDRT
BOMI 87.009	BOMI 86.005	2.3	2.9	9.0-20.0	CRH-CDRT
BOMI 87.009	BOMI 86.005	2.0	3.2	n.a.	CRH-CDIT
BOMI 87.009	BOMI 86.005	1.5[b]	n.a.	1.6[b]	CRH-LT-CDIT
BOMI 86.005	BOMI 87.009		no response		CRH-CDRT
BOMI 87.006	BOMI 87.010	2.1	1.8	1.6	CRH-CDRT
BOMI 87.006	BOMI 86.005	4.2	1.1	0.7-2.0	CRH-CDRT
BOMI 86.005	BOMI 87.006		no response		CRH-CDRT
BOMI 87.010	BOMI 86.005	n.a.	7.8	n.a.	CRH-CDRT
BOMI 86.005	BOMI 87.010		no response		CRH-CDRT

[a] average of all available single-hole transmissivities from Table 4-2

[b] results from various analyses of a long-term, constant discharge test (GEMPERLE, 1989)

n.a. not analyzed due to insufficient data quality

Data are based on flow-period data, steady-state assumption and recovery data of constant-drawdown (CDRT) and constant-discharge tests (CDIT) (compiled from Appendix B of HOEHN et al., NTB 89-15). Single hole data (SIH) and data from the long-term constant-discharge test (LTCDIT) in BOMI 87.009 are given for comparison.

Storage coefficients were calculated using the (COOPER & JACOB, 1946) approach. The results are listed in Appendix B1 and B2 of HOEHN et al. (NTB 89-15). The calculated values are very sensitive to the data quality and the position of the fitted regression lines in the pressure versus log t diagrams. Consequently, extrapolated times are inherently uncertain. In addition, basic assumptions for a strict application of these methods may not be fully satisfied and so the obtained storage coefficients cover a relatively broad range of 10^{-4} to 10^{-8} with mean values of 10^{-5} ($\pm$ an order of magnitude) for all boreholes.

Frequency Domain Analysis: Single-hole data from a set of three hydrotests performed in BOMI 86.004 in 1987 were re-analyzed by transforming the time series of the head disturbance and the response of the aquifer to the frequency domain and then calculating the transfer function of these data (MARSCHALL & BARCZEWSKI, 1990). This transfer function, defining a relationship between head disturbance in a well and the response of the aquifer system during a hydrotest, does not depend on initial conditions but only on the geometry and the hydraulic properties of the aquifer. In other words, analyses of flow and pressure data are always possible. It is not limited any more by the analytical solutions presented in Section 4.1.2 which depend on the assumption of either constant-flow or constant-pressure conditions.

Initial estimates of the transmissivity (T) based on flow-period data from constant-drawdown and constant-discharge single-hole tests were between 1.3×10^{-6} and $1.6 \times 10^{-6}\ m^2s^{-1}$. Analysis using the frequency domain approach yielded a transmissivity value of $1.3 \times 10^{-6}\ m^2s^{-1}$. Both evaluations yielded the same result, indicating a good data quality. Straight-line fitting of data in the log t diagrams was justified and no systematic error was introduced by assuming either constant-flow or constant-pressure conditions. A substantially different result would have been rather unexpected as this approach is also based on the same assumption of a homogeneous 2-dimensional aquifer of infinite extent).

The method seems to provide more reliable values for storage coefficients. Initial estimates for single-hole constant-discharge tests in BOMI 86.004 were around 2.5×10^{-7}. Frequency domain analysis yielded 1.0×10^{-6}. This is close to 1.3×10^{-6}, the mean storage coefficients of all conventional cross-hole data calculated for this borehole.

4.1.4 Results of a Long-Term Constant-Discharge Test (LTCDIT)

The objectives of the long-term (pumping duration of 35 days) test were to examine the potential existence of flow boundaries within the fracture system, to examine the effects of long-term pumping on outflow to the tunnel, and to analyze the pressure-recovery data using an analytical model developed specifically for fractured rock (BOURDET & GRINGARTEN, 1980).

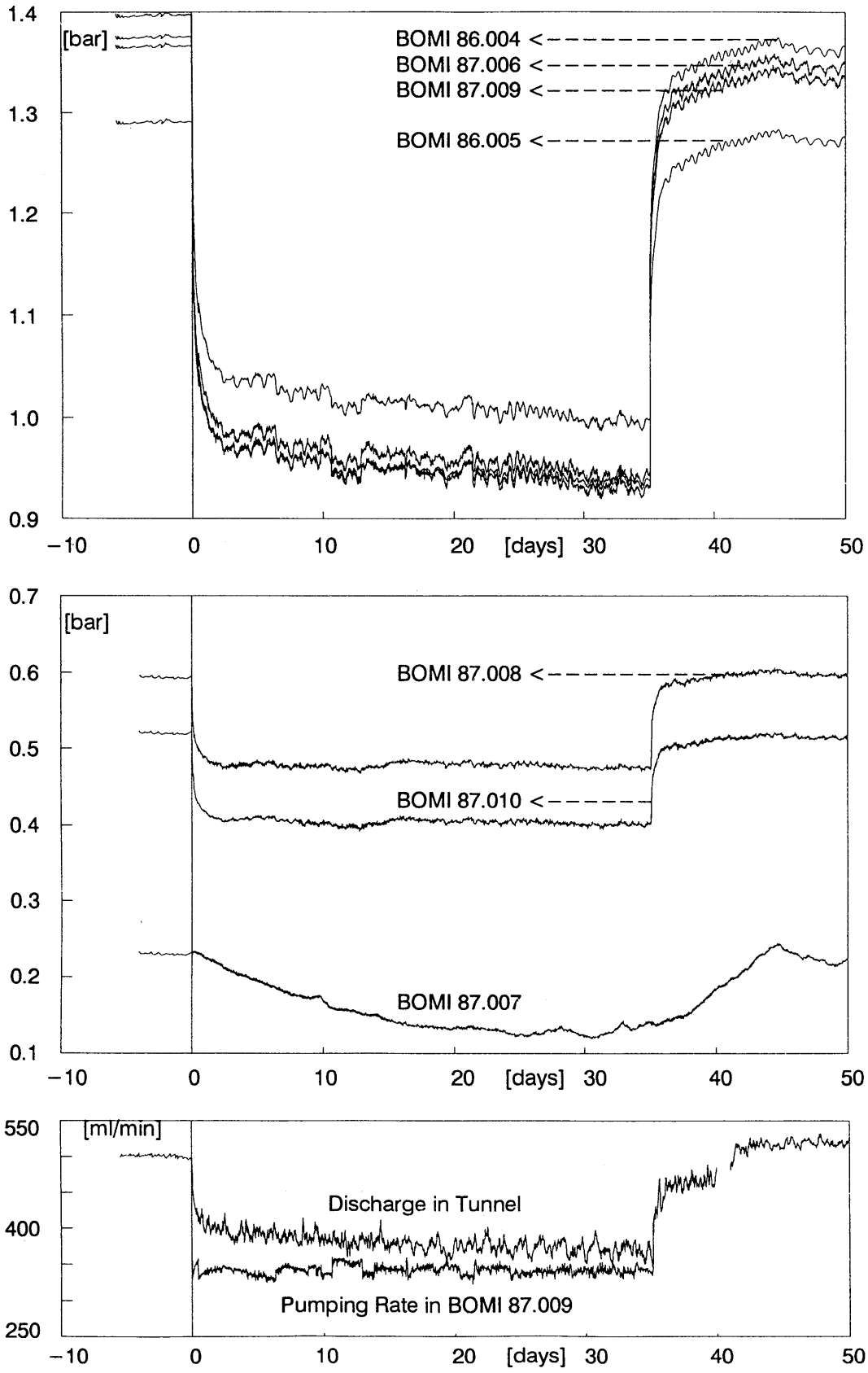

Fig. 4-1: Pressure and flow response during the long-term constant discharge test in BOMI 87.009

Initial flow rates, measured immediately after opening the flow line from the packed-off interval, were in the order 2000 ml min^{-1}. This was substantially more than the total steady outflow from the fracture to the tunnel (520 ml min^{-1}). It was estimated that a pump rate of about 100 - 400 ml min^{-1} might yield a sufficient pressure response in all the boreholes without excessively draining the site. It was feared that discharge at a rate of more than 520 ml min^{-1} from BOMI 87.009 might practically stop any outflow from the fracture to the tunnel and lead to long-lasting de-saturation of a large zone around the tunnel. As this would be undesirable from a chemical standpoint, it was decided to limit the outflow from this interval.

The pump rate for the initial 3 minutes of the test was set to approximately 150 ml min^{-1}. As this rate was unstable (due to the employed pump) the discharge was immediately increased and quickly stabilized at 340 ± 10 ml min^{-1}. Pressure and flow data of the pumped borehole were recorded during drawdown. Pressure recovery following the flow-period was monitored for an equal period of time. Additionally, pressure data for each of the observation boreholes and the outflow from the fracture to the tunnel were measured. The observed pressure and flow responses during this long-lasting hydrotest are illustrated in Figure 4-1.

All pressure and flow data obtained during the flow-period and the subsequent pressure recovery are listed in the report of GEMPERLE (1989). The drawdown in the tested borehole BOMI 87.009 caused a rapid pressure response in all boreholes, except BOMI 87.011 and BOMI 87.007 (see Fig. 4-1). The latter reacted very slowly while BOMI 87.011 did not respond at all. During pumping of 340 ± 10 ml min^{-1} from BOMI 87.009 the total outflow from the migration fracture to the tunnel dropped from initially 520 ± 10 to 360 ± 10 ml min^{-1} at the end of the 35-day pumping period (see Fig. 4-1). During the first 33 hours of the pumping period the outflow decreased by approximately 100 ml min^{-1}. Pressure recovery produced a corresponding increase over a similar time.

The measured data were analyzed for transmissivity using standard THEIS type curve-matching procedure and the JACOB straight-line approximation (GEMPERLE, 1989). While the THEIS method of analysis for transient conditions was developed for a homogeneous, 2-dimensional infinitely extending aquifer and constant-discharge (radial flow) from an infinitely small pumping well, the JACOB approach is only valid for simplified well functions (steady-state flow). Resulting transmissivity values and storage coefficients are presented in Table 4-3.

One of the goals for this test was to check for boundary effects. Typical constant-head boundary effects were not obvious but the existence of several impermeable (no-flow) boundaries in the water-bearing fracture at a distance of 25 - 30 m from the tested borehole were indicated. However, from the evaluations of GEMPERLE (1989) it was not clear whether these phenomena could be attributed to the existence of the nearby tunnel.

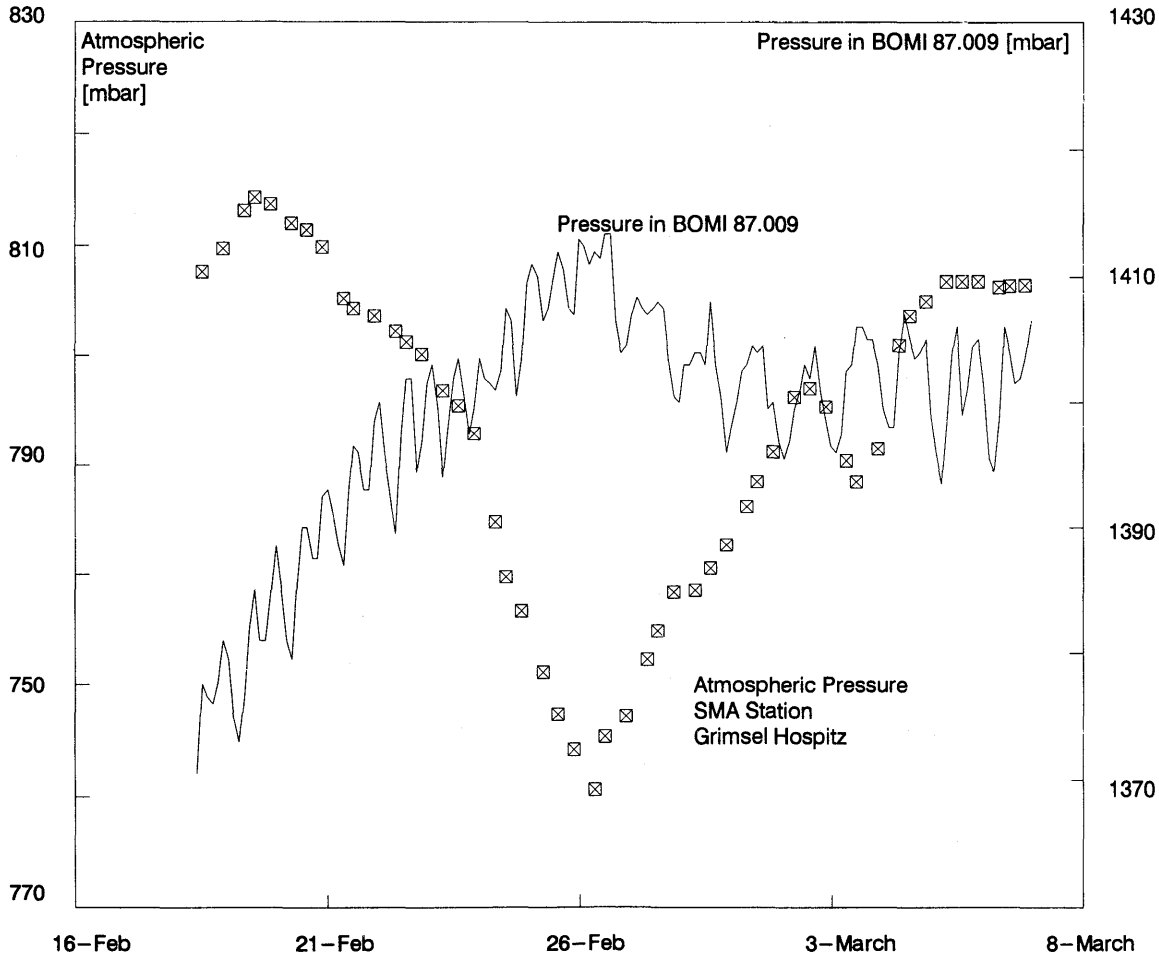

Fig. 4-2: Pressure data from the final stage during recovery after the long-term constant-discharge test are shown. The oscillations are caused by earth tides. The pressure drop in the borehole is an effect due to an increase of barometric pressure. (Barometric data by courtesy of the Swiss Meteorological Survey SMA).

A double-porosity analytical model for fracture flow (BOURDET & GRINGARTEN, 1980) was applied to analyze the early-time recovery data of the long-term constant-discharge test (LTCDIT). The analysis provided transmissivity values around $1.8 \times 10^{-6} m^2 s^{-1}$ for the fracture. The hydraulic conductivities for the rock matrix were in the order of $10^{-12} m\ s^{-1}$. Resulting storage coefficients were in the range of 0.7×10^{-6} to 2.1×10^{-6} for the fracture and 1.6×10^{-6} to 12×10^{-6} for the rock matrix. It should be mentioned, however, that the double-porosity fracture-flow model provides only one possible approach to interpret the observed responses, i.e. solutions are not unique for the observed pressure responses.

During pressure recovery following the long-term constant-discharge test pressure oscillations due to earth tides were observed (Fig. 4-2). Additionally, a phenomenon due to barometric effects was noticed. A pressure drop of 12 mbar, which affected all (except BOMI 87.011) borehole intervals, was observed during the last 10 days of monitoring (Fig. 4-2). This can be explained by a storm of the end of February 1989 which registered a barometric pressure low of about -50 mbar. The influence of atmospheric pressure on hydraulic pressure in wells is known (e.g. DAVIS & DeWIEST, 1966). As the atmospheric pressure increases the water levels in wells drilled into confined aquifers will be lowered. Pressure changes on the aquifer caused by barometric effects are distributed partly on the aquifer material and partly on the water. Therefore, the observed pressure drop in the tested boreholes (caused by the increase of the barometric pressure) outranged the simultaneously increasing pressure during the final recovery period of the test.

4.1.5 Hydraulic Properties of the Rock Matrix

A hydraulic pulse test was performed in August 1987 in the unfractured granodiorite in the deepest interval of borehole BOMI 87.009 (between the deepest packer and the end of the borehole, usually designated interval I, see Fig. 3-7). Applying the approach of SAGEEV (1986) a hydraulic conductivity of 1.3×10^{-11} m s^{-1} and a storage coefficient of 3.5×10^{-7} were obtained for the country rock.

Application of a double-porosity fracture flow model (BOURDET & GRINGARTEN, 1980) to recovery data obtained form the long-term constant-discharge test (GEMPERLE, 1989) also yielded approximate figures for matrix conductivity and storage coefficients. In the area of boreholes BOMI 86.004, BOMI 87.006 and BOMI 87.009 the inferred hydraulic conductivity of the matrix was around 10^{-12} m s^{-1}. Derived storage coefficients for the matrix were between 1.6×10^{-6} and 1.2×10^{-5}.

Both types of analyses result in the same hydraulic parameters for the solid rock matrix within the experimental error. The calculated conductivity of the matrix is 8 to 9 orders of magnitude smaller than the conductivity of the fracture, assuming a fracture width in the range of 1 - 10 mm. This large conductivity difference between the fracture and the matrix allows us to neglect hydrodynamic flow from the fracture to the matrix in transport models (see also Section 3.3.2).

An anomalous pressure field exists in the sparsely fractured rock mass on both sides of the migration shear zone. The borehole intervals between the tunnel and the fracture, as well as in the deepest intervals (intervals I; see Fig. 3-7), exhibit substantially lower pressures than measured in the fracture interval itself (see also Section 3.3.1). In Table 4-4 a typical pressure recording (February 23, 1989) from all borehole intervals is presented.

Table 4-4: Typical hydraulic pressures from the migration fracture as well as from the adjacent rock mass during the final recovery period of the long-term, constant-discharge test (February 23, 1989).

	Pressure (bar)			
Borehole	Interval I	Interval II	Interval III	Interval IV#
BOMI 86.004	0.95	1.32f	<-0.2§	-
BOMI 86.005	0.65	1.25f	<-0.2§	-
BOMI 87.006	0.52	1.27f	<-0.4§	-
BOMI 87.007	0.18f	-0.42	-0.61	-
BOMI 87.008	0.56f	0.46	-	-
BOMI 87.009	0.97	1.29f	<-0.1§	-
BOMI 87.010	0.18	0.53f	<-0.06§	-
BOMI 87.011	0.40f	0.00	-0.48	-0.21

f fracture interval

§ limit on pressure gauge, actual pressure could be smaller

interval #I is the deepest borehole section (see Fig. 3-7)

4.1.6 Assessment of Hydrotest Analyses

The objective of hydrotest analyses is to provide input for the hydrodynamic characterization of the migration fracture. Accuracy and completeness of these attempts are clearly limited by the choice of conceptual models or system boundaries. To some degree, the testing procedure may also influence the outcome of hydrotest analyses, however, the existing equipment appears to be adequate for providing reliable data.

Preliminary Conclusions: The results of single-hole analyses of the hydrotests seem to provide information on the heterogeneous transmissivity distribution, while the results from cross-hole analyses reveal a rather uniform transmissivity on the scale of the distance between the various boreholes (2-15 m). This "average" transmissivity value of 2×10^{-6} m^2 s^{-1} could be interpreted tentatively to represent the characteristic transmissivity of one or a few dominant channels within the migration fracture. Such preferential pathways are not necessarily intersected by the existing boreholes.

The number of available boreholes was kept relatively small by various reasons. Thus, the density of available information on local hydraulic parameters remains limited and construction of hydrodynamic models must include a great deal of interpolation and expert judgement. The demands on the validity of a model depends on the different applications. So it is entirely possible, for instance, that a model is able to predict reasonably well local hydraulic pressures, while it turns out to provide an inadequate basis for modeling transport. Then the hydrodynamic model should be improved by including also results of conservative tracer testing.

Conceptual Model Considerations: It is necessary to emphasize again that the results from the various hydrotest analyses may depend on the the general conceptual model of groundwater flow at the migration site:

- The constant-drawdown tests, the constant-discharge tests, and the long-term constant-discharge test were analyzed on the assumption of a 2-dimensional flow in a homogeneous porous medium of infinite extent (single-porosity flow concept).

- The long-term constant-discharge test was additionally evaluated using a double-porosity fracture flow model (BOURDET & GRINGARTEN, 1980). The data from this test were also analyzed for boundary effects (LOHMAN, 1972). The analysis of test data cannot be considered to yield a unique solution since the evaluated early-time boundaries and double-porosity behavior could both provide reasonable interpretations of the observed responses. It is also difficult to choose one interpretation over another. However, application of the dual-porosity fracture flow model to fractured granitic environments (GRINGARTEN, 1982) similar to the migration site yielded comparable results.

Hydrotest data analyses based on the two concepts (2-dimensional flow in a homogeneously porous aquifer and double-porosity fracture flow) yielded almost identical transmissivity values and storage coefficients. It appears that both conceptual models are suitable to characterize the hydraulics of the migration fracture sufficiently. However, application of more sophisticated (e.g., heterogeneous) models and more refined analytical methods may lead to an even better understanding of the groundwater flow in the fracture.

4.2 Hydrodynamic Modeling of the Migration Zone

The prime objective was to have a hydrodynamic model available as the basis for modeling solute transport. Various modeling efforts were carried out for the following purposes:

1) for selecting meaningful borehole positions (i.e. intersections with fracture) during the drilling campaigns

2) to interpret experimental results from hydraulic testing

3) to provide input, such as flowpaths and flow velocities for transport modeling

4) to assist in the planning and setup of conservative tracer breakthrough experiments

An overview of several hydraulic models using data from hydraulic testing at the migration site are presented in the following sections. Some of them were thought to provide alternative views and concepts, others were mainly used to estimate the potential impact from unknown boundary conditions or to check the validity of conventional hydrotest analyses. However, none of them was applied as a basis for modeling tracer transport.

4.2.1 The PSI Steady-State Model (HERZOG Model)

This model is described by HERZOG (NTB 89-16). Here, the migration fracture is modeled as a 2-dimensional, isotropic, heterogeneous equivalent porous medium. To develop a sufficiently high degree of detail, a hierarchical approach was followed. The boundaries for a local model (which comprised the immediate vicinity of the laboratory tunnel at the migration site) were selected by solving first the equations for a larger, regional model of coarser discretization (Fig. 4-3). The transmissivity field, ranging from 1.5×10^{-6} to approximately 1×10^{-8} m^2s^{-1} (and substantially less considering also the no-flow boreholes BOMI 87.007 and BOMI 87.011) of the model was based on the data obtained from the single-borehole tests described in Section 4.1.

The computed results for the regional model are presented in Figure 4-3. The local model results, assuming a homogeneous and heterogeneous transmissivity distribution, are presented in Figure 4-4a and Figure 4-4b, respectively. The later results match the measured pressure data at steady-state conditions, except for the two non-flow boreholes BOMI 87.007 and 87.011. The first pilot tracer test configurations were arranged based on these model predictions.

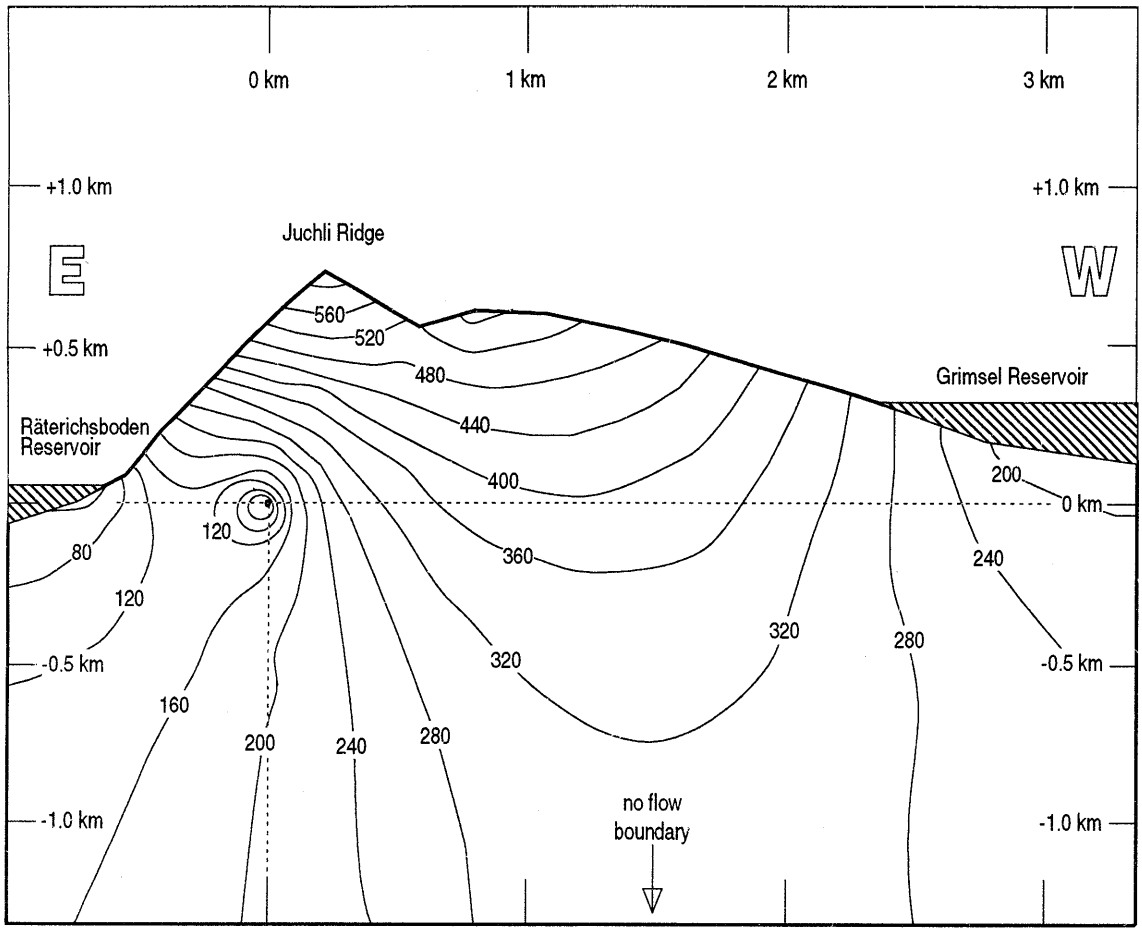

Fig. 4-3: Distribution of the hydraulic head in the far-field hydrodynamic model of HERZOG (NTB 89-16).

4.2.2 Model of a 2-D Network of Conductive Elements (The LBL Model)

An alternative approach to analyze flow and transport in fractured rock assumes that the flow of groundwater takes place in a poorly connected network of fractures rather than in a continuous porous aquifer. A new type of model for fracture hydrology has been developed at Lawrence Berkeley Laboratory (DAVEY et al., 1989). Their so called equivalent discontinuum model represents the discontinuous nature of the aquifer as a partially filled lattice of conductive elements. Initially a base model is developed based on geological and geophysical data to identify regions which are conducting groundwater. The orientation of conducting channels is also based on geological information of the site. The base model is continually modified by removing some of the conductive elements until it behaves like the observed natural system. The method used for modification is a statistical inverse technique called simulated annealing.

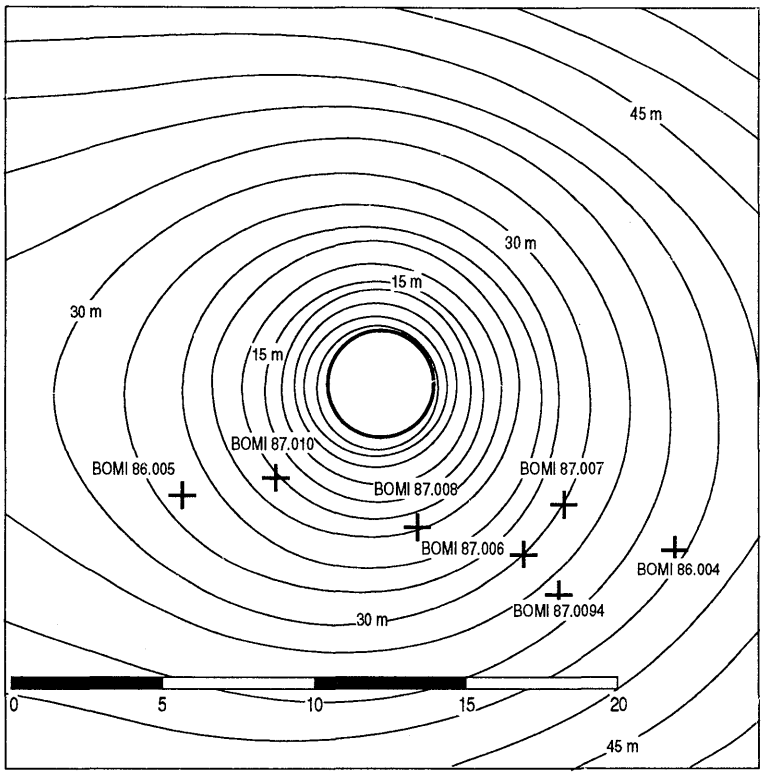

Fig. 4-4a: Potential field for the homogeneous model (from HERZOG, NTB 89-16)

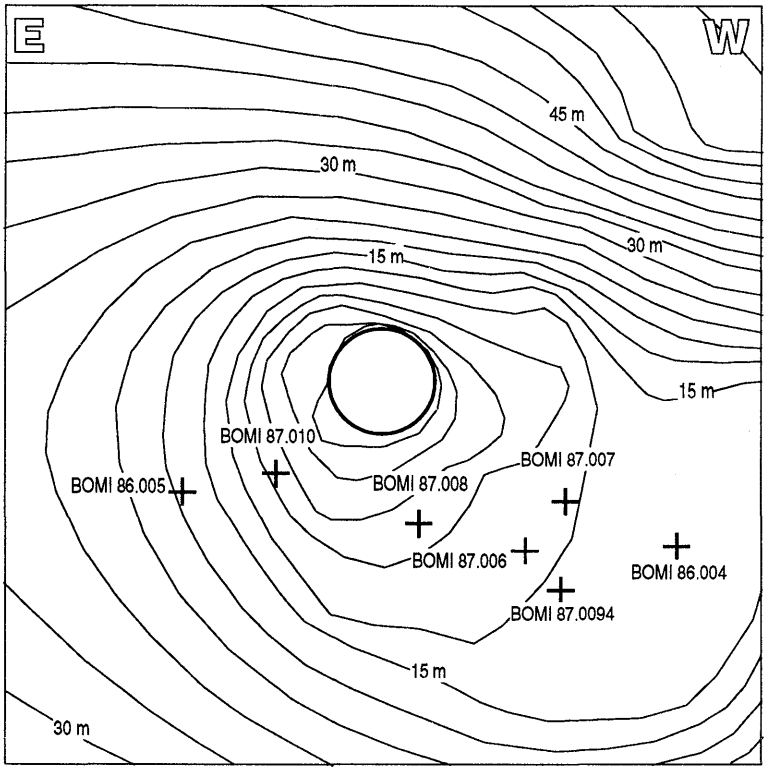

Fig. 4-4b: Heterogeneous model; all wells closed (from HERZOG, NTB 89-16

The migration site provided an unique opportunity to develop a model using geological information and hydrologic field data. The annealing algorithm was used five times to find steady-state configurations which matched the observed pressure and flow data from the migration site. (The model was not tested with tracer test data). The transient response of a system is more sensitive to the distribution of hydraulic conductivity than the steady-state response. Theoretically this makes the transient annealing more attractive. However, simulating the hydrotests could not reproduce the observed field data in the low permeable zone around BOMI 87.007 and BOMI 87.011. This indicates that a transient model defined by uniformly conductive elements probably may not adequately describe flow in the migration fracture. A model with elements of variable permeability under development.

4.2.3 Development of Type Curves using the Code NAMMU

The code NAMMU (Numerical Assessment Method for Migrations Underground; AERE Harwell, United Kingdom Atomic Energy Authority) was applied to compute type curves for constant-discharge tests in a homogeneous 2-dimensional aquifer including wellbore storage in the test interval and effects from the nearby laboratory tunnel (WYSS, 1990). The computed type curves, generated by simulation of discharge tests, varying the transmissivity values and storage coefficients, show a strong influence of the tunnel which causes steady-state flow conditions after a short time (in the order of 1000 seconds depending on the transmissivity). Evaluation of the data from the long-term constant-discharge test revealed transient flow conditions, even after a pumping period of 30 days. The test data did not match the generated type curves. Therefore, the applied homogeneous 2-dimensional model appeares not to be suitable to describe transient phenomena of the migration fracture.

4.2.4 Development of a 2-D Model for Steady-State and Transient Conditions

A model was developed (WYSS, 1990) for heterogeneous, 2-dimensional flow in the water-bearing migration fracture based on the previously obtained spatial parameter (T and S) distribution from single-hole and cross-hole analysis and the long-term constant-discharge test in BOMI 87.009. The results from the regional model (HERZOG, 1989) served as boundary conditions to the local model (Fig. 4-3).

Calibration resulted in an excellent match of predicted and observed steady-state pressures in the borehole intervals (except for the no-flow wells BOMI 87.007 and BOMI 87.011) as well as the monitored discharge rate to the tunnel. However, a simulation of the long-term constant-discharge test does not match satisfactorily the test data. Although the poor match may be due to inadequate choice of parameters or model boundaries, it is more likely that it can be attributed to the incapability to take into account the high degree of heterogeneity in the fracture.

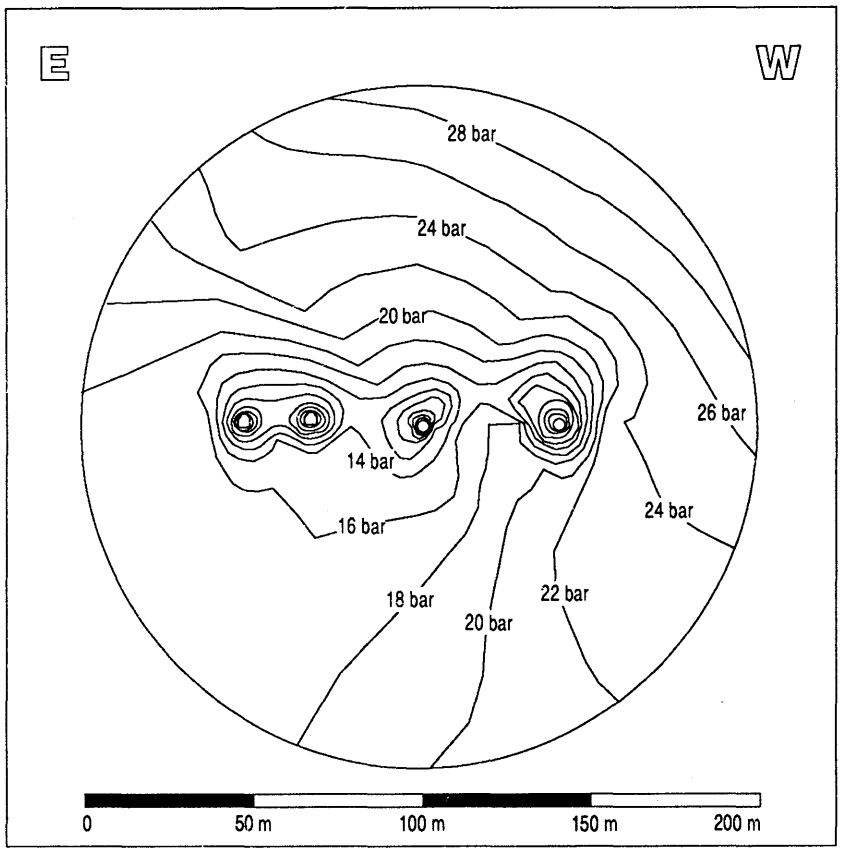

Fig. 4-5: Distristribution of the hydraulic head for steady-state conditions in the vincinity of the Grimsel Test Site. The tunnels in the central part are (from left to right) Ventilation Drift, Migration Drift, Main Access Tunnel, and Cable Tunnel (WYSS, 1990)

4.3 Tracer Dilution Experiments with the Single-Borehole Probe

Tracer dilution methods in packed-off borehole intervals can be utilized to estimate the local specific discharge and flow direction of groundwater. These values are used for estimating the groundwater flow velocity vector. A convenient tool to measure tracer dilution in a borehole is the Single-Borehole Probe (SBP) developed by the GSF Institute for Hydrology (Munich-Neuherberg). The Single-Borehole Probe was originally built for directional dilution tests in screened vertical observation wells in porous aquifers. It allows one to inject and to measure radioactive tracers downhole. The SBP was installed in boreholes of the migration fracture for the purpose of evaluating flow rates in *natural gradient tests* (i.e. testing the radial undisturbed flow field around the laboratory tunnel) and *monopole tests* (i.e. negligible mass injected into the radially converging flow into a pumped borehole; cf. also Fig. 6-2).

Table 4-5: Test arrangements and parameters for single-hole dilution tests

Test Interval	Run Nr.	Date	Test Type	Collection Hole	Collection Rate [ml/min]	$Q_{dilution}$ [ml/min]
BOMI 87.006	#9	19/10/88	monopole	BOMI 86.004	206	0.98
BOMI 87.006	#10	25/10/88	natural gradient			1.23
BOMI 87.009	#11	26/10/88	natural gradient			1.61
BOMI 86.004	#12	27/10/88	natural gradient			0.15
BOMI 86.004	#13	09/11/88	monopole	BOMI 87.006	220	0.05
BOMI 87.009	#18	12/04/89	monopole	BOMI 87.006	102	11.58
BOMI 87.009	#19	19/04/89	monopole	BOMI 87.006	33	5.47
BOMI 87.009	#20	21/04/89	natural gradient			1.53

The GSF Single-Borehole Probe consists of two gas inflated packers which seal the dilution volume. This packed-off interval is adjustable to the geometry of the borehole. For experiments conducted in the migration fracture this volume was kept constant at 0.45 l. The tracer ($^{82}Br^-$, at activities of less than 0.4 MBq) is injected by a remotely controlled syringe. Mixing between the packers is ensured with an oscillating coil. The tracer is detected with a NaI scintillation counter which is integrated in a collimator lead shield (MOSER & RAUERT, 1980). After first utilizations of the probe at Grimsel, several modifications were made by GSF to accommodate the probe for fractured rock (see THORNE, 1990b).

Eight single-hole dilution experiments were analyzed, among them four monopole tests (i.e., negligible mass injected into radially converging flow; see Section 6) and four natural gradient tests. The results are shown graphically in Figure 4-6. The dilution of the tracer differs extremely. The flow rate calculated from all eight dilution tests varies by a factor of about 200. This range is due to different hydraulic gradients and hydraulic conductivity in the three tested boreholes. The scatter of data obtained in run # 12 and # 13 originate from either a very small hydraulic gradient during the natural gradient test or from the possibility that the monopole arrangements reverse the natural radial flow field in the drift. Early time deviations of the exponential concentration decrease in run # 10 and # 12 may be an experimental artifact, due to an incomplete mixing in the test interval.

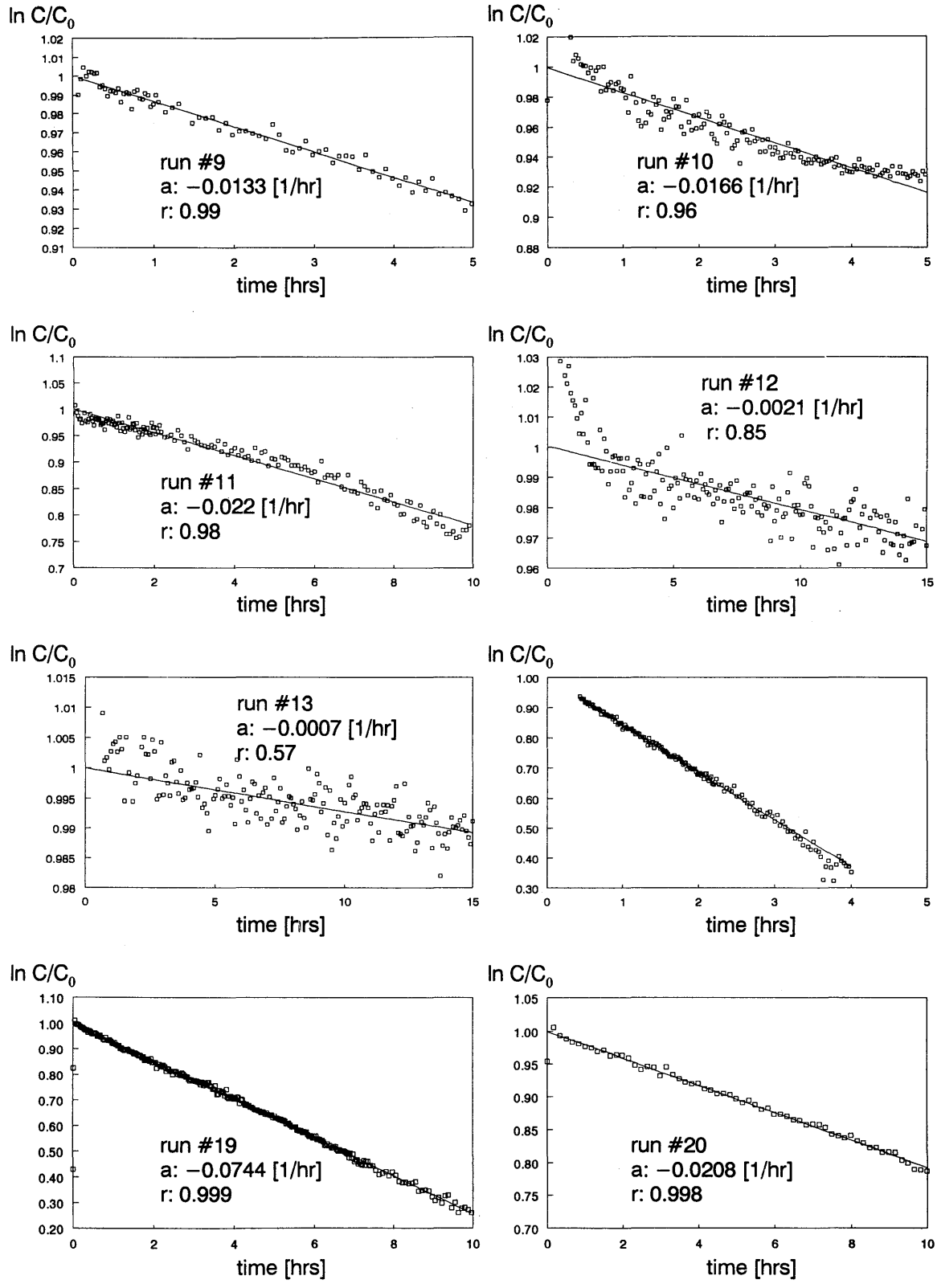

Fig. 4-6: Results of single-hole dilution tests
(*a:* slope of regression line; *r:* correlation factor)

The probe was calibrated for fracture flow conditions and the flow rates calculated from the measured dilution rates (Fig. 4-6). Details of these procedures will be documented elsewhere. Preliminary results are compiled in Table 4-6. Flow rates calculated by simple application of Darcy's law (based on measured pressure gradients) are also tabulated. The two independently derived flow rates (Q_{da} and Q_{di}, obtained from Darcy's law and from the dilution test, respectively) generally vary by less than a factor of 2. Based on this good match we concluded that both methods yield reliable results at flow rates varying by an order of magnitude.

Table 4-6: Comparison of flow rates obtained from single-hole dilution tests (Q_{di}) with results from hydrotests and applying Darcy's law (Q_{da}).

Test Interval	Run Nr.	Gradient [m/m]	Hydraulic Conductivity [cm/min]	Q_{da} Darcy [ml/min]	Q_{di} Dilution [ml/min]	Ratio Q_{di}/Q_{da}
BOMI 87.006	#9	0.1235	1.32	0.70	0.978	1.4
BOMI 87.006	#10	0.1235	1.32	0.70	1.225	1.75
BOMI 87.009	#11	0.0451	5.28	1.02	1.610	1.57
BOMI 86.004	#12	0.0117	1.68	0.08	0.154	1.82
BOMI 86.004	#13	0.0188	1.68	0.135	0.052	0.39
BOMI 87.009	#18	0.4099	5.28	9.31	11.579	1.24
BOMI 87.009	#19	0.1442	5.28	3.27	5.473	1.67
BOMI 87.009	#20	0.0451	5.28	1.02	1.531	1.50

5 LABORATORY SUPPORT PROGRAMME TO THE MIGRATION TEST

In this section a brief summary is provided of the laboratory experimental work conducted in support of the Migration experiment. Detailed descriptions of this work are reported in BAJO et al. in NTB 88-23, BAEYENS et al. in NTB 88-23, AKSOYOGLU (1990) and AKSOYOGLU et al. (NTB 91-04). The ion exchange model was introduced earlier by BAEYENS & BRADBURY in NTB 88-23 and EIKENBERG et al. (NTB 90-39).

5.1 Scope of the Laboratory Investigations

In general, the aims of the investigations are to characterize and understand the chemistry of the groundwater (see Section 3.4), and the geochemistry and physico-chemical properties of the fracture material. A more specific aim was to identify and select suitable sorbing radionuclides for tracer tests and to determine their sorption properties. The emphasis in the latter studies was placed on trying to obtain an understanding of sorption processes and mechanisms and thereby to be in a position to predict/estimate sorption behaviour in the in-situ migration tests.

Details on the fracture mineralogy, sampling procedures, laboratory sample characterization and the chemical characterization of migration site groundwater have been discussed previously in Sections 3.1 to 3.4. A description of the experimental work and the main results associated with rock-water interaction tests, the physico-chemical characterization of fracture materials and the sorption tests will be summarized in the following Sections. Since the cation exchange mechanism played a central role in the interpretation of experimental data, a separate section will be devoted to this topic.

5.2 Rock-Water Interaction Tests

The aim of these experiments was to study the interaction of fracture material, subsequently referred to as *mylonite*, with groundwater under laboratory conditions and, in particular, to examine the chemical stability of the system over relatively long times. The latter point was particularly important for the forseen batch sorption tests, as well as the planned in-situ tests, where it is essential that the system remains chemically stable over the time scale of the experiments (possibly several tens of days).

The rock-water interaction tests consisted simply of contacting disaggregated mylonite (particle size less than 2 mm) with groundwater in closed containers which were shaken periodically. The water composition was monitored regularly for times up to 200 days. Since suitable glove boxes were not available at this time, experiments were carried out under a cover gas of N_2 in an attempt to limit CO_2 contamination. (The P_{CO2} in equilibrium with natural MI water is $< 1.4 \times 10^{-5}$ bar and $3 - 8 \times 10^{-6}$ bar for measured and calculated values, respectively; BAJO et al. in NTB 88-23). The variable parameters in these tests were the water (natural and artificial water), temperature (ambient, about 25°C; "field temperature", about 12°C) and rock to water ratio (1 : 2 and 1 : 10). Details of the experimental method and results are fully described by BAJO et al. in NTB 88-23.

The most significant and interesting changes in water composition occurred within the first 2 days of the tests. The observations made during this time can be summarized as follows:

(i) *Since significant changes in the water composition were observed it was concluded that the fracture material was not in equilibrium with MI water.*

(ii) *The rock-water system rapidly attained a new steady state condition which depended on the rock / water ratio.*

(iii) *Major anion concentrations remained constant.*

(iv) *The concentration of Na, by far the most abundant cation in the MI water remained essentially constant.*

(v) *The changes in the other cation concentrations (Ca, K, Mg and Sr) were essentially complete within the first day.*

(vi) *The sum of the increases in K and Mg concentrations equalled the sum of the decreases in Ca and Sr concentrations (All cation concentrations expressed in meq* l^{-1}*).*

Observations (ii), (iii) and (vi), coupled with the fact that the cation concentration changes occurred very rapidly, are strong indicators for **cation exchange reactions** occurring on the mylonite.

In order to provide information which could be used to test the above deduction, cation exchange capacity *(CEC)* determinations were subsequently carried out on the mylonite samples used in the rock-water interaction tests. The results from these experiments showed clearly that the quantities of exchangeable cations on the mylonite were large enough to account for the observed solution changes in all of the rock-water interaction tests. Further the changes in cation concentrations in the aqueous phase were quantitatively consistent with the changes in the cation occupancies on the mylonite for each individual cation when the quantities were expressed on an equivalent scale.

Water chemistry and cation exchange data were subsequently used to predict sorption data for the major cations in this system and to propose appropriate radionuclides for the first series of migration experiments with sorbing tracers. However, in order to be able to appreciate the reasons for the choices made some background to the cation exchange model is necessary. The exchange model is therefore briefly described in the next section before presenting an analysis of the rock-water interaction results.

One final comment needs to be made regarding the rock-water interaction tests. After a stable period which lasted approximately 14 days further changes in the solution compositions began to occur. These changes were accompanied by a gradual fall in the pH. The evidence available strongly suggested a contamination of the rock-water system with atmospheric CO_2. The observed results could be explained in terms of calcite dissolution and Ca exchange on the mylonite (see BAEYENS et al. in NTB 88-23). The mylonite water system is extremely sensitive to CO_2 contamination and these results indicated the necessity of working in atmosphere controlled glove boxes. All subsequent work described in this chapter was carried out in such facilities.

5.3 Cation Exchange

5.3.1 Background Information

In general a reversible cation exchange reaction for a binary system involving cations A and B, with valences z_A and z_B, respectively, can be expressed as:

$$z_B A_x + z_A B = z_A B_x + z_B A \qquad \{5.1\}$$

in which x denote exchangeable ions on the surface of the cation exchange medium (i.e. mylonite). A *selectivity coefficient*, K_c, can be defined for reaction {5.1} by the direct application of the mass-action law:

$$K_c = \frac{(N_B)^{z_A} \; [A]^{z_B}}{(N_A)^{z_B} \; [B]^{z_A}} \qquad \{5.2\}$$

where $[A]$ and $[B]$ are the activities (or, to a first approximation, the molar concentrations) of ions A and B in solution. N_A and N_B are the fractional ion occupancies of the cations A and B on the solid phase. The fractional ion occupancy of ion B is defined as

$$N_B = \frac{\textit{Quantity of Ion B Sorbed on Mylonite [in } \mu eq\ g^{-1}]}{\textit{Cation Exchange Capacity of Mylonite [in } \mu eq\ g^{-1}]} \qquad \{5.3\}$$

For a binary cation system the sum $(A_x + B_x)$ is equal to the cation exchange capacity, CEC, and hence

$$N_B = \frac{B_x}{(A_x + B_x)} \quad \textit{and} \quad N_A = \frac{A_x}{(A_x + B_x)} \qquad \{5.4\}$$

In a system at equilibrium, where the sorption of ions A and B is determined only by ion exchange reactions, equation {5.2} can be rewritten in terms of the sorption distribution coefficient, ${}^{B}K_d$, for ion B. Remembering that the distribution coefficient is defined as

$$K_d = \frac{\textit{Quantity of Nuclide Sorbed on the Rock per Unit Rock Mass}}{\textit{Quantity of Nuclide in Solution per Unit Volume}} \qquad \{5.5\}$$

and for a cation exchange medium, this may be expressed for ion B as

$$ {}^{B}K_d = \frac{CEC/z_B \cdot N_B}{[B]} \qquad \{5.6\} $$

If the CEC is expressed in equivalents kg^{-1} (CEC/Z_B = mol kg^{-1}), and the concentration $[B]$ is in mol l^{-1} then the units of ${}^{B}K_d$ are $l\,kg^{-1}$ (or $ml\,g^{-1}$). Using equation {5.6}, equation {5.2} becomes

$$ K_c = \frac{({}^{B}K_d)^{z_A} \; [A]^{z_B}}{(CEC/z_B)^{z_A} \; (N_A)^{z_B}} \qquad \{5.7\} $$

and re-arrangement of equation {5.7} gives

$$ {}^{B}K_d = K_c^{(1/z_A)} \cdot \frac{N_A^{(z_B/z_A)}}{[A]^{(z_B/z_A)}} \cdot \frac{CEC}{z_B} \qquad \{5.8\} $$

A few important points need to be noted concerning the above equations of the ion exchange model:

i) The *cation exchange capacity (CEC)* of a material does not have a unique value but depends on the particle size, pH and is also depending on the method chosen for its determination.

ii) In most cases, *selectivity coefficients*, K_c, are not constant but depend on *fractional ion occupancies*. In order to fully characterize an ion exchange reaction, K_c values need to be measured as a function of ion occupancy (i.e. from $N_B = 0$ to $N_B = 1$) at constant ionic strength and temperature.

iii) Even in a well characterized system K_d values calculated from equation {5.8} will be highly dependent on the solution composition and the method used to prepare the solid phase.

iv) If the solid phase and the contacting liquid are not in equilibrium then ion exchange will occur and the fractional ion occupancies on the solid phase and water composition will change and a new equilibrium between the solid and liquid phase will be established. Thus, if the solid and liquid phases are initially out of equilibrium then the new equilibrium will depend on the solid/liquid $(S:L)$ ratio. Hence, the K_d value will also depend on the $S:L$ ratio.

Table 5-1: Corrected cation exchange capacity *(CEC)*, exchangeable cations [in μeq g^{-1}] and fractional ion occupancies (values in parentheses).

Origin of Mylonite Samples	Rock : Water (S:L) Ratio [g : ml]	Exchangeable Cations Na	K	Mg	Ca	Sr	<CEC> [μeq g^{-1}]
Samples taken directly from 60 kg mylonite stock	2:1	0.19 (0.05)	0.65 (0.15)	0.26 (0.06)	3.08*f* (0.73)	0.042 (0.01)	4.21*f*
		0.19 (0.04)	0.69 (0.16)	0.28 (0.06)	3.15*f* (0.73)	0.044 (0.01)	4.35*f*
Samples taken from completed rock-water interaction tests	1:2	0.18 (0.06)	0.36 (0.12)	0.16 (0.05)	2.33*f* (0.76)	0.031 (0.01)	3.06*f*
	1:10	0.16 (0.05)	0.20 (0.07)	0.086 (0.03)	2.45 (0.84)	0.035 (0.01)	2.93
		0.24 (0.05)	0.31 (0.07)	0.16 (0.04)	3.64*f* (0.83)	0.053 (0.01)	4.40*f*

f corrected with measured alkalinity, see BAEYENS et al. (in NTB 88-23)

5.3.2 Application of the Cation Exchange Model to the Results from Rock-Water Interaction Experiments

The results from cation exchange experiments (*CEC* values and fractional ion occupancies) as a function of rock to water ratio are summarized in Table 5-1 (see BAEYENS et al. in NTB 88-23 for details).

The table shows clearly that Ca^{2+} is by far the dominant cation on the mylonite. Further, the fractional cation occupancies of Na^+ ($N_{Na} \sim 0.05$) and Sr ($N_{Sr} = 0.01$) are approximately constant for the different solid/liquid ($S:L$) ratios whereas those for K^+ and Mg^{2+} decrease with decreasing $S:L$ ratio (0.15 to 0.07 and 0.06 to 0.04 for N_K and N_{Mg}, respectively). This decrease is accompanied by an increase in the fractional occupancy of Ca^{2+} (N_{Ca} from 0.73 to 0.83).

The information in Table 5-1, together with the equilibrium water chemistry data at each $S:L$ ratio, allows the *distribution coefficients* for each of the main cations to be calculated using equation {5.6}. These values are given in Table 5-2.

Each of the K_d values calculated applies only to the particular conditions under which each of the individual experiments was carried out, and, as mentioned earlier, the sorption values are a function of the $S:L$ ratio. It should be noted from Table 5-2 that the water compositions in these tests are different from that of MI water and therefore the calculated K_d values cannot be generalized to apply to the mylonite/MI water system. However, by interpreting the results in terms of a cation exchange model and applying equation {5.2}, *selectivity coefficients,* K_c, can be evaluated (Table 5-3) and these can be used to calculate K_d values at the MI water composition with equation {5.7}. Strictly speaking, equations {5.1}, {5.2}, and {5.4} are only valid for a binary cation exchange system which the mylonite/MI water system is not. The justification for the application of these equations lies in the observation that Ca is by far the dominant cation on the mylonite (fractional occupancy, N_{Ca}, 0.73 to 0.84) and consequently, if exchange between the cation pairs Ca-Na, Ca-K, Ca-Mg and Ca-Sr are considered, neglecting the presence of the other ions does not significantly influence the results of the calculation of the selectivity coefficients (see BAEYENS & BRADBURY in NTB 88-23 and EIKENBERG et al. NTB 90-39 for more details on this subject).

Table 5-2: Distribution coefficients of the major cations for mylonite at different rock to water ratios (Table taken from BAEYENS et al. in NTB 88-23)

	Na	K	Mg	Ca	Sr	<CEC> [μeq g^{-1}]
Rock : Water Ratio 2:1						
Quantity on Mylonite [μeq g^{-1}]	0.19	0.65	0.26	3.08	0.042	4.21
Concentration in Solute [meq l^{-1}]	1.3	0.70	0.15	0.98	0.016	
K_d [ml g^{-1}]	0.15	0.9	1.7	3.1	2.6	
Rock : Water Ratio 2:1						
Quantity on Mylonite [μeq g^{-1}]	0.19	0.69	0.28	3.15	0.044	4.35
Concentration in Solute [meq l^{-1}]	1.3	0.70	0.15	0.98	0.016	
K_d [ml g^{-1}]	0.15	1.0	1.9	3.2	2.8	
Rock : Water Ratio 1:2						
Quantity on Mylonite [μeq g^{-1}]	0.18	0.36	0.16	2.33	0.031	3.06
Concentration in Solute [meq l^{-1}]	0.79	0.16	0.03	0.38	0.0038	
K_d [ml g^{-1}]	0.23	2.3	5.3	6.1	8.2	
Rock : Water Ratio 1:10						
Quantity on Mylonite [μeq g^{-1}]	0.16	0.20	0.086	2.45	0.035	2.94
Concentration in Solute [meq l^{-1}]	0.76	0.048	0.009	0.24	0.0028	
K_d [ml g^{-1}]	0.21	4.2	9.6	10.2	12.5	
Rock : Water Ratio 1:10						
Quantity on Mylonite [μeq g^{-1}]	0.24	0.31	0.16	3.64	0.053	4.40
Concentration in Solute [meq l^{-1}]	0.71	0.054	0.012	0.26	0.0026	
K_d [ml g^{-1}]	0.34	5.7	13.3	14	20.4	
Concentration in Natural MI water [meq l^{-1}]	0.69	0.0038	0.0011	0.25	0.0037	

The selectivity coefficients, K_c, calculated for Ca-Na, Ca-Mg and Ca-Sr agree well in the different rock-water ratio series, particularly in view of the uncertainties in the experimental data. The mean values for these exchange reactions are also given in Table 5-3 and the relative standard deviations (1 σ) for the four samples lie between 20 and 30 %.

A constant K_c value as a function of concentration (N_B values) is an indication of linear sorption (i.e. sorbed quantities are directly proportional to concentration) for a solution of otherwise constant composition (see equation {5.8}). In the case of potassium the exchange behaviour is non-linear, e.g., $K_c \sim 38$ for $N_K \sim 0.18$ and $K_c \sim 320$ for $N_K \sim 0.08$). The inference here is that potassium sorption will be non-linear. Since the chemistry of K is similar to that of Cs, and Cs is being considered as a potential tracer, the indication here is that Cs will sorb non-linearly in this system (see Section 5.4.4).

On the basis of the calculated K_c values and the MI water composition, first estimates of the sorption values for Na, Mg, Ca and Sr in the mylonite/MI water system can be made using equation {5-8}. These calculated values are given in Table 5-4.

The values predicted for K_d depend directly on the magnitude of the *CEC*. The in-situ sorption in the migration fracture will thus depend on the in-situ *CEC* which is unknown. (However, a field scale rock-water interaction experiment provided clues as to the effective in-situ *CEC*; see Section 7.2).

Table 5-3: Selectivity coefficients (K_c) and fractional ion occupancies (N_B) for ion exchange reactions on mylonite (Table taken from BAEYENS & BRADBURY in NTB 88-23)

Mylonite Samples	Cation Exchange Reaction							
	$Ca_X+2Na = 2Na_X+Ca$		$Ca_X+2K = 2K_X+Ca$		$Ca_X+Mg = Mg_X+Ca$		$Ca_X+Sr = Sr_X+Ca$	
	N_{Na}	K_c	N_K	K_c	N_{Mg}	K_c	N_{Sr}	K_c
Rock:Water 2:1	0.06	1.02	0.18	38.2	0.08	0.57	0.013	0.87
Rock:Water 1:2	0.07	1.51	0.13	153	0.06	0.87	0.013	1.33
Rock:Water 1:10	0.06 0.06	0.82 1.01	0.08 0.08	361 280	0.04 0.04	0.95 0.91	0.015 0.014	1.26 1.41
Mean K_c Stand.Dev.		1.1 ± .3				0.8 ± .2		1.2 ± .2

Table 5-4: Calculated ion occupancies and estimated distribution coefficients (K_d) for Na, Mg, Ca, and Sr on mylonite fracture material in equilibration with natural Grimsel water (i.e., MI water; see Table 17 in BAEYENS & BRADBURY, NTB 88-23).

Cation	Concentration in Natural Grimsel Water [μeq ml^{-1}]	Ion Occupancy N_B	Quantity of Exchangeable B_X Cations on Mylonite		Range of Estimated K_d-values [ml g^{-1}]
			for a CEC of 3.0 μeq g^{-1}	for a CEC of 4.5 μeq g^{-1}	
Na	0.690	0.06	0.18	0.27	0.3-0.4
Mg	0.0011	0.004	0.012	0.018	11-16
Ca	0.250	0.92	2.76	4.14	11-17
Sr	0.0037	0.02	0.06	0.09	16-25

5.3.3 Application of the Results to the GTS Migration Experiment

An ideal non-conservative tracer for the first migration experiments, particularly from the point of view of transport modeling, would be one which exhibits linear equilibrium reversible sorption with rapid kinetics. On the basis of certain assumptions (see BAEYENS & BRADBURY, Section 6.4 in NTB 88-23), the K_d values for some of the cations in the natural system could be estimated, assuming a value for the *CEC* (see Table 5-4).

If any of the cations Na^+, Sr^{2+}, Mg^{2+} and Ca^{2+}, are added at low enough levels (say at concentrations about 100 times less than their respective equilibrium aqueous concentrations) then neither the overall equilibrium, nor the individual concentrations in the liquid phase, nor the ion occupancies on the mylonite will be significantly influenced. In other words, trace additions of such cations will not change the naturally existing distributions. If the cations are added as radioactive isotopes, **isotope exchange** will take place and their behaviour can be followed by solution activity measurements. From the point of view of the activities measured in the liquid phase, the radioactive isotopes will behave as though they were sorbing linearly. The K_d values governing the redistribution will be the same, whatever the magnitude of the added concentration, provided that it is much less than the corresponding natural equilibrium value. Hence, within a certain concentration range (in practice from the detection limit to about 1 % of the equilibrium concentration) radioisotopes of the four cations mentioned will exhibit (apparent) equilibrium linear reversible sorption with rapid kinetics, i.e. they will behave as "ideal" tracers and their estimated K_d values are given in Table 5-4 for the corresponding *CEC* values.

Of the four cations mentioned, Mg^{2+} can be excluded since no suitable long lived radioisotopes exist. Ca^{2+} can be excluded because of the possibility of precipitation reactions in a system already saturated with respect to calcite. Thus on the basis of the data presented previously, $^{85}Sr^{2+}$ and $^{22}Na^{+}$ were proposed as non-conservative tracers to be used for the sorbing migration experiments. For both Sr^{2+} and Na^{+}, precipitation reactions can be excluded in MI water.

As stated previously, the K_d values are dependent on the in-situ CEC which is unknown. However, if equation {5-6} is used to obtain an expression for the ratio of the K_d values for Sr^{2+} and Na^{+}, i.e.

$$\frac{^{Sr}K_d}{^{Na}K_d} = \frac{\dfrac{CEC / z_{Sr} \cdot N_{Sr}}{[Sr]}}{\dfrac{CEC / z_{Na} \cdot N_{Na}}{[Na]}} \qquad \{5.9\}$$

where $[Sr]$ and $[Na]$ are expressed in mol l^{-1}, the cation exchange capacity, CEC, is expressed in eq kg^{-1} and z_{Sr} and z_{Na} are the valences of Sr^{2+} and Na^{+}, respectively, then

$$\frac{^{Sr}K_d}{^{Na}K_d} = \frac{[Na] \cdot Z_{Na} \cdot N_{Sr}}{[Sr] \cdot Z_{Sr} \cdot N_{Na}} \qquad \{5.10\}$$

The ratio $^{Sr}K_d : {}^{Na}K_d$ is thus independent of the in-situ cation exchange capacity and has a value of approximately 60 (data given in Table 5-4). The implication of this for the field migration tests is that, if $^{22}Na^{+}$ and $^{85}Sr^{2+}$ are injected simultaneously, then the weakly sorbed $^{22}Na^{+}$ will break through first. From the evaluation of the breakthrough profile, a $^{Na}K_d$ value, specific to the fracture and test conditions, can be derived. If the cation exchange model is applicable and, if the N_B values generated from laboratory tests are valid in the fracture, then the sorption of $^{85}Sr^{2+}$ should be about 60 times greater than for $^{22}Na^{+}$. With model parameters calibrated on the $^{22}Na^{+}$ breakthrough, the $^{Sr}K_d$ value could then be used as an independent means of predicting the breakthrough time and characteristics for $^{85}Sr^{2+}$.

One major assumption underlying the above predictions is that ion exchange is the only significant mechanism determining sorption. Clearly, before such tracers could be used in migration experiments it is essential to test the validity of the assumptions and predictions by performing laboratory sorption experiments with $^{22}Na^{+}$ and $^{85}Sr^{2+}$ in the groundwater-mylonite system. The subject of the next section is the radiotracer batch sorption tests.

5.4 Radiotracer Batch Sorption Experiments

The purpose of the sorption measurements carried out at trace concentrations of $^{22}Na^+$ and $^{85}Sr^{2+}$ was to check experimentally the predictions for their sorption behaviour made on the basis of the cation exchange model. In addition, sorption tests using $^{82}Br^-$, $^{131}I^-$ and $^{137}Cs^+$ were performed.

Bromide and iodide are considered to be examples of non-sorbing anions and indeed, the radionuclides $^{82}Br^-$ and $^{123}I^-$ had been previously used as conservative tracers (together with uranine and ^4He) in field migration experiments at the GTS.

The sorption of $^{137}Cs^+$ was investigated since radiocesium had been proposed as a potential tracer in future migration tests using tracers exhibiting non-linear sorption. As such, the use of cesium would represent a further step in increasing the complexity of the transport process and thereby provide a test of the capabilities of the transport codes to model the breakthrough curves. Sorption isotherm data for Cs were thus required as input data for the codes and also for estimating whether breakthrough in the migration tests was likely to occur within a practical time scale.

5.4.1 Experimental

The main results of this series of laboratory investigations are documented in AKSOYOGLU et al. (NTB 91-06). All experiments were carried out in controlled atmosphere glove boxes (two different types, an IGA-Box with O_2 and CO_2 concentrations of 2-10 ppm and a MECAPLEX-Box with O_2 and CO_2 concentrations of < 1 ppm, were used at the PSI). Samples of mylonite were repeatedly crushed, until all the material passed through a 250 μm and a 63 μm sieve to obtain the < 250 and < 63 μm size fractions, which were subsequently homogenized. The homogeneity of a series of 5 g and 10 g sub-samples was checked. It was decided to use 5 g splits for sorption experiments and *CEC* determinations (made by the silver thiourea (AgTU) method). The homogeneity tests indicated that the likely sample to sample variation was less than ± 10 %. Rock-water separation, usually performed by centrifugation and filtration, is one of the most crucial steps for meaningful sorption experiments. For mylonite conditioning and part of the sorption experiments, however, dialysis bags were used to confine particulate matter inside while allowing ions to pass freely through the membrane. (Details given in AKSOYOGLU et al., NTB 91-06).

Two series of experiments were carried out: The first set included sorption experiments with $^{82}Br^-$, $^{131}I^-$, $^{22}Na^+$ and $^{85}Sr^{2+}$ on the < 250 μm particle size fractions. A second series was performed on the < 63 μm size fraction using mixtures of either of $^{22}Na^+$ plus $^{137}Cs^+$ or $^{85}Sr^{2+}$ plus $^{137}Cs^+$. An additional series was performed only with $^{137}Cs^+$. Rock to water ratios *(S : L)* of 1 : 2.5, 1 : 10 and 1 : 20 were used in these tests.

5.4.2 Results with Non-Sorbed Tracers

Experiments with $^{82}Br^-$ and $^{131}I^-$ revealed, as expected, no detectable sorption of these anions on fracture material. Observed K_d values lay within experimental error (AKSOGOGLU et al. NTB 91-06).

5.4.3 Sorption of $^{85}Sr^{2+}$ and $^{22}Na^+$

Experiments on the coarse (< 250 μm) size fraction showed pronounced kinetic effects. Sr^{2+} required at least 30 days to reach stable K_d values, whereas for Na^+, K_d values were still increasing at the termination of the experiment (49 days). Sorption tests were carried out both with and without dialysis bags. In the former case the times to equilibrium were approximately two and a half times slower than in the latter. Continuous agitation was not applied in these tests and the major cause of the slow kinetics is likely to have been the sedimentation of the samples. However, if this were to have been the only cause, then the kinetics for Na sorption would not be expected to be be slower than for Sr. Rather the reverse would be anticipated in a straightforward diffusion controlled process since Sr is more strongly sorbing. This point will be returned to when the sorption tests on mylonite samples of smaller particle size (< 63 μm) are discussed.

The sorption of $^{85}Sr^{2+}$ was linear and independent of the solid-liquid ratio. Over the whole radionuclide equilibrium concentration range (from about $2x10^{-11}$ to about 10^{-8} mol l^{-1}), $^{Sr}K_d$ values were about 67 ($\pm$ 4) ml g^{-1}. (Desorption tests yielded values of 73 ($\pm$ 7) ml g^{-1} and, hence, indicated reversible sorption). The calculated sorption values based on *CEC*, fractional ion occupancy and water chemistry data were 61 ($\pm$ 10) ml g^{-1}. Considering the experimental uncertainties this agreement was considered to be good and the sorption results were in accord with the predictions based on a cation exchange mechanism. (Note that the sorption values here are higher than those calculated from the rock/water interaction tests. The reasons for this are the higher *CEC* values and different water chemistries. This applies also to the following results for Na^+ and to the Na^+ and Sr^{2+} results on mylonite with a particle size < 63 μm).

For the < 250 μm mylonite size fraction $^{22}Na^+$ exhibited linear reversible sorption in the radionuclide concentration range about 10^{-10} to $2x10^{-8}$ mol l^{-1} with an average sorption coefficient of about 2.3 ($\pm$ 0.1) ml g^{-1}. This is a factor of about 3 greater than the sorption value of 0.7 ($\pm$ 0.1) ml g^{-1} calculated based on the *CEC*, fractional ion occupancies and water chemistry data. (Again it is to be noted that this value is higher than that calculated in the rock-water interaction tests due to the higher *CEC* and different water chemistry). This difference was considered to be too great to be caused by experimental error alone. A hypothesis, postulating the existence of Na^+ exchange sites within the < 250 μm particles which could be reached by Na^+ but not by the large AgTU complex used in the cation exchange measurements (see BAEYENS et al. in NTB 88-23), was put forward to explain this discrepancy and the slower sorption kinetics of $^{22}Na^+$ compared with $^{85}Sr^{2+}$. It should be noted, however, that the *CEC* determinations by the silver thiourea (AgTU) method were carried out over much shorter times than the sorption measurements.

Subsequently, the mylonite was crushed to < 63 μm to expose more of these internal sites and the *CEC* determinations and sorption experiments repeated. Again, excellent agreement was found between the calculated sorption of $^{85}Sr^{2+}$ and the measured K_d value, i.e. 111 (± 7) and 110 (± 10) ml g^{-1}, respectively. (Note that the calculated value is different due to the different *CEC* of the < 63 μm particles). The fractional cation occupancy of Sr for the < 250 μm and < 63 μm sized mylonite particles was virtually the same indicating little or no internal Sr sites. The calculated and measured K_d values for $^{22}Na^{+}$ (2.5 ± 0.2 and 3.5 ± 1.0 ml g^{-1}, respectively) were in much closer agreement than in the previous tests and the fractional occupancy of Na increased for the < 63 μm fraction as would be expected on the basis of the hypothesis. Both $^{85}Sr^{2+}$ and $^{22}Na^{+}$ reached equilibrium within 24 hours.

In conclusion, the sorption of $^{85}Sr^{2+}$ is described well by a cation exchange model whereas, in certain circumstances such a model may underestimate $^{22}Na^{+}$ sorption, most probably due to Na^{+} exchange sites within particles. The latter sites are not reached by large exchange complexes such as silver thiourea (AgTU) within the 3 days contact time and are therefore not included in *CEC* measurements. Though these experiments confirmed that the dominant mechanism for the sorption of Na^{+} and Sr^{2+} on fracture material is cation exchange, the sorption values obtained are most probably not directly applicable to migration tests using these cations as tracers since the laboratory conditions were not fully representative of those in the migration fracture.

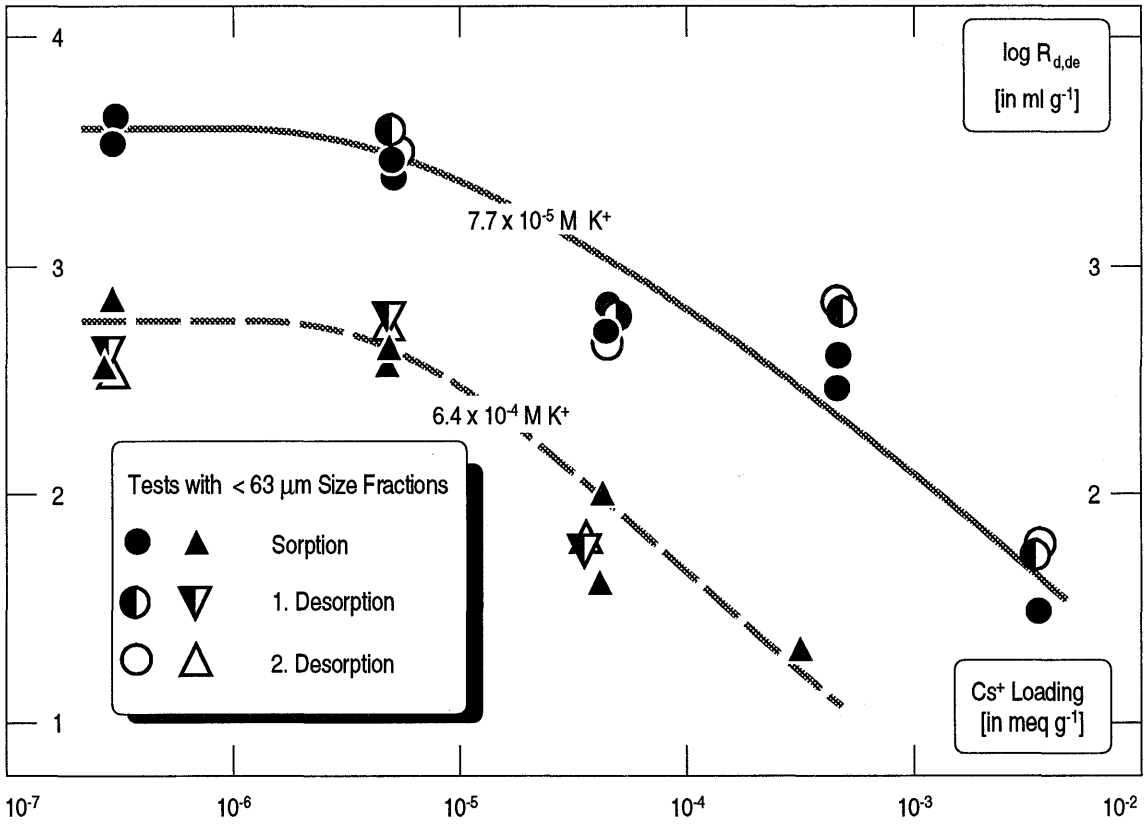

Fig. 5-1: Sorption/desorption coefficients determined for Cs^{+} on duplicate Grimsel mylonite samples as a function of the Cs^{+} loading at two different K^{+} concentrations. The graph is redrawn from AKSOYOGLU et al. NTB 91-06.

5.4.4 Sorption of ^{137}Cs

Trace quantities of cesium are known to be preferentially adsorbed at certain specific sites located at the edges of clay particles. Previous experiments on the sorption of Cs^+ on clays (e.g. CREMERS 1988 and references cited therein) have shown that, even at trace concentrations, potassium influences the sorption of cesium on illites and micas. Exchange with other cations, depending on their surface occupancy, becomes important at increasing concentrations of Cs^+. Sorption-desorption isotherms for Cs were therefore measured at different concentrations of dissolved potassium in an attempt to understand the mechanisms for Cs^+ sorption on fracture material. Substantial amounts of K^+ continuously leached from crushed mylonite fractions during conditioning experiments, indicated the rather unique behaviour of K^+. Therefore, experiments were carried out at artificially enhanced K^+ levels to guarantee constant ion concentrations of competing potassium during the experiments (AKSOYOGLU 1990; AKSOYOGLU et al. NTB 91-06).

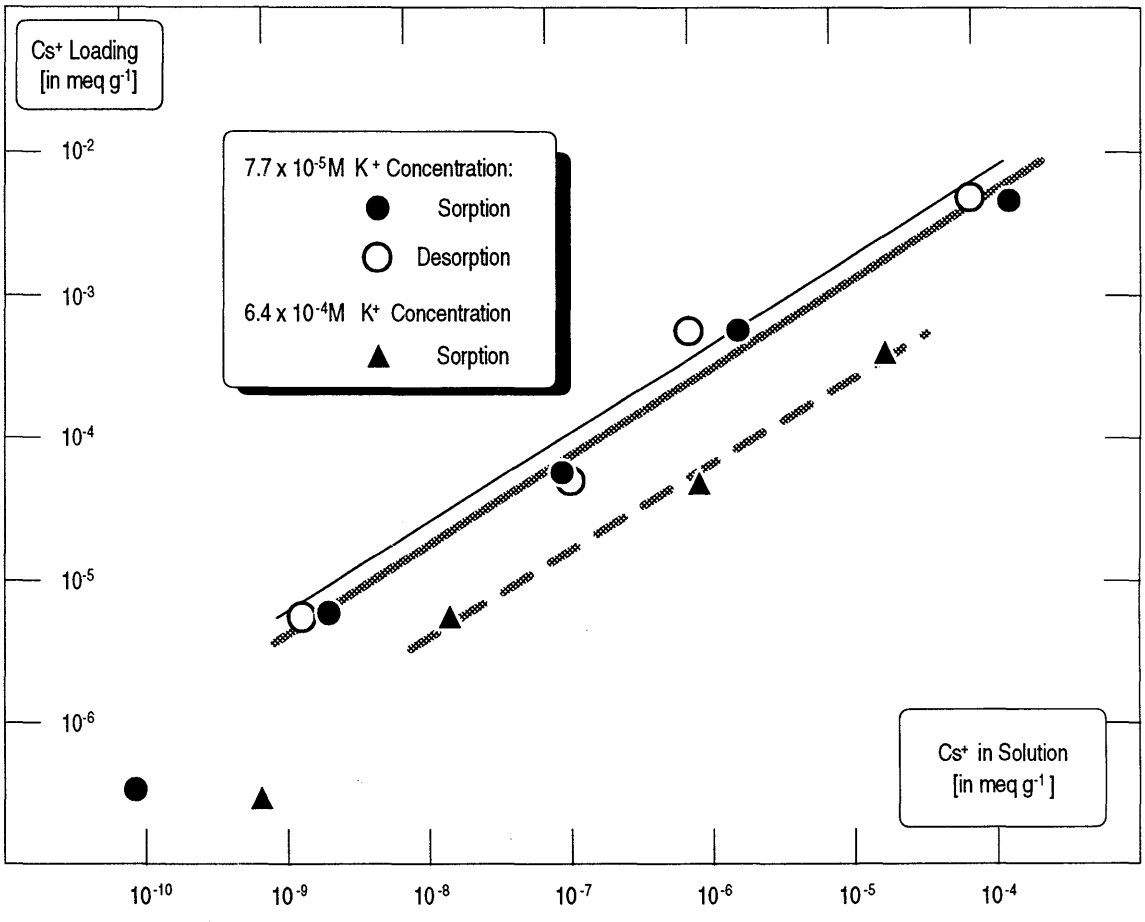

Fig. 5-2: Freundlich isotherm of $^{137}Cs^+$ sorption on Grimsel mylonite samples (< 63 µm size fraction) in solutions with artificially enhanced potassium concentrations of $7.7x10^{-5}M$ *(upper curve)* and $6.4x10^{-4}M$ *(lower curve)*. The graph is redrawn from Fig. 7 in AKSOYOGLU et al. (NTB 91-06).

Cesium sorption on crushed mylonite (< 63 μm) was measured at a solid/liquid ratio of 1 : 10, at equilibrium Cs^+ concentrations from about 10^{-9} to about 10^{-4} mol l^{-1} and two different K^+ concentrations ($7.7x10^{-5}$ and $6.4x10^{-4}$ mol l^{-1}). Sorption and desorption results are plotted in Figures 5-1 and 5-2. The sorption of Cs^+ is non-linear and is clearly influenced by the K^+ concentration. At Cs^+ concentrations below 10^{-8} to 10^{-9} mol l^{-1} (corresponding to a Cs^+ loading on the solid of about $5x10^{-6}$ mol g^{-1}) the sorption becomes constant. There is some tentative evidence to suggest that the natural level of Cs^+ in MI water lies near these concentrations. Isotope exchange is thus a possible explanation for the constant sorption values measured.

It must be emphasized, that the isotherm for Cs^+ was determined at potassium concentrations which were factors of about 20 and 170 above that in natural migration water. It is therefore difficult to justify an extrapolation of the K_d values to in-situ Grimsel conditions. At low Cs concentrations and natural K^+ concentrations, however, it is likely that the relevant K_d value for Cs^+ may exceed the measured values of approximately 4000 ml g^{-1}. For sorption values of this magnitude it is unlikely that breakthrough curves for Cs^+ can be measured for the range of conditions available for field tracer tests at the Grimsel Test Site.

5.5 Laboratory High-Pressure Infiltration Experiments

In the study of transport of sorbing radionuclides, laboratory-based, high-pressure infiltration experiments constitute an intermediate step between the large-scale field migration work and static batch-sorption experiments. For this reason, such experiments were also selected as a test case in the international INTRAVAL study, the aim of which is the validation of geosphere transport models (SKI 1987; JAKOB et al., 1989; JAKOB & HADERMANN, NTB 91-27). In connection with the experimental work on Grimsel bore cores, breakthrough curves for both sorbing and non-sorbing radionuclide tracers have been fitted to single-porosity and dual-porosity transport models, allowing transport/sorption properties of the rock/water system to be determined and the goodness-of-fit of the different models to be compared.

5.5.1 Experimental Set-up

Two cylindrical rock borecores (borecore 1 and borecore 2) consisting of fractured granodiorite from the Grimsel Test Site were used in these experiments. The borecores, were taken at 19.23 m and 20.38 m from the drill core BOMI 86.004, which intersects the test fracture for the migration experiments at 20.66 m. They were cut from the drill core in such a way that the final borecores each contained a single shear zone with an axial orientation. Both borecores were 4.6 cm in diameter. Borecores 1 and 2 were of length 3.05 cm and 4.38 cm respectively. To summarize the experimental method, infiltration fluid (natural Grimsel groundwater from the MI fracture) is forced through a borecore, which is confined within a high-pressure cell. The borecore is mounted between to stainless steel end-pieces, which are designed to distribute infiltration fluid across the surface of the borecore on the high-pressure (up-stream) side and to collect the emerging fluid on the low-pressure (downstream) side (see Fig. 5-3). Once the

system has reached a steady state, a pulse containing one or more radioactive tracers is injected into the infiltration fluid and the resulting breakthrough curves are recorded. Details of the experimental setup and procedures are documented elsewhere (see BISCHOFF et al., 1987; SMITH et al., 1990a and SMITH, NTB 91-33).

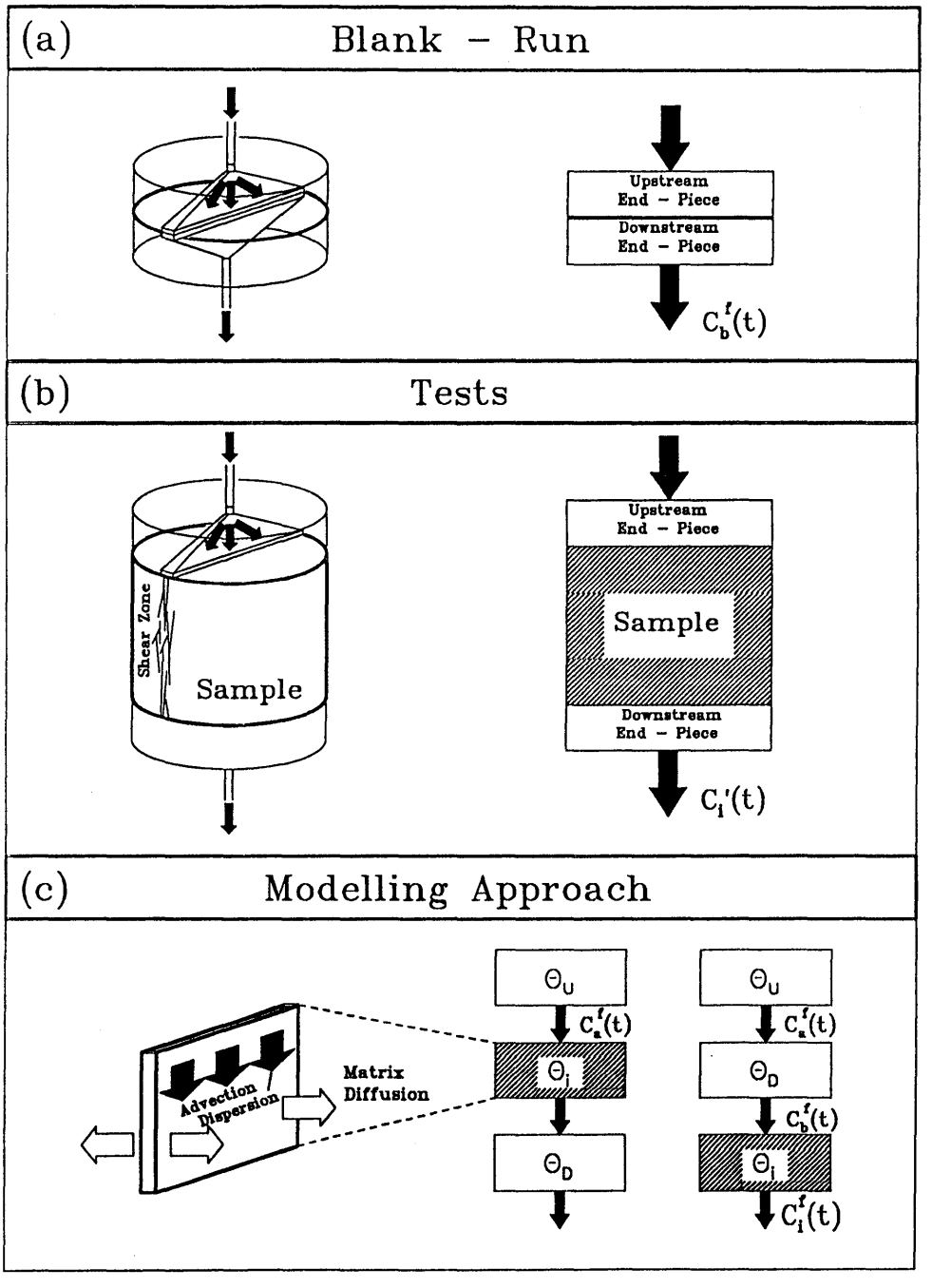

Fig. 5-3: Experimental procedure and modeling approach (Figure taken from SMITH, NTB 91-33).

It was shown in SMITH et al. (1990a) that the breakthrough curve for a single sorbing tracer contains insufficient information to enable all physical parameters of interest to be determined uniquely. To provide the additional information required for modeling, experiments were performed in which both sorbing (^{24}Na) and non-sorbing (^{82}Br) radionuclides were included in the tracer pulse. Unfortunately in the early experiments, the form of the tracer pulse as it entered the borecore was not well-delined. This was because dispersion effects produced by the apparatus on the non-sorbing radionuclide were similar in magnitude to the results of dispersion and matrix diffusion in the borecore itself. The latter processes could thus not be separated from experimental artifacts, seriously limiting the usefulness of the breakthrough curves.

The apparatus and experimental procedure were modified to allow the above artifacts to be quantified (SMITH & ALEXANDER, 1990). A "blank-run" is first carried out, in which the two end-pieces are pressed together with no borecore present. The breakthrough curve from the blank-run then gives the initial form of the tracer pulse. This is then used as input when modeling the breakthrough curves in the presence of the borecores, thus incorporating dispersion due to the apparatus into the model (see Fig. 5-3).

5.5.2 Results

Representative breakthrough curves for the non-sorbing ($^{82}Br^-$) and sorbing ($^{24}Na^+$) are illustrated in Figure 5-4. Also shown is the blank run of the $^{82}Br^-$ which depicts the apparatus effects mentioned above. The best fits for the single and dual-porosity models to the observed breakthroughs are also illustrated.

Tables 5-5 and 5-6 present the physical parameters extracted from 5 experiments on the two borecores. Six different experiments were conducted on two specimens. Experiments BOMI 58, BOMI 61 and BOMI 62 were performed on borecore 1. BOMI 60 and BOMI 69 were performed on borecore 2. (Note that for these experiments "BOMI" designates different runs on core samples and not, as usually used throughout this document, migration site boreholes). BOMI 58, BOMI 61 and BOMI 62 were carried out using practically the same infiltration flowrate. BOMI 60 was carried out using a higher infiltration flowrate than BOMI 69. γ-detection of the tracers was usually carried out using a semiconductor device, except in the case of BOMI 69, where two different measurement devices were used: BOMI 69N refers to results obtained with a sodium iodide scintillation counter and BOMI 69Z to those obtained with the semiconductor device.

The physical parameters which can be determined, using either the single- or dual porosity model, are the longitudinal dispersion length for both tracers (a_{L1} and a_{L2}), the surface-based retardation factor (R_f) and the velocity of the infiltration fluid (u). For all experiments, u was found to be in the order of 10^{-3} cm s^{-1} and a_{L2} in the range of 2 cm to 4 cm. The range of values of a_{L1} for borecore 2, between 3 cm and 6 cm, were similar to that of a_{L2} for both borecores. For borecore 1, however, a_{L1} was an order of magnitude smaller: between 1.5 mm and 3.5 mm.

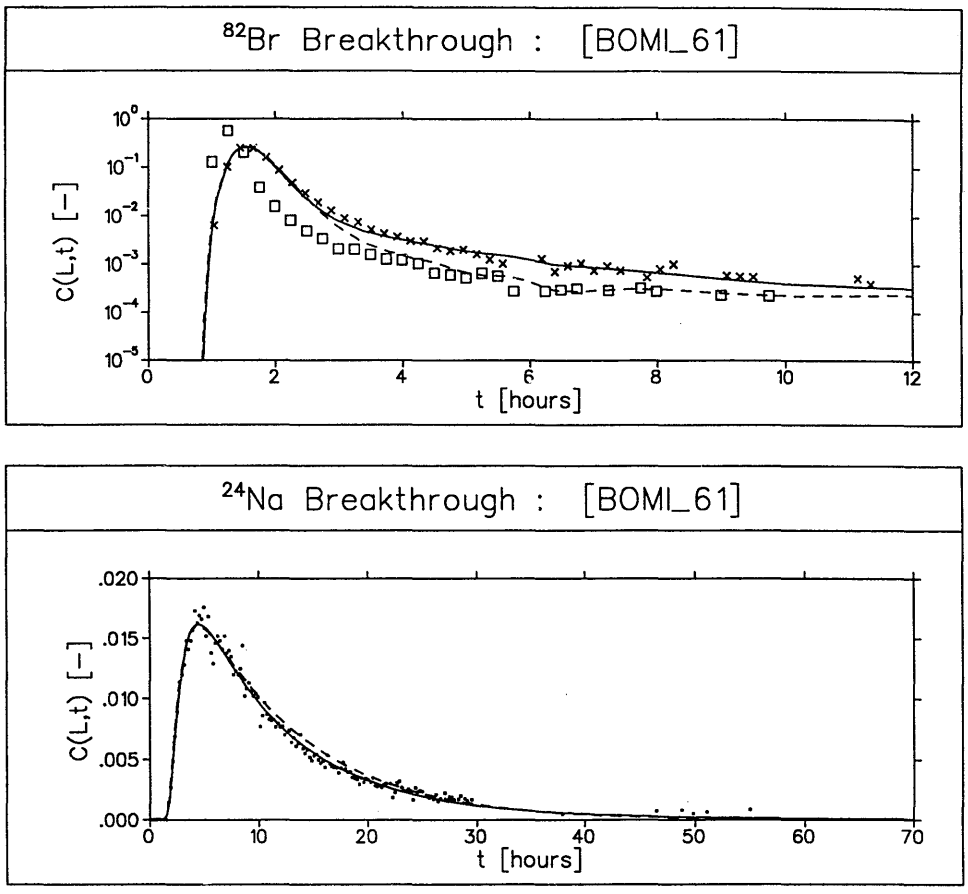

Fig. 5-4: Experimental data and models fitted to $^{82}Br^-$ and $^{24}Na^+$ breakthrough curves for infiltration experiment BOMI 61.

The magnitude of a_L is dictated by the length scales of inhomogeneities both in tracer-independent quantities, such as fracture aperture, and in tracer dependent quantities such as sorption along the flow path (GELHAR 1987). Different longitudinal dispersion lengths for non-sorbing and sorbing tracers are, therefore, to be expected if it is inhomogeneties in sorption which determine a_L for sorbing tracers. The difference between the two borecores indicates that the borecores may not be sufficiently large to provide a representative elementary volume *(REV)*. This could be tested by carrying out further experiments with borecores of different length.

Table 5-5: Physical parameters extracted from 5 experiments on two borecores using the single-porosity transport model (for details see SMITH, NTB 91-33)

Parameter	Units	Factor	Core 1 BoMI58	Core 1 BoMI61	Core 1 BoMI62	Core 2 BoMI60	Core 2 BoMI69N	Core 2 BoMI69Z
u	$cm\ s^{-1}$	$x\ 10^{-3}$	-	1.40	1.43	-	1.09	1.13
a_{L1}	cm	$x\ 10^{-1}$	-	3.44	2.44	-	32.7	60.3
a_{L2}	cm	$x\ 10^{-1}$	42.51	30.8	24.8	34.6	27.6	30.9
R_f	-		24.7	18.7	20.0	31.9	25.4	27.5
σ_1^2	-	$x\ 10^{-6}$	-	6.83	18.6	-	2.69	4.99
σ_2^2	-	$x\ 10^{-7}$	4.92	4.91	8.74	1.53	12.5	8.08

Table 5-6: Physical parameters extracted using the dual-porosity transport model (for details see SMITH, NTB 91-33)

Parameter	Units	Factor	Core 1 BoMI58	Core 1 BoMI61	Core 1 BoMI62	Core 2 BoMI60	Core 2 BoMI69N	Core 2 BoMI69Z
u	$cm\ s^{-1}$	$x\ 10^{-3}$	1.50	1.48	1.53	1.64	1.11	1.17
a_{L1}	cm	$x\ 10^{-1}$	-	2.64	1.53	-	32.0	53.0
a_{L2}	cm	$x\ 10^{-1}$	38.0 (36.6)	25.5 (24.6)	(-)	(34.2)	(1.13)	(29.5)
R_f	-		23.8 (23.2)	18.2 (18.1)	(-)	(31.6)	(25.8)	(27.7)
$\varepsilon_p \chi_{max\ 1} / b$	-	$x\ 10^{-2}$	-	20.1	17.7	-	2.5	6.51
$\varepsilon_p \chi_{max\ 2} / b$	-	$x\ 10^{-2}$	31.2	24.2	-	-	-	-
$\varepsilon_p^2 D_p / b^2$	s^{-1}	$x\ 10^{-6}$	-	2.95	5.22	-	0.069	0.428
$D_p / \chi_{max\ 1}^2$	s^{-1}	$x\ 10^{-5}$	-	6.4	16.7	-	11.0	10.1
K_d	$ml\ g^{-1}$		0.11 (0.19)	0.16 (0.26)	(-)	(0.046)	(0.029)	(0.050)
σ_1^2	-	$x\ 10^{-6}$	-	2.20	3.45	-	2.80	4.80
σ_2^2	-	$x\ 10^{-7}$	4.21 (4.22)	3.41 (3.37)	(-)	(1.53)	(12.4)	8.11)

Values of the retardation factor R_f lie within the relatively narrow range of 18 to 32. R_f, which represents sorption on the fracture walls, may be written as

$$R_f = 1 + \frac{1}{b} K_a \qquad \{5.11\}$$

where K_a [m] is a surface-based sorption constant. Assuming that the mineralogy and, hence, the chemical properties of the fracture walls are similar for the two core samples (i.e., similar values for K_a), equation 5.11 implies that the aperture half-width b may also be similar

Physical parameters which can be determined from the dual-porosity model alone are the thickness of the porous matrix for both tracers with respect to the fracture half-aperture ($\varepsilon_p \chi_{max\,1} / b$ and $\varepsilon p \chi_{max\,2} / b$), the ratio of the effective diffusion coefficient to the square of the fracture half-aperture ($\varepsilon_p^2 D_p / b^2$) and the distribution constant for the sorbing tracer (K_d). The quantities $\varepsilon_p \chi_{max\,1} / b$ and $\varepsilon_p^2 D_p / b^2$, both derived by fitting the dual-porosity model to the breakthrough curves for the non-sorbing tracer, each differ by about an order of magnitude between the two borecores. Eliminating ε_p / b from these two quantities, values of $D_p / \chi^2_{max\,1}$ are obtained (also given in Table 5-6) which show relatively little variability, taking values in the order of $10^{-4} s^{-1}$ for both borecores. This implies that it is ε_p / b , the ratio of matrix porosity to fracture aperture it is the fracture aperture, which is chiefly responsible for the differences between the two borecores. As discussed above, however, the lack of variability in R_f suggests that the aperture is similar in both cases. This would only leave matrix porosity to account for the observed differences, with borecore 2 having the lower value of ε_p .

Although it is not possible to obtain values of b (fracture half-aperture) directly from the fitting procedure, b can be estimated from $\varepsilon_p^2 D_p / b^2$ by assuming reasonable values for $\varepsilon_p D_p$. The effective diffusion coefficient can be written

$$\varepsilon_f D_p = k \cdot \varepsilon_p D_o \qquad \{5.12\}$$

where D_o is the diffusion coefficient in free water (about 10^{-9} $m^2 s^{-1}$ for the major ions found in groundwater). Values for the geometry factor k between about 0.01 and 0.5 are commonly observed in diffusion experiments for non-sorbing ions in porous geological materials (FREEZE & CHERRY, 1979). This gives a range of values for b of 14 - 140 µm for borecore 1 and 48 - 850 µm for borecore 2.

Fitted values of K_d for the sorbing tracer lie in the range 0.1 - 0.3 ml g^{-1} for borecore 1 and 0.03 - 0.05 ml g^{-1} for borecore 2. The case of borecore 2, however, the merit function for the best fit of the simulated to the observed breakthroughs $\varepsilon_{min\,2}^2$, is virtually identical for the single-porosity and dual-porosity models. An examination of

the variation of a relative merit function with K_d for each of the experiments demonstrates the reason for this (Fig. 5-5). We define the relative merit function as $\chi_2^2 / \chi_{min\ 2}^2$. It has a well defined minimum for the experiments BOMI 58 and BOMI 61 (borecore 1), whereas, for the experiments BOMI 60 and BOMI 69, the function is almost flat for K_d less than 0.1 ml g^{-1}. Since there is no well defined minimum for these experiments, no reliable value for K_d can be given.

The K_d values of 0.1 - 0.3 ml g^{-1} determined from the high pressure infiltration experiments are between a factor of 2 - 4 less than those determined from the rock-water interaction studies performed on incompletely disaggregated fracture material as described in Section 5.2 (see also Table 5-7) .

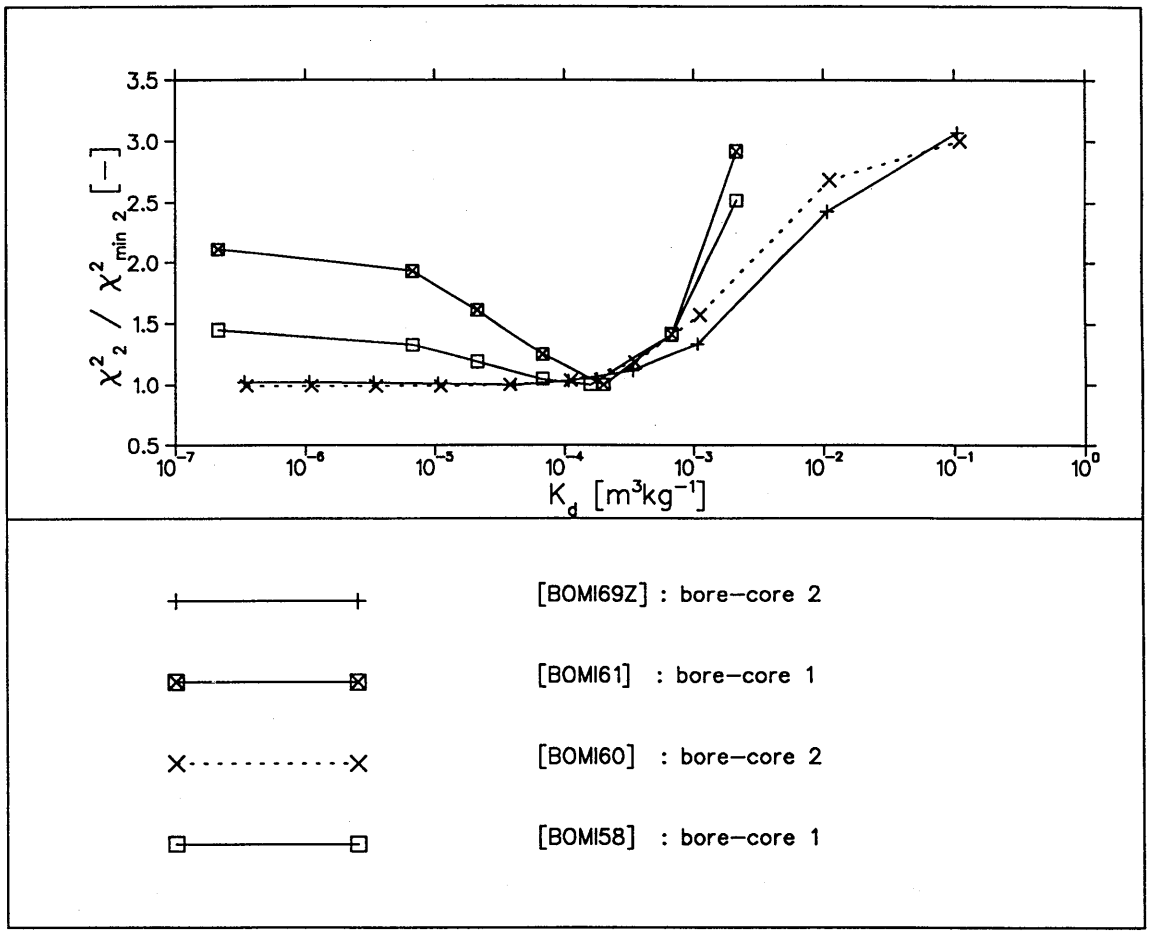

Fig. 5-5: Variation of relative merit function.

5.6 Comparison of Sorption Values

Table 5-7 summarizes the sorption values for Na and Sr determined from (1) rock-water interaction studies on < 2 mm, mylonite grains, (2) radiotracer batch sorption tests on < 250 μm and < 63 μm mylonite grains, and (3) the high-pressure infiltration tests conducted on a fractured granodiorite rock core. As expected, the apparent K_d (and CEC) increases as the grain size decreases due to the increase in the available surface area.

Table 5-7: Summary and comparison of laboratory sorption experiments.

Type of Experiments	Size Fraction	Kd [Na] [in ml/g]	Kd [Sr] [in ml/g]	Kd [Cs] [in ml/g]	CEC [in μeq/g]
Rock-Water Interaction [1]	< 2 mm	0.3 - 0.4	16 - 25	-	2 - 5
Batch Radiotracer Sorption Tests [2]	< 250 mm	1.2 - 2.4	62 - 82	-	5 - 8 [4]
	< 63 mm	2.5 - 3.5	110 ± 10	~4'000 [5]	~14 [4]
High-Pressure Infiltration on core samples [3]	(model fit)	0.1 - 0.3	-	-	-

1 Bradbury et al. (NTB 88-23)

2 Aksoyoglu et al. (NTB 91-06)

3 P. Smith (NTB 91-33)

4 Aksoyoglu et al. (1989)

5 extrapolated value for natural Grimsel hydrochemical conditions

6 CHARACTERIZATION OF THE MIGRATION FRACTURE WITH CONSERVATIVE TRACERS

During 1988 and 1989, a total of 28 conservative tracer tests were performed in the MI fracture (Table 6-1). These tests had the following objectives:

1) To provide information for designing migration experiments with reacting tracers.

2) To test the suitability of the instrumentation: packer systems, injection and collection control, tracer analysis equipment, data acquisition etc. (THORNE, 1990a, b).

3) To search for optional arrangements of borehole pairs to perform two-well injection-extraction experiments with groundwater residence times suitable for tracer experiments under different natural or artificially induced hydraulic conditions (later to be used during tracer experiments with reacting tracers).

4) To test predicted residence times and breakthrough characteristics determined from application of the PSI hydrodynamic model described in Section 4.2.1.

A brief overview of the various experiments, including applied tracers and prevailing flow conditions, is provided in THORNE (1990a, b). Experience obtained from these experiments led to extensive modifications and improvements in the equipment and methodology, and provided the basis for successfully conducted long-term experiments with reacting tracers.

6.1 Tracer Selection

The following criteria for the selection of conservative tracers were considered:

- non-reactive with fracture material
- detectable in small quantities
- below detection in the natural groundwater
- easy to handle, non toxic, environmentally safe
- relatively simple to analyze by standard techniques (preferentially, on-line analytical instruments)
- should not affect the in-situ water chemistry
- stable in Grimsel groundwater

Table 6-1: Hydrodynamic characterization of the migration fracture with conservative tracer tests.

Test Nr	Date	Test Type	Tracer utilized	Injection Borehole BOMI	Rate [ml/min]	Extraction Borehole BOMI	Rate [ml/min]
1	12/7/88	dipole p	ur, Br	86.004	259	87.009	618
2	14/7/88	dipole p	ur, Br	86.004	41	87.009	191
3	20/7/88	dipole p	ur, Br	86.004	77	87.006	219
4	26/7/88	dipole p	ur, Br	86.004	70	87.006	204
5	6/9/88	dipole p	ur, Br	86.004	78	87.006	195
6	13/9/88	dipole p	ur, Br	86.004	26	87.006	79
7	20/9/88	dipole p	ur	87.006	76	86.004	205
8	4/10/88	dipole p	ur, Br	87.006	24	86.004	82
9	18/10/88	monopole	ur, Br	87.006		86.004	206
10	25/10/88	natural	ur, Br	87.006			
11	26/10/88	natural	Br	87.009			
12	27/10/88	natural	ur, Br	86.004			
13	9/11/88	monopole	ur, Br	86.004		87.006	221
14	6/12/88	dipole p	ur	86.004	73	87.006	221
15	13/12/88	dipole p	ur	86.004	63	87.006	219
16	14/12/88	dipole p	ur	86.004	68	87.006	250
17	29/3/89	dipole p	He	86.004	46	87.006	108
18	12/4/89	monopole	ur,Br,He	87.009		87.006	102
19	19/4/89	monopole	ur,Br,He	87.009		87.006	34
20	21/4/89	natural	ur,Br	87.009			
21	26/4/89	dipole p	ur,Br,He	86.004	31	87.006	80
22	11/5/89	dipole s	He	86.004	30	87.006	76
32	25/8/89	dipole p/s	ur,He	86.004	80	87.006	160
33	14/9/89	dipole s	ur,He	86.004	78	87.006	155
40	2/10/89	dipole s	ur,He	86.004	31	87.006	86
41	7/3/90	dipole p	ur,He	86.004	30	87.006	80
42	14/3/90	dipole p	ur,He,Br	86.004	53	87.006	150
43	21/3/90	dipole s	ur,Br	86.004	53	87.006	150
44	11/6/90	dipole p	ur	86.004	10	87.006	148
45	26/6/90	dipole p	ur,Br	86.004	10	87.006	155
47	05/02/91	dipole p	ur, ^{123}I	86.004	51	87.006	150
49	19/02/91	dipole p	ur, ^{123}I	86.004	10	87.006	149
51	27/11/91	dipole p	ur	86.004	10	87.006	155

Test Type:
- dipole p: dipole with pulse injection of tracer
- dipole s: dipole with step injection of tracer
- monopole: no injection flow
- natural: natural radial flowfield to the laboratory drift

Tracer:
- ur: uranine
- He: ^{4}He
- Br: ^{82}Br

For the pilot breakthrough tests Uranine, $^{82}Br^-$ and He were used. Uranine (Na-fluorescein) is a standard dye often used for hydrogeological purposes. It can easily be detected in low concentrations by using fluorophotometric techniques. It has been shown to be stable and to be non-sorbing in granite environments such as the Stripa test site in Sweden (ABELIN et al., 1987). Its emission intensity (BEHRENS, 1986) strongly depends upon the pH in the groundwater; therefore special care was necessary to avoid pH changes due to aeration of the relatively high-pH Grimsel water during calibration or on-line analyses.

The radioactive tracer $^{82}Br^-$ ($t_{1/2}$ = 35.5 h) also is often employed in short-term groundwater investigations (see Section 4.3) and is known to be non-reacting in practically any natural hydrochemical environment. The third conservative tracer is the noble gas helium which has been used as a tracer in previous groundwater studies (CARTER et al., 1959). As dissolved helium is uncharged, its penetration into the rock matrix may differ somewhat when compared with anion tracers. Helium was expected to provide some additional information on matrix diffusion due to its small molecular size (EIKENBERG & KIPFER, 1989). A novel technique for on-line helium analysis was developed (see Section 6.5.3). Whenever possible ^4He was analyzed simultaneously with the other tracers. Details of tracer injection and analytic equipment are documented in THORNE (1990b).

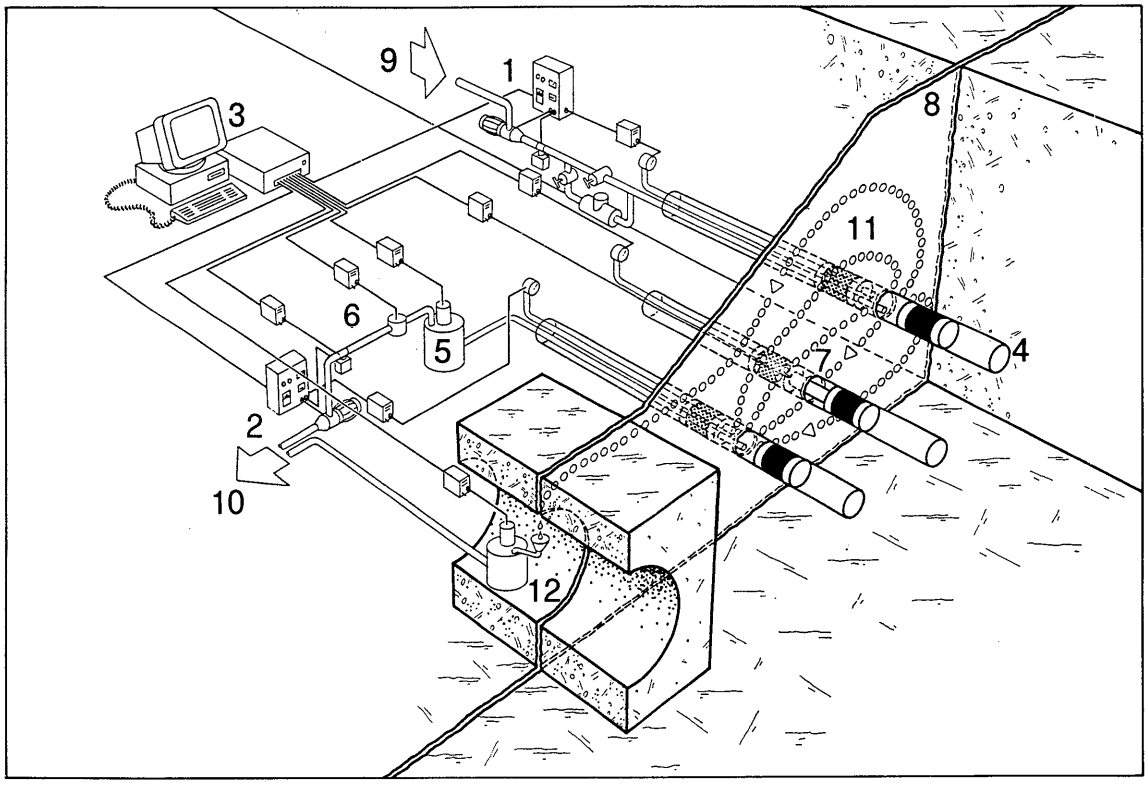

1 Injection Control
2 Extraction Control
3 Data Aquisition System
4 Multi Packer
5 Flow-Through Scintillometer
6 Tracer Analyses
7 Down-Hole Scintillometer
8 Water Filled Fracture
9 Untraced Water
10 Traced Water Flow
11 Artificial Flow Field
12 Monitoring in the Drift

Fig. 6-1: Typical experimental setup for tracer experiments.

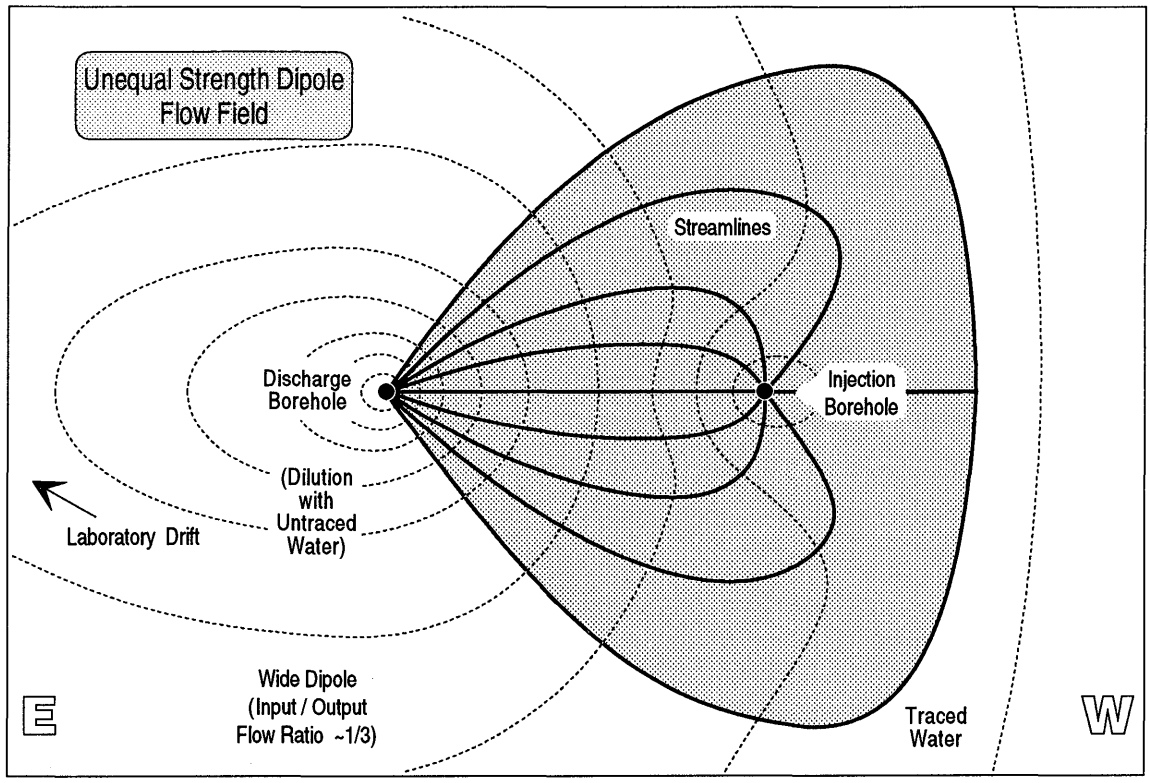

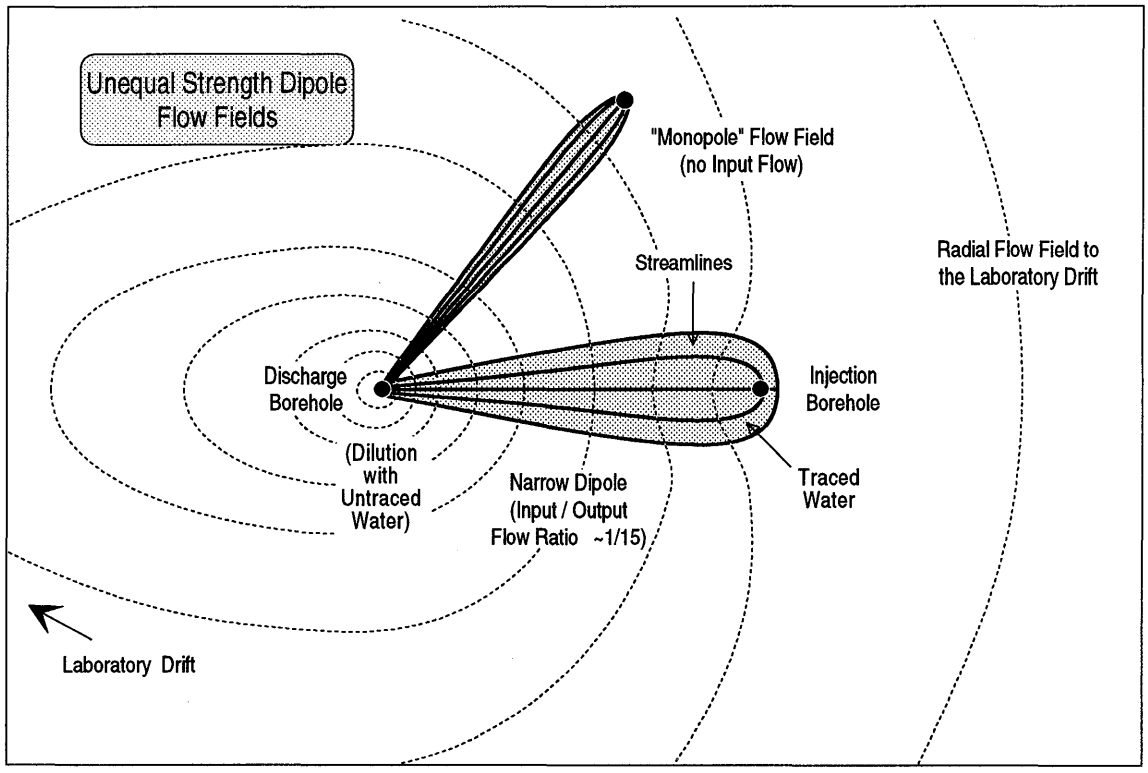

Fig. 6-2: Schematic illustration of monopole and various dipole flow conditions

6.2 Experimental Set-up

Injection and collection systems for the pilot tests are schematically illustrated in Figure 6-1 and are described in detail in THORNE (1990b). Most of the pilot tracer tests have been conducted within a nearly steady-state flow field established by pumping water at a constant rate (Q_{in}) into the fracture interval of one borehole while extracting water from the fracture interval of another borehole at a higher rate (Q_{out}). Such tests are usually referred to as **dipole** or doublet tests. A schematic illustration of various types of converging flow fields, simplified for a homogeneously transmissive 2-dimensional aquifer, are presented in Figure 6-2. The flow field is usually dominated by the drawdown of the discharge borehole while the "natural", radially converging flow into the tunnel can be neglected for practical purposes.

The first series of pilot tests with non-sorbed tracers were carried out with an imported water (EM water, see Section 7.2). During later tests, the injection flow was maintained with MI water after uncontaminated collection and storage of water from the migration fracture became available. The experimental setup for these tests is depicted in Figure 6-3. Typical experiments were carried out with injection into BOMI 86.004 and collection from BOMI 87.006. A prerequisite for the breakthrough tests was tracer recovery as complete as possible for safety reasons and for later comparison with reactive tracers. For experiments carried out so far the ratio $Q_{out} / Q_{in} = \beta$ was always greater than 2. There must be a minimal drawdown on the order of about 0.2 bar in the collection borehole to ensure 100 % recovery, otherwise some flow lines escape the dipole flow field and tracer may be lost or discharge into the drift. This minimal drawdown in BOMI 87.006 can be achieved by controlling the flow from the extraction well to about 100 ml min^{-1}. From this borehole, maximum flow rates were limited to about 200 ml min^{-1}, resulting in a drawdown of approximately 0.6 bar. Higher pump rates caused degassing of water (oversaturated with nitrogen, see Table 2-3) in the tubing and accumulating gas bubbles caused malfunction of control equipment.

Pulses of tracer were generally added as a slug to the injection flow. A typical pulse injection was performed with a few ml of tracer solution containing 1-10 ppm Uranine and 0.07-4 MBq $^{82}Br^-$. Detection limits were about 0.001 ppb for Uranine (PERKIN ELMER Spectrofluorometer LS-3B and Filterfluorometer LS-2B) and in the order of 30 Bq l^{-1} $^{82}Br^-$ ($3^1/_2$" NaI scintillator).

Four of the pilot tests (see THORNE, 1990a,b) were conducted with a flow field created by only extracting water from the fracture zone without water injection. These test were performed under close to radially converging flow conditions and are referred to as **monopole** tests (see Fig. 6-2). They were conducted utilizing a GSF Single-Borehole Probe for tracer injection. Tracer flow was induced by the drawdown in the pumped collection borehole.

Four pilot tests have also been conducted under **natural gradient** conditions with no water being injected or extracted at any of the boreholes. This natural flow is driven by drainage from the migration fracture to the drift and is very small. A GSF Single-Borehole Probe was installed in the injection borehole and breakthrough of tracers was determined in the collected outflow in the drift. An additional GSF Single-Borehole Probe was installed in a (passive) observation borehole for monitoring tracer breakthrough during some dipole and monopole tests as well as in experiments with a natural gradient.

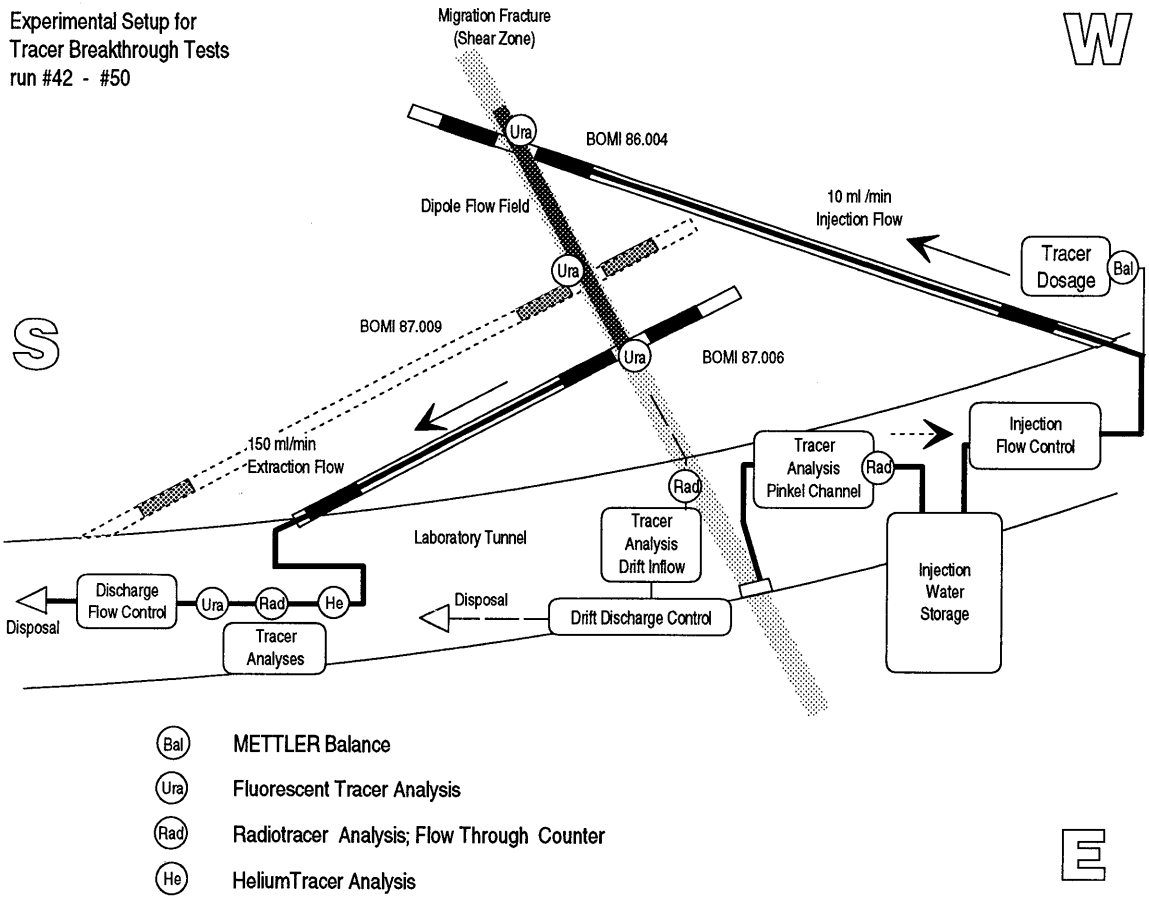

Fig. 6-3: Experimental setup for tracer experiments with MI water.

6.3 Tracer Breakthrough Results

The non-reactive tests were carried out with various flow fields and borehole constellations. The effects of equipment improvement and modifications were carefully monitored and these tests provided extensive information on the experimental area in the migration fracture. The most relevant results were:

- Several viable cross-hole connections were found for tracer experiments, providing a useful range of distances from 2 to 5 m.

- Steady-state flow conditions could be sufficiently maintained during the times required to complete conservative tracer experiments.

- By varying the hydraulic conditions as much as practicable, constraints for future tests were established. For distances of 2 - 5 m, the following time span for pulse breakthrough was established: first detection (= first arrival) of tracers was after 0.5 - 4 hours and corresponding peak travel times were 1.5 to 12 hours. Complete monitoring of the breakthrough tail required continuing tracer analyses for 3 to 10 days (these timescales are particularly useful for planning tests with sorbing tracers).

- Complete tracer recovery is possible for several different flow conditions, mainly depending on the drawdown in the extraction borehole (c.f. Fig. 6-4).

- Depending on the flow conditions, monomodal or bimodal breakthrough curves were observed (see Fig. 6-4). These differences have been postulated to be a result of transmissivity heterogeneities or somewhat channelized flow within the migration fracture (e.g., the variable aperture concept by TSANG et al., 1991; MORENO & TSANG, 1991).

- Prototype injection and extraction equipment worked satisfactorily.

- All three applied tracers (Uranine, $^{82}Br^-$, and helium) yielded practically identical breakthrough curves (see Fig. 6-5).

- To examine the short-term reproducibility of the system two pulse test were conducted within a week in the same flow field ($\beta = 3$). Both breakthrough curves compare favorably (Fig. 6-6). A test to validate long-term effects is planned.

Based on the extensive experience obtained during these pilot tests a series of adjustments and modifications were made prior to conducting the reactive tracer testing described in Section 7.

Knowledge of the shape of the tracer input signal (injected tracer concentrations versus time) is important for modeling tracer breakthrough. Initially, no information was available on dispersion effects within the tubing from the injection device down to the packed-off fracture interval. Later, down-hole Uranine analysis was made possible by installing a fibre optic system (cf. Section 4.5.1) at the end of the injection line in the packer interval. In principle, tracer injection could have been carried out utilizing the GSF down-hole tool (see Section 4.3) for down-hole radiotracer analysis, however, its gas inflated double-packer system was considered inadequate by many reasons (e.g., the range of γ - rays precludes point measurements and depends on geometric factors as well; in addition, it could not be excluded that small amounts of gas may leak from the packers; etc.).

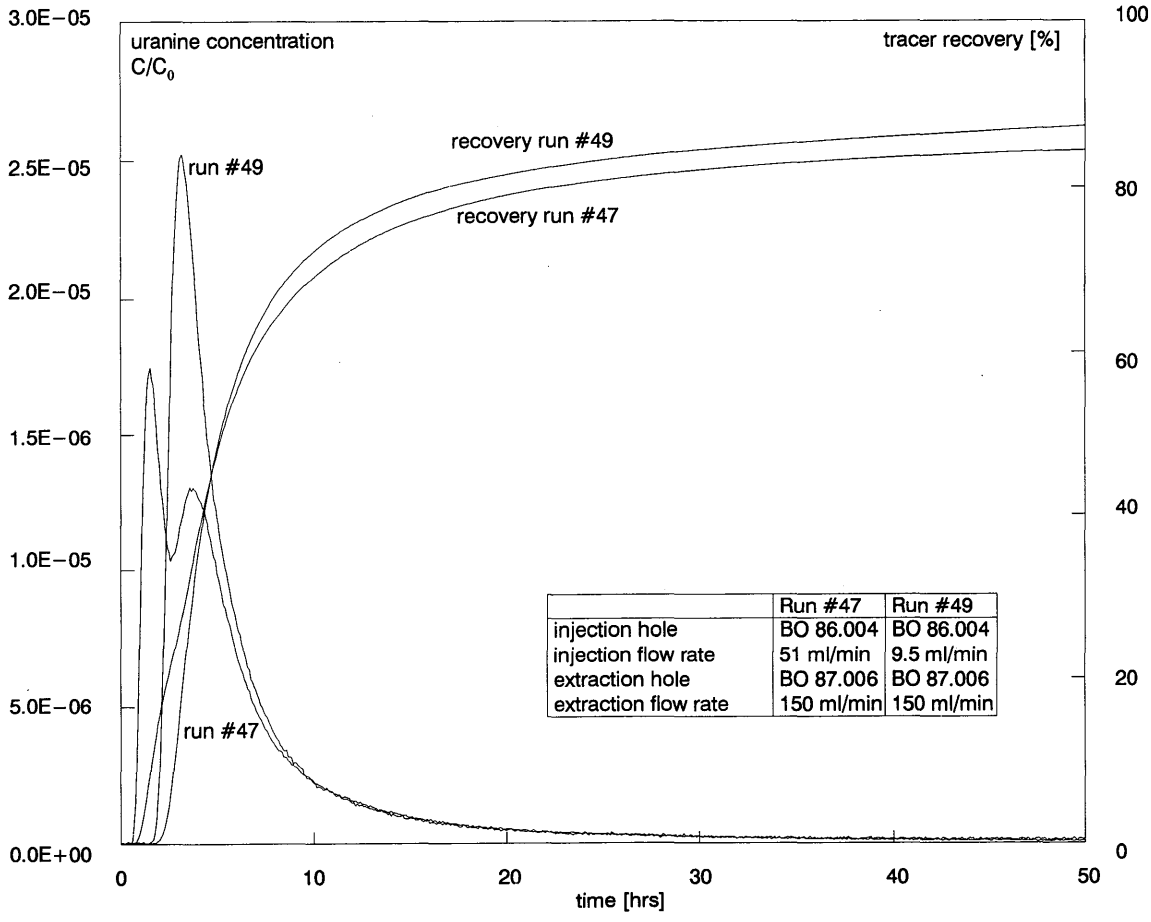

Fig. 6-4: Uranine breakthrough during runs # 47 and # 49.

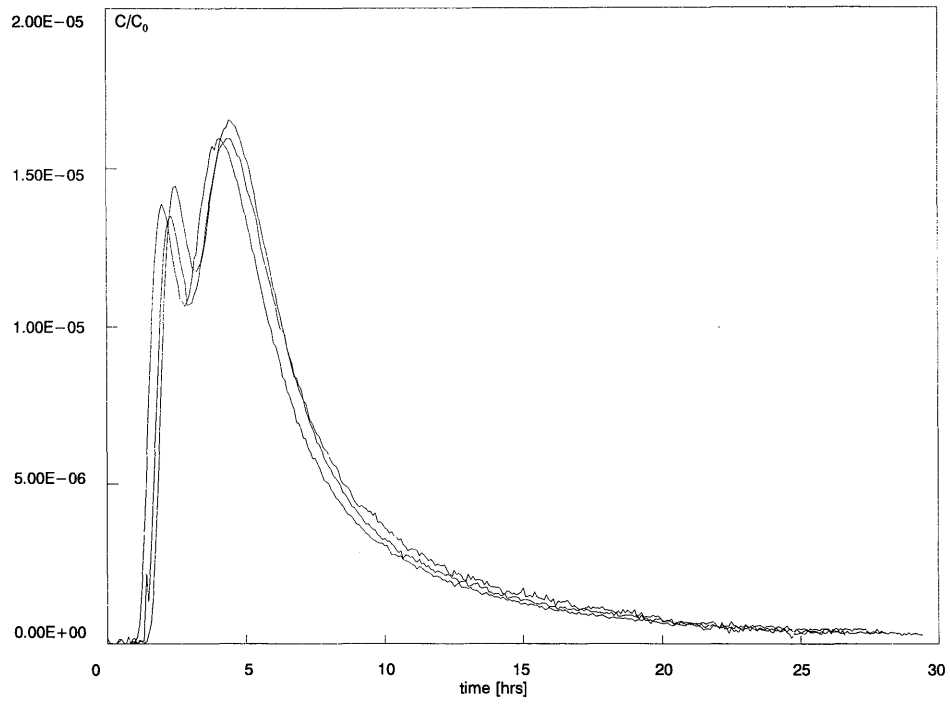

Fig. 6-5: Breakthrough of Uranine, $^{82}Br^-$ and ^4He during test # 42

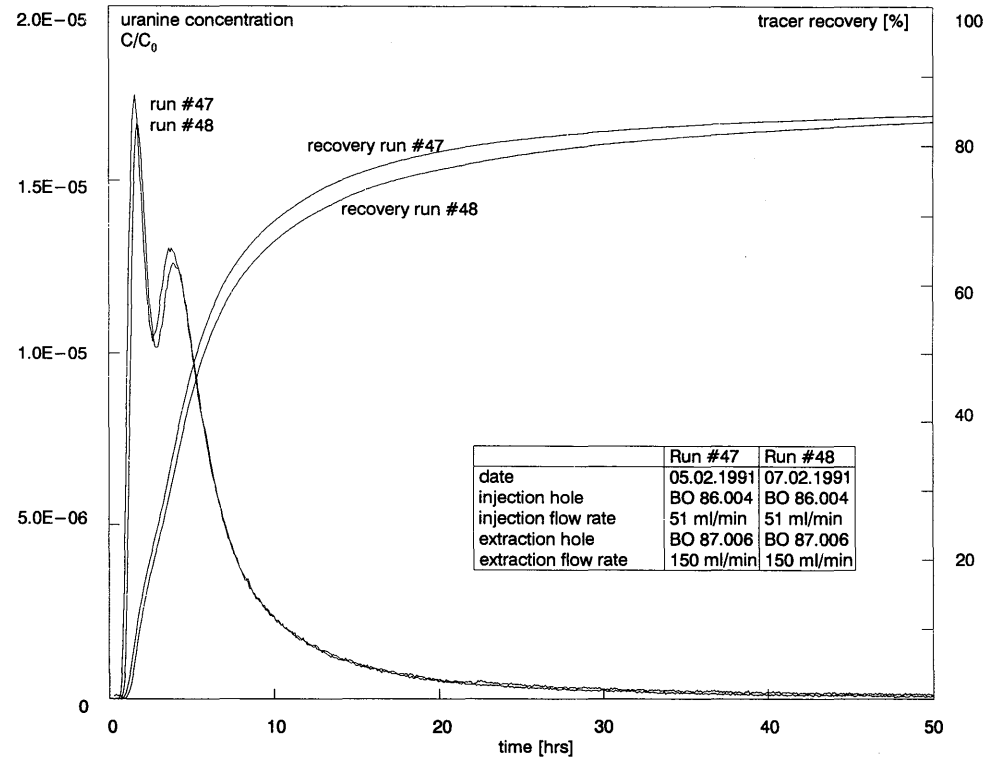

Fig. 6-6: A comparison of tracer breakthrough characteristics and recovery from run #47 and run #48 (see Table 7-1) performed under identical conditions.

6.4 Conservative Tracer Breakthrough Analysis

Preliminary analysis of the conservative tracer allows us to estimate some of the key hydrogeologic parameters required in subsequent interpretations of the sorbing tracer tests. Numerous analyses of the observed breakthrough curves have been conducted by researchers at PSI. An early test analysis, described in HERZOG (1991, NTB 91-31), was fit with both single-porosity (no matrix diffusion; see Fig. 6-7a) and dual-porosity conceptual models (including matrix diffusion; see Fig. 6-7b). The parameters used in these fits are summarized in Table 6-2. Modified modeling of more recent field tests, performed under improved experimental conditions will be documented by HEER (1992).

By comparing the results from the single porosity and dual porosity modeling, the following is worth to mention:

i) the velocity V_o in case of the matrix diffusion model is larger than in the case of the model without matrix diffusion. As the matrix has a retarding effect, the velocity has to be increased in order to fit the experimental data.

ii) The broadening of the curve in the case of no matrix diffusion is governed by the dispersion lenght a_L only, whereas in the case of matrix diffusion, the matrix contributes to the broadening. Thus, fitted a_L are smaller when modeling with matrix diffusion.

Table 6-2: Selected and preliminary model derived parameters for matching conservative tracer breakthrough curves measured during early test runs

distance between boreholes:	$L_o = 490\ cm$	
channel half width:	$b = 1.49 \times 10^{-2}\ cm$	
number of channels:	$n = 10$	flow porosity $\varepsilon_f = 30\ \%$
width of fracture:	$a = 1\ cm$	
maximum penetration depth:	$D = 3.51 \times 10^{-2}\ cm$	
porosity of the matrix:	$\varepsilon_p = 10\ \%$	
bulk density of matrix:	$\rho(1-\varepsilon_p) = 2.670\ g\ cm^{-3}$	
sorption coefficients:	$K_a = K_d = 0$	
Average velocity:	$V_o = 200\ cm\ h^{-1}$	(with matrix diffusion)
	$V_o = 163\ cm\ h^{-1}$	(without matrix diffusion)
Longitudinal	$a_L = 8\ cm$	(with matrix diffusion)
Dispersion length:	$a_L = 10\ cm$	(without matrix diffusion)
Diffusivity:	$\varepsilon_p D_p = 5 \times 10^{-7}\ cm^2\ s^{-1}$	(for matrix diffusion)

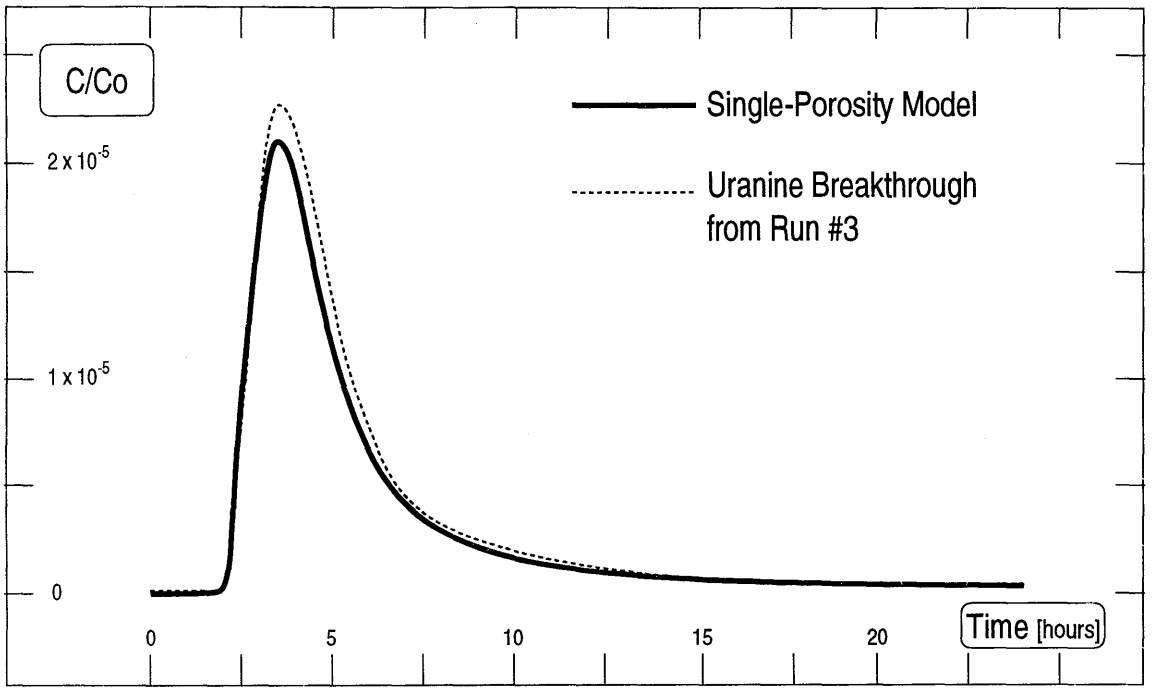

Fig. 6-7a: Results of a single-porosity model (i.e., no matrix diffusion) and the observed tracer breakthrough during run #3

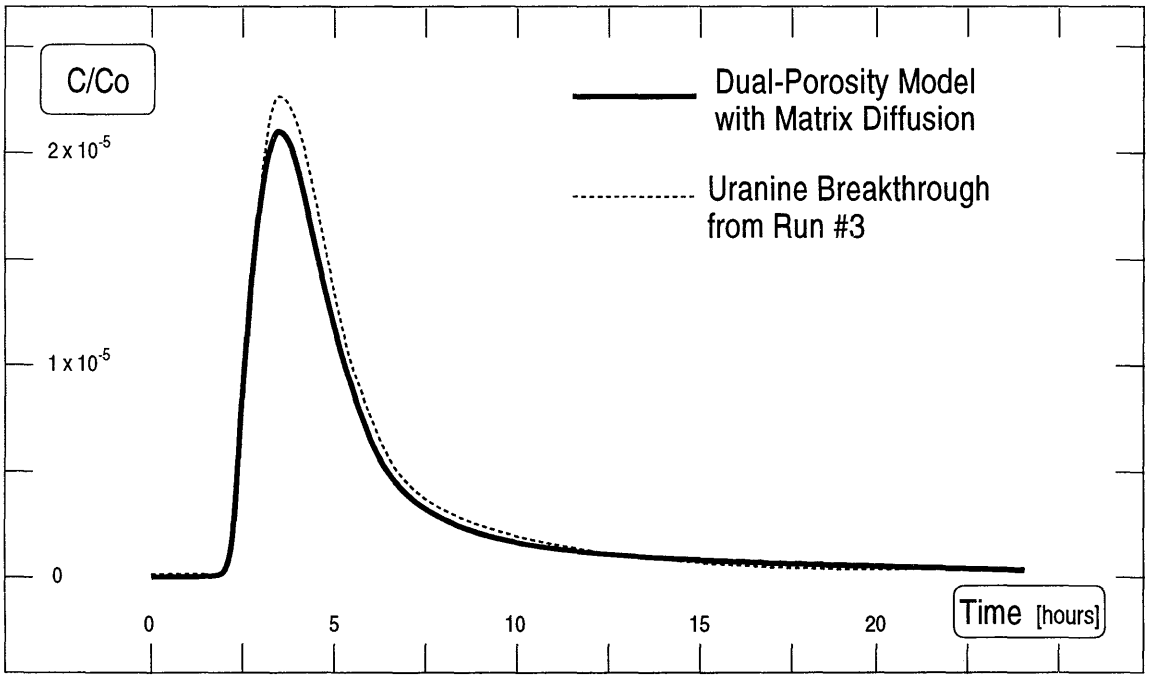

Fig. 6-7b: Results of a dual-porosity model including matrix diffusion and data from field tracer run #3 (conservative tracers)

6.5 Technique Development

Aside from numerous changes of the tracer experimental setup, three novel techniques have been developed which merit to be briefly mentioned as substantial improvements of tracer hydrogeology. These are: low-volume packer intervals, single-fiber fluorometry and the application of the noble gas helium as a tracer.

6.5.1 Low-Volume Packer Intervals

Pilot tracer tests revealed that minimizing equipment volume substantially reduces travel time and uncertainties from mixing processes within the apparatus. Therefore, new low-volume interval pieces were developed with small mechanical packers being activated by the movement of the adjacent water-inflated, main packers (THORNE, 1990a). The modified packer system is depicted in Figure 6-8.

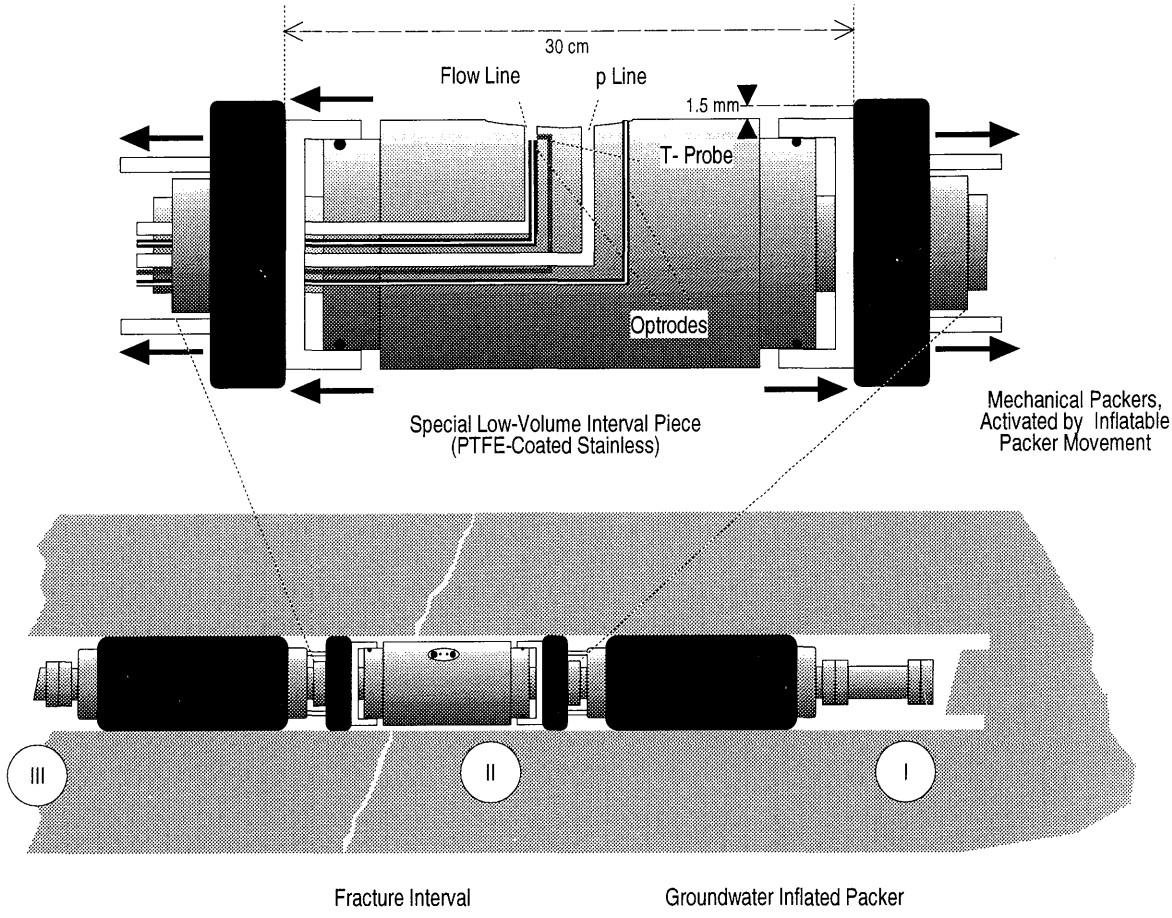

Fig. 6-8: Modified borehole packer setup for fracture intervals.

6.5.2 Optical Fiber Fluorometry (Optrodes)

A fiber optic system for in-situ measurement of Uranine was developed by the University of Stuttgart (quartz fiber fluorometry or optrode technique, BARCZEWSKI & MARSCHALL, 1987). This method allows highly sensitive, down-hole point analysis of fluorotracers over considerable distances without taking samples. This technique is particularly useful to determine instrumental dispersion effects and accurate tracer residence times in the packed-off section of the injection interval during migration experiments. The components of the fiber optic system for downhole measurements of Uranine are illustrated schematically in Figure 6-9.

Based on results obtained with the University of Stuttgart prototype, a modified system was built. Two optical fiber pairs were placed into each packer interval piece, one at the end of the flow line, the other on the surface of the interval tubing. Usually, one of the fiber optic systems is installed in the injection interval, one in the extraction interval, and, if possible, an additional one in the fracture interval of a neighboring borehole (see Fig. 6-3). They allow one to determine exact residence times of the conservative tracer Uranine. For the modified system an argon laser (maximum ouput 100 mW) was chosen as a light source. With a specifically developed detection system Uranine concentrations ranging from 0.001 ppb to 1 ppm could be measured down-hole. Details of the modified low-volume packer intervals and positioning of optrodes are provided in THORNE (1990b) (see also Figure 6-9).

The fiber optic system provides a novel and useful technique for downhole analysis of fluorotracers. The first results of the modified system are most encouraging. Because of its high sensitivity the system appears to be suitable for down-hole analysis in deep boreholes (several hundred m deep). Equipped with an tracer injection and mixing device, and installed in a packer system, it may also be used for single-hole dilution tests.

The optrode technique was used in more recent tests (e.g., run #50; see Table 7-1) to determine the exact shape of the Uranine concentration function in the injection interval following a 3 minute pulse injection with an HPLC pump. Figure 6-10 illustrates the actual tracer input function observed in the packed-off injection interval. This function differs substantially from any theoretically derived mixing function. The mean residence time of the tracer in the injection equipment may, particularly for low injection flow rates, represent a significant portion of the total breakthrough time and, thus, the actually measured tracer input function should be considered during modeling of tracer tests.

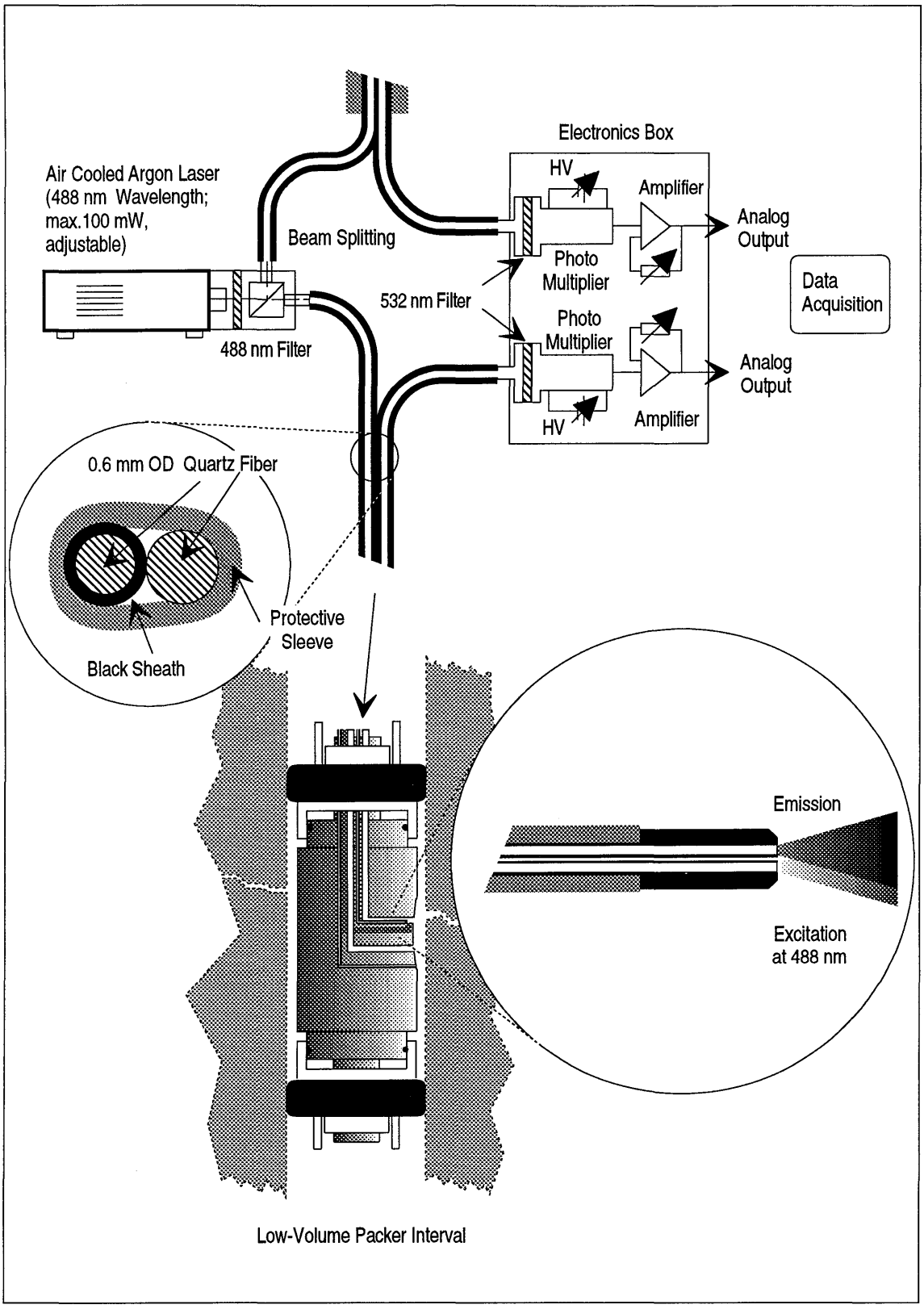

Fig. 6 - 9 Components of the dual-fiber optic system for high-sensitivity down- hole uranine analyses (optrodes)

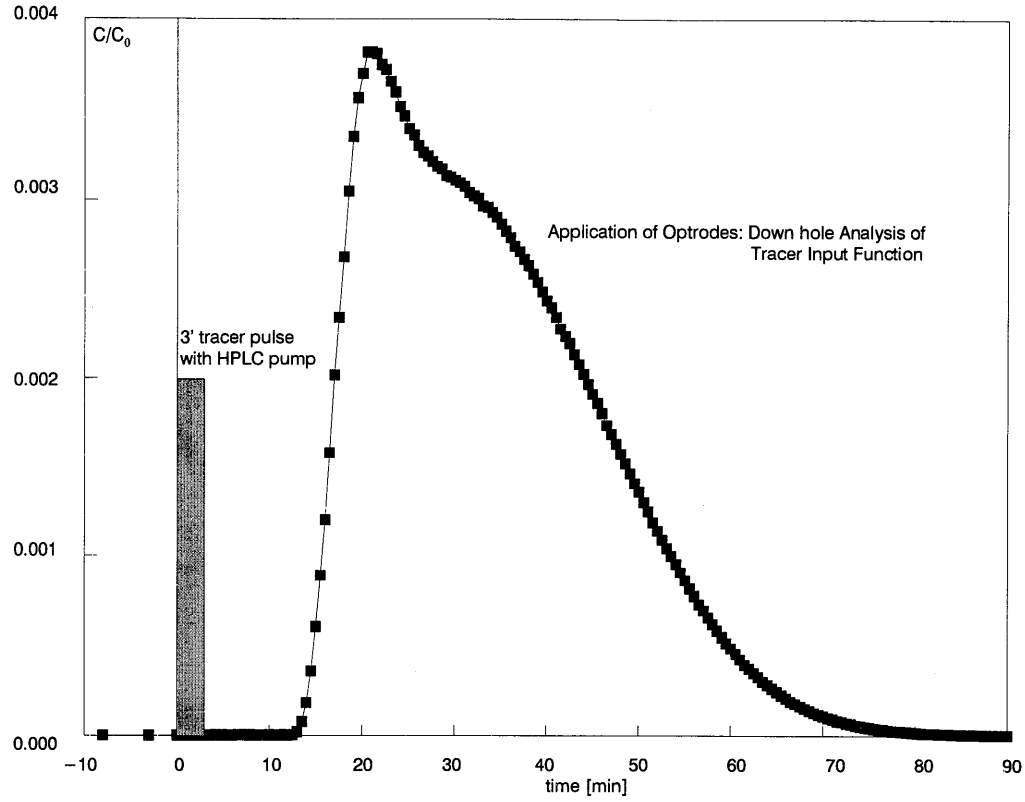

Fig. 6-10: Uranine concentration versus time, measured down-hole by the fiber optic system (optrode) within the injection packer interval.

6.5.3 Helium Tracer Method

It is often useful and informative to complement anionic conservative tracers by inert, neutral species. Therefore an additional conservative tracer was required to detect charge related phenomena (e.g., anion repelling or exclusion in the rock matrix). Preliminary breakthrough tests were conducted by injecting ^{4}He (together with $^{82}Br^{-}$ and Uranine). Samples of extracted water were analyzed mass spectrometrically in the laboratory. The preliminary results indicated that dissolved ^{4}He can be used as a tracer for closed groundwater systems (EIKENBERG & KIPFER, 1989).

A novel analytical in-situ technique was developed, based on a flow-through vacuum dialysis, with a 1 mm thick silicon rubber membrane as a permeation leak and a commercial helium leak detector (BALZERS HLT-100 with a quadrupole mass spectrometer as a ^{4}He or ^{3}He partial pressure gauge). The principle of online He analysis is illustrated in Figure 6-11. The method and the experimental setup is also described by THORNE (1990b) and in a recent paper by EIKENBERG et al. (1992a). The effective detection limit of this method is about 1ng ^{4}He per liter water (corresponding to about 3×10^{-8} ccSTP ml^{-1}). Natural Grimsel water exhibits (during early tests) a nearly constant He content of about 4×10^{-6} ccSTP ml^{-1}. Pulse injection of 5-20 ml of He-saturated water produces a peak signal of about twice the background concentration.

EIKENBERG et al. (1992) indicated that the method could be useful to check water flow fields for completely saturated conditions (as He tends to penetrate gas-filled pore space, its breakthrough under unsaturated conditions is expected to be retarded with respect to dissolved anion tracers). In addition, it was initially hoped that utilizing the He detection technique might allow us to verify effects attributed to matrix diffusion. Matrix diffusion is an effect related to the double porosity nature of the flow system in the migration shear zone. Tracers may diffuse from the major water conductive channels into porous fracture infill material. It was hoped that the simultaneous injection of He and Uranine could reveal a slightly different breakthrough which could be ascribed to the comparatively larger diffusion coefficient of dissolved He. To date it has not been possible to observe effects that could unambiguously be attributed to the uncharged helium particles penetrating the (negatively charged) rock matrix more readily than anionic tracers.

The resolution of ^{4}He concentration measurement is rather limited due to temporal variations of the ^{4}He background in the Grimsel groundwater. Experiments with ^{3}He are planned to improve measurement accuracy.

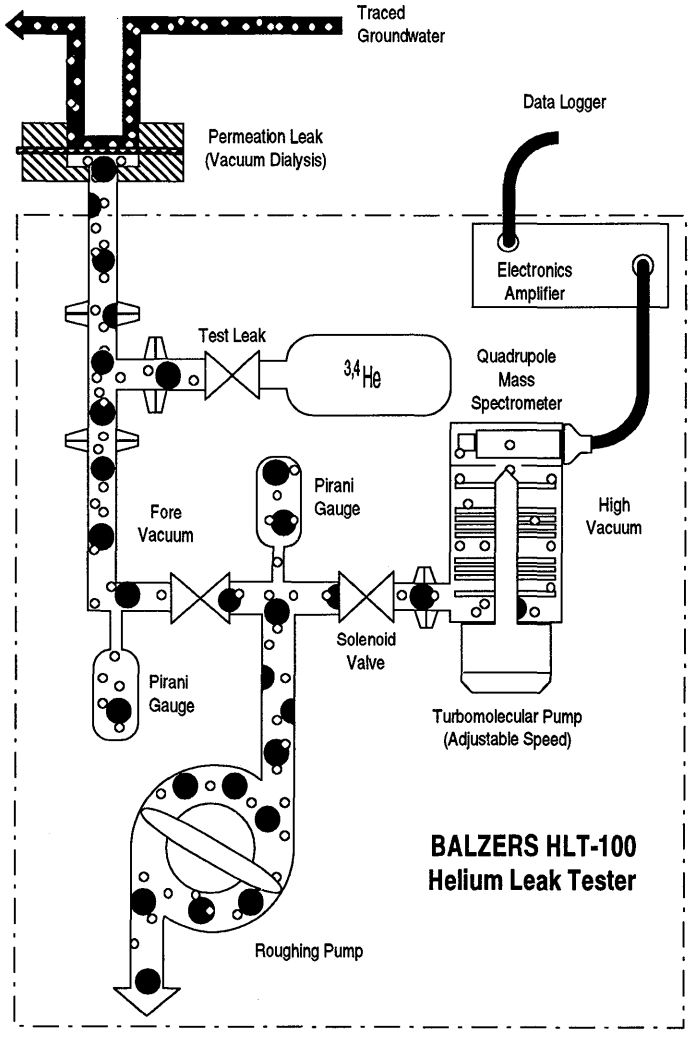

Fig. 6-11: Principle of ^{3}He or ^{4}He on-line tracer analysis based on vacuum dialysis and a standard industrial helium leak detector.

7 REACTIVE TRACER TESTS IN THE MIGRATION FRACTURE

This section focuses on the field migration tests performed with substances which interact with the fracture rock material. In particular, a hydrogeochemical equilibration test (i.e. a dynamic field scale rock/groundwater interaction or conditioning experiment) and tracer breakthrough experiments with ^{22}Na and ^{24}Na are discussed.

Initially it was planned to perform migration experiments with $^{85}Sr^{2+}$ during 1990, but since equipment tests at the migration site revealed substantial sorption of Sr^{2+} on standard equipment (mainly on stainless steel as well as polyamide 11 tubings), the experiments with Sr had to be delayed. As Na^+ did not sorb on these materials, a suite of migration experiments was first carried out with $^{22}Na^+$ and $^{24}Na^+$. Major equipment modifications have been undertaken including the replacement of polyamide by teflon tubings and teflon coating of the packer intervals. Recent material tests showed extremely little (reversible) sorption of Sr^{2+} (and Na^+) on the modified equipment. After these material tests, tracer analytical equipment was again calibrated and a series of short-term pulse experiments were recently carried out with Uranine, $^{123}I^-$ and $^{24}Na^+$. The recent results from tests with $^{123}I^-$, with its breakthrough characteristic closely matching the other conservative tracers, is presented elsewhere (EIKENBERG et al., 1992b). A first pulse injection of $^{85}Sr^{2+}$ together with$^{22}Na^+$ and Uranine (run # 50) was started in February 1991. Monitoring of Sr is still underway during the preparation of this manuscript. Preliminary results of this migration experiment indicate the need of prolonged tracer monitoring of on the order of at least 4 months. Thus, no Sr results will be included in this report (Some preliminary details are given by EIKENBERG et al., 1992b).

7.1 Summary of Field Tests with Reactive Tracers

During the Winter of 1989 a field scale rock-water interaction experiment (run # 17) was performed, with monitoring of the main dissolved cations as the reactive component. Between Summer 1989 and February 1991 four migration experiments with pulse injection of short lived $^{24}Na^+$ and one continuous injection experiment with $^{22}Na^+$ were carried out (run # 46). A list of all experiments with reactive tracers is provided in Table 7-1. This table also gives information on the flow conditions and the tracers used for the various tests. During all of the tracer experiments, at least one non-sorbing substance (i.e Uranine, ^{82}Br or ^4He) was simultaneously injected to enable a direct comparison of the breakthrough profiles of conservative and reactive tracer. A compilation of all previous field tracer tests up to October 1989, involving conservative tracers only, is summarized in Table 6-1.

Table 7-1: List of all dipole field tests involving reactive tracers.

Run Nr.	Test Date (start)	Tracers (injected simultaneously)	Tracer Injection Mode	Dipole Flow Field			
				Injection		Collection	
				Input Rate ml/min	Borehole BOMI	Output Rate ml/min	Borehole BOMI
#17	29.03.89	EM water [1]	step	46	86.004	108	86.006
#29	27.06.89	^{24}Na ^{4}He Uranine	pulse	78	86.004	166	86.006
#30	04.07.89	^{24}Na ^{4}He Uranine	pulse	21	86.004	72	86.006
#31	10.07.89	^{24}Na ^{4}He ^{82}Br Uranine	pulse	5	86.004	80	86.006
#46	03.07.90	^{22}Na ^{4}He ^{82}Br Uranine	step [2]	10	86.004	153	86.006
#47	05.02.91	^{123}I Uranine [3]	pulse	51	86.004	150	86.006
#48	07.02.91	^{24}Na Uranine [4]	pulse	51	86.004	151	86.006
#49	19.02.91	^{123}I Uranine [3]	pulse	9.5	86.004	149	86.006
#50	27.02.91	^{22}Na ^{85}Sr Uranine [4]	pulse	9.5	86.004	148	86.006

1 hydrochemical field equilibration experiment with a water of slightly different composition, i.e. EM water is replacing MI water in the fracture.

2 Uranine and ^{22}Na were injected continously over 220 hours, ^{82}Br was added as a single pulse, ^{4}He as multiple pulses during run #46.

3 run #47 and run #49 are already listed in Table 6-1 (conservative tracer tests). However, I^- might be a very weakly interacting species, although the relatively short-termed field experiments performed so far did not provide unambiguous indication of any iodine retardation.

4 Uranine concentrations were also monitored by quartz fiber optrodes in the fracture intervals of the injection/extraction boreholes as well as of the passive borehole BOMI 87.009.

7.2 A Hydrogeochemical Equilibration Experiment

The first series of pilot tests with non-sorbed, anionic tracers were carried out with an imported water (EM water; see Table 7-1) from borehole BOEM 85.012 located about 300 m south of the migration site in the main access tunnel. The chemical composition of this groundwater was slightly different from that in the migration fracture (MI water; see also Section 7.2.1). For a correct interpretation of any migration experiment with reactive tracers, however, it is important that the groundwater and the fracture material are in chemical equilibrium. Thus, prior to the first tests with sorbing tracers, it was decided to monitor the concentration changes in the extracted water during equilibration of the fracture with EM water.

The initial objectives of the hydrogeochemical equilibration experiment were the following:

- to determine the timescale of equilibration for different anions and reactive cations and
- to obtain clues on how the fracture responded to injection of a foreign water.

This field-scale rock-water interaction experiment turned out particularly helpful

- to estimate the in-situ cation exchange capacity and in-situ sorption coefficients,
- to estimate the effects of water composition on sorption coefficients for Na^+ and Sr^{2+}, and
- to improve the understanding of equilibration (and transport) processes in Grimsel groundwater (EIKENBERG et al., NTB 90-39)

Such experiments may provide a convenient method to more reliably extrapolate laboratory sorption data (usually determined under different physical conditions) to the conditions prevailing in the field.

7.2.1 Experimental Set-up

The pilot tracer tests 1988 (see Section 6) potentially could have contaminated the MI water in the migration fracture with EM water. Although there are some differences in their ionic composition (mainly in the proportions of Na^+ and Ca^{2+} contents; see Table 7-2), the major characteristics are very similar in that both waters are poorly mineralized with an ionic strength of roughly 10^{-3} M, with O_2 and CO_2 below the detection limit (less than 0.1 ppm and 10^{-6} M, respectively). The pH is relatively high with values of 9.6 and 8.9 in the MI and EM water, respectively. Prior to any field experiments with reactive tracers, the fracture was purged from any such contamination by (1) thoroughly re-equilibrating with MI water by recurring strong drawdown during removal of different packer systems for equipment modification, (2) prolonged radial (natural gradient) flow to the drift and (3) the 35-day long-term constant-discharge hydrotest LTCDT in BOMI 87.009.

The hydrogeochemical equilibration experiment is described in detail by EIKENBERG et al. (NTB 90-39). The resident groundwater in the migration fracture (MI water) was, within a closed flow field, replaced by continuously injecting a slightly foreign groundwater (EM water) with modified equipment for doublet flow field control (see Section 6). Electrical conductivity and pH were measured by electrodes in the injection and extraction flow. During the course of the experiment, a total of 22 water samples were taken and subsequently analyzed at the Paul Scherrer Institute (PSI) for the analysis of the major anion and cation concentrations, alkalinity, and pH.

Table 7-2: Mean chemical composition° of MI water and EM water.

Parameter	MI water [1]	MI water [2]	EM water [2]
Na^+	692 ± 9	692 ± 6	264 ± 7
K^+	3.84 ± 0.50	4.96 ± 0.22	24.0 ± 0.8
Rb^+	-	0.025 [4]	0.051 [4]
Mg^{2+}	1.08 ± 0.25	1.24 ± 0.06	7.74 ± 0.16
Ca^{2+}	254 ± 2	284 ± 1	422 ± 11
Sr^{2+}	3.67 ± 0.04	3.92 ± 0.02	7.76 ± 0.23
Sr^{2+}	-	4.14 [4]	7.5 [4]
SO_4^{2-}	115 ± 11	118 ± 16	88 ± 20
F^-	330 ± 5	355 ± 19	77.9 ± 4.2
Cl^-	155 ± 8	158 ± 12	5.9 ± 1.1
pH	9.6 ± 0.1	9.5 ± 0.1	8.9 ± 0.1
Ionic Strength [M]	0.0012	0.0013	0.0010
Temperature [°C]	12	12	10.4 [3]
Alkalinity	420 ± 10	450 ± 10	600 ± 10
Conductivity [$\mu S\ cm^{-1}$]	103 ± 3	106 ± 3	75 ± 3

° all concentrations are in $\mu eq\ l^{-1}$

1 data from BAJO et al. (NTB 88-23)

2 data from EIKENBERG et al. (NTB 90-39)

3 injection temperature into the migration fracture was 12°C (ambient temperature at the experimental site)

4 isotope dilution data from KRALIK (1991)

7.2.2 Results

A thorough discussion of measured and expected chemical effects is documented in EIKENBERG et al. (NTB 90-39). Generally, different equilibration times for anions and various cations were observed: F^- and Cl^- reached steady state concentrations in the extracted water within about 50 hours (i.e. consistent with conservative tracer breakthrough experiments carried out under similar flow conditions; see Section 6) whereas the major cations, Na^+ and Ca^{2+}, required about 150 hours. Mg^{2+}, K^+, and Sr^{2+} showed evidence of being retarded more strongly. Sr^{2+} did not reach a steady state until about 250 hours and K^+ and Mg^{2+} concentrations were still increasing slowly when the experiment was terminated after 312 hours.

7.2.3 General Conclusions from the Hydrogeochemical Equilibration Experiment

For the pilot tests performed with conservative (non-sorbed) tracers, it can be safely concluded that the use of chemically different water has no detectable effects on their breakthrough characteristics. For reactive tracers, however, any changes of the water chemistry within the flow path could lead to chemical disequilibrium and, thus, ill defined sorption conditions.

The ion concentrations were changing somewhat during the course of the field equilibration experiment, i.e. the conditions were slightly different from the (intended) chemical equilibrium during tracer experiments. Therefore, application of the usual transport models does not allow us to deduce effective K_d values for Na^+ and Sr^{2+} (valid for the MI fracture and MI water). For reactive tracer experiments, therefore, a new source of injection water (MI-water) had to be explored.

The temporary (elemental) concentration changes were analyzed and interpreted by EIKENBERG et al. (NTB 90-39) on the basis of mixing processes (within the flow field and in the drawdown borehole interval) and the assumption that the fracture material behaved as a weak cation exchange medium. Although during this experiment multi-ionic cation exchange processes occurred simultaneously, the dominating mechanism was cation exchange between Na^+ (sorbed on fracture minerals under equilibrium conditions with MI water) and dissolved Ca^{2+} in EM water (c.f. Table 7-2). The exchange reaction for the binary system involving the cations Na^+ and Ca^{2+} may be written as

$$Ca^{2+} + 2\,Na^{+}{}_{x} \;=\; 2\,Na^{+} + Ca^{2+}{}_{x} \qquad \{7.1\}$$

in which x denote exchangeable (or sorbed) ions on the surface of the cation exchange medium (see Section 5.3). The evolution of Na^+ and Ca^{2+} concentrations in the extracted water is illustrated in Figure 7-1. The mixing-sorption controlled breakthrough curves of both cations are similar.

From the concentration changes of the different species, an **interacting component** could be deduced for each of the cations (e.g. by graphically subtracting from its breakthrough curve the mixing, i.e. dispersive component which is represented by the breakthrough of any non-reactive anion; see Fig. 7-2). This interacting component corresponds to the mass of cations being sorbed (e.g. Ca^{2+}) or desorbed (e.g. Na^+) during the equilibration process. Applying laboratory derived ion selectivities for the fracture material, the data provide *a direct measurement of the flow field exchange capacity*. This quantity is termed *FEC* in EIKENBERG et al. (NTB 90-39) and is in the order of 300-400 meq for the applied doublet flow field within the migration fracture (see e.g., the shaded area in Fig. 6-2).

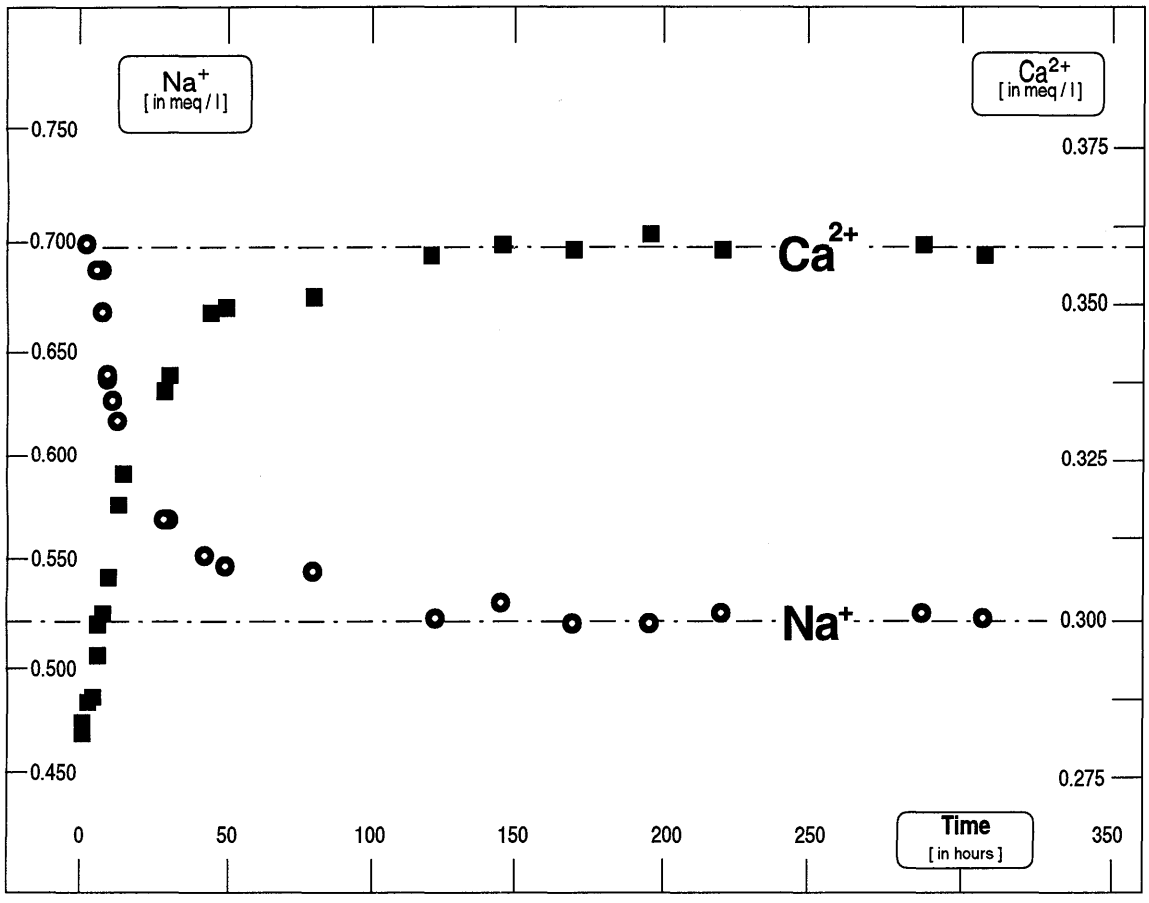

The dashed lines represent calculated steady-state concentrations for the two cations based on known mixing (i.e. dispersion, dilution) processes.

Fig.7-1: Concentrations of Na^+ and Ca^{2+} as a function of time in extracted groundwater from the migration fracture during replacement of MI water with EM water within an unequal-strength dipole flow field.

7.2.4 Comparison of the Field Equilibration Experiment with Laboratory Data

Under simplifying assumptions on porosities and the geometry of the flow field, rough estimates of mass-related parameters can be deduced. The in-situ cation exchange capacity *(CEC)* is in the order of 2 μeq g^{-1}, the in-situ sorption coefficients for Na^+ were 0.05 - 0.25 ml g^{-1} and ranged from 2 - 10 ml g^{-1} for Sr^{2+}. These values are somewhat lower than those determined from rock-water interaction experiments and are, substantially smaller than those measured during batch radiotracer sorption experiments in the laboratory (cf. Table 5-7).

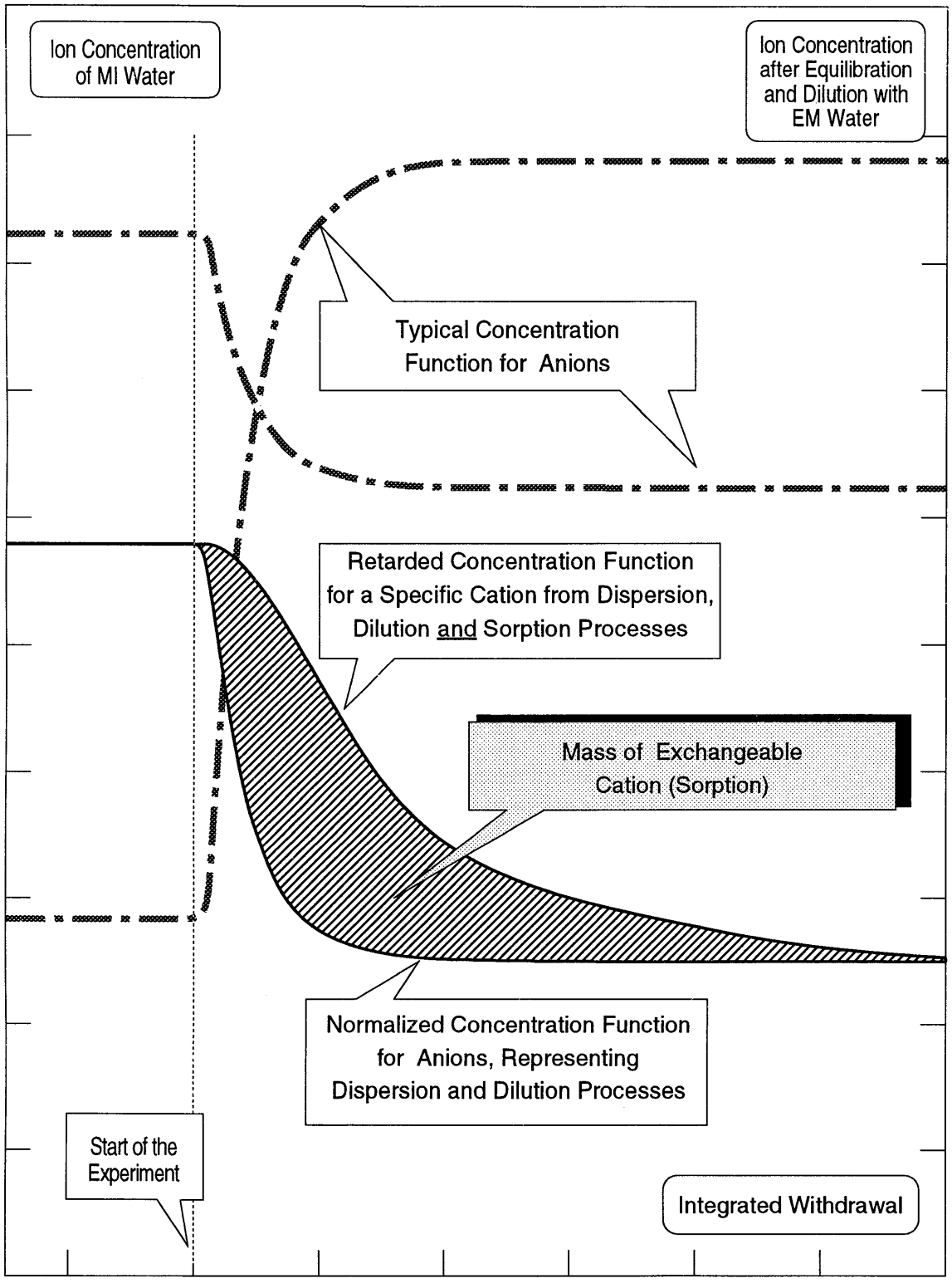

Fig. 7-2: Principle to derive the effective cation exchange capacity *(FEC, in eq)* by replacing the resident MI water by the slightly different EM water in an unequal-strength dipole flow field (concentrations are in arbitrary units).

The values of the in-situ CEC and sorptions coefficients are, not unexpectedly, smaller than the laboratory values. This is mainly due to there being less accessible mineral (i.e. mainly phyllosilicate) surfaces in the MI fracture than in laboratory samples (where the disaggregation of the rock exposes more fresh mineral surfaces). The ratio of the sorption coefficients for Sr^{2+} and Na^{+} is, however, independent of the CEC value (for systems of similar mineralogy and surface properties, i.e. ion selectivities; see Section 5.3.3). EIKENBERG et al. (NTB 90-39) obtained a $K_d[Sr]/K_d[Na]$ ratio of approximately 40 for their field rock-water interaction experiment. This value is close to the ratio from laboratory rock-water interaction experiments (ratio of approximately 60, see Section 5.2) and from batch sorption experiments (ratio of 25 - 45, see Section 5.4). This is considered a good agreement between field and laboratory results, particularly in view of the involved complexities.

Assuming the ion-exchange model to be valid, in-situ rock-water interaction experiments provide a direct measure of the actually available exchange sites (termed FEC in units of [eq]) for the studied flow field. It is therefore recommended to include this parameter as an option in transport models as it is related to such in-situ parameters as the CEC and K_d.

7.3 Pulse Tests with ^{24}Na

A series of experiments was performed with short-lived ^{24}Na ($t_{1/2}$=15h). This isotope was very useful to obtain first clues on the behaviour of Na^{+} because any contamination of the equipment would have decayed within a rather short time. However, its halflife was too short for complete monitoring of the whole Na^{+} breakthrough. The experimental setup and the results of these experiments will be summarized in this section. The $^{24}Na^{+}$ and Uranine breakthrough data of run # 29 were analyzed applying preliminary versions of a transport model (HERZOG, 1990; HERZOG, NTB 91-31). A short discussion of measured and model derived K_d [Na] values is given at the end of this section.

7.3.1 Experimental Set-up

During the first suite of migration experiments with $^{24}Na^{+}$ (runs # 29-31 in the summer 1989), injection water (MI-water) was pumped from the fracture interval in BOMI 87.010. Prior tests by pumping up to 100 ml min^{-1} from this borehole resulted in only a small drawdown and non-detectable pressure interferences (< 10 mbar) in any other borehole. Otherwise, the setup is identical to the one used for the pilot tests with conservative tracers (Fig. 6-1; see also THORNE, 1990a, b). During the more recent migration experiments (e.g. run # 48, January 1991) injection water was collected (without atmospheric contamination) from a discharge channel at the tunnel wall and subsequently stored under a pure nitrogen atmosphere in a 1'500 l stainless steel tank (see Fig. 6-3). Repeated checks of the chemical composition of MI water during storage did not reveal any detectable changes.

The first three pulse injection experiments with short-lived $^{24}Na^{+}$ were carried out

under varied flow conditions (see Table 7-1) in order to obtain different tracer travel times (and, possibly, clues on the Na^+ sorption kinetics). As always the same fracture interval was tested (between BOMI 86.004 and BOMI 87.006), the mean travel time was mainly effected by the drawdown, i.e. the output flow rate in the extraction borehole. The width of the dipole flow field was attributed to the various ratios for input/output flow rates. Mean values were 78/165 ml min^{-1} for run #29 (fast dipole,), 21/72 ml min^{-1} for run #30 (slow dipole), 5/80 ml min^{-1} for run #31 (narrow, slow dipole) and 51/151 ml min^{-1} for run #48 (fast dipole; see also Fig. 6-2).

The stability of the flow rates was precisely monitored and varied from 1 - 10 % during runs #29 - 31 (MOINEAU pumps) and less than 1 % during run #48 due to the more precise HPLC pumps. Monitoring the groundwater discharge of the tunnel indicated that small quantities of injected radiotracers (i.e. less than 1 %) appeared in the tunnel whenever the output flow in the collector borehole was less than about 100 ml min^{-1}. Therefore, all migration experiments after 1989 were carried out with output flow rates of around 150 ml min^{-1} and input/output flow ratios of 1/3 (wide unequal-strength dipole) or 1/15 (narrow unequal-strength dipole flow field; see Fig. 6-2).

Table 7-3: List of used tracers quantities, method of tracer dosage, approximate equipment volumes and analytical sensitivities[1] during pulse injection breakthrough experiments

Test:		run #29	run #30	run #31	run #48
Date:		27/06/1989	04/07/1989	10/07/1989	07/02/1991
Tracer:	$^{24}Na^+$ [1]	4.06 MBq ± 10%	5.16 MBq ± 10%	4.09 MBq ± 10%	5.44 MBq ± 10%
	Uranine [2]	1 ml ± 4%	1 ml ± 4%	5 ml ± 4%	3.242 ml ± 0.5%
Dosage Device:		Syringe	Syringe	Syringe	HPLC Pump
Equipment Volumes:					
Injection Line		210 ml	210 ml	210 ml	280 ml [3]
Input Borehole Interval		900 ml	900 ml	900 ml	80 ml [3]
Output Borehole Interval		1200 ml	1200 ml	1200 ml	80 ml [3]
Flow-Through Scintillation Counter		1000 ml [4]	1000 ml [4]	1000 ml [4]	600 ml [3]

1 scintillation counter accuracy is ± 1.5% for $^{24}Na^+$ based on calibration runs; sensitivity for $^{24}Na^+$ analysis in the flow-through detector is ~ 0.02 Bq ml^{-1}

2 taken from a 10 ppm stock solution; relative accuracy of Uranine measurements in MI water is better than 1%; detection limit is 0.001-0.002 ppb

3 all teflon or PTFE coated equipment; flow-through coil around scintillation counter

4 cylindrical flow-through tank around scintillation detector.

Narrow flow fields (or monopole arrangements) are of interest for the modeling exercise since, ideally, the flow path would be expected to follow the most direct connection between injection and extraction borehole intervals (see e.g., MORENO & TSANG, 1991).

The different methods of tracer dosage, the amounts of tracers injected, approximate detection limits for tracer analyses as well as typical equipment dead volumes during the various pulse runs are set out in Table 7-3. Although the $^{24}Na^{+}$ solutions were not carrier free (about 100 MBq were obtained by neutron activation of 1 mg $NaCO_3$ in a PSI research reactor and subsequently split for laboratory and field measurements), the increase of the natural Na^{+} concentration in the input water flow after pulse injection was always much less than 1 %.

7.3.2 Results of Migration Experiments with $^{24}Na^{+}$

Breakthrough Characteristics: Figures 7-3 and 7-4 show the results of the four pulse migration experiments with $^{24}Na^{+}$ (runs # 29-# 31 and # 48). Measured concentrations of $^{24}Na^{+}$ and the simultaneously injected conservative tracers in the output flow are normalized to C/C_0. For pulse injection, C_0 is defined by dissolving the amount of injected tracer in 1 ml MI water. Tracer recoveries corrected for flow rate variations are also shown. Figure 7-5 illustrates a comparison of the four breakthrough curves of $^{24}Na^{+}$. The injection and extraction flow rates caused differences of the peak travel times by a factor of about three. Experiments # 30 and # 48 resulted in clearly bimodal characteristics (the bimodality of # 29 is more subdued) of the concentration versus time curve, while experiment # 31 yielded monomodal breakthrough profiles for both, conservative and reactive tracers. These differences were already noticed during the pilot experiments (see Section 6) and attributed to channeling or by the heterogeneous transmissivity distribution within the migration fracture.

Although experimental conditions during 1988 and the most recent $^{24}Na^{+}$ pulse tests might have differed due to significant changes of equipment volumes, the input/output flow rates during runs # 29 and # 48 were similar and, thus, should allow a comparison of the breakthrough characteristics of these two tests. First tracer arrival, peak width, and recovery were roughly similar (see Fig. 7-5), however, important details (e.g. lower peak height and more pronounced bimodality during run #48) are different. It is not clear whether these differences can be entirely attributed to the reduced equipment volumes or whether the flow conditions within the migration fracture had changed somewhat over the last 2-3 years. Such changes could have occured by local erosion and redeposition of unconsolidated fracture infill (fault gouge) during the annual cycles of local dislocations (see Section 2.1) or short periods of enhanced flow velocities (mainly caused by free outflow from the boreholes during packer replacement or equipment modification).

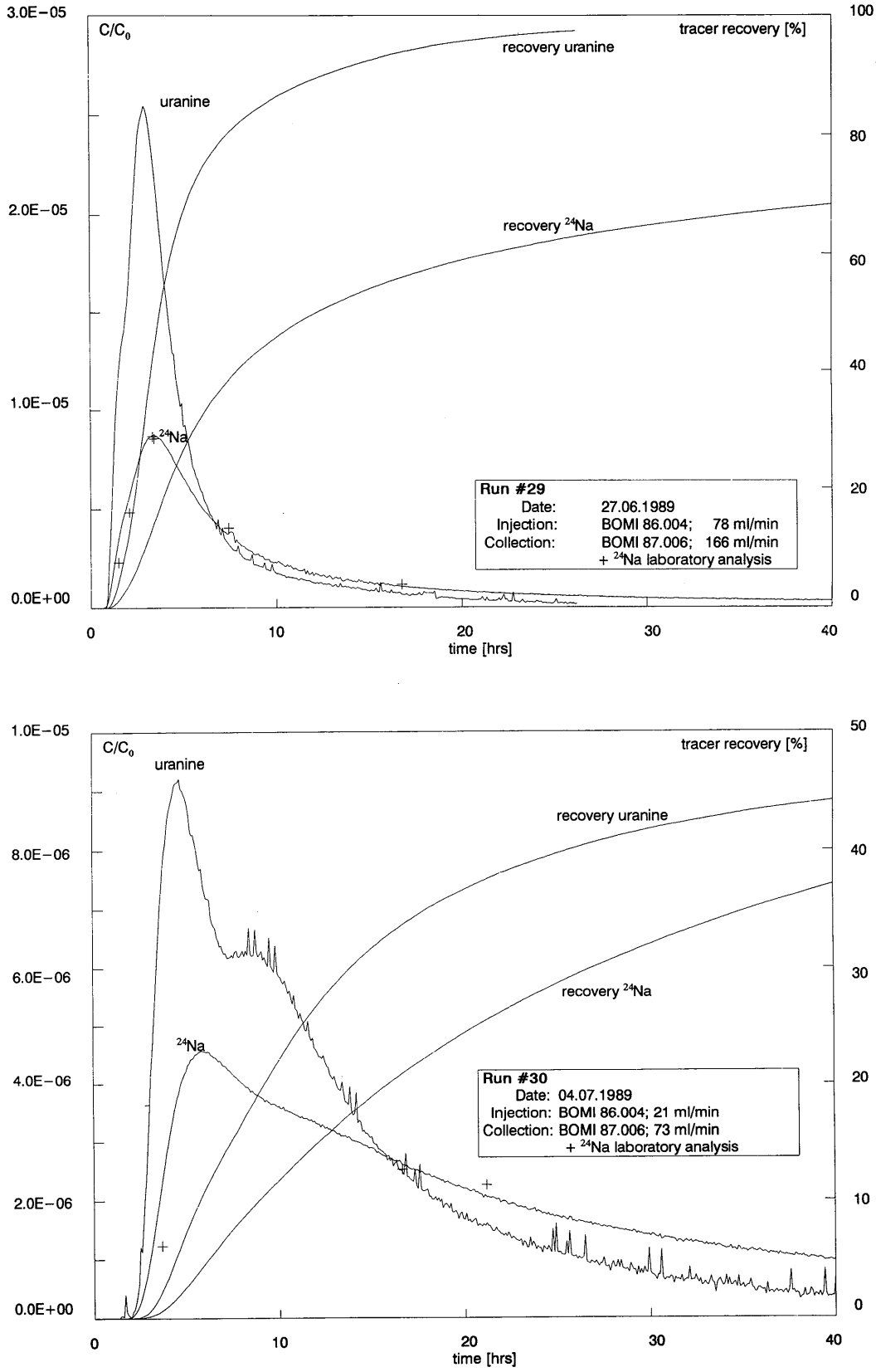

Fig. 7-3: Tracer breakthrough profiles and recovery after pulse injection of $^{24}Na^{+}$ and Uranine during run #29 and run #30.

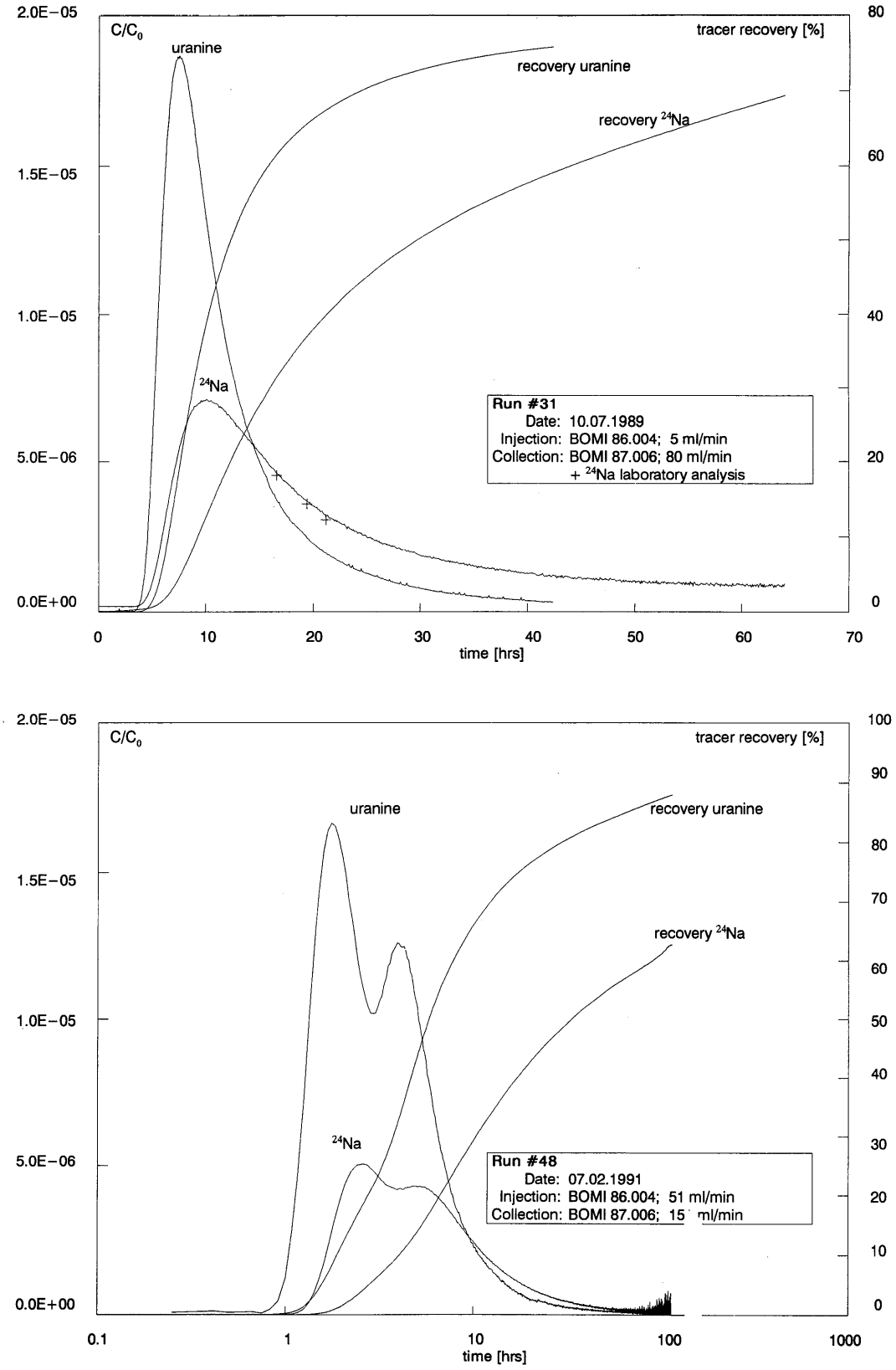

Fig.7-4: Tracer breakthrough profiles and recovery after pulse injection of $^{24}Na^{+}$ and Uranine during run #31 and run #48.

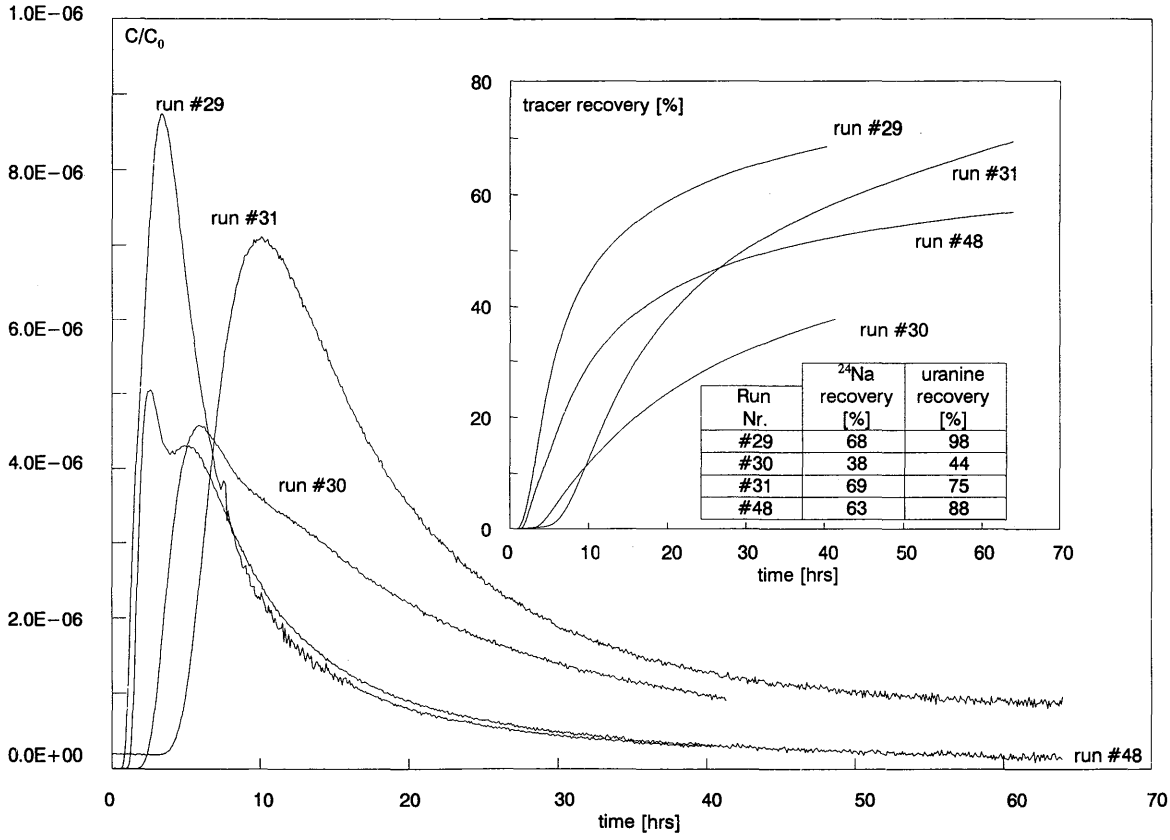

Fig. 7-5: Comparison of all $^{24}Na^{+}$ breakthrough curves from pulse injection experiments.

Retardation of Na^{+}: When compared with breakthrough profiles from non-sorbing tracers, $^{24}Na^{+}$ breakthroughs are characterized by little retardation for the first tracer arrival, a rather modest peak retardation of approximately 1.3 but, nevertheless, noticable peak depression and a pronounced tailing (particularly in experiment # 30). In an attempt to mimic a monopole-like flow field (by maintaining small injection flow rates) run #31 resulted in noticeably longer travel times (with higher injection rates), somewhat less pronounced tailing (probably due to tighter bundling of the water flow lines) and a similar peak retardation than during run #30.

The relatively small peak retardation of $^{24}Na^{+}$ was unexpected. An initial rough guess (based on the single-porosity column concept) a laboratory derived K_d of ~ 0.3 ml g^{-1} and an estimated porosity of 10 % yielded retardation factors in the order of 10. Obviously, such considerations were overly simplistic, as already indicated from the observed characteristics of the water filled pore space (cf. Fig. 3-4; Section 3.1). Indeed, various applications of (dual-porosity) transport models (see Section 7.3.4) show that the results from modeling field migration experiments are consistent with laboratory derived sorption values (see Table 5-7).

Recovery of Conservative Tracers: While Uranine recovery was approximately 100 % for run #29 and # 48 (estimated error on integrated Uranine quantities is 5 - 10 %), recovery during the two other runs (particularly for # 30) was incomplete, indicating that the flow field was not any longer closed for experiments with relatively small drawdown in the extraction well. A portion of the mass flow was diverted by the radial flow field to the laboratory tunnel, although tracer monitoring of discharging MI water was not sensitive enough to detect any traces of $^{24}Na^{+}$. However, as pilot tracer experiments conducted in 1988 occasionally revealed only small mass losses (< 1 %) to the tunnel under similar flow conditions, it cannot be excluded that some of the tracer flow escaped into more remote areas of the migration fracture.

Additional equipment for radiotracer analysis was installed during later field experiments. Analyses of input water revealed that, unexpectedly, pumping MI water from the fracture interval of BOMI 87.010 caused partial recycling of tracered groundwater through the supply borehole and, probably, long tailing of the breakthrough by the additional mixing/dilution processes. Meaningful modeling of such constellations is virtually impossible, thus, a new source of injection water had to be developed (see Fig. 6-3). For any subsequent field tracer experiments (including run #48), injection flow was provided by collecting water (up to 80 ml min^{-1}) from a discharge channel of the migration fracture into the tunnel (for details, see Section 7.4.1).

Recovery of $^{24}Na^{+}$: Due to its short halflife and difficulties to obtain precise laboratory measurements of $^{24}Na^{+}$ to calibrate on-line radiotracer analyses, recovered quantities may be somewhat uncertain. It is useless to discuss the low recoveries of Na^{+} and Uranine during run #30 and # 31, due to the distorted flow conditions as mentioned above. However, the substantially lower tracer recovery for $^{24}Na^{+}$ than for Uranine during run #29 and # 48 were initially attributed to the following two reasons:

i) kinetic effects (as also observed during laboratory sorption studies with Na^{+}; see Section 5), may apparently lead to an irreversibly sorbed component, and/or

ii) a significant portion of the tracer may be hidden in the long, pronounced tail of the breakthrough curves, with small tracer concentrations converging extremely slowly to the detection limit.

Subsequent field experiments indicated reversible transport processes (see Section 7.4.2) which seem to rule out a significant irreversibly sorbed component. It appears more likely that the short halflife of $^{24}Na^{+}$ ($t_{1/2}$=15 h) prevents complete monitoring of its long breakthrough tail and, thus, accurate determination of the total percent recovery. Indeed, recovery during later experiments (e.g. run #46; see Section 7.3.3) with long-lived $^{22}Na^{+}$ ($t_{1/2}$=2.6 a) was practically complete when the sodium tracer can be monitored over several weeks.

7.3.3 Conclusions from the $^{24}Na^{+}$ Pulse Tests

The first reactive tracer breakthrough experiments (runs # 29, # 30 and # 31) with short lived $^{24}Na^{+}$, provided a useful test of the equipment and the analytical setup and yielded valuable input for the first applications of newly developed transport models (see the next section). A more recent experiment (run #48), performed under much better defined experimental conditions, basically confirmed the major characteristics of the earlier tests. For these pulse tests, the following preliminary conclusions were drawn:

- The 4 pulse tests with $^{24}Na^{+}$, although involving different travel times, yielded virtually identical peak retardation and, thus, did not imply major kinetic effects.

- The apparently small retardation of the Na^{+} breakthrough might be attributed to relatively small cation exchange capacities under in-situ field conditions. It is interesting to note that an effective *CEC*, inferred from the hydrogeochemical equilibration experiment (see Section 7.2.3), was estimated to be in the order 2 $\mu eq\ g^{-1}$, substantially less than the values (up to 13 $\mu eq\ g^{-1}$) determined on laboratory material).

- Incomplete $^{24}Na^{+}$ recovery is, almost certainly, an experimental flaw due to the inability to monitor the breakthrough tail of short-lived isotopes over sufficiently long times, rather than the result of irreversible sorption.

- As a reliable interpretation of tracer experiments requires complete recovery of the conservative and reactive tracers and, because Grimsel migration experiments result in long tailing breakthrough curves, only sufficiently long-lived tracers provide adequate data.

- it cannot be excluded that pulse tests provide an inadequate time-scale for rock-tracer interaction, i.e. the most effective sites for cation exchange cannot be reached within the typical duration of pulse tests.

It was also concluded that continuous injection (step input) of the sodium tracer (i.e. $^{22}Na^{+}$) would offer several advantages because (a) substantially prolonged tracer-rock interaction times are possible, (b) less rapid changes of tracer concentrations and smaller concentration gradients may improve equilibrium conditions, and (c) the basic assumptions for transport modeling (including the fundamental geochemical requirement of fully reversible cation exchange reactions with rapid kinetics) can be conveniently tested. HERZOG (1990, NTB 91-31) predicted that during reasonably long injection times, conservative tracers as well as Na^{+} would reach a plateau concentration. Subsequently, intensive efforts were spent to modify the experimental setup for continuous injection of tracers (see Section 7.4).

7.3.4 Modeling of a $^{24}Na^{+}$ Pulse Test

A transport model has been developed (HERZOG, 1990 and HERZOG, NTB 91-31) which can be used to predict tracer breakthrough curves of in-situ migration experiments. Transport is calculated in a number of streamtubes to account for idealized unequal-strength dipole flow fields in a planar fracture of homogeneous transmissivity (see Fig. 6-2). As the natural pressure gradients were relatively small (see Fig. 3-8; Section 3.3). The radially converging flow to the laboratory tunnel was neglected, and only artificially induced dipole flow fields were considered. The conceptual dual-porosity model, together with a simplified view of the water-filled pore space of the migration fracture, is depicted in Figure 3-4. With this model sorption coefficients can be extracted for cases of known sorption mechanisms.

One of the critical parameters is the assumed flow width of the fracture. The breakthrough curves of experiment # 29 with the non-sorbing Uranine (i.e., Na fluorescein) and the sorbing nuclide $^{24}Na^{+}$ were used for a first adjustment, taking into account information from independent measurements such as porosity, density of fracture infill or the fracture width (see Section 3.1). The results of modeling are presented in Table 7-4.

A comparison of the calculated breakthrough curves (using these parameters) with the experimental results is given in Figure 7-6. The figure shows a reasonable agreement between measured and calculated concentration versus time data and the parameters, especially the sorption constant for sodium, are consistent with independent information. Table 7-4 demonstrates that the model derived $K_d[Na]$ value well match with the sorption data derived from the field-scale (in-situ) equilibration experiment (c.f. Section 7.2) as well as with results from laboratory rock-water interaction experiments, carried out on rather coarse-grained (< 2 mm) samples of fracture material (c.f. Section 5.2, see also Table 5-7). It is also interesting to note, that similar $K_d[Na]$ values were obtained when analyzing dynamic infiltration experiments (SMITH, NTB 91-33) with a model of dual-porosity (Section 5.5; see also Fig. 5-7).

Although there still exists uncertainties in basic parameters such as the porosity, the model has already provided good insight into the basic behaviour of the migration system and is able to describe important features of field breakthrough experiments. Clearly, the model has now to be applied to a wider range of experimental results (e.g., including more strongly sorbing tracers) to achieve better adjustment of crucial parameters and more information on the validity and the limits of the model.

Although the basic concept remained unchanged, substantially improved transport modeling is currently underway at PSI. However, it is outside the scope of this paper to present the details of ongoing research by the PSI group which will be documented elsewhere (HEER, 1992).

Table 7-4: Selected and preliminary model derived parameters for matching experimental Na^+ breakthrough curves (from HERZOG, NTB 91-31).

Distance between input and output interval:	L_o	= 490 cm
Width of the fracture:	a	= 1 cm
Half width of the water layers:	b	= $1.49 \cdot 10^{-2}$ cm
Half width of the infill[f] layers:	d	= $3.51 \cdot 10^{-2}$ cm
Longitudinal dispersion length:	a_L	= 8 cm
Porosity of the infill[f]:	ε_p	= 0.01
Bulk density of the infill[f]:	$\delta(1 - \varepsilon_p)$	= 2.67 g cm^{-3}
(Porosity·diffusion constant) of the infill[f]:	$\varepsilon_p D_p$	= $2 \cdot 10^{-8}$ cm^2 s^{-1}
Sorption constant for ^{24}Na of the infill[f]:	K_d	= 0.3 ml g^{-1}

[f] for modeling only, "infill" is defined as the zone of width a = 1 cm in which only (limited matrix) diffusion occurs; "infill" comprises the total water-filled pore space in the mylonitic shear zone, including fault gouge filled openings (cf. Section 3.1).

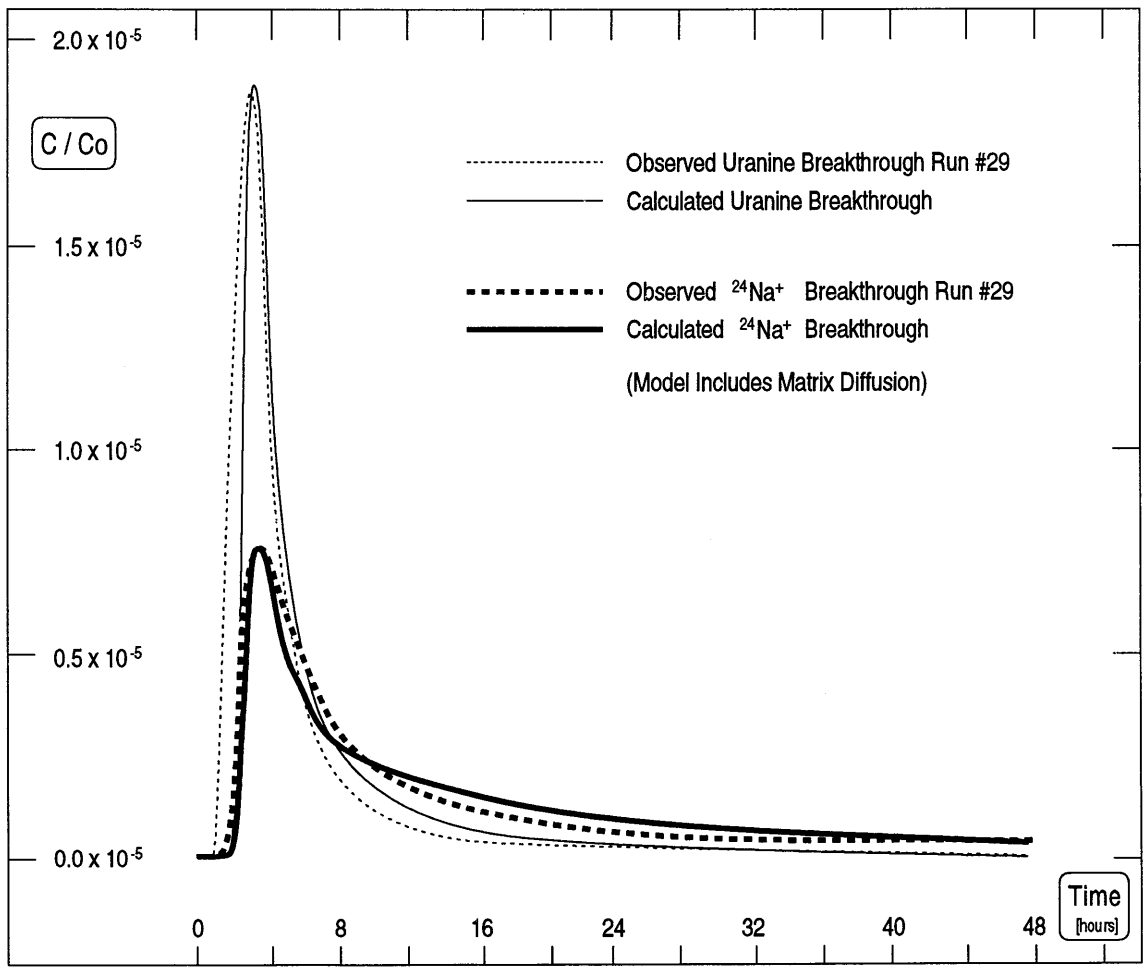

Fig. 7-6: Comparison of modeled and experimental breakthrough curves for run #29.

7.4 A Continuous Injection Test with ^{22}Na

As pointed out in the previous Section, the pulse injection tests with $^{24}Na^{+}$ showed the need for prolonged exposure of the tracer to the rock. Therefore, it was necessary to modify the experimental setup (designed for tracer pulse injection) and to develop techniques for continuously injecting constant tracer concentrations over several days or weeks *(= step input).* From the previous pulse tests it was already known that the time required to approximately reach a plateau concentration for conservative tracers was in the order of 3 days for the usual flow conditions between BOMI 86.004 and BOMI 87.006 (for Na^{+}, about 5 days were predicted).

The requirements for continuous injection experiments were much more stringent than for the relatively short-term pulse tests:

- All systems must be designed to run without interruption over prolonged times (up to several months)
- High demands on the accuracy and longtime stability of flow control devices and analytical instruments

7.4.1 Experimental Set-up

Based on the experience from numerous pulse injection tests with conservative and reactive tracers, equipment was extensively modified by a variety of innovative measures. Some of the most important improvements are summarized below.

Source of Injection Water: Injection flow was provided by collecting water (up to 80 ml min^{-1}) from a discharge channel of the migration fracture into the tunnel (see Fig. 6-3). This was achieved without any atmospheric contamination. As minute amounts of tracers were frequently detected in the discharging groundwater, storage of large quantities (1'500 l) under a protective gas atmosphere was installed and successfully tested.

Tracer Analyses and Data Acquisition: In an attempt to increase the sensitivity of on-site radiotracer analyses, additional lead shielding was installed around the scintillator detectors to reduce the natural γ background. Cylindrical flow-through tanks were replaced by a teflon spirals of slightly less volume to minimize any sorption effects near the detectors. The sensitivity of the various detectors was then calibrated for actually used flow rates and tracer concentrations. The data acquisition system described by THORNE (1990b) was replaced by a FLUKE Helios I data logger to process the 40 analog signals (pressures, flow rates, tracer concentrations, etc.). The data logger is PC controlled and data are handled by LABTEC Notebook software. The data acquisition system can be monitored remotely via the telephone line and two modems.

Minimizing of Equipment Volume: If equipment volumes (see Table 7-3) are in the order of flow field volumes, tracer travel times could be delayed and breakthrough characteristics may be significantly effected. Because mixing in equipment volumes is highly uncertain, the diameters of the flow lines were reduced and special low-volume packer interval pieces were built and installed during October 1988. The unique design of this interval is depicted in Fig. 6-8 (see also THORNE (1990b). It is particularly suited to pack-off smooth boreholes and short intervals (30 cm). Two short mechanical rubber packers are longitudinally compressed when the hydraulic packers on both sides are inflated, sealing off a borehole interval of less than 30 cm length and a volume as low as 80 ml. During the $^{22}Na^{+}$ step input experiment, a stainless steel prototype was installed in the injection borehole. For experiments after 1990, three of these interval pieces were PTFE coated to avoid sorption of Sr^{2+} and each was equipped with 2 quartz fiber optrodes to allow down hole fluorescent tracer analysis in the injection/extraction boreholes (BOMI 86.004 and BOMI 87.006) as well as in a passive observation borehole (e.g. BOMI 87.009; see Fig. 6-3). The optrodes can now measure precisely the tracer input function and also provide information on dispersion and travel time in the apparatus.

Preliminary Step Input Experiments: Various trial runs were performed with continuous dosage of Uranine over several days at a rate of 10 µl min^{-1} utilizing an HPLC pump (SHIMADZU Model LC-5; 1µl -10 ml min^{-1}), while injection and extraction flow control was provided as usual by MOINEAU pumps. This setup was judged to be inadequate as measured tracer concentrations in the extracted groundwater were unstable; input and output pump rates drifted over a few % within a few days and responded (sometimes erratically) to the small earth tidal pressure variations, causing daily oscillations of tracer concentration (up to 10 %) in the discharge flow.

Sorption Proofing of Apparatus: Equipment tests were also performed to calibrate radiotracer analysis for $^{22}Na^{+}$ and $^{85}Sr^{2+}$. As workers performing field migration experiments with Sr^{2+} elsewhere never mentioned any difficulties by utilizing standard equipment materials, it was rather surprizing to find substantial sorption of $^{85}Sr^{2+}$ on etched or polished stainless steel surfaces and even on polyamide 11 (nylon) tubing. Considerable efforts were spent to confirm that teflon exhibits negligible sorption. Subsequently, extensive modifications were required to rebuild the apparatus for migration experiments with Sr. Packer interval pieces (see Fig. 6-8) were coated with PTFE and nylon tubing was replaced by teflon tubing. Special provisions (e.g., lining filled with flowing MI water) had to be taken to counter its permeability for atmospheric O_2 and CO_2. After completion of the 7-day continuous injection test with $^{22}Na^{+}$ (see Section 7.4.2), i.e. after October 1990, field tracer experiments were performed with the modified, sorption-proofed equipment.

Modification of Input and Output Flow Control: The two excenter drive MOINEAU pumps were replaced by standard laboratory HPLC (High Performance Liquid Chromatography) pumps (SHIMADZU Model LC-8; 0.1-150 ml min^{-1}) which were specified to provide extremely stable flow over a large pressure range (~200 bar). First tests of the new setup with HPLC pumps revealed very stable and constant input and output flow rates. However, prolonged use of these pumps revealed some unexpected problems (see below) which could not be solved immediately. During step input run #46,

therefore, the extraction flow was maintained again by a MOINEAU pump, while 2 HPLC pumps were installed to provide the input flow. Two pumps were used to ensure that one of them could always be serviced and maintained alternately during regular intervals. The modified setup for run #46 is depicted in Figure 7-7. For later experiments (after 1990), a heavy duty HPLC pump (LABOMATIC Model HD-200) designed for flow rates up to 1'100 ml min^{-1} was used to control the groundwater flow from the extraction well.

Initial Problems with HPLC Pumps: During the first step input experiment with $^{22}Na^{+}$ ($t_{1/2}$=2.6 y), lasting for over two months, the highly precise injection and extraction pumps had to be frequently replaced and maintained due to leakage problems. The pistons (i.e. sapphire plungers) of the HPLC pumps showed visible scratches after a few days of operation. In addition, erosion products frequently clogged the tiny valves of the pumps. This was surprizing as sapphire (i.e. γ-Al_2O_3) is an extremely hard and chemically resistant material. The white sediment which accumulated in the plunger chamber was analyzed by X-ray diffractometry. Aside from various amorphous phases, it contained secondary Al phases such as zeolites. Hydrogeochemical modeling revealed that the rather high pH and fluorine level in MI water may lead to substantial corrosion (i.e. dissolution) of the Al_2O_3 plungers (EIKENBERG & BÜHLER, 1990). Continuous removal of the corrosion products by the gaskets during pumping and continuous exposure to aluminum unsaturated water obviously led to substantial dissolution of plunger material within a few days, causing first minor leaking, then clogging of the tiny (passive) pump valves by the precipitates and, if unnoticed, to full gasket failure or mechanical drive damage.

These corrosion problems were adequately solved by replacing the original sapphire plungers of the LABOMATIC pump by silicon carbide which is extremely resistant against mechanical abrasion and chemical attack. The sapphire plungers from the SHIMADZU pumps were replaced by pistons made from a hard tungsten-titanium alloy. After these modifications, all the HPLC pumps worked reliably during uninterrupted use over several months with MI water.

Tracer Dosage for Continuous Injection: During run #46 was performed by feeding with a SHIMADZU Model LC-5 HPLC (single-piston) pump at a rate of 10 µl min^{-1} the tracer solution, a mixture of Uranine and $^{22}Na^{+}$ from a small reservoir (260 ml aerated MI water, containing about 4.7 ppm Uranine and 17 kBq ml^{-1}) into the input flow of 10 ml min^{-1}. The injection rate must be very precisely known and, therefore, the weight loss of the tracer reservoir is continuously monitored by a METTLER balance which is linked to an IBM type Personal Computer. A total of 4.4 MBq $^{22}Na^{+}$ was injected during 220 hours. Adding the tracers to the input flow did not at all affect the ionic composition of the MI water.

For ^{4}He pulses, the tracer solution was obtained by equilibrating MI water at ambient pressure and temperature with helium gas. 10 to 20 ml of He-saturated water were then taken with a syringe and immediately injected through a thick rubber membrane into a bypass of the input flow line. During more recent tests, helium tracer dosage was also accomplished by HPLC pumps (see EIKENBERG et al. 1992).

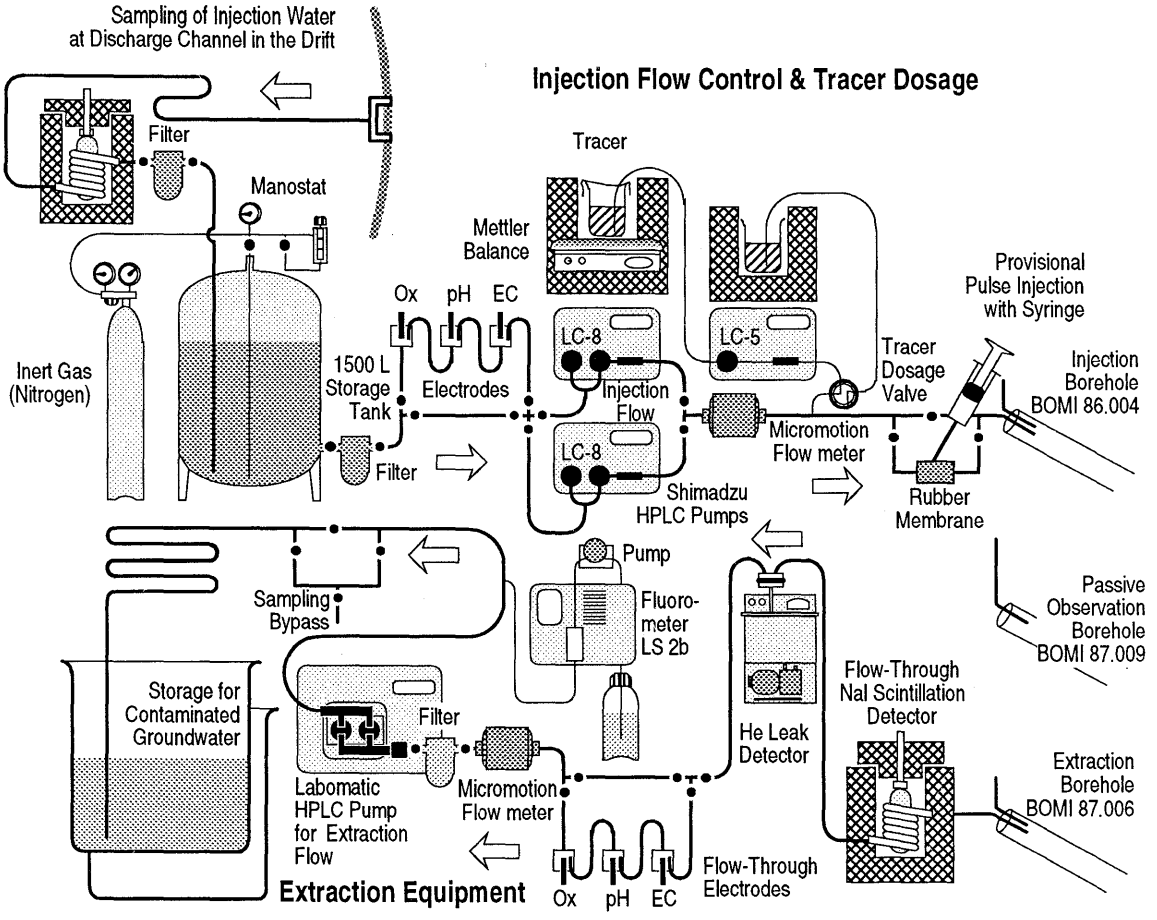

Fig. 7-7: Experimental Set-up for the $^{22}Na^{+}$ step input run #46

7.4.2 Results and Discussion of the first $^{22}Na^{+}$ Step Input

Results: A first step input experiment (run #46) over a distance of 4.9 m (from BOMI 86.004 to BOMI 87.006) involved simultaneous injection of Uranine and $^{22}Na^{+}$. Injection started during the first days of July 1990 (cf. Table 7-1) and lasted ~ 9 days with subsequent monitoring of the tracers over more than 2 months. A total of 7 pulse injections with dissolved ^{4}He and in one case $^{82}Br^{-}$ were added for flow field checks (see Fig. 7-8). The responses from these pulse tests are virtually identical, indicating stable flow conditions throughout the whole duration of run #46.

After interruption of tracer injection, the elution tail of Uranine required about 1 week to drop to 1 % of the plateau value (Fig. 7-9) while $^{22}Na^{+}$ required substantially longer (> 4 weeks) to drop to 1 % (Fig. 7-10).

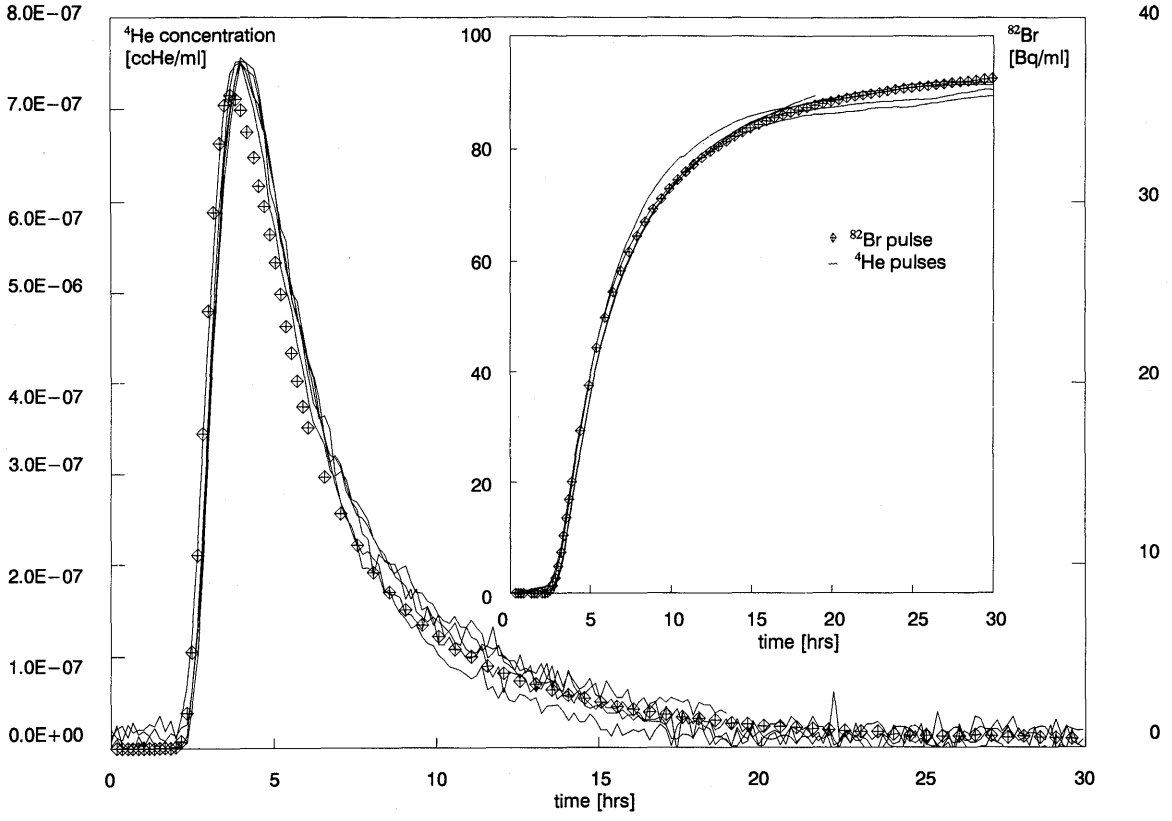

Fig. 7-8: Comparison of breakthrough curves obtained from 7 different pulse injections of $^{82}Br^-$ or dissolved ^4He during run #46.

Data from the field flow-through radiotracer counting were checked by collecting 20 water samples (in 50 ml PE bottles) which were subsequently analyzed at the Paul Scherrer Institute with a high-resolution γ - counter. Figure 7-10 demonstrates the excellent agreement between field data and laboratory $^{22}Na^+$ activity measurements and the high quality of radiotracer analysis. The estimated error on recovered $^{22}Na^+$, eluted from the Ml fracture over 500 hours, is less than 2 %.

After about 100 hours of tracer injection, one of the two pistons of the HPLC pump for injection flow malfunctioned (see above) and, for known time intervals, input flow rates were only 5 instead of the preset 10 ml min^{-1}. This did not substantially alter the flow field (drawdown of 153 ml min^{-1}), however, resulted in temporary concentration "anomalies". The quantities of injected/recovered tracers are not affected. In an attempt to provide an undisturbed breakthrough curve, the mirror image of the $^{22}Na^+$ concentration versus time function after termination of tracer injection is depicted in Fig. 7-12. A justification of this procedure is given below.

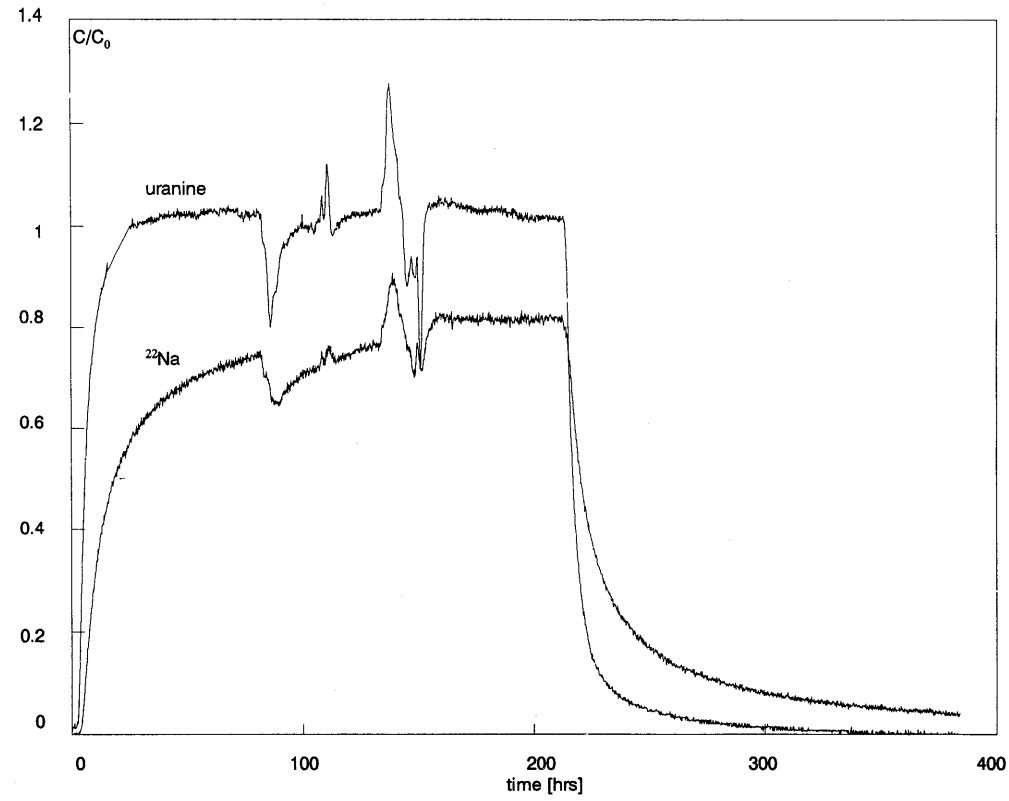

Fig. 7-9: Field breakthrough after a 220 hour continuous injection of of Uranine and $^{22}Na^{+}$ during run #46.

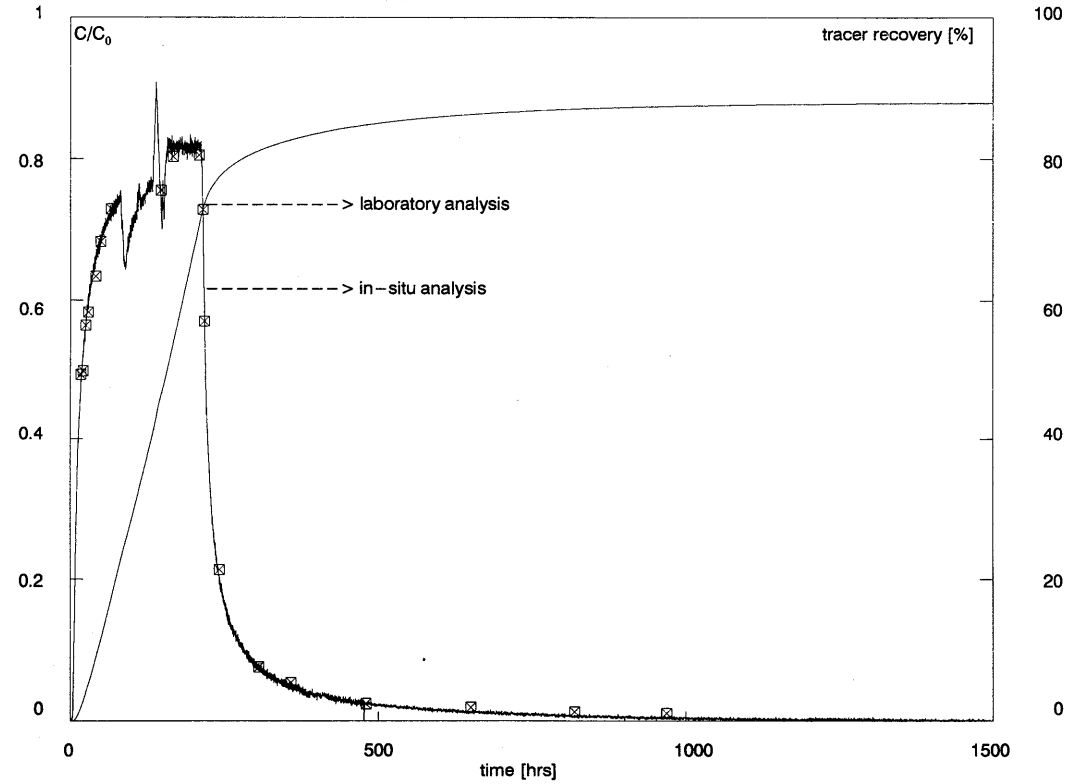

Fig. 7-10: Field breakthrough of $^{22}Na^{+}$ during run #46; comparison of laboratory γ-counting and on-line flow-through scintillation counter analysis.

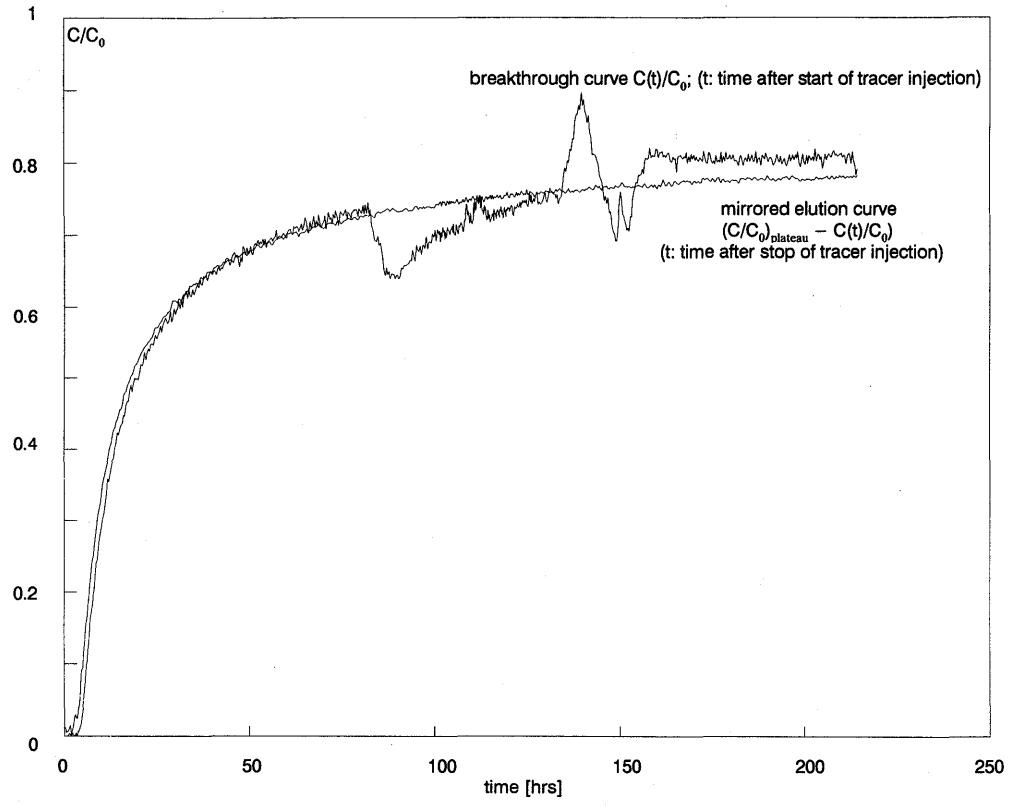

Fig. 7-11: Normalized $^{22}Na^{+}$ concentration versus time function for step-input breakthrough and mirrored elution curve section during run #46.

Important Observations: The major observations during the continuous injection experiment with Uranine and $^{22}Na^{+}$ were:

i) Uranine reached predicted plateau concentrations and recovery was approximately 100 %.

ii) $^{22}Na^{+}$ did not reach the calculated plateau concentration during the injection period and only about 90 % recovery was reached after 2 months.

iii) The breakthrough part (defined during tracer injection) and elution part (after termination of tracer injection) of the measured concentration versus time function are, on a mirror image, almost identical (Figs. 7-11 and 7-12).

iv) Under identical flow conditions the first derivative of the concentration versus time function during step input closely matches the response observed after pulse injection (i.e. the response from the step input test corresponds to the integrated breakthrough curve after pulse injection; c.f. Fig. 7-13)

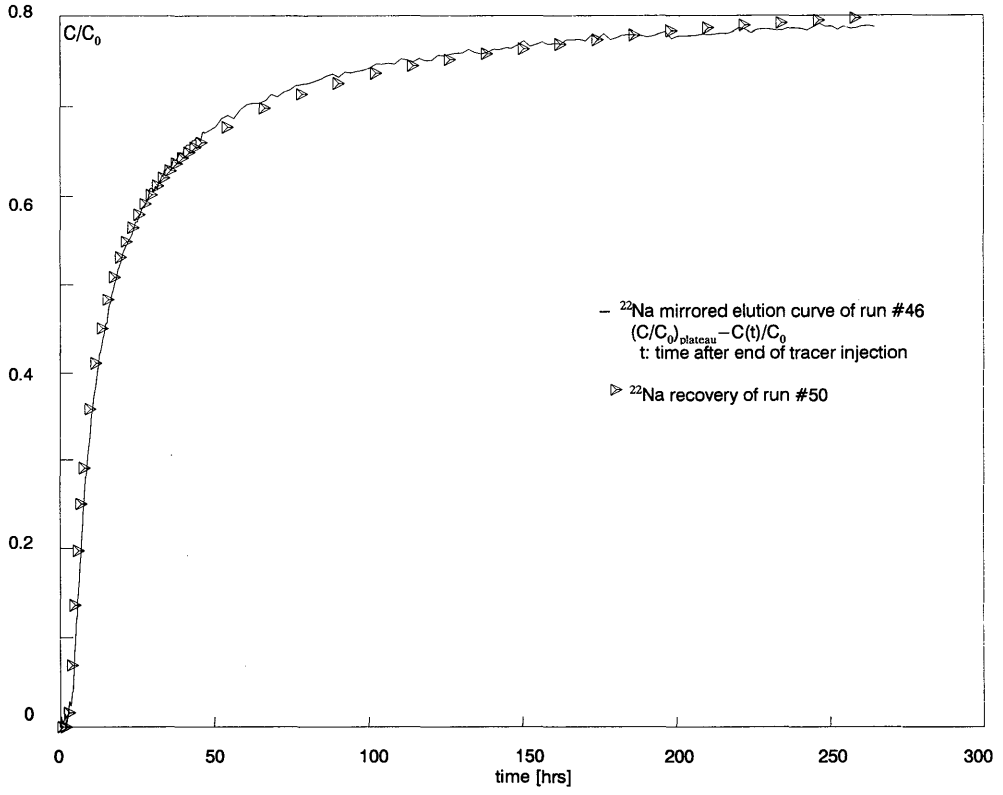

Fig. 7-12: Normalized $^{22}Na^{+}$ concentration function during step input breakthrough (mirrored elution curve of run #46) and the recovery curve section of a pulse test (run #50) performed under identical flow conditions.

Preliminary Conclusions: Although the step experiment has not yet been interpreted in detail by transport modeling, some preliminary conclusions are based on the above observations during the continuous injection experiment:

i) *From scoping transport model predictions (HERZOG, 1990), the hydrogeochemical equilibration experiment (EIKENBERG et al., NTB 90-39) and the Na^{+} pulse tests a constant plateau for Na^{+} was expected to stabilize after approximately one week. On a first view such a plateau had apparently been attained after ca 150 hours. However, extraction flow rates, maintained by a MOINEAU pump, were drifting somewhat and caused the Uranine concentrations to decrease somewhat during the last 2-3 days of tracer injection.*

ii) *Although, the $^{22}Na^{+}$ activities in extracted groundwater remained essentially constant before termination of tracer injection, more stable flow conditions (see i) would have resulted in still slightly increasing $^{22}Na^{+}$ concentrations (see Fig. 7-11 and Fig. 7-12). It is therefore likely that the discrepancy between calculated and measured plateau concentration is, at least partially, due to still incomplete saturation of the fracture with $^{22}Na^{+}$. Incomplete sodium recoveries are considered to be*

caused by insufficiently long monitoring of the long breakthrough tails as already concluded from the various pulse runs with Na^+ (see Section 7.3).

iii) The virtually identical shape of the breakthrough portion and the mirrored elution portions of the concentration versus time function for $^{22}Na^+$ (Fig. 7-13) convincingly demonstrate that, within experimental errors, breakthrough and elution must largely include reversible transport processes.

iv) The close match of a pulse response (preliminary $^{22}Na^+$ data from run #50) and a differentiated step (mirrored derivative of the recovery data from run #46) is illustrated in Figure 7-14. This is an additional indication that for both pulse and step injection experiments (performed under identical flow conditions) advection dispersion, and sorption processes are essentially identical and reversible during typical experiments in the migration fracture.

Thus, the tracer experiments clearly indicate that the major transport processes (i.e. dispersion and sorption) in the migration fracture appear reversible and, thus, seem to rule out any substantial kinetic effects for sorption. If diffusion processes should control a significant portion of the mass transport, such processes must also be largely reversible. It is still an open question, however, to what extent diffusion processes contribute to the breakthrough/elution characteristics.

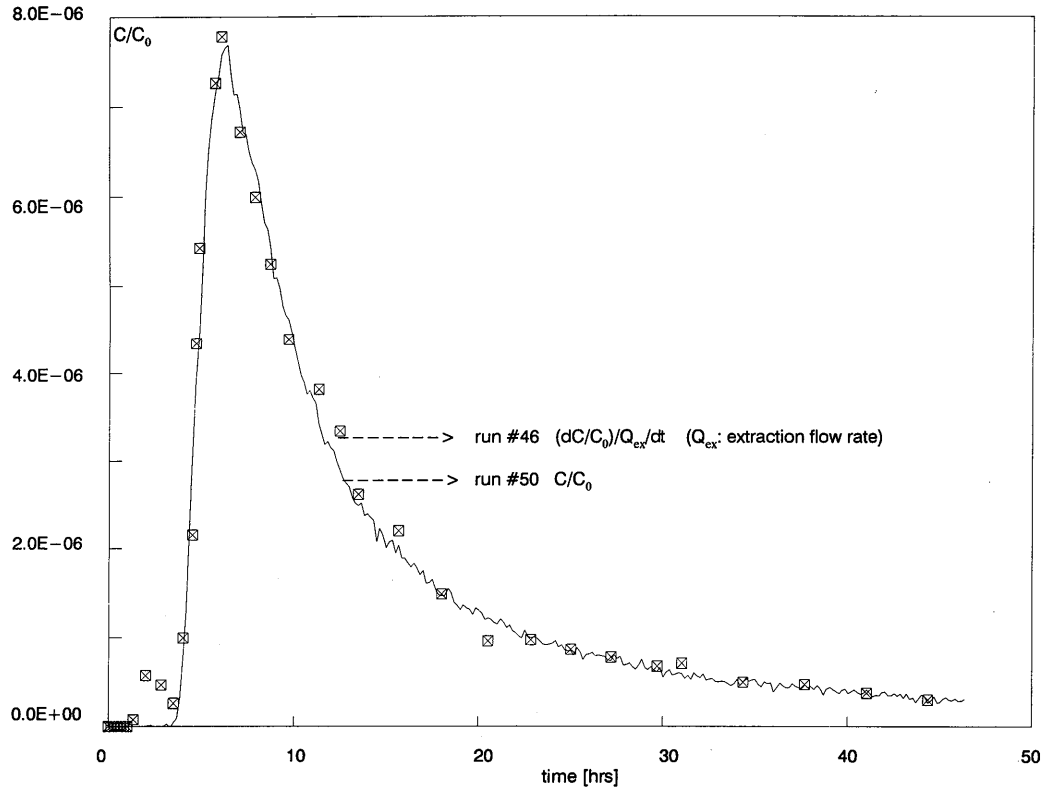

Fig. 7-13: Comparison between the $^{22}Na^+$ breakthrough functions after pulse injection (run #50) and the derivative of the concentration function during continuous injection (elution function from run #46). Both runs were carried out under practically identical experimental conditions. The similarity also holds for conservative tracers (not shown).

7.4.3 Modeling of the $^{22}Na^{+}$ Step Input Experiment

Modeling of the step input experiment, based on a somewhat improved version of HERZOG's (1990) transport model is still underway. However, measured concentration versus time functions can be compared with earlier model predictions. Figure 7-14 (taken from HERZOG, 1990) shows calculated breakthrough curves for continuous injection of Uranine, Na^{+} and Sr^{2+}, based on the model calibrated for Na^{+} (see Section 7.3.4) and an input/output flow ratio of ~ 1/3 (i.e. $\beta \cong 3$). For Sr^{2+} a K_d of 18 ml g^{-1} (see first row in Table 5-7) was taken. Although the field experiment (run #46) was then executed with an input/output flow ratio of 1/15 ($\beta = 15$), the major characteristics between Uranine and $^{22}Na^{+}$ appear adequately depicted (cf. Fig. 7-9; the drawdown in the discharge interval predominantly effects water flow time). If a pulse run were carried out with $^{85}Sr^{2+}$ predicted peak time would be around 20-40 hours after tracer injection.

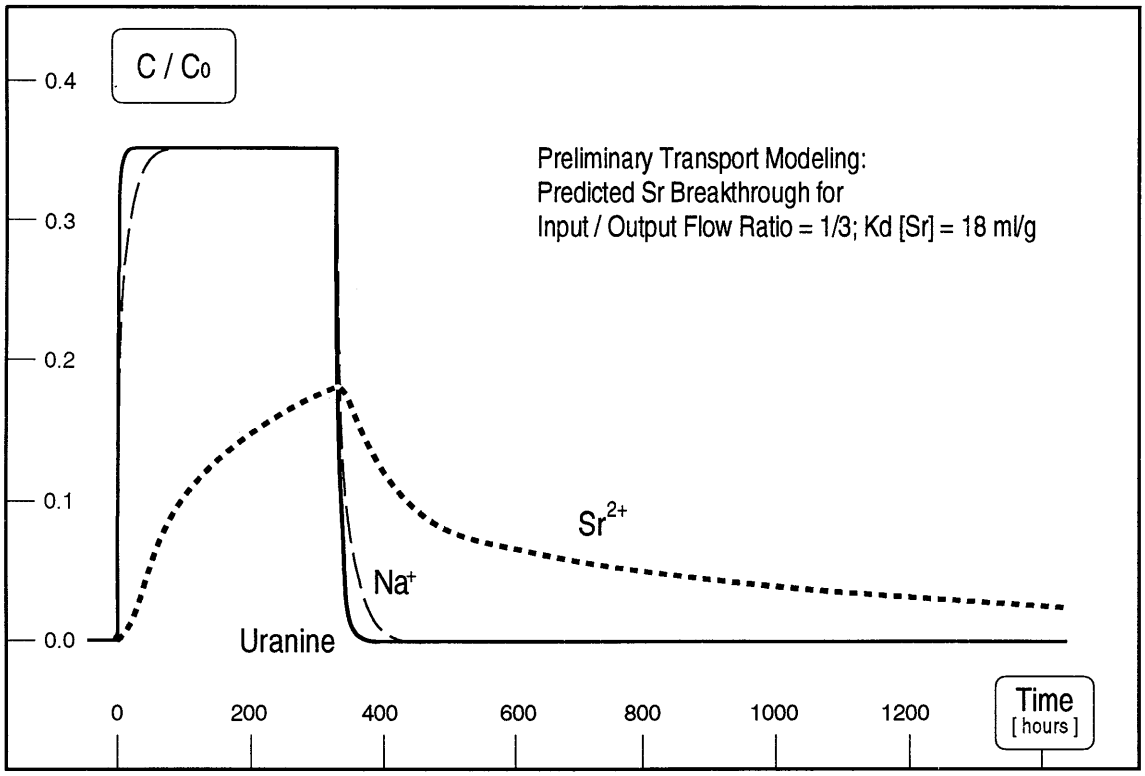

Fig. 7-14: Transport modeling: predicted concentration versus time functions for step injection (336 hours) of Uranine, Na^{+} and Sr^{2+}.

8 CONCLUSIONS

It is clear from this document that the Grimsel migration experiment is a monumental undertaking involving a large number of people utilizing a wide variety of approaches to solve the numerous problems associated with conducting a field experiment of this nature. In itself, this is no bad thing since one of the stated aims of the Grimsel research facility is the training of personnel in the methodology of a proper site characterization along with the development and application of new techniques.

The planning of the MI experiment has benefited from the experience gained in prior studies (e.g. Stripa, Finnsjön). In such early work, it was usually found that the system was under-defined - i.e. there were many unmeasured (free) parameters that field results could be equally well simulated by a wide range of models which involved completely different mechanistic bases. From its earliest conception in 1985, therefore, this project was envisaged as a multi-disciplinary study of the transport system as a whole. This approach greatly increased the work load involved but, in addition to improving the value of the experiment as an examination of radionuclide retardation and a test of transport models, it has provided the opportunity for modelers to work closely with those people actually conducting the laboratory and field experiments. The importance of this cannot be over-emphasized; in this way modelers have a chance to work on real problems which test the validity of their models and experimenters learn much about the major constraints under which most modelers must work. More, the building up of such multi-disciplinary groups will be necessary during the actual safety assessment of a repository site and so the experiences gained here will be put to concrete use later in the Nagra/PSI/PNC programmes.

Obviously, with these points in mind, the MI experiment was always intended to be more wide ranging than a simple radiotracer field experiment and so has grown to encompass many fields including engineering, chemistry and hydrology. With a synthesis report of the Grimsel migration experiment being planned after termination of experimental and modeling activities, it is worth noting here some major findings of what has been covered so far:

The Grimsel Environs

- The migration site and the surrounding environs were extensively characterized in terms of structural geology, mineralogy, petrography, hydrochemistry and hydrology prior to performing the actual migration experiments. Outside the migration site, however, there was no systematic water sampling carried out for hydrochemical or isotope studies. Therefore, conclusions from the latter investigations are of rather preliminary nature.

- The hydrogeological setting of the Grimsel area appears relatively simple: meteoric waters, mainly as melting snow, infiltrate at low temperatures. Subsequent rock-water interaction leads to progressive take-up of leachable elements. Generally, groundwaters discharging into the tunnel system are weakly mineralized, may show some local chemical variations, but do not reveal any significant temporal changes. They are virtually oxygen-free and over-saturated with other dissolved atmospheric gases (i.e., mainly nitrogen).

- The major water flow paths through the overlying rock mass are provided by two steeply dipping fault systems. Both have been reactivated by the relatively recent brittle deformation processes which continually occurred in old ductile shear zones along lamprophyre dykes (striking NW - SE) and shear zones oriented along the direction of regional alpine foliation (principal strike from NE - SW).

- Some of the groundwaters discharging into the access tunnel contain anthropogenic tritium at levels of 5 - 25 TU. No tritium was found neither at the migration site nor in any discharge within the Grimsel underground laboratory, indicating an age of these waters of at least 40 years.

- Stable isotope compositions of groundwater discharging at various locations in the tunnel system do not reveal systematic trends. Mixing (on a scale of 0.1 - 1 km) of meteoric waters infiltrating at different altitudes could be provided by water bearing fracture systems (probably associated with lamprophyre dyke zones); these transsect the main fault zones which run from the mountain ridge straight down to the main access tunnel.

The Migration Site

- The characteristics of the various water flow systems within the Grimsel rock mass are the result of the specific regional tectonic history, metamorphism, and ongoing hydrogeochemical processes. The migration shear zone exhibits all the major structural, mineralogical and petrographic features which are typical for any shear zone of this region. However, its characteristics may differ considerably from fractures in other crystalline rocks of different geological settings (e.g., shield rocks in Canada or Sweden; bedrock in N-Switzerland, etc.).

- The field experiments are carried out in a narrow, water conducting shear zone (= migration fracture) within a tectonically active, granitic rock mass. On the scale of several meters, this fracture can be described as a two-dimensional feature. The major water flow paths are the product of relatively recent tectonic deformation (alpine uplift). Brittle processes reactivated older, ductile shear zones and led to the formation of a few centimeter wide, asymmetric array of conducting fractures in an otherwise relatively impermeable mylonitic fabric. These openings are partially filled with highly porous, unconsolidated micaceous fault gouge and have been identified as the main pathways for water flow.

- Although a variety of observations demonstrate that the migration fracture is part of a rather fragile hydrogeological setting (varying reservoir levels may induce rock-mechanical movement within the migration shear zone and seasonnally varying pressures; artificial flow fields potentially could erode infilling fault gouge; etc.), the site, so far, has appeared to be sufficiently stable during most tracer breakthrough experiments. For long-term experiments, however, checks of the stability of the flow fields should be carried out by repeated pulse injections of a conservative tracer.

Hydrochemistry

- The groundwater in the migration fracture has been thoroughly characterized with respect to the hydrochemistry and acid/base equilibria as well as the temporal stability of the system. No significant seasonal nor long-term variations have been observed. The water is anoxic, has a high pH (~ 9.6) and a low ionic strength of 0.0012 M with the cation content dominated by Na^+ and Ca^{2+} while F^-, HCO_3^-, Cl^-, SO_4^{2-} and $SiO(OH)_3^-$ are the major anions.

- The Eh state of migration water is not clear, due to marked disequilibrium between various redox couples. The Eh buffer capacity should be defined experimentally under simulated in situ conditions using fracture material and MI water.

- Further studies include the definition of ambient microbiological and colloidal populations. However, the full significance of these with respect to radionuclide transport remains unclear.

- Trace element and natural radioisotope transport processes were also studied in the migration fracture as well as in its immediate vicinity. These so-called natural analog studies conclusively demonstrate (as mainly indicated by the pronounced disequilibrium of ^{226}Ra with respect to other U decay products) that the pore space along the narrow shear zone has been open to rock-water interaction over several thousand years.

Hydrogeology of the Migration Fracture

- Hydrogeological exploration involved the drilling of 8 boreholes (6 to 24 m long). Subsequent hydraulic testing revealed local heterogeneities of the transmissivity from $5 \cdot 10^{-6}$ to about 10^{-8} m^2s^{-1} (single hole tests). On a scale of several meters, however, the fracture appears rather homogeneous with an average transmissivity of about $2 \cdot 10^{-6}$ m^2s^{-1} based on the results of cross-hole tests.

- Various hydrodynamic models satisfactorily predict stationary hydrological conditions (pressure distribution, flow) but have some difficulty in reproducing the observed transient response from long-term pumping tests. In addition, the detailed hydraulic characterization has allowed the testing of several hydrodynamic models and development of a better understanding of the unsaturated zones around underground constructions.

- Tunnel ventilation causes drying-out of the unfractured rock mass. The associated capillary suction induces substantially decreased hydraulic pressures within the adjacent rock. Noticeable effects have been measured up to more than 15 meters from the tunnel wall. It appears, however, that these do not disturb the flow within the transmissive portions of the migration fracture.

Flow Fields and Scale of Tests

- At distances between 6 and 12 m from the tunnel wall, hydraulic pressures in the migration fracture initially average around 1.5 bar. Continuous drainage caused by the earlier tunnel excavation led to an exponential decrease to about 1.3 bar over the first few years. This hydraulic setting is well suited to maintain artificially stressed, closed flow fields (unequal strength dipoles with input/output flow ratios always less than 1/2) for tracer experiments. Thereby, the natural, radially converging flow field towards the laboratory tunnel can practically be neglected.

- A series of pilot experiments utilizing conservative tracers (uranine, ^{4}He and $^{82}Br^{-}$ was performed in order to test the equipment and to identify appropriate borehole constellations and flow conditions (travel times) for the planned migration experiments. Hydraulic connections were found in the fracture sections between at least 4 boreholes. This would allow, in principle, to test the migration fracture on a scale from approximately 1.7 to 15 m.

- A variety of flow conditions were chosen for subsequent tracer breakthrough experiments. Conservative tracer pulse injection yielded monomodal or bimodal breakthrough curves, depending on the tested fracture section or the input/output water flow ratios. Peak times varied from 1 to about 12 hours, while monitoring of the complete tail breakthrough required 2 - 7 days. These timescales appeared adequate to allow practicable experiments with weakly to moderately sorbing species which were expected to be retarded considerably.

Laboratory Programme

- A large laboratory-based support programme has been developed to aid the field programme and this includes rock- water interaction experiments, radionuclide batch sorption studies, and dynamic (high-pressure) infiltration experiments, all carried out under simulated in-situ conditions.

- As it was judged inappropriate to collect the required sample mass from the migration fracture, laboratory material was taken from an adjacent, much wider shear zone of similar origin. A careful characterization of the samples indicated that, at least mineralogically, mylonitic material from both locations is virtually identical and that disaggregated material from the sampling fault may adequately represent the micaceous, porous infill (e.g., fault gouge) of the migration shear zone.

- An ion-exchange model was proposed on the basis of laboratory rock-water interaction experiments which were performed with loosely disaggregated fracture material. These studies indicated that the sorption of chemically simple cations is dominated by reversible cation (isotope) exchange under equilibrium conditions and that the distribution coefficient K_d is proportional to the available cation exchange capacity (CEC). The model also predicts that, for a system of constant CEC, increasing contents of dissolved ions generally cause decreasing sorption coefficients (K_d).

- K_ds for Na and Sr under the chemical conditions prevailing in the migration fracture were expected to range from 0.3 - 0.4 ml g^{-1} and from 16 - 25 ml g^{-1}, respectively. Therefore isotopes of Na^+ and Sr^{2+} were proposed for the first series of field experiments with reactive tracers. At relevant tracer concentrations, these too species are linearly sorbing (i.e., constant K_d).

- Radionuclide batch sorption studies on mylonite material demonstrated the relationship between water chemistry, grain-size, CEC and K_d and basically confirmed the results obtained from rock-water interaction experiments.

- Further laboratory sorption experiments clearly show the concentration dependent distribution coefficient of non-lineraly sorbing Cs^+. For fine-grained fracture material (< 63 μm) and the chemical conditions prevailing in the migration fracture, a relatively high K_d of around 4'000 ml g^{-1} was measured.

Field Tests with Reactive Tracers

- A field-scale equilibration experiment within the migration fracture was performed by replacing the water in the migration fracture (MI water) by continuously injecting a foreign groundwater (EM water), characterized by a similar ionic strength but slightly different elemental composition. The measured concentration changes in the extraction flow were interpreted on the basis of the above cation exhange model which allowed determination of the actually available cation exchange capacity of the applied flow field. This total fracture exchange capacity (FEC) was 360 $\pm$ 100 μeq for a closed, unequal strength dipole flow field over a distance of approximately 5 m and characterized by input and extraction water flow rates of 48 ml min^{-1} and 108 ml min^{-1}, respectively. This experiment was also helpful to estimate the in-situ CEC and, therefore, in-situ sorption coefficients for Na^+ and Sr^{2+}, which were roughly compatible with data obtained from coarse-grained, rather incompletely disaggregated laboratory samples.

- The first field tests performed, using pulse injection of short-lived $^{24}Na^{+}$, showed only a small retardation of the breakthrough peak (factors of 1.2 - 1.5). To prolong the interaction time of the tracer with fracture materials, a complex setup for continuous injection was constructed with tracer dosage and input/output flow being provided by highly precise (modified) HPLC pumps. A 7-day continuous injection of $^{22}Na^{+}$, together with uranine (and pulses of $^{82}Br^{-}$ and ^{4}He) was monitored over 2 months. Preliminary examination of this test, however, did not reveal any detectable differences arising from the prolonged exposure of the tracers to the fracture.

- Utilizing the same equipment, several pulse injection runs with $^{24}Na^{+}$, uranine, $^{82}Br^{-}$ and $^{123}I^{-}$, and input/output ratios of 1/3 and 1/15, were carried out. Pulse tests with moderately sorbing $^{85}Sr^{2+}$ were still underway at the end of the period considered in this report.

- To date, field radionuclide migration tests have been carried out for several years using a variety of non-active tracers but only relatively simple sorbing species (Na^{+}, Sr^{2+}; Sr data are not covered in this report). The latters were used testing a single section of the migration fracture over a distance of approximately 5 m, only. Further experiments are currently underway, utilizing the same tracers in experiments over a section of considerably shorter straight line travelling distance (i.e. 1.7 m).

- After these tests with chemically simple and weakly sorbing tracers, it is planned to use chemically more complex (e.g. redox sensitive) nuclides of relevance to repository safety assessment studies (including isotopes of Cs, Se, Ni, Tc, and potentially Pd, Sn and Np). The final stage of the migration experiment is intended to be an excavation of part or all of the tracer flow path.

Technique Development

- Various engineering concepts have been tested and several novel and innovative techniques were developed and successfully tested. Much of the experimental apparatus utilized has been significantly improved and, in cases, represent state-of-the-art technology, some of which will be deployed during detailed characterization of potential repository host formations.

- Major efforts were necessary to modify the experimental setup for long-term tracer experiments with Sr^{2+}:

  (a) in an attempt to minimize uncertainties from instrumental dispersion, equipment volumes were reduced as much as possible. This required the construction of special low-volume packer interval pieces; these small mechanical packers are activated by the movement of the adjacent water-inflated, main (standard) packers.

(b) sorption proofing of the equipment required replacement of nylon by teflon tubing and coating of stainless steel surfaces by PTFE

(c) modification of commercially available HPLC pumps for maintaining highly stable, long-term flow rates.

- Dual quartz fiber fluorometry (optrodes), utilizing an adjustable Argon laser as the excitiation light source, was developed to enable continuous, precise and highly sensitive down-hole analyses of uranine. These measurements are needed to define the actual tracer input function.

- The He tracer method, utilizing a permeation leak (= vacuum dialysis) and a standard He leak detector, was developed for on-line continuous analysis of dissolved He which is now routinely used as a redundant tracer. The method is useful to check de-saturation phenomena in the flow system and, potentially, might be useful to unambiquously identify diffusion processes. Helium as a truly inert and uncharged species is expected to penetrate somewhat easier into the rock matrix.

Preliminary Results from Transport Modeling

- A specific transport model has been developed at the Paul Scherrer Institute in parallel to the field and laboratory experiments. It is based on a standard code (RANCHMD) utilized in repository safety assessment to describe the migration of radionuclides in the geosphere. Although single hole testing revealed a heterogeneous transmissivity distribution, a homogenenous transmissivity is assumed for transport modeling. The code allows the inclusion of the particular flow conditions (unequal-strength dipoles) utilized during field migration experiments.

- Preliminary versions of the model have been used to predict the breakthrough characteristics or retardation of sorbing radiotracers. The results of the field experiment are then compared with the model prediction. Not only does this act as a test of the predictive capabilities of the models utilized but also gives an indication of the relevance of the large mass of laboratory based, radionuclide sorption data (being produced worldwide) to an actual field environment.

- Experimental data were fit with dual-porosity and single porosity concepts. Both concepts produce satisfactory results when fitting conservative tracer breakthrough, while for Na^+ only dual-porosity modeling yields reasonable parameters.

- The dual-porosity modeling concept, with diffusion and sorption occuring in a pore space of limited width (actually a few mm), is consistent with the findings of extensive petrographic examination of the water-bearing pore space. Thus, the breakthrough peak after pulse injection of tracers is mainly the result of hydrodynamic flow in the major transmissive openings within the mylonitic fabric, while the breakthrough tail involves the compounded characteristics of hydrodynamic dispersion as well as reversible retention by diffusion and sorption processes in the highly porous fault gouge (10-30% porosity).

- Preliminary modeling show that the interpretation of Na tracer breakthrough experiments by a dual-porosity modeling approach yield roughly consistent sorption values laboratory rock-water interaction studies, a field-scale equilibration experiment and. With the transport model now calibrated by the Na experiments, detailed predictions for the breakthrough of Sr are available. Ongoing field experiments with $^{85}Sr^{2+}$ will provide a critical test for the applicability of the radionuclide retardation model.

- Confident modeling can only be achieved when experimenters meet a variety of requirements:

  (a) as tracer travel time within the tubing and instrumental dispersion effects cannot always be neglected, down-hole analyses is required to obtain the actual input function of the tracer entering the flow field in the migration fracture

  (b) it is important to maintain very stable, steady-state flow conditions over prolonged periods. Specially designed equipment is needed as the standard pumps for hydrogeological investigations may not provide the required stability. The stability of the flow conditions must be continuously checked by precise monitoring of flow rates and hydraulic pressures even outside the applied flow field.

  (c) steady-state, undisturbed chemical conditions must be maintained during tracer experiments. Hence, specially designed methods or apparatus are necessary during water injection and tracer dosage. Application of radioisotopes, due to their low elemental concentrations, may effectively preclude any chemical disturbance during tracer injection.

  (d) it is helpful to carry out migration experiments in closed flow fields and to achieve, at least for non-retarded species, complete (i.e., 100%) recovery of the injected tracers.

  (e) in addition to conservative tracers, simultaneous application of tracers with various distribution coefficients may drastically narrow the viable range of model derived parameters.

(f) As monitoring of the breakthrough tail section could provide important clues for modeling, tracer analytical equipment should be highly stable and sensitive. A dynamic range of at least 3 orders of magnitude is required.

(g) a thorough structural geological and petrographical investigation of the water-filled pore space is important for selecting an appropriate modeling concept

(h) laboratory sorption experiments must be carried with well characterized material under relevant physical and chemical conditions and the sorption mechanisms must be identified for the selected tracers.

Overall then, the migration experiment is an excellent demonstration of the value of combining efforts on field experiments, laboratory studies and modeling and in showing how such an approach can significantly improve the understanding of radionuclide retardation in the geosphere. Many exciting results have already been produced by this method and it is intended to maintain the high standards already attained in the project when the new experiments with complex (strongly sorbing, redox sensitive) tracers begin and are, eventually, followed by an excavation of the MI fracture. Here the MI experiment will, once again, be quite literally breaking new ground and success is by no means ensured but at least those involved will have the support of the massive body of experience build up within the project in the six years since its inception.

9. FUTURE PLANS

9.1 **Mid-Term Activities** (until summer 1993)

After field experiments utilizing chemically simple tracers, the first pulse injection migration experiments with $^{85}Sr^{2+}$ (together with uranine and $^{22}Na^{+}$) were initiated. Several months of tracer monitoring will be required. These experiments will be analysed by a somewhat modified and improved transport model (HEER, 1992) which will allow the first rigorous test of model predictions (i.e. relative retardation of Na^{+} and Sr^{2+}; HERZOG, 1990 and HERZOG, NTB 91-31).

It is planned to repeat tracer breakthrough experiments with weakly to moderately retarded $^{22}Na^{+}$ and $^{85}Sr^{2+}$ (including conservative tracers) with different flow fields (and over a shorter distance between injection and extraction borehole). The major purpose is to check the validity of the model parameters obtained from earlier experiments.

After the experiments with chemically simple and weakly sorbing tracers, it is intended to use chemically more complex nuclides of relevance to repository safety assessment studies (possibly including isotopes of Cs, Se, Ni, Tc, Pd, Sn, and Np). Laboratory studies on non-linearly sorbing Cs have already been carried out so, in principle, field tests with Cs or Rb (a chemical analog of Cs with a conveniently short-lived isotope) could be instigated soon. Of particular interest are redox-sensitive tracers. Preliminary laboratory results are available for Se, Ni (and Co, chemically analogous to safety relevant Ni). The final selection will be taken on the basis of laboratory studies and suitability of field equipment. Immediately related activities to achieve the objectives of the next planned phase with more complex tracers include

- laboratory experiments to select safety-relevant tracers (based on appropriate solubitity and sorption criteria) followed by detailed characterisation of these elements in this particular groundwater system (sorption, redox system, speciation)

- designing field tests with complex tracers

- carrying out field tests to check the suitability of the available apparatus (and material) for use with more complex tracers (e.g. Cs, Se, Co, etc.)

In addition models must be continually refined or modified based on the results of new field tracer experiments and laboratory studies.

Important input for transport modeling or for the design and execution of field tracer experiments can be obtained from **laboratory high-pressure infiltration experiments** on fractured core samples. Additional tests are planned with other conservative and, perhaps, also reactive tracers.

Many additional field experiments have been proposed but then shelved due to time limitations, technical problems or potential perturbations of the field site.

9.2 **The Final Stage** (until summer 1994)

The final stage of the Grimsel migration experiment is intended to be an excavation of part (or all) of the shear zone between the tracer input borehole and the output borehole. The main aims of the project are to check the validity of model derived parameters and to obtain additional data on the actual transport processes in the field.

Ideally, the excavation experiment should allow a direct definition of radionuclide migration in the MI fracture by physically mapping the tracer distribution in the accessible pore space. This will then allow a comparison of sorption or retardation processes established in the laboratory and a verification of important assumptions implicit in the transport models used to interpret the tracer experiments.

Similar experiments have been attempted in the past (ABELIN, 1985; ABELIN, 1986; BOURKE, 1987) but this particular study is somewhat more demanding in that rather than a simple, planar fracture, it is intended to excavate a more complex, narrow shear zone (see Section 3), including the highly friable and uncompacted fracture infill material. A feasibility study, examining potential methodologies for both the field excavation, fracture conservation, subsequent laboratory analyses and modeling studies, is currently underway.

ACKNOWLEDGEMENTS

The authors gratefully acknowledge the efforts of a large number of individuals from different countries who have contributed to the Grimsel migration experiment. Here, some of those who are not referred to as authors of available documentation, but merit special thanks for their special contribution to the project, are mentioned. Particularly appreciated is the dedicated and extensive experimental support for on-site radiotracer analyses, in particular, by E. Reichlmayr and W. Drost from the Institute of Hydrology, GSF Munich.

During the early stages, the project benefitted from invaluable geological advice of H.P. Keusen (GEOTEST, Zollikofen). Important contributions to improve uranine analyses were obtained from H. Behrens (GSF Munich) and P. Steffen (GEMAG, Albertswil). A variety of novel hydraulic equipment was designed and built by the creative staff (especially P. Giger) of the SOLEXPERTS workshop. The suitability of quartz-fiber optics for down-hole fluorometry was efficiently demonstrated at Grimsel by B. Barczewski and P. Marschall (University of Stuttgart). Extremely helpful hints and assistance to develop the novel He tracer technology were obtained from Prof. P. Signer and his crew of the Mass Spectrometry Group (Institute for Mineralogy, ETH Zürich) and from Dr. Coprio (BALZERS AG, Liechtenstein). Continuous support and assistance for radiotracer experiments was provided by the staff of PSI Hotlab (especially S. Aksoyoglu and K. Bischoff). Numerous hydrochemical analyses were performed by R. Keil, O. Antonsen (PSI) and H.Senften (Mineralwasser Labor, Zürich). Decontamination of traced water discharge was skillfully provided by M. Furrer and P. Leupi (PSI).

During many stages of the project, field work at the Grimsel Test Site depended wholly upon the support and assistance from the local crew (T. Bär, H. Abplanalp and W. Kickmaier). The numereous unexpected findings have required unusual flexibility and improvisation.

The manuscript greatly benefited from R.W.Andrews' review and editing suggestions.

The collaborating staff involved are aware that the Grimsel migration experiment is quite an unusual collaborative venture, as Nagra and PSI generously provided the facilities, manpower and funding to develop, improve, and utilize the most suitable experimental techniques. Since 1989, the Japanese Power Reactor and Nuclear Fuel Development Corporation (PNC) has co-sponsored the project.

REFERENCES

List of Cited Nagra Technical Reports (NTB)

NGB 85-09E: Project Gewähr 1985 - Nuclear Waste Management in Switzerland: Feasibility Studies and Safety Analyses. Nagra Project Report; Nagra, Baden, Switzerland (January 1985)

NTB 81-07: Sondierbohrungen Juchlistock - Grimsel. Nagra Technical Report; Nagra, Baden, Switzerland; (November 1981)

NTB 84-46: B. Wernli, C. Bajo, K. Bischoff (1984) Bestimmung des Sorptions-koeffizienten von Uran (VI) an Grimsel- und Böttsteingranit. Nagra Technical Report; Nagra, Baden, Switzerland (September 1984); also published as EIR Bericht Nr. 543, Paul Scherrer Institute, Villigen, Switzerland

NTB 85-40: Hadermann J. and F. Roesel (1985) Radionuclide Chain Transport in Inhomogeneous Crystalline Rocks; Limited Matrix Diffusion and Effective Surface Sorption. Nagra Technical Report; Nagra, Baden, Switzerland (February 1985); also published as EIR Bericht Nr. 551; Paul Scherrer Institute Villigen (Switzerland)

NTB 85-42: Bischoff K., Wolf K. and Heimgartner B. (1987) Hydraulische Leitfähigkeit, Porosität und Uranrückhaltung von Kristallin und Mergel: Bohrkern-Infiltrationsversuche. Nagra Technical Report; Nagra, Baden, Switzerland; also published as EIR Bericht Nr. 628, Paul Scherrer Institute, Villigen, Switzerland; April 1987

NTB 85-46: Grimsel Test Site - Overview and Test Programs. Nagra Technical Report, Nagra Baden, Switzerland; August 1985

NTB 85-47: Felslabor Grimsel - Übersicht und Untersuchungsprogramme. Nagra Technical Report, Nagra Baden, Switzerland; August 1985

NTB 87-08: Alexander W.R., MacKenzie A.B., Scott R.D., and McKinley I.G. (1990) Natural Analogue Studies in Crystalline Rock: The Influence of Water-bearing Fractures on Radionuclide Immobilization in a Granitic Rock repository. Nagra Technical Report; Nagra, Baden, Switzerland; June 1990

NTB 87-13: Falk L., Magnusson K.-Å., Olsson O., Ammann M., Keusen H.R., and Sattel G. (1988) Grimsel Test Site: Analysis of Radar Measurements Performed at the Grimsel Rock Laboratory in October 1985. Nagra Technical Report; Nagra, Baden, Switzerland; February 1988

NTB 87-14: Keusen H.R., Ganguin J., Schuler P. and Buletti M. (1987) Felslabor Grimsel - Geologie. Nagra Technical Report; Nagra, Baden, Switzerland; February 1989

NTB 87-40/1: Abelin H., L. Birgersson, J. Gidlund, I. Neretnieks, L. Moreno, I. Neretnieks, H. Widén and T. Ågren (1987) Stripa Project: 3-D Migration Experiment - Report 3: Performed Experiments, Results and Evaluation. Nagra Technical Report; Nagra, Baden, Switzerland; also published as Stripa Project Technical Report TR 97-21 (November 1987)

NTB 87-40/2: Abelin H., L. Birgersson, J. Gidlund, I. Neretnieks, L. Moreno, I. Neretnieks, H. Widén and T. Ågren (1987) Stripa Project: 3-D Migration Experiment - Report 3: Performed Experiments, Results and Evaluation. Nagra Technical Report; Nagra, Baden, Switzerland; also published as Stripa Project Technical Report TR 97-21 (November 1987)

NTB 88-01: F.J. Pearson Jr., W. Balderer, H.H. Loosli, B.E. Lehmann, A. Matter, Tj. Peters, H. Schmassmann, A. Gautschi (1991) Applied Isotope Hydrogeology - A Case Study in Northern Switzerland. Nagra Technical Report; Nagra, Baden, Switzerland; also published in Studies in Environmental Sciences 43, Elsevier, Amsterdam (May 1991)

NTB 88-06: Seismische Durchschallungstomographie (WBK, Westfälische Berggewerkschaftskasse). Nagra Technical Report; Nagra, Baden, Switzerland; June 1988

NTB 88-23: Bradbury M.H., editor (1989) Grimsel Test Site - Laboratory Investigations in Support of the Migration Experiments. Nagra Technical Report; Nagra, Baden, Switzerland; also published as PSI Bericht Nr. 28; April 1989

NTB 88-31: Niva B., Olsson O., and Blümling P. (1988) Radar Crosshole Tomography with Application to Migration of Saline Tracer Through Fracture Zones. Nagra Technical Report; Nagra, Baden, Switzerland; October 1988

NTB 88-37: Bräuer V., B. Kilger and A. Pahl (1989) Felslabor Grimsel - Ingenieurgeologische Untersuchungen zur Interpretation von Gebirgsspannungsmessungen und Durchströmungsversuchen. Nagra Technical Report; Nagra, Baden, Switzerland; April 1989

NTB 88-39E: Pahl A., Heusermann St., Bräuer V., and Glöggler W. (1989) Grimsel Test Site - Rock Stress Investigations. Nagra Technical Report; Nagra, Baden, Switzerland; April 1989

NTB 88-39: Pahl A., Heusermann St., Bräuer V., and Glöggler W. (1989) Felslabor Grimsel - Gebirgsspannungsuntersuchungen. Nagra Technical Report; Nagra, Baden, Switzerland; April 1989

NTB 88-40: Schneefuss J., Gläss F., Gommlich G., and Schmidt M. (1989) Felslabor Grimsel - Wärmetest; Abschlussbericht. Nagra Technical Report; Nagra, Baden, Switzerland; May 1989

NTB 89-01: Wyss E. (1989) Felslabor Grimsel: Hydrogeologische Untersuchungen zur Bestimmung hydraulischer Potentiale. Nagra Technical Report; Nagra, Baden, Switzerland (June 1989)

NTB 89-11: Flach D. and Noell U. (1990) Neigungsmessungen zur Ermittlung neotektonischer Vorgänge (Untersuchungen zur Erkundung ausgewählter Eigenschaften von kristallinen Felsformationen für die Endlagerung radioaktiver Abfälle). Nagra Technical Report; Nagra, Baden, Switzerland; in preparation

NTB 89-15: Hoehn E., Fierz T., and Thorne P. (1990) Grimsel Test Site - Hydrogeological Characterisation of the Migration Experimental Area. Nagra Technical Report; Nagra, Baden, Switzerland; also published as PSI Bericht Nr. 60; June 1990

NTB 89-16: Herzog F. (1989) Hydrologic Modelling of the Migration Site in the Grimsel Rock Laboratory - the Steady State. Nagra Technical Report; Nagra, Baden, Switzerland; also published as PSI Bericht Nr. 23; July 1989

NTB 90-01: Degueldre C., G. Longworth, V. Moulin and P. Vilks. Grimsel Test Site - Grimsel Colloid Exercise: An International Intercomparison Excercise on the Sampling and Characterisation of Groundwater Colloids. Nagra Technical Report; Nagra, Baden, Switzerland (January 1990); also published as PSI Bericht Nr. 39; Paul Scherrer Institute, Villigen

NTB 90-13: Jakob A., J. Hadermann and F. Roesel (1989) Radionuclide chain transport with matrix diffusion and non-linear sorption. Nagra Technical Report, Nagra, Baden, Switzerland (October 1990); also published as PSI Bericht Nr. 54; Paul Scherrer Institute, Villigen, Switzerland

NTB 90-15: Baertschi P., Alexander W.R., and Dollinger H. (1990) Uranium Migration in the Crystalline Rock: Capillary Solution Transport in the Granite of the Grimsel Test Site. Nagra Technical Report; Nagra, Baden, Switzerland; February 1991

NTB 90-39: Eikenberg J., Baeyens B., and Bradbury M. (1990) The Grimsel Migration Experiment - A Hydrogeochemical Equilibration Test. Nagra Technical Report; Nagra, Wettingen, Switzerland; also published as PSI Bericht Nr. 100; May 1991

NTB 91-01E (English Version): Grimsel Test Site - Fracture Flow Test. Nagra Technical Report; Nagra, Wettingen, Switzerland; in print

NTB 91-02E (English Version): Grimsel Test Site - Ventilation Test. Nagra Technical Report; Nagra, Wettingen, Switzerland; in print

NTB 91-03: Voborny O., Adank P., Hürlimann W., Vomvoris S., Mishra S. (1991) Grimsel Test Site: Modeling of Groundwater Flow in the Rock Body Surrounding the Underground Laboratory. Nagra Technical Report; Nagra, Wettingen, Switzerland; October 1991

NTB 91-06: Aksoyoglu S., C. Bajo and M. Mantovani (1990) Grimsel Test Site: Batch Sorption Experiments with iodine, bromine, strontium, sodium and cesium on Grimsel mylonite. Nagra Technical Report NTB 91-06, Nagra, Wettingen, Switzerland (February 1991); also published as PSI Bericht Nr. 83; Paul Scherrer Institute, Villigen, Switzerland (February 1991)

NTB 91-12: Bossart P. and M. Mazurek (1991) Grimsel Test Site: Structural Geology and Water Flow-Paths in the Migration Shear-Zone. Nagra Technical Report; Nagra, Wettingen, Switzerland; November 1991

NTB 91-27: JAKOB, A. & HADERMANN, J. (1990): INTRAVAL Test Case 1b - Modelling results; Nagra Technical Report; Nagra, Wettingen, Switzerland; also published as PSI Bericht Nr. 105, Paul Scherrer Institute, Villigen, Switzerland (July 1991).

NTB 91-31: Herzog F. (1991) Grimsel Test Site: A Simple Transport Model for the Grimsel Migration Experiments. Nagra Technical Report; Nagra, Wettingen, Switzerland; also published as PSI Bericht Nr. 106; September 1991

NTB 91-33: Smith P.A. (1991) Grimsel Test Site: Modelling of Laboratory High-Pressure Infiltration Experiments. Nagra Technical Report; Nagra, Wettingen, Switzerland; also published as PSI Bericht Nr. 117; January 1992

REFERENCES: List of Cited Authors

ABELIN, H., NERETNIEKS, I., TUNBRANT, S. & MORENO, L. (1985): Migration in a single fracture - Experimental results and Evaluation. Stripa Project Internal Report 85-03, SKB Stockholm, Sweden.

ABELIN, H. (1986): Migration in a Single Fracture - an in-situ Experiment in a Natural Fracture. Ph. D. Thesis, Dept. Chemical Engineering, Royal Institute of Technology, Stockholm, Sweden.

ABELIN, H., BIRGERSSON, L., GIDLUND, J., NERETNIEKS, I., MORENO, L., NERETNIEKS, I., WIDÉN, H. & ÅGREN, T. (1987): Stripa Project: 3-D Migration Experiment - Report 3: Performed Experiments, Results and Evaluation. Nagra Technical Report NTB 87-40/1+2; Nagra, Baden, Switzerland; also published as Stripa Project Technical Report TR 97-21, SKB Stockholm, Sweden (November 1987).

AKSOYOGLU, S., BAJO, C. & MANTOVANI, M. (1990): Grimsel Test Site: Batch Sorption Experiments with iodine, bromine, strontium, sodium and cesium on Grimsel mylonite. Nagra Technical Report NTB 91-06, Nagra, Baden, Switzerland (February 1991); also published as PSI Bericht Nr. 83; Paul Scherrer Institute, Villigen, Switzerland (December 1990).

AKSOYOGLU, S. (1990): Cesium Sorption on Mylonite, J. Radioanal. Nucl. Chem. 140, 301-313.

ALEXANDER, W.R. (1991): Redox State of the Grimsel Test Site (GTS) Radionuclide Migration Experiment (MI), Groundwater/Rock System. Nagra Internal Technical Note AN/90-216 (January 1991).

ALEXANDER, W.R., McKINLEY, I.G., MacKENZIE, A.B. & SCOTT, R.D. (1990a): Verification of matrix diffusion by means of natural decay series disequilibria in a profile across a water-conducting fracture in granitic rock. Sci. Basis Nucl. Waste Manag. XIII, 567-576.

ALEXANDER, W.R., MacKENZIE, A.B., SCOTT, R.D. & McKINLEY, I.G. (1990b): Natural Analogue Studies in Crystalline Rock: The Influence of Water-bearing Fractures on Radionuclide Immobilisation in a Granitic Rock repository. Nagra Technical Report NTB 87-08; Nagra, Baden, Switzerland; June 1990.

BAERTSCHI, P., ALEXANDER, W.R. & DOLLINGER, H. (1990): Uranium Migration in the Crystalline Rock: Capillary Solution Transport in the Granite of the Grimsel Test Site. Nagra Technical Report NTB 90-15; Nagra, Baden, Switzerland; February 1991

BAERTSCHI, P., ANTONSEN, O., MEIER, W.R., KEIL, R. (1982): Untersuchungen an Wasserproben der Sondierbohrungen SB1-SB4 im Hauptstollen des Pumpkraftwerks Grimsel/Oberaar (Nagra Auftrag), EIR Internal Technical Report TM-44-82-13, Paul Scherrer Institute, Villigen, Switzerland.

BAEYENS, B. & BRADBURY, M.H. (1989): Selectivity Coefficients and Estimates of In-Situ Sorption values for Mylonite. In Grimsel Test Site - Laboratory Investigations in Support of the Migration Experiments; in M. Bradbury ed.; Nagra Technical Report NTB 88-23; Nagra, Baden, Switzerland; also published as PSI Bericht Nr. 28; April 1989.

BAEYENS, B., AKSOYOGLU, S. & BRADBURY, M.H. (1989): Cation Exchange Characteristics of Mylonite. In Grimsel Test Site - Laboratory Investigations in Support of the Migration Experiments; in M. Bradbury ed.; Nagra Technical Report NTB 88-23; Nagra, Baden, Switzerland; also published as PSI Bericht Nr. 28; April 1989.

BAJO, C., HOEHN, E., KEIL, R. & BAEYENS, B. (1989): Chemical Characterisation of the Groundwater from Fault Zone AU 96 m. In Grimsel Test Site-Laboratory Investigations in Support of the Migration Experiments; in M. Bradbury ed.; Nagra Technical Report NTB 88-23; Nagra, Baden, Switzerland; also published as PSI Bericht Nr. 28; April 1989.

BAJO, C., AKSOYOGLU, S. & MANTOVANI, M. (1989): Groundwater Stability and Rock-water Interaction Experiments. In Grimsel Test Site - Laboratory Investigations in Support of the Migration Experiments; in M. Bradbury ed.; Nagra Technical Report NTB 88-23; Nagra, Baden, Switzerland; also published as PSI Bericht Nr. 28; April 1989.

BALDERER, W. (1987): Unpublished Nagra Data; private communication.

BARCZEWSKI, B. & MARSCHALL, P. (1987): Neue Methoden zur Bestimmung kleinster Strömungsgeschwindigkeiten und zur Messung von Markierungsfarbstoffen in Grundwassermessstellen. Wissenschaftlicher Bericht 87/13 (HWV 086), 43 p.; Institut für Wasserbau, Universität Stuttgart; September 1987.

BEHRENS, H. (1986): Water Tracer Chemistry: A Factor Determining Performance and Analytics of Tracers. Proceedings of the 5th International Symposium on Underground Water Tracing; Institute of Geology and Mineral Exploration, Athens; 121-123.

BISCHOFF, K., WOLF, K. & HEIMGARTNER, B. (1987): Hydraulische Leitfähigkeit, Porosität und Uranrückhaltung in Bohrkernproben von Böttstein und Grimsel: Bohrkern-Infiltrationsversuche. Nagra Technical Report NTB 85-42, Nagra, Baden, Switzerland; also published as an EIR Bericht Nr. 628; Paul Scherrer Institute, Villigen.

BLÜMLING, P. & SATTEL, G. (1988): Tomographic Investigations. In Nagra Informiert 1/2 1988 or Nagra Bulletin, special English edition 1988; p. 35-40.

BOSSART, P. & MARTEL, S. (1990): Hydrogeological Implications of Ductile and Brittle Deformations in the Grimsel Crystalline, Upper Aare Valley, Switzerland. Nagra Internal Report 90-19; Nagra, Baden, Switzerland; May 1990.

BOSSART, P. & MAZUREK, M. (1990): Felslabor Grimsel: Strukturgeologische Charakterisierung und Geometrie der Wasser-Fliesswege in der Migrationsscherzone. Nagra Internal Report 90-44, Nagra Wettingen, Switzerland (August 1990).

BOSSART, P. & MAZUREK, M. (1991): Grimsel Test Site: Structural Geology and Water Flow-Paths in the Migration Shear-Zone. Nagra Technical Report NTB 91-12; Nagra, Wettingen, Switzerland; November 1991.

BOURDET, D. & GRINGARTEN, A.C. (1980): Determination of fissure volume and block size by type curve analysis. Soc. Pet. Eng. Journal; Trans. AIME 9293.

BOURKE, P.J. (1987): Channeling of Flow Through Fractures in Rock. AERE Report 12305; Harwell, United Kingdom.

BRADBURY, M.H. & BAEYENS, B. (1989): Application of the results to the GTS Migration Experiment. In Grimsel Test Site - Laboratory Investigations in Support of the Migration Experiments; in M. Bradbury ed.; Nagra Technical Report NTB 88-23; Nagra, Baden, Switzerland; also published as PSI Bericht Nr. 28; April 1989.

BREWITZ, W., BRASSER, Th., KULL, H. & HUFSCHMIED, P. (1988): The ventilation Test. In Nagra Informiert 1/2 1988 or Nagra Bulletin, special English edition 1988; p. 46-49.

CACAS, M.C., LEDOUX, E., DE MARSILY, G., TILLIE, B., BARBEAU, A., DURAND, E., FEUGA, B. & PEAUDECERF, P. (1990a): Modeling Fracture Flow with a Stochastic Discrete Fracture Network: Calibration and Validation, 1. The Flow Model. Water Resources Research, Vol. 26/3, 479-490.

CACAS, M.C., LEDOUX, E., DE MARSILY, G., BARBEAU, A., CALMELS, P., GAILLARD, B. & MARGARITTA, R. (1990b): Modeling Fracture Flow with a Stochastic Discrete Fracture Network: Calibration and Validation, 2. The Transport Model. Water Resources Research, Vol. 26/3, 491-500.

CARTER, R.C., KAUFMAN, W.J., ORLOB, G.T. & TODD, D.K. (1959): Helium as a ground-water tracer. J. Geophys. Res., 64, 2433-2438.

CHOUKRONE, P. & GAPAIS, D. (1983): Strain pattern in the Aare Granite (Central Swiss Alps): orthogneiss developed by bulk inhomogeneous flattening. J. Struct. geol., Vol. 5, Nr. 3/4, 411-418.

CHRISTOFI, N. & MILNER, C.R. (1985): Microbial Examination of Groundwater from the Grimsel Test Site: the Results of two Studies Carried out by the Napier Polytechnic of Edinburgh. Nagra Internal Report NIB 90-23; Nagra, Baden, Switzerland, September 1990.

COOPER, H.H. JR. & JACOB, C.E. (1946): A generalised graphical method for evaluating formation constants and summarising well-field history. Am. Geophys. Union Trans., 27 (4), 526-534.

CREMERS, A., ELSEN, A., DE PRETER, P. & MAES, A. (1988): Quantitative Analysis of Radiocesium Retention in Soils. Nature, 335, 247-249.

DAVEY, A., KARASAKI, K., LONG, J.C.S., LANDSFELD, M., MENSCH, A. & MARTEL, S.J. (1990): Analysis of Hydraulic data from the MI Fracture Zone at the Grimsel Rock Laboratory, Switzerland. Nagra-DOE Cooperative Project Report NDC-15/LBL-27864; December 1990

DAVIS, S.N. & DE WIEST, R.J.M. (1966): Hydrogeology. John Wiley & Sons, New York, USA.

DEGUELDRE, C., BAEYENS, B., GOERLICH, W., GRIMMER, H., MOHOS, M., PORTMANN, A., RIGA, J. & VERBIST, J. (1987a): In-laboratory, on site, in situ sampling and characterisation of Grimsel colloids - Phase I. Internal Technical Report EIR TM-42-87-20; Paul Scherrer Institute, Villigen, Switzerland.

DEGUELDRE, C., DENNEMONT, J. & STADELMANN, P. (1987b): Sampling and Characterisation of Grimsel Colloids - Phase II by use of microbeam techniques. Internal Technical Report EIR TM-42-87-27, 20 p.; Paul Scherrer Institute, Villigen, Switzerland.

DEGUELDRE, C., BAEYENS, B., GOERLICH, W., RIGA, J., VERBIST, J. & STADELMANN, P. (1989): Colloids in Water from a Subsurface Fracture in Granitic Rock, Grimsel Test Site, Switzerland. Geochim. Cosmochim. Acta 53, p. 603-610.

DEGUELDRE, C., LONGWORTH, G., MOULIN, V. & VILKS P. (1990): Grimsel Test Site - Grimsel Colloid Exercise: An International Intercomparison Excercise on the Sampling and Characterisation of Groundwater Colloids. Nagra Technical Report NTB 90-01; Nagra, Baden, Switzerland (January 1990); also published as PSI Bericht Nr. 39; Paul Scherrer Institute, Villigen, Switzerland.

DROST, W. (1984): Single Well techniques. - In: Tracer methods in isotope hydrology: 8, Vienna, Austria (IAEA).

DROST, W. (1968): Groundwater measurements by means of radioactive tracers. Atomenergie-Kerntechnik, 48(2), 81-86.

DROST, W., KLOTZ, D., KOCK, A., MOSER, H., NEUMAIER, F. & RAUERT, W. (1968): Point dilution methods of investigating groundwater flow by means of radioisotopes. Water Resources Res. 4/1; 125-146.

EGGER, P. (1986): Grimsel Test Site: Tests for Excavation Effects (Machine Excavated Tunnel)- a Preliminary Summary. Nagra Internal Report 86-28; Nagra, Baden, Switzerland.

EIKENBERG, J. (1989): Abschätzung von geochemischen Veränderungen bei Stollenluftinfiltrationen in die Grimsel Migrationskluft. PSI Internal Technical Note AN-41-89-04, 8 p. Paul Scherrer Institute, Villigen, Switzerland.

EIKENBERG, J. (1990): Water Chemistry Calculations for the Hydrogeochemical Equilibration Experiment at the GTS. PSI Internal Technical Report TM-41-89-20, 27 p., Paul Scherrer Institute, Villigen, Switzerland.

EIKENBERG, J. & BÜHLER, Ch. (1990): Grimsel-Grundwasser als chemisches Lösungsmittel von Korund. PSI Internal Technical Note AN-41-90-58, Paul Scherrer Institut, Würenlingen, Switzerland.

EIKENBERG, J. & KIPFER, R. (1989): ^{4}He als Tracer bei Migrationsexperimenten. PSI Internal Technical Report TM-41-89-12, 26 p.; Paul Scherrer Institute, Villigen, Switzerland; June 1989.

EIKENBERG, J., BAEYENS, B. & BRADBURY, M.H. (1991): The Grimsel Migration Experiment: A Hydrogeochemical Equilibration Test. Nagra Technical Report NTB 90-39; Nagra, Wettingen, Switzerland, also printed as PSI Bericht Nr. 100; May 1991

EIKENBERG, J., FRICK, U., FIERZ, Th. & BÜHLER, Ch. (1992): On-line detection of stable helium isotopes in migration experiments. Proceedings of the 6th International Symposium on Water Tracing, September 21 - 26, 1992; Karlsruhe, Germany

FALK, L., MAGNUSSON, K.-Å., OLSSON, O., AMMANN, M., KEUSEN, H.R. & SATTEL, G. (1988): Grimsel Test Site: Analysis of Radar Measurements Performed at the Grimsel Rock Laboratory in October 1985. Nagra Technical Report NTB 87-13; Nagra, Baden, Switzerland; February 1988.

FINSTERLE, S., SCHLUETER, E. & PRUESS, K. (1990): Exploratory Simulations of Multiphase Effects in Gas Injection and Ventilation Tests in an Underground Rock Laboratory. Nagra-DOE Cooperative Project Report NDC-13/LBL-28810; June 1990.

FLACH, D. & NOELL, U. (1990): Neigungsmessungen zur Ermittlung neotektonischer Vorgänge (Untersuchungen zur Erkundung ausgewählter Eigenschaften von kristallinen Felsformationen für die Endlagerung radioaktiver Abfälle). Nagra Technical Report NTB 89-11; Nagra, Baden, Switzerland

FREEZE, R.A. & CHERRY, J.A. (1979): Groundwater. Prentice Hall Inc., Eagle Cliffs, New Jersey, USA

FRESENIUS (1986,1987): Unpublished Nagra Data.

FRICK, U., BAERTSCHI, P. & HOEHN, E. (1988): Migration Investigations. In Nagra Informiert 1/2 1988 or Nagra Bulletin, special English edition 1988; p. 23-34.

FRICK, U., BAERTSCHI, P. & HOEHN, E. (1988): Migration investigations. Nagra Bulletin, Special Edition 1988; 23-24, Nagra, Baden.

FRICK, U., ALEXANDER, W.R. & DROST, W. (1991): The radionuclide migration experiment at Nagra's Grimsel underground test site - a comprehensive program including field, laboratory, and modeling studies. Paper IAEA-SM-319/27 in the Proceedings of the International Symposium on the Use of Isotope techniques in Water Resources Development, Vienna, 11-15 March 1991.

GARNIER, J.M., CRAMPON, N., PREAUX, C., POREL, G. & VREULX, M. (1985): Traçage par ^{13}C, $^{2}H^{+}$, I^{-} and uranine dans la nappe de la craie sénonienne en écoulement radial convergent (Béthune, France). J. Hydrol. Amsterdam, 78, 379-392.

GELHAR, L.W. (1987): Applications of stochastic models to solute transport in fractured rocks. SKB Technical Report 87-05; SKB Stockholm, Sweden.

GEMPERLE, R. (1989): Migration GTS: Test description and first ananlysis of a 35-day constant-flow test in BOMI 87.009. Nagra Internal Report 89-14; Nagra, Baden, Switzerland.

GEOTEST (1981): Sondierbohrungen Juchlistock-Grimsel. Nagra Technical Report NTB 81-07; Nagra, Baden, Switzerland, November 1981.

GEOTEST (1986): Grimsel Migration Experiment: Structural Geology of Migration Fracture and Drillcore descriptions (Geologie der Bohrungen BOMI 86.004 and BOMI 86.005). Geotest Report # 86025.

GEOTEST (1987): Grimsel Migration Experiment: Drillcore descriptions BOMI 87.006 to BOMI 87.011. Unpublished Nagra Data; Nagra, Baden, Switzerland.

GEOTEST (1988): Felslabor Grimsel - Geologie (Rohdatenbericht). Nagra Internal Report 87-42; Nagra, Baden, Switzerland (October 1988).

GRINGARTEN, A.C. (1982): Flow test evaluation of fractured rocks. Geol. Soc. of America Spec. Paper 189, 237-263.

HADERMANN, J. & ROESEL, F. (1985): Radionuclide Chain Transport in inhomogeneous Crystalline Rocks; Limited Matrix Diffusion and Effective Surface Sorption. Nagra Technical Report NTB 85-40; Nagra, Baden, Switzerland (February 1985); also published as EIR Bericht Nr. 551; Paul Scherrer Institute, Villigen, (Switzerland).

HEER W. (1992): Grimsel Migration Experiment - Transport Modeling of Reactive Tracer Breakthrough. Issued simultaneously as Nagra Technical Report and PSI Report; Paul Scherrer Institute, Villigen, (Switzerland). In preparation

HERZOG, F. (1989): Hydrologic Modelling of the Migration Site in the Grimsel Rock Laboratory - the Steady State. Nagra Technical Report NTB 89-16; Nagra, Baden, Switzerland; also published as PSI Bericht Nr. 23; July 1989.

HERZOG, F. (1990): Transport-Modelling for the Grimsel Migration Experiments: Streamtube Approach, First Results and Predictions. PSI Internal Technical Report TM-41-90-18; 34 p.; Paul Scherrer Institute, Villigen, Switzerland.

HERZOG, F. (1991): Grimsel Test Site: A Simple Transport Model for the Grimsel Migration Experiments. Nagra Technical Report NTB 91-31; Nagra, Wettingen, Switzerland; also published as PSI Bericht Nr. 106; September 1991.

HOEHN, E. (1987): Distribution of the fracture openings of the migration fault (unpublished data); private communication.

HOEHN, E., FRICK, U. & HADERMANN, J. (1988): Exploration Methods and Instrumentation of a Single Fracture for radionuclide Migration Experiments at the Grimsel Rock Laboratory. In: Hydrology and Safety of Radioactive and Industrial Hazardous Waste Disposal, Symposium Orléans June 3-10, 1988; Documents du B.R.G.M. Nr. 160, p. 407-417.

HOEHN, E., FIERZ, T. & THORNE, P. (1990): Grimsel Test Site - Hydrogeological Characterisation of the Migration Experimental Area. Nagra Technical Report NTB 89-15; Nagra, Baden, Switzerland; also published as PSI Bericht Nr. 60; June 1990.

HOEHN, E. & EIKENBERG, J. (1992): Injection-extraction migration experiments in a single fracture with uranine and the reactive radionuclides $^{22}Na^{+}$, $^{24}Na^{+}$ and $^{85}Sr^{2+}$. Proceedings of the 6th International Symposium on Water Tracing, September 21 - 26, 1992; Karlsruhe, Germany

HORNER, D.R. (1951): Pressure build-up in wells; 3rd World Petrol. Congr., 2, 503-521. The Hague, Netherlands.

HUFSCHMIED, P. & ADANK, P. (1988): Modelling Groundwater Flow in the Rock Body Surrounding the Grimsel Test Site. In Nagra Informiert 1/2 1988 or Nagra Bulletin, special English edition 1988; p. 50-52.

HUFSCHMIED, P. & FRIEG, B. (1989): Observation of Hydraulic Heads in the Nagra Boreholes in Northern Switzerland. In Nagra Informiert December 1989 or Nagra Bulletin, Special English edition 1989; p. 39-49.

IVANOVICH, M. & WILKINS, M.A. (1984): Harwell Report on the analysis of Nagra groundwater samples from deep boreholes: uranium series disequilibrium measurements (Nagra data). AERE-G 3135, April 1984.

JACOB, C.E. & LOHMAN, S.W. (1952): Nonsteady flow to a well of a constant drawdown in an extensive aquifer. Am. Geophys. Union Trans., 33, 559-569.

JAKOB, A., HADERMANN, J. & ROESEL, F. (1989): Radionuclide chain transport with matrix diffusion and non-linear sorption. Nagra Technical Report NTB 90-13, Nagra, Baden, Switzerland; October 1990; also published as PSI Bericht Nr. 54; Paul Scherrer Institute, Villigen, Switzerland.

JAKOB, A. & HADERMANN, J. (1990): INTRAVAL Test Case 1b - Modelling results; Nagra Technical Report NTB 91-27; Nagra, Wettingen, Switzerland; also published as PSI Bericht Nr. 105, Paul Scherrer Institute, Villigen, Switzerland (July 1991).

KELLEY, V.A. & FRIEG, B. (1990): Grimsel Test Site: Field Investigations (Interference tests, Fluid Logging, and Constant-Rate Withdrawal Test) in the BK Area, December 1989 - March 21, 1990. Nagra Internal Report 90-31; Nagra, Baden, Switzerland; September 1990.

KEUSEN, H.R., GANGUIN, J., SCHULER, P. & BULETTI, M. (1987): Felslabor Grimsel - Geologie. Nagra Technical Report NTB 87-14 (NTB 87-14E English version); Nagra, Baden, Switzerland; February 1989.

KRALIK, M. (1991): private communication; tritium, stable isotope and hydrochemical data analyzed at the Geotechnical Institute, Federal Research Institute Arsenal (Bundesversuchs- und Forschungsanstalt), Vienna.

KUHLMANN, U. (1989): Applications of NAMMU: results of four test examples; Nagra Internal Report 89-71; Nagra, Baden, Switzerland.

KUHLMANN, U., VOMVORIS, S. & HUFSCHMIED, P. (1990): Evaluation of earth tide induced matrix dispersion; Proceedings of the GEOVAL Symposium May 14-17, 1990; Stockholm, Sweden.

KULLIN, M. & SCHMASSMANN, H. (1991): Isotopic Composition of Modern Recharge. In: Applied Isotope Hydrogeology - A Case Study in Northern Switzerland. Nagra Technical Report NTB 88-01; Nagra, Wettingen, Switzerland; also published in Studies in Environmental Sciences 43, Elsevier, Amsterdam, Netherland (May 1991), 65-89.

LABHART, T.P. (1966): Mehrphasige alpine Tektonik am Nordrand des Aarmassivs. Beobachtungen im Druckstollen Trift-Speicherberg (Gadmental) der Kraftwerke Oberhasli AG. Eclogae Geol. Helv. 59/2, p. 803-830.

LANDSTRÖM, O., KLOCKARS, K.E., PERSSON, O., TULLBORG, E.L. LARSON, S.Å., ANDERSSON, K., ALLARD, B., TORSTENFELT, B. (1982): Migration Experiments in Studvik. SKBF-KBS Technical Report 82-18, SKB Sockholm, Sweden.

LIEDKE, L. & ZUIDEMA, P. (1988): The Fracture System Flow Test. In Nagra Informiert 1/2 1988 or Nagra Bulletin, special English edition 1988; p. 41-45.

LINDBERG R.D. & RUNNELS D.D. (1984) Ground water redox reactions: an analysis of equilibrium state applied to Eh measurements and geochemical modeling. Science 225, p.425-427

LOHMAN, S.W. (1972): Groundwater hydraulics; U.S. Geol. Survey Prof. Pap. 708, U.S. Governement Print. Office, Washington, USA.

LONG, J.C.S., MAJER, E.L., MARTEL, S.J., KARASAKI, K., PETERSON Jr. J.E., DAVEY, A. & HESTIR, K. (1990): Hydrologic Characterisation of Fractured Rocks-an Interdisciplinary Methodology. Nagra-DOE Cooperative Project Report NDC-12/LBL-27863; November 1990.

LOOSLI, H.H., LEHMANN, B.E. & DÄPPEN, G. (1991): Dating by Radionuclides. In: Applied Isotope Hydrogeology - A Case Study in Northern Switzerland. Nagra Technical Report NTB 88-01; Nagra, Wettingen, Switzerland; also published in Studies in Environmental Sciences 43, Elsevier, Amsterdam, Netherland (May 1991), 153-174.

MAJER, E.L., PETERSON, Jr. J.E., BLÜMLING, P. & SATTEL, G. (1990a): p-Wave Imaging of the FRI and BK Zones at the Grimsel Rock Laboratory. Nagra-DOE Cooperative Project Report NDC-4/LBL-28807; August 1990.

MAJER, E.L., PETERSON, Jr. J.E., BLÜMLING, P. & SATTEL, G. (1990b): Shear Wave Experiments at the US Site at the Grimsel Rock Laboratory. Nagra-DOE Cooperative Project Report NDC-7/LBL-28808; July 1990.

MAJER, E.L., MYER, L.R., PETERSON, Jr., J.E., KARASAKI, K., LONG, J.C.S., MARTEL, S.J., BLÜMLING, P. & VOMVORIS, S. (1990c): Joint Seismic, Hydrogeological, and geomechanical Investigations of a Fracture Zone in the Grimsel Rock Laboratory. Nagra-DOE Cooperative Project Report NDC-14/LBL-27913; June 1990.

MARQUER, D., GAPAIS, D. & CAPDEVITA, R. (1985): Comportement chimique et orthogneissification d'une granodiorite en faciès schistes verts (Massif de l'Aar, Alpes centrales). Bull. Minéral. 108; 209-221.

MARSCHALL, P. & BARCZEWSKI, B. (1990): Evaluation of single borehole hydrotests in the frequency domain by a univariate statistical method. Conf. Proceedings of Model CARE 90: Calibration and Reliability in Groundwater Modelling. The Hague Sept. 1990, IAHS Publ. Nr. 195.

MARTEL, S.J. & PETERSON, Jr. J.E. (1990): Use of an Integrated Geologic and geophysical Information for Characterizing the Structure of Fracture Systems at the US/BK Site, Grimsel Laboratory, Switzerland. Nagra-DOE Cooperative Project Report NDC-16/LBL-27912; May 1990.

MARTEL, S.J. & PETERSON, Jr. J.E. (1991): Interdisciplinary Characterisation of Fracture Systems at the US/BK Site, Grimsel Laboratory, Switzerland. Int. J. Rock Mech. Min. Sci. & Geomech. Abstr. Vol 28/4, pp. 295-323.

MAZUREK M., BOSSART P. ALEXANDER W.R., LOWSON R. & MACKENZIE A.B. (1991): Microscale fluid flowpaths and the mobility of U, Th and Ra in the migration fracture (in preparation)

McKINLEY, I.G., ALEXANDER W.R., BAJO, C., FRICK, U., HADERMANN J., HERZOG, F. & HOEHN, E. (1988): The Radionuclide Migration Experiment at the Grimsel Rock Laboratory, Switzerland. Sci. Basis Nucl. Waste Manag. XI, p. 179-187.

McKINLEY, I.G. & GROGAN, H. (1984): Specification of an experimental study of geochemistry and elemental migration at the Grimsel rock laboratory. EIR Internal Technical Report TM-45-84-37, Paul Scherrer Institute, Villigen, Switzerland; 51 p.

MEYER, J., MAZUREK, M. & ALEXANDER, W.R. (1989): Petrographic and Mineralogical Characterisation of fault Zones AU 96 m and AU 126 m. In Grimsel Test Site: Laboratory Investigations in Support of the Migration Experiments; in M. Bradbury ed.; Nagra Technical Report NTB 88-23; Nagra, Baden, Switzerland; also published as PSI Bericht Nr. 28; April 1989.

MILNER, C. & CHRISTOFI, N. (1985): A microbial examination of groundwater from the Grimsel Test Site (Appendix). In West J.M. and Grogan H., editors; Nagra Internal Technical Report NIB 86-13, Nagra, Baden, Switzerland.

MORENO, L., NERETNIEKS, I. & KLOCKARS, C.E. (1983): Evaluation of some tracer tests in granitic rock at Finnsjön. SKBF/KBS Technical Report 83-38, Nuclear Fuel Safety Project; SKB, Stockholm, Sweden.

MORENO L. & TSANG, C.F. (1991): Multiple peak response to tracer injection tests in single fractures: a numerical study. Water Resources Research. Vol. 27, Nr. 8, pp. 2143-2150.

MOSER, H. & RAUERT, H. (1980): Isotopenmethoden in der Hydrologie. Lehrbuch der Hydrogeologie 8, Gebr. Borntäger, Berlin, Deutschland.

MÜLLER, W. (1988): The Grimsel Test Site: Geological Background of the Area and Special Aspects of water Flow. In Nagra Informiert 1/2 1988 or Nagra Bulletin, special English edition 1988; p. 13-20.

NAGRA (1985): Felslabor Grimsel: Rahmenprogramm und Statusbericht. Nagra Technical Report NTB 85-34; Nagra, Baden, Switzerland.

NAGRA (1988): In Nagra Informiert 1/2 1988 or Nagra Bulletin, English edition 1988; special issue devoted to the research projects at the Grimsel Test Site.

NAGRA (1990): Grimsel Test Site: The Grimsel Radionuclide Migration Experiment-Status Autumn, 1990. Nagra Internal Report 90-14; Nagra, Baden, Switzerland.

NERETNIEKS, I. (1990): Solute transport in fractured rock - applications to radionuclide waste repositories. SKB Technical Report 90-38, SKB Stockholm, Sweden, December 1990.

NOELL, U. & ZÜRN, W. (1991): Detaillierte Interpretation der Neigungsmessungen im Felslabor Grimsel. Nagra Internal Report 90-30; Nagra, Baden, Switzerland; March 1991.

NOWAKOWSKI, K.S., EVANS, G.V., LEVER, D.A. & RAVEN, K.G. (1985): A field example of measuring hydrodynamic dispersion in a single fracture. Water Resources Research, Vol. 21, Nr. 8, 1165-1174.

OHSE, W. (1983): Lösungs- und Fällungserscheinungen im System oberflächennahes unterirdisches Wasser / gesteinsbildende Minerale - eine Untersuchung auf Grundlage der chemischen Gleichgewichts-Thermodynamik; Ph.D. Thesis of the Christian Albrecht University, Kiel; Germany.

PAHL, A., HEUSERMANN, St., BRÄUER, V., GLÖGGLER, W. (1989): Felslabor Grimsel: Gebirgsspannungs-Untersuchungen. Nagra Technical Report NTB 88-39; Nagra, Baden, Switzerland; April 1989.

PAHL, A., BRÄUER, V., HEUSERMANN, St., KILGER, B. & LIEDKE, L. (1986): Results of Engineering Geological Research in Granite. Bull. Int. Assoc. Eng. Geol., 34, p. 59-65.

PHOTODOCUMENTATION (1987): Grimsel Migration Experiment: Colorphotos from drillcores of all boreholes (BOMI 86.004 to BOMI 87.011). Unpublished Nagra Data; Nagra, Baden, Switzerland.

RABER, E., GARRISON, J. & OVERSBY, V. (1983): The Sorption of selected radionuclides on various metal and polymeric materials. Radioactive Waste Management and the Nuclear Fuel Cycle, Vol 4/1, 41-52.

RAMSAY, J.G. & HUBER, M.I. (1983): The Techniques of Modern Structural Geology, Vol 1: Strain Analysis. Academic Press, London, Great Britain.

RAMSAY, J.G. & HUBER, M.I. (1987): The Techniques of Modern Structural Geology, Vol 2: Folds and Fractures. Academic Press, London, Great Britain.

SAGEEV, A. (1986): Slug test analysis. Water Resour. Res. Vol. 22, Nr. 8, 1323-1333.

SCHNEEBELI, M., LÄSER, H.P., WYDLER, H. & FLÜELER, H. (1990): Wasserpotential und Wassergehalt in ungesättigten Graniten des Felslabors Grimsel: Labormessungen. Nagra Internal Report 90-20, Nagra, Baden, Switzerland; May 1990.

SKI (1987): INTRAVAL Project Proposal, SKI 87:3; Swedish Nuclear Power Inspectorate, Stockholm, Sweden.

SMITH, P.A. & ALEXANDER, W.R. (1990): Proposed Experimental programme for the High Pressure Infiltration Apparatus. PSI Internal Technical Note, AN-41-90-25/PES-90-525; Paul Scherrer Institute, Villigen, Switzerland.

SMITH, P.A., HADERMANN, J. & BISCHOFF, K. (1990): Dual Porosity Modelling of Infiltration Experiments on Fractured Granite, Proc. GEOVAL Symposium, May 14-17, 1990, Stockholm, Sweden.

SMITH P.A. (1991) Grimsel Test Site: Modelling of Laboratory High-Pressure Infiltration Experiments. Nagra Technical Report NTB 91-33; Nagra, Wettingen, Switzerland; also published as PSI Bericht Nr. 117; January 1992

STALDER, H.A. (1981): Sondierbohrungen Juchlistock-Grimsel: Mineralogisch-Petrographische Untersuchungen. Nagra Internal Report 81-01; Nagra, Baden, Switzerland; September 1981.

STECK, A. (1968): Die alpidischen Strukturen in den zentralen Aaregraniten des westlichen Aaremassivs. Eclogae Geol. Helv. 61, p. 19-48.

STIESS, H. (1990): Berechnungen zum Wärme-, Stoff- und Nuklidtransport in einer Einzelkluft mit Hilfe von NAMMU: Theoretische Grundlagen, Verifikation und Berechnung der Wärmeausbreitung in einem zweidimensionalen Kluft-Matrix-System. Nagra Internal Report 90-15; Nagra, Baden, Switzerland.

THORNE, P. (1990a): Grimsel Test Site: The Grimsel Migration Experiment - Borehole equipment used for hydrotesting and pilot tracer tests. Nagra Internal Report 89-10; Nagra, Baden, Switzerland (October 1990).

THORNE, P. (1990b): Grimsel Test Site: The Grimsel Migration Experiment - Equipment used for tracer analysis during pilot tests. Nagra Internal Report 89-11; Nagra, Baden, Switzerland (October 1990).

TSANG, Y.W., TSANG, C.F., NERETNIEKS, I. & MORENO, L. (1988): Flow and Tracer Transport in Fractured Media: A Variable Aperture Channel Model and Its Properties. Water Resources Research. Vol. 24, Nr. 12, pp. 2049-2060.

TSANG, C.F., TSANG, Y.W. & HALE, F.V. (1991): Tracer Transport in Fractures: Analysis of Field data Based on a Variable-Aperture Channel Model. Stripa Project Technical Report 91-14; SKB Stockholm, Schweden. June 1991.

VILKS, P. & DEGUELDRE, C. (1991): Sorption behaviour of ^{85}Sr, ^{131}I, ^{137}Cs on colloids and suspended particles from the Grimsel Test, Switzerland. Applied Geochemistry, Vol. 6, Nr.5, pp. 553-563, Pergamon Press.

VOMVORIS, S. (1988): Some Results for Unequal Dipole Tracer Tests; Nagra Internal Technical Note.

WATANABE, K. (1991): Evaporation Measurements in the Grimsel Test Site. Nagra Internal Report 90-15; Nagra, Wettingen, Switzerland.

WYSS, E. (1989): Felslabor Grimsel: Hydrogeologische Untersuchungen zur Bestimmung hydraulischer Potentiale. Nagra Technical Report NTB 89-01; Nagra, Baden, Switzerland (June 1989).

WYSS, E. (1990): Felslabor Grimsel Migrationstest: Drei Beispiele für das weitere Verständnis des hydraulischen Verhaltens. Nagra Internal Report 90-49; Nagra, Baden, Switzerland (August 1990).